THE UNIVERSITY OF HULL

Problems Involving Heat Transfer with Change of Phase

being a thesis submitted for the Degree of

Doctor of Philosophy

in the University of Hull

by

Peter Michael Beckett, M.A. (Oxon.).

April 1971.

To

Jo, Rachel and Caroline

Abstract

In Part I, two-dimensional laminar film condensation is investigated on the basis of boundary layer theory. The case of flow past a semi-infinite flat plate, which is aligned parallel to a uniform mainstream with velocity $u_m^*(x) = u_o^*$, is discussed by means of a perturbation analysis for both small and large rates of cooling at the surface. Predictions, for this similar solution of the boundary layer equations, are compared with exact numerical solutions in the case of steam-water condensation. The perturbation analysis is then extended to non-similar flows and results for steam-water condensation are compared with numerical solutions obtained using the Hartree-Womersley method. The cases $u_m^*(x) = u_o^* \sin\left(\frac{x}{2}\right)$ and $u_m^*(x) = u_o^*\left(1-\frac{1}{3}\frac{x}{2}\right)$ are used for comparison. The numerical solutions are also studied to discuss separation in these condensation problems.

Part II is devoted to the solidification of a cylindrical bar, initially at fusion temperature, when the outer surface temperature is lowered below fusion. The governing equations are solved numerically to obtain accurate results for the solidification process and in addition a power series in the non-dimensional time is developed. Terms of this series are found both analytically and numerically. Interest surrounds the radius of convergence of such a series because of the similarity between the movements of the solidification front and the growth of the boundary layer for flow through a cylinder.

Acknowledgments

It is a pleasure to express my gratitude to Dr. Graham Poots for suggesting such interesting work, and for being a constant source of help and encouragment throughout the time I have been associated with him.

I also owe a debt of gratitude to Miss Tessa Blackmore and Miss Lindis Robinson for typing the thesis.

Contents

Nomenclature

Part I

C_f	non-dimensional shear stress
C_p	specific heat at constant pressure
$f(\eta)$	similarity function
$F(\xi,\eta)$	function in non similar solution
G	temperature similarity function
h_{fg}	latent heat of condensation
k	thermal conductivity
m	exponent in Falkner-Skan velocity, $u_m^*(x) = u_0^* (x/c)^m$.
Nu	Nusselt number
p	pressure
P	Prandtl number
q	velocity
Re_x	local Reynolds number
$t(x)$	measure of condensate thickness
T	temperature
u, v	velocity components
U, V	thick film perturbation velocity functions
$u_m^*(x)$	general vapour mainstream velocity
u_0^*	constant vapour mainstream velocity
x, y	physical co-ordinates
x, y_1	Howarth-Dorodnitsyn co-ordinates
X, Y	Similarity co-ordinates; range of Y is $[0,1]$.

Γ condensation rate

$\xi(x)$ form of interface

δ_1 vapour boundary layer displacement thickness

δ_2 vapour boundary layer momentum thickness

$\Delta(x)$ interface location (Howarth-Dorodnitsyn co-ordinates)

ΔT $= T_S - T_W$.

ε $x^{1/3}$

ξ, η similar co-ordinates

θ non-dimensional temperature; $\theta = (T-T_W)/(T_S-T_W)$.

λ dimensionless parameter; $\lambda = \left(\frac{\rho_s \mu_s}{\rho_s^* \mu_s^*}\right)^{1/2}$.

μ dynamic viscosity

ρ density

$\tau_w^*(x)$ interfacial shear stress

ϕ condensate thickness (similar solution)

χ dimensionless parameter;

ψ stream function

Subscripts

s saturated

w wall

I interface

Superscript

$*$ vapour phase

Part II

a radius of cylinder

c specific heat

e_r coefficients in series expansion of ε

$E(t)$ depth of penetration of solidification front

$f_r(\eta)$ function in series expansion of θ

k thermal conductivity

L latent heat of solidification.

r cylindrical polar co-ordinate

t time

T temperature

β $L/C(T_f - T_o)$.

ε E/a, non-dimensional penetration depth.

ς $\frac{1}{2}e_0\eta$.

η dimensionless co-ordinate; $\eta = (a-r)/a\varepsilon$.

θ dimensionless temperature; $\theta = (T-T_o)/(T_f-T_o)$

τ dimensionless time; $\tau = tk/a^2$.

Subscripts

f evaluation at fusion temperature

o evaluation at wall temperature

PART I

LAMINAR FILM CONDENSATION

Chapter 1

Introduction to Condensation problems

When a cold surface at temperature, T_W, below saturation temperature, T_S, is exposed to vapour, either saturated or superheated, liquid condensate forms on the surface. If the liquid wets the surface it spreads out and establishes a stable film; this process is referred to as film condensation. The vapour continues to condense at the liquid-vapour interface, the heat being transferred through the liquid film. In contrast the liquid may not wet the surface and the condensate forms into droplets which coalesce as they are driven along the surface. This is called dropwise condensation.

The mechanism of dropwise condensation is not fully understood, but it is very apparent that the heat transfer rate is up to twenty times higher than for film condensation. It has been generally supposed that heat goes through the bare surfaces that exist between the drops, but if this is what occurs, the means by which the condensing vapour reaches the existing drops or forms into new drops is not certain.

Emmons [1] has suggested a possible mechanism. Molecules reflected from the bare surface would have energies less than that of the saturated vapour and may lead to a layer of subcooled vapour next to the surface. Emmons also suggested rapid condensation sets up violent eddy currents that move the subcooled layer into drops.

Umur and Griffith [2] concluded that condensate films greater than one-molecular thickness do not form on the 'bare' surface, and that

condensation actually takes place on the drops. This was also the view of Trefethen [3] who recognised that surface tension effects could cause circulation within the drops.

The mechanism is further complicated by the fact that experimental evidence exists to show that the effect of thermal properties of the surface material are significant. Mikic [4] proved that the non-uniformity in surface temperature, under the conditions of dropwise condensation, causes different heat fluxes for different materials.

Although dropwise condensation occurs initially on contaminated surfaces after a certain period of time the drops usually all join together to form a film. Consequently most condensing equipment is designed on the assumption that the less efficient mode, that is film condensation, will exist. Part I of this thesis is devoted to film condensation.

———— o ————

Moreover interest will be confined to laminar film condensation. To show this is reasonable note that there are two general classes of problems. On the one hand there are natural convection flows in which the vapour is usually at rest far from the body and movement of the condensate is due to gravitational effects. On the other hand there are forced convection flows in which the mainstream vapour velocity relative to the wall is non-zero and the condensate motion is due to the sweeping effect of the vapour. In the former class it is the condensate phase

which may become turbulent, and it is relevant to note that a free falling film has been observed by McAdams [5] to change to turbulent flow at $4\Gamma/\mu = 1800$, where $4\Gamma/\mu$ is the film Reynolds number based on the condensation rate. Turbulence in forced flow however would occur in the vapour phase, which admits solution by boundary layer theory. As is well known suction stabilizes the laminar boundary layer, and since the condensing vapour causes an effective suction at the liquid-vapour interface, under certain conditions it completely eliminates the possibility of transition to turbulent flow. According to Schlichting [6] the condition of complete stability of the laminar boundary layer flow, subject to the no-slip condition, is expressed by

$$\frac{w_s^*}{u_o^*} > 1.18 \times 10^{-4},$$

where w_s^* is the vapour inflow velocity at the interface and u_o^* is the free stream vapour velocity. The vapour suction in most condensation processes is much greater than this value.

In a paper concerning the flow of thin films, without condensation, on vertical plates Kapitsa [7] has shown that for Reynolds numbers greater than 33, waves begin to form on the surface due to surface tension effects. To date no-one has accounted for this complication applied to condensation problems and in the work presented here it will again be ignored; not because the effect is insignificant but by way of necessity.

The last decade has witnessed growing interest in laminar film condensation. In the main this has concerned the condensation of pure vapours at saturation temperature under the assumption that there is no interfacial resistance, that is there is no temperature jump at the interface between the condensate and vapour. However the effects of vapour superheating, interfacial resistance and the presence of non-condensables in the vapour have all been studied. Sparrow and Minkowycz [8] , and together with Saddy [9] have studied combinations of these effects. The overall conclusion is that the effect of superheating is not important in a pure vapour, but the presence of even a small amount of air in steam, for example, leads to a significant decrease in the heat transfer rate. Even if both these effects had proved to be significant it would still be permissible to stipulate the vapour being both pure and saturated, however neglecting interfacial resistance is a simplifying assumption consequent on taking such a model. Kinetic theory indicates that a temperature jump exists; if it did not, no condensation could occur.

The magnitude of the jump varies directly with the rate of condensation, m; consequently the interfacial resistance is most strongly manifested in the case of a pure vapour. A widely accepted representation of the temperature jump for a pure saturated vapour is

$$\dot{m} = \Omega (T_s - T_i),$$

where T_S is the saturation temperature, T_i the interfacial temperature and

$$\Omega = \left(\frac{\sigma}{2-\sigma}\right)\left(\frac{2}{\pi R}\right)^{1/2} \frac{h_{fg} \cdot p_s^*}{T_s^{5/2}} .$$

Here h_{fg} is the latent heat of condensation, R is the gas constant of the vapour, p_s^* is the pressure in the free stream and σ is the condensation coefficient characterizing the fraction of the vapour molecules which actually condense. For the case of steam water condensation σ is almost unity, and it has been concluded [9] that interfacial resistance has a negligible effect on condensation for this fluid.

The aim of the preceding part of the introduction has been to outline the nature and applicability of the simplifications involved if we consider laminar film condensation of pure saturated vapours. The remainder of the introduction will be devoted to describing the previous work in this field and outlining the motivation for the present work.

The first theoretical study of laminar film condensation was made by Nusselt [10] who considered the problem of vapour condensing onto a vertical flat plate. Nusselt looked for the steady state solution in which the condensation, under the influence of gravity, moved down the wall while newly condensed vapour maintained the interface in a

fixed position. The dominant features of condensation problems are not always obvious so this solution is remarkable, not simply because Nusselt was a pioneer, but because he also recognised the essential physics of the flow. The model ignored momentum and heat convection effects and supposed there was no interfacial shear. The motion of the condensate was governed by a balance between viscous shear, gravity and pressure forces. Nusselt also applied the same reasoning for vapour condensing onto a circular cylinder in a gravitational field.

Since then the analysis has been modified to include the effects Nusselt neglected, and also the variation of condensate properties. The most recent contribution is by Poots and Miles [11] who solved the complete system numerically.

It is the intention in this thesis only to investigate flows in the absence of a body force so the preceding work is not directly relevant to anything that follows. It has been mentioned because of the historical importance and because the simplicity and accuracy of Nusselt's model make it the outstanding contribution to the field.

One problem which will be studied concerns the condensation of vapour, having constant mainstream velocity, onto a semi-infinite flat plate. This has already received the attention of Cess [12] and Koh [13] both of whom formulated the problem using boundary layer theory, Koh solved the full equations numerically while Cess neglected inertia forces and convected energy. The two sets of results were in general agreement, indicating that Cess' assumptions are generally valid, except for large Prandtl numbers, but certainly so for steam-water

condensation. Further support for Cess' ideas is provided by the order of magnitude arguments applied to this problem by Shekriladze and Gomelauri [14] . The re-investigation will start with the basic model assumed by Koh and Cess, except that here variable condensate properties will be included. The effect of these is known to be significant (see [11]), but the real motivation for solving the problem again only appears when it is considered together with the following problems.

The case of condensation onto the cylinder in the absence of body forces has been touched on by Shekriladze and Gomelauri [14] , but they avoid the most interesting aspect, that is the effect condensation has on separation. Presumably the effective suction at the interface will delay separation so if the condensation rate is high enough separation might not occur. According to the analysis of Prandtl [15] , the suction rate, C_Q, sufficient to prevent separation should satisfy the following inequality:

$$C_Q \cdot Re_D^{1/2} > 4 \cdot 33.$$

The Russian authors assume C_Q is large enough for this to hold and only make obvious conclusions about the delaying effect. The current work will study the case of steam condensing onto the cylinder and will provide the first quantitative description of separation in condensation problems.

As further illustration of this phenomenon, condensation onto the plate will be investigated in the presence of a linearly retarded mainstream and also the Falkner-Skan type mainstream.

It will transpire that the numerical labour involved in such problems is considerable and some approximate models are highly desirable. These will be based on perturbation expansions, and in addition to providing data on the flow, they will prove extremely valuable in pinpointing the dominant features of a particular problem.

To illustrate that the essential physics sometimes does need highlighting, it is only necessary to compare Cess' model for the plate with that proposed by Sparrow and Gregg [16] for condensation onto a rotating disk. In the former the effects of vapour drag were included but the inertia terms ignored, whilst in the latter the exact opposite was assumed. Hudson [17] recently investigated the disk problem numerically and approximately. The exact solution did not agree with the results of Sparrow and Gregg, and the approximate models, analogous to those developed here, clearly showed the interfacial shear is not insignificant.

The motivation then for the present work is two-fold. Firstly no quantitative description of separation in condensation problems is known to exist, and to this end accurate numerical solutions of the governing equations will be found. Secondly much of the work which has been presented embodies assumptions, which are often only intuitive, and it is the intention to develop uniformly valid approximations which give accurate data and give assistance in describing the essential physics.

Chapter 2

Governing Equations of Laminar Film Condensation

Throughout this part of the thesis attention will be confined to two dimensional laminar film condensation in which the vapour is at the saturated vapour temperature, T_S, and the condensation process maintained be keeping a boundary at a temperature T_W; $T_W < T_S$. In addition only problems in which the flow is steady are to be studied, so the manner in which the wall temperature is lowered to T_W is of no consequence. If the condensate properties can be taken as known functions of temperature then such problems are completely described by knowing the pressure, velocity and temperature distributions throughout the two phases together with the location of the liquid-vapour interface.

For two-dimensional flows the equations from which these will be determined are two components of the momentum transport equation together with the continuity equation in each phase, the thermal energy equation applied to the condensate layer and an energy balance associated with the liberation of latent heat at the interface.

Let $\underline{q} = (u,v)$ denote the condensate velocity with components in the (x,y) directions, where x measures the distance along the surface and y measures the distance normal to it. Let T denote the temperature of the condensate such that $T_W \leq T \leq T_S$, and denote the liquid-vapour interface by

$$y = \delta(x). \tag{2.1}$$

The condensate momentum equation is then

$$\rho \frac{D\underline{q}}{Dt} = -\underline{\nabla} p + \underline{F} - \underline{\nabla} \wedge \left[\mu \underline{\nabla} \wedge \underline{q}\right] + \underline{\nabla}\left[\left(\varsigma + \tfrac{4}{3}\mu\right)\underline{\nabla}.\underline{q}\right] \tag{2.2}$$

where ρ is the density, p the pressure, $\underline{F}$ the external body force, μ the dynamic viscosity, ζ a second coefficient of viscosity and $\frac{D}{Dt}$ is the convective derivative.

The continuity equation is:

$$\operatorname{div}(\rho \underline{q}) = 0. \tag{2.3}$$

The energy equation is:

$$\rho C_p \frac{DT}{Dt} = \underline{\nabla}\cdot(k \underline{\nabla} T) + W_i + T\beta \frac{Dp}{Dt} + \mu \Phi, \tag{2.4}$$

where C_p is the specific heat at constant volume, k is the thermal conductivity, W_i represents the energy associated with a heat source, β is the coefficient of cubical expansion and Φ is the viscous dissipation function.

For the vapour phase let x^* measure distance along the interface and y^* normal to it. Denoting all vapour quantities by a star, the velocity is $\underline{q}^* = (u^*, v^*)$, the components taken in the (x^*, y^*) directions, ρ_s^* is the density, μ_s^* is the dynamic viscosity and p^* is the pressure. The momentum and continuity equations are then:

$$\rho_s^* \frac{D\underline{q}^*}{Dt} = -\underline{\nabla} p^* + \underline{F} - \mu_s^* \underline{\nabla} \wedge (\underline{\nabla} \wedge \underline{q}^*), \tag{2.5}$$

$$\operatorname{div} \underline{q}^* = 0. \tag{2.6}$$

Here the fluid properties are considered constant since the vapour is isothermal.

This system is simplified if the body forces are neglected in the momentum equations, and the terms representing viscous dissipation and compressibility effects are excluded from the thermal energy equation. Also, although the interface is a heat source this occurs at the edge of each phase and the liberation of latent heat is accounted for in the

boundary conditions, and so W_i is also omitted from (2.4).

It is now assumed that the thickness of the condensate layer is small compared with the radius of curvature of the body so that $x = x^*$. Further, on the assumption that all changes in physical quantities normal to the surface, or interface, are large compared with changes in the x-direction, it is possible to invoke the boundary layer approximation (see Miles [18]). Thus the equations reduce to:

Condensate phase $(x \geq 0, \quad 0 \leq y \leq \delta(x))$,

$$\rho\left(u\frac{\partial u}{\partial x} + v\frac{\partial u}{\partial y}\right) = \rho_s^* U_m^*(x)\frac{dU_m^*(x)}{dx} + \frac{\partial}{\partial y}\left(\mu\frac{\partial u}{\partial y}\right), \tag{2.7}$$

$$\frac{\partial}{\partial x}(\rho u) + \frac{\partial}{\partial y}(\rho v) = 0, \tag{2.8}$$

and

$$\rho c_p\left(u\frac{\partial T}{\partial x} + v\frac{\partial T}{\partial y}\right) = \frac{\partial}{\partial y}\left(k\frac{\partial T}{\partial y}\right). \tag{2.9}$$

together with the variable property relations

$$\rho = \rho(T), \quad \mu = \mu(T), \quad c_p = c_p(T), \quad k = k(T). \tag{2.10}$$

For the case of steam-water condensation the forms of the variable properties are available from experimental data (see Appendix I).

Vapour phase $(x \geq 0, \quad 0 \leq y^* \leq \infty)$

$$\frac{\partial u^*}{\partial x} + \frac{\partial v^*}{\partial y^*} = 0, \tag{2.11}$$

and

$$u^*\frac{\partial u^*}{\partial x} + v^*\frac{\partial u^*}{\partial y^*} = U_m^*(x)\frac{d}{dx}U_m^*(x) + \nu_s^*\frac{\partial^2 u^*}{\partial y^{*2}}, \tag{2.12}$$

where $\nu_s^* = \mu_s^*/\rho_s^*$, the kinematic viscosity.

The boundary conditions which are imposed on these equations are the following.

On the body surface $(x \geq 0, y = 0)$ the non-slip condition gives

$$u = v = 0, \tag{2.13}$$

and

$$T = T_w. \tag{2.14}$$

In the vapour mainstream we have:

$$u^* \longrightarrow u_{m^*}(x) \quad \text{as} \quad y \longrightarrow \infty.$$

At the liquid-vapour interface ($x \geq 0$, $y = \delta(x)$, $y^* = 0$) the continuity of velocity tangential to the interface yields:

$$[u]_{y=\delta(x)} = [u^*]_{y^*=0} \tag{2.15}$$

If surface tension effects are neglected at the interface then the continuity in interfacial stress components yield:

$$p = p^*, \tag{2.16}$$

$$\mu_s \left[\frac{\partial u}{\partial y}\right]_{y=\delta(x)} = \mu_s^* \left[\frac{\partial u^*}{\partial y^*}\right]_{y^*=0}. \tag{2.17}$$

where the subscript, S, denotes the value of the condensate evaluated at the saturated vapour temperature T_S. Similarly μ_w will be the value of μ when $T = T_W$ etc.

Note that (2.16) has already been used in deriving (2.7) and (2.12).

The continuity in mass flow across the interface yields:

$$\left[\rho\left(v - u\frac{d\delta}{dx}\right)\right]_{y=\delta(x)} = \rho_s^* [v^*]_{y^*=0}.$$

Now since

$$\frac{\partial}{\partial x}(\rho u) + \frac{\partial}{\partial y}(\rho v) = 0$$

then

$$[\rho v]_{y=\delta(x)} = -\int_0^{\delta(x)} \frac{\partial}{\partial x}(\rho u)\, dy,$$

and

$$\rho_s^* [v^*]_{y^*=0} = -\frac{d}{dx}\left(\int_0^{\delta(x)} \rho u\, dy\right). \tag{2.18}$$

Finally it is left to express the fact that the latent heat liberated at the interface as the vapour condenses is conducted through the body surface together with convective cooling in the downstream direction.

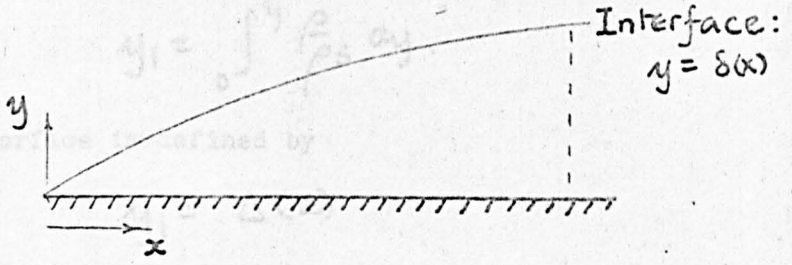

Applying the energy balance to the volume depicted above we have;

$$k_w \int_0^x \left(\frac{\partial T}{\partial y}\right)_{y=0} dx = h_{fg} \int_0^\delta \rho u \, dy + \int_0^\delta \rho u \left(c_{ps} T_s - c_p T\right) dy, \qquad (2.19)$$

where h_{fg} is the latent heat of condensation, and T is measured in absolute units. Alternatively the energy balance can be applied locally at the interface and then gives:

$$- h_{fg} \cdot \rho_s^* \left[v^*\right]_{y^*=0} = k_s \left(\frac{\partial T}{\partial y}\right)_{y=\delta(x)}. \qquad (2.20)$$

A first step common to some of the work when solving the system (2.7)-(2.18) together with either (2.19) or (2.20) is to introduce stream functions for the two phases.

The vapour phase admits the conventional incompressible stream function $\psi^*(x,y^*)$ defined by

$$u^* = \frac{\partial \psi^*}{\partial y^*}, \quad v^* = - \frac{\partial \psi^*}{\partial x}, \qquad (2.21)$$

and the condensate is treated, for convenience, as a compressible fluid so $\psi(x,y)$ is given by

$$\rho u = \rho_s \frac{\partial \psi}{\partial y}, \quad \rho v = - \rho_s \frac{\partial \psi}{\partial x}. \qquad (2.22)$$

However if x and y are retained as independent variables for the condensate phase then it becomes necessary to differentiate the density, a difficulty which is overcome by employing the Howarth-Dorodnitsyn transformation:

$$y_1 = \int_0^y \frac{\rho}{\rho_s}\, dy . \tag{2.23}$$

Then the interface is defined by

$$y_1 = \Delta(x) \tag{2.24}$$

where

$$\Delta(x) = \int_0^{\delta(x)} \frac{\rho}{\rho_s}\, dy. \tag{2.25}$$

It is also convenient to introduce a dimensionless temperature function $\theta(x, y_1)$ by:

$$T = T_w + \theta . \Delta T , \quad \Delta T = T_s - T_w , \tag{2.26}$$

so that the boundary conditions on T yield :

$$\theta = 0 , \; y_1 = 0 \; ; \; \theta = 1 , \; y_1 = \Delta(x). \tag{2.27}$$

Introducing (2.21)-(2.26) into (2.7)-(2.20) the following set of equations results:

Condensate: $(x \geq 0 , \; 0 \leq y_1 \leq \Delta(x))$.

$$\rho\left(\frac{\partial \psi}{\partial y_1}\frac{\partial^2 \psi}{\partial x \partial y_1} - \frac{\partial \psi}{\partial x}\frac{\partial^2 \psi}{\partial y_1^2}\right) = \rho_s^* u_m^* \frac{d u_m^*}{dx} + \frac{\rho}{\rho_s}\frac{\partial}{\partial y_1}\left(\frac{\mu}{\rho_s}\frac{\partial^2 \psi}{\partial y_1^2}\right), \tag{2.28}$$

$$\rho_s c_p \left(\frac{\partial \psi}{\partial y_1}\frac{\partial \theta}{\partial x} - \frac{\partial \psi}{\partial x}\frac{\partial \theta}{\partial y}\right) = \frac{\partial}{\partial y_1}\left(\frac{k}{\rho_s}\frac{\partial \theta}{\partial y_1}\right), \tag{2.29}$$

Vapour $(x \geq 0, \; 0 \leq y^* \leq \infty)$,

$$\left(\frac{\partial \psi^*}{\partial y^*}\frac{\partial^2 \psi^*}{\partial x \partial y^*} - \frac{\partial \psi^*}{\partial x}\frac{\partial^2 \psi^*}{\partial y^{*2}}\right) = u_m^* \frac{d u_m^*}{dx} + \nu_s^* \frac{\partial^3 \psi^*}{\partial y^{*3}} . \tag{2.30}$$

Boundary conditions: At the body surface

$$\frac{\partial \psi}{\partial x} = \frac{\partial \psi}{\partial y_1} = 0 , \; \theta = 0 , \quad y_1 = 0 , \; x \geq 0 . \tag{2.31}$$

Interfacial conditions: $\left(x>0,\ y_1=\Delta(x),\ y^*=0\ ;\ \Delta(x)=\int_0^{\delta(x)}\frac{\rho}{\rho_s}\,dy\,.\right)$.

$$\theta = 1, \tag{2.32}$$

$$\rho_s \psi = \rho_s^* \psi^*, \tag{2.33}$$

$$\frac{\partial \psi}{\partial y_1} = \frac{\partial \psi^*}{\partial y^*}, \tag{2.34}$$

$$\mu_s \frac{\partial^2 \psi}{\partial y_1^2} = \mu_s^* \frac{\partial^2 \psi^*}{\partial y^{*2}}. \tag{2.35}$$

Mainstream condtion:

$$\frac{\partial \psi^*}{\partial y^*} \longrightarrow u_m^*(x) \quad \text{as} \quad y^* \longrightarrow \infty. \tag{2.36}$$

Finally the local and global forms of the energy balance are:

$$k_s . \Delta T . \left(\frac{\partial \theta}{\partial y_1}\right)_{y_1=\Delta(x)} = h_{fg}\, \rho_s^* \left[\frac{\partial \psi^*}{\partial x}\right]_{y^*=0} \tag{2.37}$$

and

$$\frac{\rho_w k_w . \Delta T}{\rho_s} \int_0^x \left(\frac{\partial \theta}{\partial y_1}\right)_{y_1=0} dx = h_{fg} \int_0^{\Delta(x)} \rho_s \frac{\partial \psi}{\partial y_1}\, dy_1 + \int_0^{\Delta(x)} (C_{ps} T_s - C_p T) \rho_s \frac{\partial \psi}{\partial y_1}\, dy_1. \tag{2.38}$$

———— o ————

Chapter 3

Numerical similar solutions

Introduction

It has been established in the previous chapter that the equations and boundary conditions governing the transport of momentum and energy are (2.28)-(2.38). Having constructed these for the general mainstream vapour flow $U_m^*(x)$, the intention in this Chapter is to restrict ourselves to $U_m^*(x) = U_o^*(x/c)^m$ and seek similar solutions. Falkner and Skan [19] first used this as the mainstream velocity for a single phase flow and it has proved to be a most fruitful source of information about the behaviour of both compressible and incompressible boundary layers. It would take far more than this volume to extend all the work which has been done in one phase case to the two phase problems arising in condensation, but guided by the work of Hartree [20] and Stewartson [21] a wealth of information should be at hand.

With the velocity distribution in the vapour we are looking simultaneously at the problems of condensation in the neighbourhood of the forward stagnation point on the circular cylinder by taking $m = 1$, and the forced flow over a flat plate by taking $m = 0$. The former problem has recently been extensively studied by Hudson [17], while the latter has been investigated by Cess [12], and it is to this problem that much of the effort of this chapter will be devoted. Cess considered a constant property condensate and solved the problem by utilising appropriate solutions which were available from work on a single phase flow. This work will be shown to be largely consistent with the ideas

and results of this thesis, but the limitations of 'Cess' method and sources of innacuracy will be explained.

In addition to this particular problem, m will be allowed to vary in order that some tentative conclusions concerning separation in condensation flows might be given.

Hartree and Stewartson both studied the results for $m < 0$, and though somewhat artificial because of the singularity in the mainstream velocity at $x = 0$, these have been of considerable interest. It is found that for $0 > m > m_0$ ($m_0 = -0.0904$) then an infinity of solutions exist, and moreover for $m = m_0$ a solution results which would have zero shear at the wall. Guided by the reasoning which dictates which of the infinity of solutions is physically acceptable, we find the corresponding solution for the condensation problem and the relevant value of m_0.

The similarity solution

For the condensate layer make the change of variables

$$\psi = \left(\frac{2u_0^* \xi^{m+1} v_s}{c^m}\right)^{\frac{1}{2}} f(\eta), \quad \xi = x, \quad \eta = \left(\frac{u_0^* x^{m-1}}{2c^m v_s}\right)^{\frac{1}{2}} y_1. \tag{3.1}$$

Then $$\frac{\partial}{\partial x} = \frac{\partial}{\partial \xi} + \frac{(m-1)}{2\xi}\eta \frac{\partial}{\partial \eta}, \quad \frac{\partial}{\partial y_1} = \left(\frac{u_0^* \xi^{m-1}}{2 v_s c^m}\right) \frac{\partial}{\partial \eta}.$$

Therefore $$u = \frac{\partial \psi}{\partial y_1} = \left(\frac{u_0^* \xi^m}{c^m}\right) f'(\eta) = u_m^*(\xi) f'(\eta) \tag{3.2}$$

and $$v = -\frac{\partial \psi}{\partial x} \cdot \frac{\rho_s}{\rho} = -\frac{\rho_s}{\rho}\left(\frac{u_0^* \xi^{m-1} v_s}{2c^m}\right)^{1/2}\left[(m+1) f(\eta) + (m-1)\eta f'(\eta)\right], \tag{3.3}$$

where dashes denote differentiation with respect to η .

Then also $$\frac{\partial^2\psi}{\partial x\,\partial y_1} = \left(\frac{u_0^* \xi^{m-1}}{c^m}\right)\left[m f'(\eta) + \tfrac{1}{2}(m-1)\eta f''(\eta)\right]$$

and $$\frac{\partial^2\psi}{\partial y_1^2} = \left(\frac{u_0^* \xi^{m-1}}{2\nu_s c^m}\right)^{1/2}\left(\frac{u_0^* \xi^m}{c^m}\right) f''(\eta).$$

Hence the condensate momentum equation becomes

$$\left(\frac{\rho\mu}{\rho_s\mu_s} f''(\eta)\right)' + (m+1) f(\eta) f''(\eta) + 2m\left[\frac{\rho_s^*}{\rho} - f'(\eta)^2\right] = 0. \quad (3.4)$$

The thermal energy equation (2.29) becomes, on putting $\theta(x,y_1) = G(\eta)$, the following:

$$\left(\frac{\rho k}{\rho_s k_s} G'(\eta)\right)' + (m+1)\frac{c_p}{c_{ps}} . P_s . f(\eta) G'(\eta) = 0, \quad (3.5)$$

where $P_s = c_{ps}\mu_s/k_s$, the Prandtl number.

For the vapour phase introduce corresponding functions and variables by

$$\psi^* = \left(\frac{2u_0^* \xi^{m+1} \nu_s^*}{c^m}\right)^{1/2} f^*(\eta^*), \quad (3.6)$$

where $\eta^* = \left(\frac{u_0^* x^{m-1}}{2c^m \nu_s^*}\right)^{\frac{1}{2}} y^*$ and $\xi = x$.

Consequently $$u^* = \left(\frac{u_0^* \xi^m}{c^m}\right) f^{*\prime}(\eta^*) = u_m^*(\xi) f^{*\prime}(\eta^*)$$

$$\text{and } v^* = -\left(\frac{u_0^* \xi^{m-1} \nu_s^*}{2c^m}\right)^{\frac{1}{2}}\left[(m+1) f^*(\eta^*) + (m-1)\eta^* f^{*\prime}(\eta^*)\right]. \quad (3.7)$$

The vapour momentum equation becomes

$$f^{*'''}(\eta^*) + (m+1) f^*(\eta^*) f^{*''}(\eta^*) + 2m\left(1 - [f^{*'}(\eta^*)]^2\right) = 0 \quad (3.8)$$

where dashes here denote differentiation with respect to η^*.

The boundary conditions on the functions $f(\eta)$, $f^*(\eta^*)$, $G(\eta)$ are:

$$f(0) = f'(0) = 0 \; ; \quad G(0) = 0 \, , \quad G(\phi) = 1 \; ; \quad (3.9)$$

$$f^{*'}(0) = 1. \quad (3.10)$$

The interface between the condensate and vapour is given by $\eta = \phi$, and the equalities of normal mass flow, tangential velocity and continuity of shear at the interface yield:

$$\left(\frac{\rho_s \mu_s}{\rho_s^* \mu_s^*}\right)^{1/2} f(\phi) = f^*(0) \, , \quad (3.11)$$

$$f'(\phi) = f^{*'}(0) \, , \quad (3.12)$$

$$\left(\frac{\rho_s \mu_s}{\rho_s^* \mu_s^*}\right)^{1/2} f''(\phi) = f^{*''}(0). \quad (3.13)$$

The remaining condition that can be applied is the so called energy balance which is given in local and global forms (2.37) and (2.38). Naturally bothyield the same results when included in the numerical scheme, and though the global one is not necessary in the numerical work which is entailed in solving the problems of this chapter it proves to be more stable when investigating retarded flows. The required form of the local energy balance is

$$\left(\frac{C_{ps}.\Delta T}{P_s.h_{fg}}\right) G'(\phi) = (m+1) f(\phi). \qquad (3.14)$$

One of the unknowns we are trying to find is the dimensionless thickness of the condensate layer, namely ϕ . To ease the numerical scheme a further transformation is made which fixes the range of integration, normal to the wall, as $[0,1]$, and casts the unknown ϕ into the equations.

We take $X = \xi$, $Y = \eta/\phi$,

then $\frac{\partial}{\partial \xi} = \frac{\partial}{\partial x}$, $\frac{\partial}{\partial \eta} = \frac{1}{\phi}\frac{\partial}{\partial Y}$

and we have the following equations to solve for the condensate layer:

$$\left(\frac{\rho\mu}{\rho_s/\mu_s} f''(Y)\right)' + (m+1)\phi f(Y) f''(Y) + 2m\left(\phi^3\frac{\rho_s}{\rho} - \phi f(Y)^2\right) = 0, \qquad (3.15)$$

$$\left(\frac{\rho k}{\rho_s k_s} G'(Y)\right)' + (m+1)\frac{C_p}{C_{ps}}.P_s\,\phi\, f(Y) G'(Y) = 0 . \qquad (3.16)$$

Here the dash denotes differentiation with respect to Y.

The vapour equation remains unaltered:

$$f^*(\eta^*)''' + (m+1) f^*(\eta^*) f^*(\eta^*)'' + 2m\left(1 - [f^{*\prime}(\eta^*)]^2\right) = 0. \qquad (3.17)$$

The above system (3.15)-(3.17) must now be solved subject to the following boundary conditions:

$$f(0) = f'(0) = 0 \; ; \; G(0) = 0, \; G(1) = 1. \tag{3.18}$$

and $$f^{*\prime}(\infty) = 1, \tag{3.19}$$

at the interface:

$$\left(\frac{\rho_s \mu_s}{\rho_s^* \mu_s^*}\right)^{1/2} f(1) = f^*(0), \tag{3.20}$$

$$f'(1) = \phi \, f^{*\prime}(0), \tag{3.21}$$

$$\left(\frac{\rho_s \mu_s}{\rho_s^* \mu_s^*}\right)^{\frac{1}{2}} f''(1) = \phi^2 f^{*\prime\prime}(0), \tag{3.22}$$

$$\frac{C_{ps}.\Delta T}{P_s.h_{fg}} G'(1) = (m+1)\,\phi\, f(1). \tag{3.23}$$

Two distinct numerical schemes have been employed to solve these equations. Initially an iterative method involving Runge-Kutta integration was employed, but work on the more complicated problems in the following chapters demands the use of a matrix scheme. Once this has been developed the present simpler set of equations is readily introduced into the program. Appendix C is largely devoted to the matrix scheme, which is also used to find solutions for the problems on solidification in part II, but a brief note on the Runge-Kutta method is found in appendix B. The great advantage of the matrix scheme is that it does not require such good initial approximations as that involving the Runge-Kutta integration. The problem of finding acceptable starting data is not difficult if $m = 0$, which was the first problem studied, but for $m < 0$ the problem is very

real and solutions in this range of m were found using the matrix iterative method.

Later in this project (see Chapters 4 and 6) approximate solutions of a range of condensation problems are found. These yield quantitative information which proves to be accurate enough to dispense with the need for such detailed calculations, but they could be used as starting values for the preceding iterative methods.

In order to describe the flow behaviour in each of the condensation problems the following information will be provided: velocity distributions in the two phases, the thermal field in the condensate layer, the displacement and momentum thicknesses for the vapour phase, skin friction coefficients at the wall and interface, wall heat transfer and finally the rate of condensation.

These quantities of practical interest are now defined for the case of a general vapour mainstream with velocity $u_m^*(x)$.

Condensate thickness: $\delta(x)$, (3.24)

Displacement thickness: $$\delta_1 = \int_{\delta(x)}^{\infty} \left(1 - \frac{u^*}{u_m^*(x)}\right) dy, \tag{3.25}$$

Momentum thickness: $$\delta_2 = \int_{\delta(x)}^{\infty} \frac{u^*}{u_m^*(x)} \left(1 - \frac{u^*}{u_m^*(x)}\right) dy, \tag{3.26}$$

Condensation rate $$\Gamma = \int_0^x - \rho_s^* \left[v_s^*\right]_{y=\delta(x)} dx, \tag{3.27}$$

Wall skin friction: $$Cf_{w.} = \frac{\left(\mu \frac{\partial u}{\partial y}\right)_{y=0}}{\frac{1}{2}\rho_s U_m^{*2}(x)}, \qquad (3.28)$$

Interfacial shear: $$Cf_I = \frac{\left(\mu \frac{\partial u}{\partial y}\right)_{y=\delta(x)}}{\frac{1}{2}\rho_s U_m^{*2}(x)}, \qquad (3.29)$$

Nusselt number: $$Nu = \frac{x}{\Delta T}\left(\frac{\partial T}{\partial y}\right)_{y=0}. \qquad (3.30)$$

The characteristics actually plotted are:

$$\frac{\delta(x)}{x}.Re_x^{1/2}, \quad \frac{\delta_1}{x}.Re_x^{1/2}, \quad \frac{\delta_2}{x}.Re_x^{1/2}, \quad \frac{\Gamma}{\sqrt{2}\mu_s^*}Re_x^{*1/2}, \qquad (3.31)$$

$$Cf_w.Re_x^{1/2}, \quad Cf_I.Re_x^{1/2} \quad \text{and} \quad Nu.Re_x^{-1/2},$$

where $Re_x = U_m^*(x).x/\nu_s$ and $Re_x^* = U_m^*(x).x/\nu_s^*$.

Discussion of results for forced flow over the semi-infinite flat plate (m = 0).

This is the problem tackled by Cess who treated the condensate as a constant property fluid. Cess introduced similarity variables and having noted that the resulting equations and boundary conditions for the vapour phase were analogous to the case of vectored blowing or suction, a fictitious origin was introduced in order to utilise the work of Emmons and Leigh [22], who tabulated the Blasius function with suction and blowing. Cess then assumed linear velocity and thermal profiles in the condensate and proceeded to find formulae for $Cf_w.Re_x^{1/2}$ and $Nu.Re_x^{-1/2}$

involving the suction velocity and corresponding wall shear from the Emmons and Leigh problem.

The accuracy of Cess' work will be discussed later, but it is important to note now, that the necessity for detailed numerical knowledge of the corresponding single phase problem is a severe restriction on applying his technique to the two phase problem.

Velocity distribution

The dimensionless velocity $\frac{u}{u_o^*} = \frac{1}{\phi}\frac{\partial f}{\partial Y}$ and $\frac{u^*}{u_o^*} = \frac{\partial f^*}{\partial \eta^*}$ are given in Tables (3)-(6) for the case of T_W = 0, 70, 90 and 99.99°C, and the information is also displayed graphically in figure 1.

When T_W = 0°C it is quite apparent that u is not proportional to Y, and so Cess is not justified in assuming a linear profile. The same observation can be made for the other values of T_W, though the effect is not as marked. However though $\frac{\partial u}{\partial Y}$ is by no means constant, table 3 shows that the shear stress, $\mu \frac{\partial u}{\partial y} = \left(\frac{\rho\mu}{\rho_s\mu_s}\right)\frac{1}{\phi^2}\frac{\partial^2 f}{\partial y^2}$, is almost constant. This fact indicates that it is the absence of variable fluid properties, and not the exclusion of the non-linear terms from the momentum equations, which is the major source of error in Cess' model. For the particular case of T_W = 0°C the value of μ falls from 1.78×10^{-2} g/cm.sec. at the body surface to 2.812×10^{-3} g/cm.sec. at the interface, and it is at this extreme value of T_W that Cess' results will be seen to be in error most.

The non-dimensional condensate thickness $\frac{\delta(x)}{x} \cdot Re_x^{1/2}$, previously defined for the general mainstream velocity $U_m^*(x)$ becomes:

$$\frac{\delta(x)}{x}.\ Re_x^{1/2} = \sqrt{2}\ \phi \int_0^1 \frac{\rho_s}{\rho}\, dY, \qquad (3.32)$$

and this is included in table 7. As expected the film increases in thickness as T_W falls.

The vapour boundary layer characteristics for this problem become

$$\frac{\delta_1}{x}.\ Re_x^{*\,1/2} = \sqrt{2}\ \left(f^*(0) + \lim_{\eta^* \to \infty} [\eta^* - f^*(\eta^*)] \right), \qquad (3.33)$$

and

$$\frac{\delta_2}{x}.\ Re_x^{*\,1/2} = \sqrt{2}\ \left(f^{*\prime\prime}(0) - f^*(0)\,[1 - f^{*\prime}(0)] \right), \qquad (3.34)$$

which are also tabulated for $T_W = 0(10)90$ and $99.99^\circ C$ in table 7.

A glance at the velocity profiles in figure 1 indicates why profiles were not sketched at regular intervals of T_W. The variation in flow pattern does not vary as much with T_W when T_W is near $0^\circ C$ as it does when $T_W \sim 100^\circ C$. The extreme case of $T_W = 99.99^\circ C$ has been included as this verifies the assertion that the vapour flow tends to the Blasius solution as $\Delta T \longrightarrow 0$. In contrast to the thickening condensate layer as ΔT increases, the vapour boundary layer thicknesses decrease. The displacement thickness when $T_W = 90^\circ C$ is less than 50% of the Blasius value and when $T_W = 0^\circ C$ the factor is less than 10%.

The non-dimensional condensation rate becomes

$$\frac{1}{\sqrt{2}}\,\frac{\Gamma}{\mu_s^*}\ Re_x^{*\,-1/2} = f^{*\prime}(0), \qquad (3.35)$$

and this is to be found in table 7. The rate increases markedly as T_W

falls and this allied to the considerably thinned vapour layer suggests the vapour may be treated as a strong suction layer, an idea which proves to be most fruitful later.

Skin friction coefficients

These take the form

$$C_{fw}.Re_x^{1/2} = \sqrt{2}.\left(\frac{\rho_w \mu_w}{\rho_s \mu_s}\right)\frac{1}{\phi^2} f''(0), \qquad (3.36)$$

and

$$C_{f_I}.Re_x^{1/2} = \sqrt{2}\ \frac{1}{\phi^2}\ f''(1), \qquad (3.37)$$

which are tabulated along with the other characteristics.

The variation of $C_{fw}.Re_x^{1/2}$ with T_W is displayed in figure 2 where comparison is made with Cess' results. The greatest error between the numerical results and Cess' solution occurs in $C_{fw}.Re_x^{1/2}$ (at $T_W = 0^\circ C$). This is not surprising since it is the viscosity that is the most sensitive of all the properties to change in temperature (see Appendix A).

It is also relevant to note that at each value of T_W the wall shear is greater than the interfacial shear for this problem.

Temperature distribution and heat transfer results

The non-dimensional thermal profile G is given in tables 3-6 and is observed to be linear for $T_W = 99.99$ and $90^\circ C$. When $T_W = 70$ and $0^\circ C$

there is a slight concavity and this is due to the variation in thermal conductivity with temperature. The expression involving the Nusselt number is

$$Nu.\,Re_x^{-\frac{1}{2}} = \frac{1}{\sqrt{2}.\phi}\left(\frac{\rho_w}{\rho_s}\right) G'(0), \qquad (3.38)$$

the values of which are found in table 7. Also $Nu.\,Re_x^{-\frac{1}{2}}$ is compared in figure 3 with the results obtained by Cess. It is again at $T_W = 0^\circ C$ where the largest discrepancy occurs and for the heat transfer is approximately 10%.

Discussion of results for the Falkner-Skan mainstream velocity

It has already been noted that for $0 > m > m_o$ ($m_o = -0.0904$) that the solution of the equations arising in the one phase flow is not unique. Hartree [20] selected that solution in which his function $f'(\eta)$ (equivalent to $f^{*\prime}(\eta^*)$ in this chapter) tended to unity from below faster than any other solution, and supported his choice by continuity arguments. Such arguments are not entirely satisfactory because it is possible to produce solutions different from Hartree's but satisfying his continuity arguments. Stewartson [21] offered an alternative and more convincing condition and this will be used to select the physically acceptable solution when dealing with condensation.

Suppose that we replace the boundary condition (3.20) by

$$f^{*\prime}(\eta^*_\alpha) = 1, \qquad (3.24)$$

and call the solutions satisfying (3.15)-(3.19), (3.21-3.24) and (3.24) $f_\alpha, G_\alpha, \phi_\alpha$ and f^*_α. We also require $|f^{*\prime}| < 1$, so that the vapour velocity is less in the boundary layer than in the mainstream. Now let $\alpha \to \infty$, corresponding to prescribing the velocity component parallel to x further and further from the plate. The solution obtained by a continuous process as $\alpha \to \infty$ is the one we accept.

In the range $0 > m > m_o$ Stewartson found two families of acceptable solutions, one in which the wall shear is positive and the other in which the wall shear is negative and typifies a reversed flow region. At $m = m_o$ then the wall shear is zero indicating a separation point type velocity profile.

It has not been possible to find the second branch solutions with flow reversal, but in view of the hitherto unknown nature of separation in condensing flows we will content ourselves with finding only the first branch solutions, and the value of m at which either $f''(0)$ or $f''(1)$ is zero. Any attempt to use this model to describe the behaviour of the vapour and condensate layers in the presence of an adverse pressure gradient must be regarded as tentative in view of the simplifying nature of the model.

When steam flows over a cylinder it is first accelerated from the stagnation point and later retarded. In the model the velocity profiles at stagnation are given by $m = 1$ and afterwards its form is determined by giving decreasing values to m. When $m = 0$ the maximum velocity is obtained in the mainstream and as m decreases below zero the mainstream is retarded

up to the separation point at which in the condensation problems either the wall or interfacial shear will vanish.

When discussing the problem of condensation on to the plate with constant mainstream velocity, a range of wall temperatures was used to illustrate the dependence of the flow characteristics on T_W. In this section the single extreme value $T_W = 0^oC$ is used.

For this case the dimensionless velocities $\frac{u}{u_{m^*}(x)} = \frac{1}{\phi}\frac{\partial f}{\partial y}$ and $\frac{u^*}{u_{m^*}(x)} = \frac{\partial f^*}{\partial \eta^*}$ can be deduced from Table 8 and they are also displayed graphically in figure 4 . The change in the velocity profiles is evident in the graphs but a more satisfactory argument can be based on the data given in Table 9.

Not surprisingly both the wall and interfacial non-dimensional shear stresses decrease as m decreases. However the observation made in the last section, that the wall shear is the greater, is not a universal feature for as $m \longrightarrow m_o$, $(m_o = -0.7633)$, $C_{fw}.Re_x^{1/2}$ tends to zero faster than $C_{fI}\,Re_x^{1/2}$.

Ideally a smaller value of m yielding a lower value of $C_{fw}\,Re_x^{1/2}$ should be given, but when m is near m_o convergence is very slow, and in order to successively reduce the third significant figure in the wall shear by unity it is necessary to reduce m by a quarter of the previous increment in m. This sequence barely changes m and figure 5, with $C_{fw}.Re_x^{1/2}$ plotted against m, shows this behaviour of the wall shear rapidly decreasing over a small range of m.

If a conclusion concerning separation is to be offered it must be then that separation first occurs at the wall, not at the interface, and, because physically acceptable solutions have been found for smaller values of m than in the one phase flow, separation is delayed by the presence of the condensate layer.

Chapter 4

Approximate analytical solutions for the condensation onto the flat plate

Introduction

The object of the present chapter is to develop approximate solutions for the problem of condensation onto the semi-infinite flat plate given a constant vapour mainstream velocity. Parallel research by Hudson [17] has shown that the arguments in this chapter can be applied to the case of condensation onto a rotating disk. This, together with the generalisations which follow (see Chapter 6), enables the method to be offered for use on all problems which admit similar solutions.

From physical reasoning it seems that if the difference between the wall and vapour temperatures is small, then the condensation rate will be slight and in the limit as $\Delta T \to 0$ the condensate layer will disappear and the vapour flow will become the Blasius flow. (The numerical solution for $T_W = 99.99^{\circ}C$. established these facts). The small temperature differences correspond to small values of $\chi = \frac{c_{ps}.\Delta T}{P_s.h_{fg}}$ and it is found that a uniformly valid perturbation expansion in terms of $\chi^{1/3}$ meets all the requirements we make, and the nature of the flow, compared with the numerical solution, is modelled very well for $\Delta T < 1^{\circ}C$. Since in the case of steam-water condensation the largest value attained by χ is approximately 0.2, it might be surprising to find that the results are not in good agreement for the range of wall temperatures $0 \leq T_W < 100^{\circ}C$, but this is the case and the reasons for the limitations will become apparent.

Outside the range of validity of this so called thin film approximation there is the case of appreciable condensation, which because of the ratio of the vapour and condensate densities demands a strong vapour inflow towards the interface. In contrast to the first model, here we have the thick film model which involves a strong suction vapour boundary layer and a perturbation expansion in terms of $(\frac{1}{\lambda^2})$, $\lambda = \left(\frac{\rho_s \mu_s}{\rho_s^* \mu_s^*}\right)^{1/2}$, is found to fit the requirements.

Thin film approximation

The equations governing the forced flow over the flat plate are (3.15)-(3.24) with m = 0. Since we are only seeking an approximation valid for small temperature differences between the wall and the vapour, the condensate will be considered as having constant fluid properties. The equations then simplify to:

Condensate $$f''' + \phi f f'' = 0, \tag{4.1}$$

$$G'' + P_s \phi f G' = 0, \tag{4.2}$$

Vapour $$f^{*'''} + f^* f^{*''} = 0 \tag{4.3}$$

and the boundary conditions become :

$$f(0) = f'(0) = 0, \tag{4.4}$$

$$G(0) = 0, \quad G(1) = 1, \tag{4.5}$$

$$f^{*'}(\infty) = 1. \tag{4.6}$$

Interface conditions: $(\gamma = 1, \eta^* = 0)$.

$$\lambda f(1) = f^*(0), \tag{4.7}$$

$$f'(1) = \phi f^{*'}(0) \tag{4.8}$$

$$f''(1) = \phi^2 f^{*''}(0), \tag{4.9}$$

and $$\chi . G'(1) = \phi f(1). \tag{4.10}$$

In the limit as $\Delta T \to 0$, i.e $\chi \to 0$, then condensation will not occur and the vapour flow will tend to the Blasius flow over the semi-infinite plate. Consequently as $\chi \to 0$ then $f(Y,\chi) \to 0$, $\delta(x) \to 0$ (which implies $\phi(\chi) \to 0$), $f^* = O(1)$ and $\theta = O(1)$.

Therefore let $f = O(\chi^m)$ and $\phi = O(\chi^n)$.

Substitution into the governing equations yields:

from (4.1) $\quad O(1) + O(\chi^{m+n}) = 0$,

(4.2) $\quad O(1) + O(\chi^{m+n}) = 0$,

(4.7) $\quad f^*(0) = O(\chi^m) \to 0$,

(4.8) $\quad f^{*\prime}(0) = O(\chi^{m-n}) \to 0$,

(4.9) $\quad f^{*\prime\prime}(0) = O(\chi^{m-2n}) \to \text{const.}$,

} from the Blasius boundary condtions

(4.10) $\quad \chi = O(\chi^{m+n})$.

From these we conclude $m = {}^2/_3$ and $n = {}^1/_3$.

It is now possible to seek expansions for f, θ, ϕ and f^* as follows :

$$f = \varepsilon^2 f_2 + \varepsilon^3 f_3 + \varepsilon^4 f_4 + \cdots \qquad (4.11)$$

$$\theta = \theta_0 + \varepsilon \theta_1 + \varepsilon^2 \theta_2 + \cdots \qquad (4.12)$$

$$\phi = \varepsilon \phi_1 + \varepsilon^2 \phi_2 + \varepsilon^3 \phi_3 + \cdots \qquad (4.13)$$

$$f^* = f_0^* + \varepsilon f_1^* + \varepsilon^2 f_2^* + \cdots \qquad (4.14)$$

where $\varepsilon = \chi^{1/3}$, so that the limiting form as $\Delta T \to 0$ is the correct one. Substitution of (4.11)-(4.14) into the governing equations (4.1)-(4.10) and the subsequent comparison of coefficients of the various powers of ε yields a series of equations for the functions f_2, θ_0 etc.

Comparing the coefficients of the lowest powers of ε from (4.3), (4.7), (4.8) and (4.6) the function f_o^* is seen to satisfy the equation

$$f_o^{*'''} + f_o^* f_o^{*''} = 0,$$

subject to the conditions

$$f_o^*(0) = f_o^{*'}(0) = 0, \quad f_o^{*'}(\infty) = 1.$$

This will be referred to as the zeroth outer solution, to be denoted by O_0, and it is the desired Blasius flow. This must be solved numerically but it is well known that $f_o^{*''}(0) = A_0 = 0.4696$

Utilising the remaining equations from the basic set in a similar manner, the following are obtained.

From (4.1) $f_2''' = 0,$

(4.2) $\theta_0'' = 0,$

(4.4) $f_2(0) = f_2'(0) = 0,$

(4.5) $\theta_0(0) = 0, \quad \theta_0(1) = 1,$

(4.9) $\phi_1^2 f_o^{*''}(0) = \lambda f_2''(1),$

(4.10) $\theta_0'(1) = \phi_1 f_2(1).$

Since $f_o^{*''}(0)$ is already known, this is a determinate set of equations the solution of which yields the first approximation to the condensate flow. This will be denoted by I_1 and is:

$$\phi_1 = (2\lambda/A_0)^{1/3}, \tag{4.15}$$

I_1: $$f_2 = (A_0/2\lambda)^{1/3} \cdot Y^2, \tag{4.16}$$

$$\theta_0 = Y. \tag{4.17}$$

The first vapour perturbation follows by considering the same equations

from the basic set which were used to find the zeroth approximation but now powers of ε one degree higher are equated.

For O_1 there then result the following:

from (4.3) $$f_1^{*'''} + f_0^* f_1^{*''} + f_0^{*''} f_1^* = 0, \tag{4.21}$$

which is to be solved subject to

$$f_1^*(0) = 0,$$

$$\phi_1 f_1^{*'}(0) + \phi_2 f_0^{*'}(0) = f_2'(1),$$

and $$f_1^{*'}(\infty) = 0.$$

Since $f_0^{*'}(0) = 0$ then ϕ_2 is not needed at this stage, and the second of these boundary conditions becomes $f_1^*(0) = f_2'(1)/\phi_1 = 2(A_0/2\lambda)^{2/3}$.

So that repeated solution of (4.21) is not necessary as λ varies, a change of dependent variable is convenient. Put $f_1^* = 2(A_0/2\lambda)^{2/3} F_1^*$ then the new function satisfies

$$F_1^{*'''} + f_0^* F_1^{*''} + f_0^{*''} F_1^* = 0, \tag{4.22}$$

the boundary condtions for which are

$$F_1^*(0) = 0, \quad F_1^{*'}(0) = 1, \quad F_1^{*'}(\infty) = 0. \tag{4.23}$$

The solution of this is $$F_1^* = f_0^{*'} / f_0^{*''}(0).$$

This satisfies the boundary conditons (4.23) because:

$$F_1^*(0) = f_0^{*'}(0) / f_0^{*''}(0) = 0,$$

$$F_1^{*'}(0) = f_0^{*''}(0) / f_0^{*''}(0) = 1,$$

$$F_1^{*'}(\infty) = f_0^{*''}(\infty) / f_0^{*''}(0) = 0,$$

and the equation (4.22) becomes on substitution:

$$F_1^{*'''} + f_0^* F_1^{*''} + f_0^{*''} F_1^* = \frac{1}{f_0^{*''}(0)} \left\{ f_0^{*iv} + f_0^* f_0^{*'''} + f_0^{*''} f_0^{*'} \right\}$$

$$= \frac{1}{f_0^{*''}(0)} \frac{d}{d\eta^*} \left\{ f_0^{*''} + f_0^* f_0^{*''} \right\} = 0.$$

There then results $F_1^{*''}(0) = \frac{1}{f_0^{*''}(0)} f_0^{*'''}(0) = 0$,

and thus $f_1^{*''}(0) = 0$.

~~It will have been recognised that the method employed is essentially that of inner and outer matched expansions where the vapour flow is the outer region and the condensate the inner.~~ Proceeding then to match the inner flow to that just obtained for the vapour, (4.1), (4.2), (4.4), (4.5), (4.9) and (4.10) yield for I_2:

$$f_3''' = 0,$$
$$\theta_1'' = 0,$$
$$f_3(0) = f_3'(0) = 0,$$
$$\theta_1(0) = \theta_1(1) = 0,$$
$$2\phi_1\phi_2 f_0^{*''}(0) + \phi_1^2 f_1^{*''}(0) = \lambda f_3''(1),$$

and $$\theta_1'(1) = \phi_1 f_3(1) + \phi_2 f_2(1).$$

Introducing the known values of ϕ_1, $f_0^{*''}(0)$, $f_1^{*''}(0)$ and $f_2(1)$ there results:

$$I_2: \qquad f_3 \equiv \theta_1 \equiv \phi_2 \equiv 0. \tag{4.25}$$

The next approximation to the vapour flow is obtained by continuing the matching technique to derive the governing equation for the function f_2^* which is:

$$f_2^{*'''} + f_0^* f_2^{*''} + f_2^* f_0^{*''} + f_1^* f_1^{*''} = 0. \tag{4.26}$$

The boundary conditions for this are:

$$f_2^{*'}(\infty) = 0,$$
$$f_2^*(0) = \lambda f_2(1) = \lambda (A_0/2\lambda)^{1/3},$$

and $$\phi_3 f_0^{*'}(0) + \phi_2 f_1^{*'}(0) + \phi_1 f_2^{*'}(0) = f_3'(1).$$

On substitution of the known values for $f_0^{*\prime}(0)$, ϕ_2, $f_1^{*\prime}(0)$, ϕ_1 and $f_3'(1)$ this last equation becomes

$$f_2^{*\prime}(0) = 0.$$

Setting $A_2 = f_2^{*\prime\prime}(0)$ it must be noted that A_2 is dependent upon λ. For the case of steam-water condensation $\lambda = 190.2$, $A_2 = 14.76$ and the function f_2^* is displayed in Figure 6. For completeness this figure also displays f_0^* and f_1^*.

Returning to the condensate phase the next terms in the expansions for f, G and ϕ involve f_4, θ_2, ϕ_3 and these are found to satisfy:

$$f_4''' = 0, \quad \theta_2'' = 0,$$

under the conditions

$$f_4(0) = f_4'(0) = 0,$$

$$\theta_2(0) = \theta_2(1) = 0,$$

$$(\phi_2^2 + 2\phi_1\phi_3) f_0^{*\prime\prime}(0) + 2\phi_1\phi_2 f_1^{*\prime\prime}(0) + \phi_1^2 f_2^{*\prime\prime}(0) = \lambda f_4''(1),$$

and $$\theta_2'(1) = \phi_1 f_4(1) + \phi_2 f_3(1) + \phi_3 f_2(1).$$

The solution of this set is

$$I_3: \quad f_4 = \frac{A_2}{6\lambda}\left(\frac{2\lambda}{A_0}\right)^{2/3} y^2,$$

$$\phi_3 = -\frac{A_2}{3A_0}\left(\frac{2\lambda}{A_0}\right)^{1/3},$$

$$\theta_2 = 0. \qquad (4.27)$$

It is now possible to write down appropriate formulae for $\frac{\delta(x)}{x} Re_x^{1/2}$ Cfw. $Re_x^{1/2}$ and Nu. $Re_x^{-1/2}$.

$$\frac{\delta(x)}{x} Re_x^{1/2} = \sqrt{2}\,\phi_0 \int_0^1 \frac{\rho_s}{\rho}\, dy = \sqrt{2}\,\phi,$$

since the thin film model is assumed to have constant fluid properties,

$$\text{therefore} \quad \frac{\delta(x)}{x}.Re_x^{1/2} = \sqrt{2}.\left(\frac{2\lambda\chi}{A_0}\right)^{1/3} - \frac{\sqrt{2}\,A_2}{3\,A_0}\left(\frac{2\lambda}{A_0}\right)^{1/3}\chi + O(\chi^{4/3}). \qquad (4.28)$$

$$C_{fw}.Re_x^{1/2} = \frac{\mu_w\left(\frac{\partial u}{\partial y}\right)_{y=0}}{\frac{1}{2}\rho_s u_0^2}\left(\frac{u_0 x}{\nu_s}\right)^{1/2} = \frac{\sqrt{2}.}{\phi^2}f''(0)$$

$$= \frac{\sqrt{2}}{\phi_1^2}\{f_2''(0) + \varepsilon^2 f_4''(0)+\cdots\}.\{1-2\varepsilon^2\phi_3/\phi_1+\cdots\}$$

$$\text{Hence} \quad C_{fw}.Re_x^{1/2} = \frac{\sqrt{2}.A_0}{\lambda} + \left[\sqrt{2}.\frac{A_2}{\lambda}\right]\chi^{2/3} + O(\chi). \qquad (4.29)$$

$$Nu.Re_x^{-1/2} = \frac{x}{\Delta T.}\left(\frac{\partial T}{\partial y}\right)_{y=0}.\left(\frac{u_0 x}{\nu_s}\right)^{-1/2} = G'(0)/\sqrt{2}\phi.$$

$$= \frac{1}{\sqrt{2}\,\phi_1\,\varepsilon}\{\theta_0'(0)+\cdots\}.\{1-\varepsilon^2\phi_3/\phi_1+\cdots\}$$

$$Nu.Re_x^{-1/2} = \frac{1}{\sqrt{2}}\left(\frac{A_0}{2\lambda\chi}\right)^{1/3} + \frac{A_2\chi^{1/3}}{3\sqrt{2}\,A_0}\left(\frac{A_0}{2\lambda}\right)^{1/3} + O(\chi^{2/3}). \qquad (4.30)$$

The merits of the thin film approximation are considered now by comparing the results for steam-water condensation given by the model with those derived by the numerical procedure of Chapter 3. Table 10 shows these results for T_W = 99.99, 99.9, 99.5, 99 and 98°C. and we deduce that the model is extremely accurate in the first case but that the precision is

is not maintained even when $T_W = 99°C$. This may be a little surprising because the value of $\chi^{1/3}$ is small in each instance ($\chi^{1/3} = 0.0109$ when $T_W = 99.99$ and $\chi^{1/3} = 0.1025$ when $T_W = 99$). Indeed when dealing with steam-water condensation the maximum value attained by χ is $\chi = 0.1077$ ($\chi^{1/3} = 0.4757$) when $T_W = 0°C$, so that convergence of the expressions (4.28), (4.29) and (4.30) might be expected throughout the range $0 \leq T_W < 100°C$.

~~The limitations however become clear if we look at the assumptions made in the formulation of the zeroth order boundary condition $f_0^*(0) = 0$. The result of substituting (4.11) and (4.14) into (4.7) is~~

$$\lambda \varepsilon^2 f_2(1) = f_0^*(0),$$

~~so that the condition $f_0^*(0) = 0$ only holds if $\lambda \varepsilon^2 f_2(1) \ll 1$. Now the thin film approximation yields $f_2(1) = (A_0/2\lambda)^{1/3}$ so that $\lambda \varepsilon^2 f_2(1) = \lambda^{2/3} \varepsilon^2 (\frac{1}{2} A_0)^{1/3}$ and the boundary condtion can only be valid if $\lambda^{1/3} \varepsilon = (\lambda\chi)^{1/3} \ll 1$. In the case of steam-water condensation this demands $\Delta T \ll 4°C$, which is compatible with the observation made above.~~

If one accepts that the model displays all the characteristics of condensation for this range of T_W it is possible to make several further deductions from noting that the shear on the interface is dependent on $f^{*\,\prime\prime}(0)$, the tangential vapour velocity at the interface on $f^{*\,\prime}(0)$ and the normal velocity on $f^*(0)$.

The model has been constructed so that in the limit as $T_W \to 100°C$. condensation will not occur and the vapour flow then becomes the Blasius flow. The zeroth order solution, given by f_0^*, is the Blasius solution, so $f_0^{*\,\prime\prime}(0)$ is known from the one phase flow ($f_0^{*\,\prime\prime}(0) = 0.4696$).

The first condensate approximation, I_1, involves only λ (which is a fluid property) and $f_0^{*\,\prime\prime}(0)$, so can be determined with just the solution

of the one phase flow over the plate, an observation which will be greatly utilised later. Physically the condensate, to the first approximation, is driven by the interfacial shear.

Moving back to the vapour phase, the first amendment is given by f_1^*, and since $f_1^*(0) = f_1^{*\prime\prime}(0) = 0$ and $f_1^{*\prime}(0) \neq 0$ the deduction is made that only the tangential velocity at the interface is modified to match that of the first condensate approximation.

This has no effect on the inner flow (4.25) and it is in the second approximation to the vapour that the inflow and shear stress at the interface are altered, both $f_2^*(0)$ and $f_2^{*\prime\prime}(0)$ being non-zero.

A further observation is that no account has yet been taken of the inertia terms in the condensate phase.

At this stage it is possible to confirm that Cess' model for this problem is correct when ΔT is small. In fact his formulae for $Cf_W\, Re_x^{\frac{1}{2}}$ and $Nu.Re_x^{-\frac{1}{2}}$ in this range are identical to the first terms of (4.29) and (4.30) respectively.

However having only one term in each series Cess concluded that the rate of change of $Cf_W.Re_x^{\frac{1}{2}}$ with ΔT, as $\Delta T \to 0$ is zero, whereas the correct limiting form is only apparent when the second term is available.

When the thin film model is applied to other problems far more fundamental errors than the foregoing can be exposed. For example it has been shown by Hudson [17] that a thin film model, applied to the problem of condensation onto a rotating disk, pinpointed the flaw in the basic assumptions made by Sparrow and Gregg [16], particularly their assumptions on the effects of interfacial shear.

The thick film approximation

An essential feature of the thin film approximation is the slight condensation rate and the thin liquid layer. At the other end of the range of possible wall temperatures, i.e. when $\Delta T/T_s = O(1)$, appreciable condensation is to be expected, which, because of the small ratio of vapour to liquid density, requires a large vapour inflow at the interface. Although physically the liquid layer is of course still thin, an expansion referred to as the thick film approximation is now constructed based on the concept of a strong suction vapour boundary layer.

With λ as a convenient large parameter involving the ratio of vapour and liquid properties, new suction boundary layer variables for the vapour flow are introduced:

$$\eta^* = \frac{1}{\lambda} y^*, \quad f^* = \lambda F^*. \tag{4.31}$$

It has been established in Chapter 3 that account must be taken of the variation in fluid properties when $T_W \sim 0^\circ C$, so the full forms of (3.15)-(3.23), with m = 0, are used here. Introducing (4.31) the basic equations become:

$$\left(\frac{\rho\mu}{\rho_s\mu_s} f''(y)\right)' + \phi f(y) f''(y) = 0, \tag{4.32}$$

$$\left(\frac{\rho k}{\rho_s k_s} G'(y)\right)' + \phi P_s \frac{c_p}{c_{ps}} f(y) G'(y) = 0, \tag{4.33}$$

and

$$\frac{d^3F^*}{dy^{*3}} + F^* \frac{d^2F^*}{dy^{*2}} = 0. \tag{4.34}$$

The boundary conditions are:

when $Y = 0$; $f = f' = 0$, $G = 0$ (4.35)

when $Y = 1$, $Y^* = 0$; $G = 1$. (4.36)

$$F^*(0) = f(1), \tag{4.37}$$

$$\phi F^{*\prime}(0) = \frac{1}{\lambda^2} f'(1), \tag{4.38}$$

$$\phi^2 F^{*\prime\prime}(0) = \frac{1}{\lambda^2} f''(1), \tag{4.39}$$

and $$\phi f(1) = \chi G'(1) \tag{4.40}$$

and as $Y^* \to \infty$ $F^{*\prime}(Y^*) \to 1/\lambda^2$. (4.41)

Compatible asymptotic expansions for the condensate and vapour phases are

$$f(Y) = F_0(Y) + \frac{1}{\lambda^2} F_2(Y) + \cdots, \tag{4.42}$$

$$G(Y) = H_0(Y) + \frac{1}{\lambda^2} H_2(Y) + \cdots, \tag{4.43}$$

$$\phi = \Phi_0 + \frac{1}{\lambda^2} \Phi_2 + \cdots, \tag{4.44}$$

and $$F^*(Y^*) = F_0^*(Y^*) + \frac{1}{\lambda^2} F_2^*(Y^*) + \cdots. \tag{4.45}$$

Substitution of (4.45) into (4.34) yields the following governing equation for F_0^* ;

$$F_0^{*\prime\prime\prime} + F_0^* F_0^{*\prime\prime} = 0,$$

and into (4.38), (4.39) and (4.41) yields the boundary conditions :

$$F_0^{*\prime}(0) = F_0^{*\prime\prime}(0) = F_0^{*\prime}(\infty) = 0.$$

Hence the solution for F_o^* is

$$F_o^*(y^*) = S^*, \tag{4.45}$$

where S^* is an arbitrary suction parameter.

Comparison of the coefficients of $\frac{1}{\lambda^2}$ when (4.45) is substituted in (4.34) gives

$$F_2^{*\,'''} + F_2^* F_o^{*\,''} + F_2^{*\,''} F_o^* = 0,$$

and introducing (4.45) this becomes

$$F_2^{*\,'''} + S^* F_2^{*\,''} = 0. \tag{4.46}$$

Integrating (4.46) twice then we have

$$F_2^{*\,'}(y^*) = A^* + B^* e^{-S^* y^*}.$$

Comparison of the coefficients of $\frac{1}{\lambda^2}$ in (4.41) yields

$$F_2^{*\,'}(\infty) = 1,$$

which demands $A^* = 1$, so that

$$F_2^{*\,'}(y^*) = 1 + B^* e^{-S^* y^*}. \tag{4.47}$$

Attention must now be turned to the condensate phase for which the zeroth order solutions follow from (4.32) and (4.33). They are

$$\left(\frac{\rho\mu}{\rho_s \mu_s} F_o''\right)' + \Phi_o F_o F_o'' = 0, \tag{4.48}$$

and

$$\left(\frac{\rho k}{\rho_s k_s} H_o'\right)' + P_s \frac{C_p}{C_{ps}} \Phi_o F_o H_o' = 0. \tag{4.49}$$

These must be solved subject to:

$$F_0(0) = F_0'(0) = 0, \quad H_0(0) = 0, \quad H_0(1) = 1,$$

$$F_0(1) = S^*,$$

$$F_0'(1) = \Phi_0 F_2^{*\prime}(0) = \Phi_0 (1 + B^*), \tag{4.50}$$

$$F_0''(1) = \Phi_0^2 F_2^{*\prime\prime}(0) = \Phi_0^2 (-B^* S^*),$$

and $$\Phi_0 F_0(1) = \chi H_0'(1).$$

Alternatively the constants B^* and S^* can be eliminated from (4.50) and we are left with the six boundary conditions:

$$F_0(0) = F_0'(0) = 0, \quad H_0(0) = 0, \quad H_0(1) = 1,$$

$$\chi H_0'(1) = \Phi_0 F_0(1), \tag{4.51}$$

and $$F_0''(1) = \Phi_0 F_0(1) (\Phi_0 - F_0'(1)).$$

The equations (4.48) and (4.49) are solved numerically subject to (4.51) and this solution is referred to as the first term of the full thick film approximation. The relevant characteristics ϕ, $f''(0)$ and $G'(0)$ are compared in Table 11 with the exact numerical solutions obtained in Chapter 3. Agreement with the exact values is excellent in the range $0 \leq T_W < 60^\circ C$ and even when $T_W = 90^\circ C$ the error in ϕ is only about 7 per cent.

The thick film approximation has been developed on the assumption that λ is large but has in no way utilised the fact that $\chi < 1$ for $0 \leq T_W < 100^\circ C$. The aim now is to find the limiting form of the system (4.48), (4.49) and (4.51) as $\chi \to 0$.

The required expansions for the unknowns of the first term of the full thick film approximation are:

$$F_0 = \chi \tilde{f} + \cdots , \quad H_0 = \tilde{H} + \cdots , \quad \Phi_0 = \tilde{\Phi} + \cdots ,$$
$$B^* = -1 + B\chi + \cdots , \quad S^* = \chi \tilde{S} + \cdots . \tag{4.52}$$

Substituting these into (4.48) and (4.49) then the functions f and $\tilde{H}$ are found to satisfy,

$$\left(\frac{\rho\mu}{\rho_s \mu_s} \tilde{f}''\right)' = 0 \quad (4.53); \qquad \left(\frac{\rho k}{\rho_s k_s} \tilde{H}'\right)' = 0 , \quad (4.54).$$

The boundary conditions (4.51) yield ;

$$\tilde{f}(0) = \tilde{f}'(0) = 0, \quad \tilde{H}(0) = 0, \quad \tilde{H}(1) = 1,$$
$$\tilde{f}(1) = \tilde{S}, \quad \tilde{f}'(1) = B\tilde{\Phi} , \quad \tilde{f}''(1) = \tilde{\Phi}^2 \tilde{S} , \tag{4.55}$$
$$\text{and} \quad \tilde{\Phi} \tilde{f}(1) = \tilde{H}(1).$$

Numerical solution of this system using the variable properties described in Appendix A presents no problems, however complete analytical solution is possible if the fluid properties are approximated as follows:

$$\rho = \rho_s , \quad c_p = c_{ps},$$
$$k = k_w + (k_s - k_w)\tilde{H} , \quad \frac{1}{\mu} = \frac{1}{\mu_w} + \left(\frac{1}{\mu_s} - \frac{1}{\mu_w}\right)\tilde{H} . \tag{4.56}$$

Assuming the density remains constant (4.54) gives

$$\frac{d\tilde{H}}{dY} = E \frac{k_s}{k}, \tag{4.57}.$$

where E is a constant. Hence we have,

$$E.Y = \int_0^{\tilde{H}} \frac{k}{k_s}\, d\tilde{H} ,$$

and since $\tilde{H}(1) = 1$ the constant E is given by

$$E = \int_0^{1} \frac{k}{k_s}\, d\tilde{H} . \qquad (4.58)$$

To the same approximation (4.53) yields

$$\frac{\mu}{\mu_s} \frac{d^2\tilde{f}}{dy^2} = D , \qquad (4.59)$$

where D is a constant, and upon changing from Y to $\tilde{H}$ as the independent variable, using (4.57), it follows that:

$$E.\frac{k_s}{k} \frac{d}{d\tilde{H}} \left(E \frac{k_s}{k} \frac{d\tilde{f}}{d\tilde{H}} \right) = D \frac{\mu_s}{\mu} . \qquad (4.60)$$

Hence we obtain

$$\tilde{f} = \frac{D}{E^2} \int_0^{\tilde{H}} \frac{k}{k_s} \left[\int_0^{\tilde{H}} \frac{\mu_s k}{\mu k_s}\, d\tilde{H} \right] d\tilde{H} . \qquad (4.61)$$

The conditions from (4.55) which remain to be satisfied are

$$\tilde{f}(1) = \tilde{S} , \quad \tilde{f}'(1) = \tilde{B}\,\tilde{\Phi} , \quad \tilde{f}''(1) = \tilde{\Phi}^2 \tilde{S} , \quad \tilde{\Phi} f(1) = \tilde{H}'(1) ,$$

from which are obtained

$$\tilde{f}''(1) = \tilde{\Phi}^2 \tilde{f}(1) \quad \text{and} \quad \tilde{\Phi} f(1) = \tilde{H}'(1)$$

$$\text{or} \quad \tilde{f}''(1) = \tilde{\Phi}\, \tilde{H}'(1) \quad \text{and} \quad \tilde{\Phi}\, \tilde{f}(1) = \tilde{H}'(1) . \qquad (4.62)$$

Then substituting from (4.59) and (4.57) we have

$$D = \tilde{\Phi} E , \qquad (4.63)$$

and from (4.62) and (4.57)

$$\tilde{\Phi}\,\frac{D}{E^2}\,\frac{\varepsilon_p^2}{2} = E\,, \tag{4.64}$$

where $$\varepsilon_p^2 = 2\int_0^1 \frac{k}{k_s}\left[\int_0^{\tilde{H}} \frac{\mu_s k}{\mu k_s}\, d\tilde{H}\right] d\tilde{H}\,. \tag{4.65}$$

The integrals (4.58) and (4.65) are analagous to those obtained by Voskresenskiy [23] when modifying Nusselt's theory to account for the variation in the physical properties throughout the condensate. Labuntsov [24] used (4.56) to evaluate the integrals approximately. Using analysis similar to that employed by Labuntsov then we have on substituting (4.56) into (4.58) and (4.65):

$$E = (k_s + k_w)/2k_s\,,$$

$$\varepsilon_p = \left\{\left(8 + 9\frac{k_w}{k_s} + 3\frac{k_w^2}{k_s^2} + \frac{\mu_s}{\mu_w}\left[7 + 21\frac{k_w}{k_s} + 12\frac{k_w^2}{k_s^2}\right]\right)/60\right\}^{1/2}. \tag{4.66}$$

For the case of steam-water condensation these quantities, evaluated for $T_w = 0(10)90^\circ C$, are given in table 12.

From (4.63) and (4.64) D and $\tilde{\Phi}$ are given in terms of E and ε_p by:

$$D = \sqrt{2}\,E^2/\varepsilon_p\,, \qquad \tilde{\Phi} = \sqrt{2}\,E/\varepsilon_p. \tag{4.67}$$

Any desired information can now be deduced for the thick film model, and in particular expressions for ϕ, $C_{fw}\,Re_x^{1/2}$ and $Nu.Re_x^{-1/2}$ are available.

$$C_{fw}.Re_x^{1/2} = \frac{\mu_w}{\mu_s}.\sqrt{2}\,\frac{f''(0)}{\phi^2} = \chi\varepsilon_p ,$$

$$Nu.Re_x^{-1/2} = \frac{1}{\sqrt{2}.\phi}\,G'(0) = \frac{k_s}{k_w}.\frac{\varepsilon_p}{2} \qquad (4.68)$$

and $\phi = \sqrt{2}.E/\varepsilon_p$ or $\frac{\delta(x)}{x}.Re_x^{1/2} = 2E/\varepsilon_p$.

In table 13 comparison is made between these approximate formulae and the exact results for steam-water condensation. The agreement is excellent for $0 \leq T_W < 60^\circ C$ and ϕ is within 10 per cent when $T_W = 90^\circ C$. When $\Delta T < 10^\circ C$ accuracy is soon lost, and in particular the limiting form as $\chi \to 0$ is invalid because (4.68) predicts $\phi \to \sqrt{2}$ whereas the correct limit, given by the thin film approximation, is $\phi \to 0$.

The loss in accuracy as $\chi \to 0$ may be surprising considering the formulae (4.68) are the result of finding a perturbation expansion in terms of χ. The reason is illustrated in figure 7, where the variation of ϕ with ΔT is displayed. When $\Delta T > 40^\circ C$ the form of ϕ, say ϕ_n, given by the numerical solution agrees well with, ϕ_T say, the form predicted by the first term of the full thick film approximation. However as $\Delta T \to 0$ the agreement is lost ($\phi_n \to 0$ and $\phi_T \to \sqrt{2}$) because the basic assumption that a strong vapour boundary layer exists is no longer true. The limiting solution, $\phi_{T,\chi}$ say, as $\chi \to 0$ is seen in figure 7 to be in good agreement with ϕ_T for $0 \leq T_W < 100^\circ C$, but since ϕ_T itself is not a valid solution for $\Delta T \sim 0^\circ C$ then $\phi_{T,\infty}$ cannot be expected to agree with ϕ_n in this region.

The solution given by Cess of this problem also utilises the concept of a suction boundary layer and includes a limiting form equivalent to (4.68). Indeed if variable condensate properties are excluded from the

thick film approximation then $E = \varepsilon_p = 1$, and the simplified formulae would be the same as those given by Cess. In the author's opinion however the current method is of greater value in four ways. Firstly no knowledge is needed of the corresponding single phase problem, secondly the physical assumptions are minimised, thirdly the model can be readily extended and finally it is more accurate, as it takes account of variable condensate properties.

Conclusions

It has been established that analytical formulae can be obtained for all the physically interesting coefficients, and these are in excellent agreement with the results of direct numerical integration.

This evidence justifies extending the ideas to non-~~singular~~ similar flows and thus avoiding the problems of solving coupled non-linear partial differential equations with an unknown interface.

Chapter 5

Numerical solution of non-similar condensation problems

Introduction

The aim of the present chapter is to find solutions of equations (2.28)-(2.38) when the form of $u_m^*(x)$ is such that similar solutions do not exist. Two examples are considered, firstly $u_m^*(x) = u_0^*(1-\frac{1}{8}\frac{x}{c})$, which represents a linearly retarded flow over a semi-infinite plate, and secondly $u_m^*(x) = u_0^* \sin(\frac{x}{c})$ which is the potential flow past a circular cylinder.

Both of these configurations have been extensively studied for a one phase flow and many extensions to two phase problems occurring in condensation are no doubt possible, albeit with considerable complications. However since no information is to hand concerning these condensation problems attention will be focused on the basic description of the flow, particularly in regions of adverse pressure gradient where the nature of separation in condensing fluids will be discussed. An important question which will be answered is: "Does condensation delay separation and where does separation first occur, at the wall or at the interface?"

Transformation of equations into forms suitable for numerical techniques

The governing equations were introduced in Chapter 2 and simplified by introducing the stream functions ψ and ψ^* and the non-dimensional temperature

$$\theta = (T - T_w) / (T_s - T_w).$$

There resulted the following equations:

Condensate: $(x \geqslant 0, \quad 0 \leq y_1 \leq \Delta(x))$

$$\frac{\partial \psi}{\partial y_1}\frac{\partial^2 \psi}{\partial x \partial y_1} - \frac{\partial \psi}{\partial x}\frac{\partial^2 \psi}{\partial y_1^2} = \frac{\rho_s^*}{\rho} u_m^* \frac{d u_m^*}{d x} + \frac{1}{\rho_s}\frac{\partial}{\partial y_1}\left(\frac{\rho \mu}{\rho_s}\frac{\partial^2 \psi}{\partial y_1^2}\right), \tag{5.1}$$

$$C_p\left(\frac{\partial \psi}{\partial y_1}\frac{\partial \theta}{\partial x} - \frac{\partial \psi}{\partial x}\frac{\partial \theta}{\partial y_1}\right) = \frac{1}{\rho_s}\frac{\partial}{\partial y_1}\left(\frac{\rho k}{\rho_s}\frac{\partial \theta}{\partial y_1}\right), \tag{5.2}$$

Vapour: $(x \geqslant 0, \quad 0 \leq y^* \leq \infty)$.

$$\frac{\partial \psi^*}{\partial y^*}\frac{\partial^2 \psi^*}{\partial x \partial y} - \frac{\partial \psi^*}{\partial x}\frac{\partial^2 \psi^*}{\partial y^{*2}} = u_m^* \frac{d u_m^*}{d x} + v_s^* \frac{\partial^3 \psi^*}{\partial y^{*3}}. \tag{5.3}$$

Boundary conditions:

$$\psi = \frac{\partial \psi}{\partial y_1} = 0, \quad y_1 = 0, \; x \geqslant 0, \tag{5.4}$$

$$\theta = 0, \; y_1 = 0; \quad \theta = 1, \; y_1 = \Delta(x). \tag{5.5}$$

$$\frac{\partial \psi^*}{\partial y^*} \longrightarrow u_m^*(x) \quad \text{as} \quad y^* \to \infty, \tag{5.6}$$

$$\left[\frac{\partial \psi}{\partial y}\right]_{y_1 = \Delta(x)} = \left[\frac{\partial \psi^*}{\partial y^*}\right]_{y^* = 0}, \tag{5.7}$$

$$\mu_s \left[\frac{\partial^2 \psi}{\partial y_1^2}\right]_{y_1=\Delta(x)} = \mu_s^* \left[\frac{\partial^2 \psi^*}{\partial y^{*2}}\right]_{y^*=0}, \tag{5.8}$$

$$\rho_s \left[\psi\right]_{y_1=\Delta(x)} = \rho_s^* \left[\psi^*\right]_{y^*=0}, \tag{5.9}$$

and the integrated form of the energy balance

$$\Delta T.\, k_w \int_0^x \frac{\rho}{\rho_s}\left(\frac{\partial \theta}{\partial y_1}\right)_{y_1=0} dx = \int_0^{\Delta(x)} \left[\rho_s h_{fg} + C_{ps} T_s - C_p . T\right] \frac{\partial \psi}{\partial y_1} . dy_1 . \tag{5.10}$$

In the condensate phase the stream function is taken in the form;

$$\psi = \left(\frac{2 \mu_s \mu_0^* \xi^{m+1}}{(m+1) \rho_s c^m}\right)^{1/2} F(\xi, \eta), \tag{5.11}$$

where $$\xi = x \quad \text{and} \quad \eta = \left(\frac{(m+1) \rho_s \mu_0^* \xi^{m-1}}{2 \mu_s c^m}\right)^{\frac{1}{2}} y_1 . \tag{5.12}$$

The flat plate problem is solved by taking m = 0 and that for the cylinder by taking m = 1. The seemingly unnecessary introduction of the factor (m + 1) occurs because the analysis for the two problems was initially done independently and it is now desirable to unify the approach.

Introducing (5.11) and (5.12) into (5.1) and (5.2) then the differential equations for the condensate layer become:

$$\frac{\partial}{\partial\eta}\left(\frac{\rho\mu}{\rho_s\mu_s}\frac{\partial^2F}{\partial\eta^2}\right) + F\frac{\partial^2F}{\partial\eta^2} - \frac{2m}{(m+1)}\left(\frac{\partial F}{\partial\eta}\right)^2$$

$$+ \frac{2\xi}{(m+1)}\left\{\frac{\partial F}{\partial\xi}\frac{\partial^2F}{\partial\eta^2} - \frac{\partial F}{\partial\eta}\frac{\partial^2F}{\partial\xi\partial\eta}\right\} + \frac{2\xi}{(m+1)}\frac{\rho_s^*}{\rho}\left(\frac{c}{\xi}\right)^{2m}\frac{u_{in}^*(\xi)}{u_0^*}\frac{d\left(\frac{u_{in}^*(\xi)}{u_0^*}\right)}{d\xi} = 0, \quad (5.13)$$

and $$\frac{\partial}{\partial\eta}\left(\frac{\rho k}{\rho_s k_s}\frac{\partial\theta}{\partial\eta}\right) + P_s\frac{C_p}{C_{p_s}}F\frac{\partial\theta}{\partial\eta} + P_s\frac{C_p}{C_{p_s}}\frac{2\xi}{(m+1)}\left\{\frac{\partial F}{\partial\xi}\frac{\partial\theta}{\partial\eta} - \frac{\partial F}{\partial\eta}\frac{\partial\theta}{\partial\xi}\right\} = 0. \quad (5.14)$$

The boundary conditions (5.4) yield;

$$F(\xi,0) = \frac{\partial F}{\partial\eta}(\xi,0) = 0, \quad (5.15)$$

and the equation of the interface will be denoted by

$$\eta = t(x). \quad (5.16)$$

The vapour layer is treated in a similar manner introducing ψ^* as:

$$\psi^* = \left(\frac{2\nu_s^* u_0^* \xi^{m+1}}{(m+1)c^m}\right)^{1/2} F^*(\xi,\eta^*), \quad (5.17)$$

where $$\xi = x, \quad \eta^* = \left(\frac{(m+1)u_0^*\xi^{m-1}}{2\nu_s^* c^m}\right)^{1/2} y^*. \quad (5.18)$$

Hence we obtain:

$$u^* = \frac{\partial\psi^*}{\partial y^*} = u_0^*\left(\frac{\xi}{c}\right)^m \frac{\partial F^*}{\partial\eta^*},$$

$$v^* = -\left(\frac{2u_0^*\nu_s\xi^{m-1}}{(m+1)c^m}\right)^{1/2}\left\{\frac{1}{2}(m+1)F^* + \xi\frac{\partial F^*}{\partial\xi} + \frac{(m-1)}{2}\eta^*\frac{\partial F^*}{\partial\eta^*}\right\}; \quad (5.19)$$

and the boundary condition (5.6) becomes:

$$\left(\frac{\partial F^*}{\partial \eta^*}\right) \longrightarrow \left(\frac{c}{\xi}\right)^m \frac{u_m^*(\xi)}{u_0^*} \quad \text{as} \quad \eta^* \longrightarrow \infty. \tag{5.20}$$

Introducing (5.17) and (5.18) into the vapour momentum equation (5.3) gives:

$$\frac{\partial^3 F^*}{\partial \eta^{*3}} + F^* \frac{\partial^2 F^*}{\partial \eta^{*2}} - \frac{2m}{(m+1)} \left(\frac{\partial F^*}{\partial \eta^*}\right)^2 +$$

$$+ \frac{2\xi}{(m+1)} \left(\frac{\partial F^*}{\partial \xi} \frac{\partial^2 F^*}{\partial \xi \partial \eta^*} - \frac{\partial F^*}{\partial \eta^*} \frac{\partial^2 F^*}{\partial \xi \partial \eta^*} \right) + \frac{2\xi}{(m+1)} \left(\frac{c}{\xi}\right)^{2m} \frac{u_m^*(\xi)}{u_0^*} \frac{d}{d\xi} \left(\frac{u_m^*(\xi)}{u_0^*} \right) = 0. \tag{5.21}$$

At the interface $(\eta = t(\xi) , \eta^* = 0)$ we have

$$\left(\frac{\rho_s \mu_s}{\rho_s^* \mu_s^*}\right)^{1/2} F(\xi, t(\xi)) = F^*(\xi, 0), \tag{5.22}$$

$$\left(\frac{\partial F}{\partial \eta}\right)_{(\xi, t(\xi))} = \left(\frac{\partial F^*}{\partial \eta^*}\right)_{(\xi, 0)}, \tag{5.23}$$

$$\left(\frac{\rho_s \mu_s}{\rho_s^* \mu_s^*}\right)^{1/2} \left(\frac{\partial^2 F}{\partial \eta^2}\right)_{(\xi, t(\xi))} = \left(\frac{\partial^2 F^*}{\partial \eta^{*2}}\right)_{(\xi, 0)}, \tag{5.24}$$

and finally the energy balance transforms to give;

$$\left(\frac{\rho_w k_w}{\rho_s k_s}\right) \cdot \frac{1}{P_s} \left(\frac{m+1}{2}\right) \cdot \xi^{-\frac{1}{2}(m+1)} \int_0^{\xi} \xi^{\frac{1}{2}(m-1)} \left(\frac{\partial \theta}{\partial \eta}\right)_{\eta=0} d\xi$$

$$= \int_0^{t(\xi)} \left\{ \frac{h_{fg}}{c_{ps} \cdot \Delta T} + \frac{T_s}{\Delta T} - \frac{c_p}{c_{ps}} \cdot \frac{T_\infty}{\Delta T} \right\} \frac{\partial F}{\partial \eta} \, d\eta. \tag{5.25}$$

An awkward feature of programming these equations involves the non-constant condensate thickness $t(\xi)$. This difficulty is overcome by making one more change of independent variable;

$$X = \xi \quad , \quad Y = \eta / t(\xi) . \tag{5.26}$$

This fixes the range of integration across the condensate layer as $[0,1]$ and casts the unknown function $t(x)$ into the differential equations, which become the following.

Summary of Equations

Condensate phase

$$\frac{\partial}{\partial y}\left(\frac{\rho\mu}{\rho_s \mu_s}\frac{\partial^2 F}{\partial y^2}\right) + t(x).F\frac{\partial^2 F}{\partial y^2} - \frac{2m}{(m+1)}t(x)\left(\frac{\partial F}{\partial y}\right)^2 + \frac{2x}{(m+1)}t(x)^3\frac{\rho_s^*}{\rho}\left(\frac{c}{x}\right)^{2m}\frac{u_m^*}{u_0^*}\frac{d}{dx}\left(\frac{u_m^*}{u_0^*}\right)$$

$$+ \frac{2x}{(m+1)}t(x).\left\{\frac{\partial F}{\partial x}\frac{\partial^2 F}{\partial y^2} - \frac{\partial F}{\partial y}\frac{\partial^2 F}{\partial x \partial y}\right\} + \frac{2x}{(m+1)}\frac{dt}{dx}\left(\frac{\partial F}{\partial y}\right)^2 = 0 , \tag{5.27}$$

$$\frac{\partial}{\partial y}\left(\frac{\rho k}{\rho_s k_s}\frac{\partial \theta}{\partial y}\right) + t(x).\frac{c_p}{c_{ps}}.P_s F\frac{\partial \theta}{\partial y} + \frac{c_p}{c_{ps}}.P_s.t(x)\left\{\frac{\partial F}{\partial x}\frac{\partial \theta}{\partial y} - \frac{\partial F}{\partial y}\frac{\partial \theta}{\partial x}\right\} = 0 . \tag{5.28}$$

Vapour phase, (putting $X = \xi$, $Y^* = \eta^*$),

$$\frac{\partial^3 F^*}{\partial y^{*3}} + F^*\frac{\partial^2 F^*}{\partial y^{*2}} - \frac{2m}{(m+1)}\left(\frac{\partial F^*}{\partial y^*}\right)^2 + \frac{2x^*}{(m+1)}\left\{\frac{\partial F^*}{\partial x}\frac{\partial^2 F^*}{\partial y^{*2}} - \frac{\partial F^*}{\partial y^*}\frac{\partial^2 F^*}{\partial x \partial y^*}\right\}$$

$$+ \frac{2x}{(m+1)}\left(\frac{c}{x}\right)^{2m}\frac{u_m^*(x)}{u_0^*}\frac{d}{dx}\left(\frac{u_m^*(x)}{u_0^*}\right) = 0 . \tag{5.29}$$

At the body surface , $Y = 0$, $X \geq 0$,

$$F = \frac{\partial F}{\partial Y} = 0 \quad , \quad \theta = 0 . \tag{5.30}$$

the interfacial conditions are, (Y = 1, Y* = 0),

$$\theta = 1 , \tag{5.31}$$

$$\left(\frac{\rho_s \mu_s}{\rho_s^* \mu_s^*}\right)^{1/2} \frac{1}{t(x)^2} \frac{\partial^2 F}{\partial Y^2} = \frac{\partial^2 F^*}{\partial Y^{*2}} , \tag{5.32}$$

$$\frac{1}{t(x)} \frac{\partial F}{\partial Y} = \frac{\partial F^*}{\partial Y^*} , \tag{5.33}$$

and $$\left(\frac{\rho_s \mu_s}{\rho_s^* \mu_s^*}\right)^{1/2} F = F^* . \tag{5.34}$$

The mainstream vapour condition is

$$\frac{\partial F^*}{\partial Y^*} \longrightarrow \left(\frac{C}{x}\right)^m \frac{u_m^*(x)}{u_0^*} \quad \text{as} \quad Y^* \to \infty , \tag{5.35}$$

and the energy equation is:

$$\left(\frac{\rho_w k_w}{\rho_s k_s}\right) \cdot \frac{1}{P_s} \frac{(m+1)}{2 x^{\frac{1}{2}(m+1)}} \int_0^x \frac{x^{\frac{1}{2}(m-1)}}{t(x)} \left(\frac{\partial \theta}{\partial Y}\right)_{Y=0} dx$$

$$= \int_0^1 \left\{ \frac{h_{fg}}{C_{ps} \cdot \Delta T} + \frac{T_s}{\Delta T} - \frac{C_p}{C_{ps}} \cdot \frac{T}{\Delta T} \right\} \frac{\partial F}{\partial Y} dY \tag{5.36}$$

It will be shown that to commence the numerical integration of these equations it is necessary to know the form of the functions F, F^*, θ and t when $X = 0$. The limiting form of the system as $X \to 0$ is:

Condensate phase: $0 \leq Y \leq 1,\ x \geq 0,$

$$\frac{\partial}{\partial Y}\left(\frac{\rho\mu}{\rho_s\mu_s}\frac{\partial^2 F}{\partial Y^2}\right) + t(0)\,F\frac{\partial^2 F}{\partial Y^2} - \frac{2m}{(m+1)}t(0)\left(\frac{\partial F}{\partial Y}\right)^2 + t(0)^3\frac{\rho_s^*}{\rho}N = 0, \tag{5.37}$$

$$\frac{\partial}{\partial Y}\left(\frac{\rho k}{\rho_s k_s}\frac{\partial\theta}{\partial Y}\right) + t(0)\frac{C_p}{C_{ps}}.P_s.F.\frac{\partial\theta}{\partial Y} = 0. \tag{5.38}$$

Vapour phase:

$$\frac{\partial^3 F^*}{\partial Y^{*3}} + F^*\frac{\partial^2 F^*}{\partial Y^{*2}} - \frac{2m}{(m+1)}\left(\frac{\partial F^*}{\partial Y^*}\right)^2 + N = 0, \tag{5.39}$$

Boundary conditions, $Y = 0,\ x \geq 0,$

$$F = \frac{\partial F}{\partial Y} = 0\ ,\quad \theta = 0. \tag{5.40}$$

Interface conditions; $(Y = 1,\ Y^* = 0,\ x \geq 0)$

$$\theta = 1, \tag{5.41}$$

$$\left(\frac{\rho_s\mu_s}{\rho_s^*\mu_s^*}\right)^{1/2}\frac{1}{t(0)^2}\frac{\partial^2 F}{\partial Y^2} = \frac{\partial^2 F^*}{\partial Y^{*2}}, \tag{5.42}$$

$$\frac{1}{t(0)}\frac{\partial F}{\partial Y} = \frac{\partial F^*}{\partial Y^*}, \tag{5.43}$$

and $$\left(\frac{\rho_s\mu_s}{\rho_s^*\mu_s^*}\right)^{1/2} F = F^*. \tag{5.44}$$

the mainstream velocity condition is,

$$\frac{\partial F^*}{\partial y^*} \longrightarrow \lim_{x\to 0}\left\{\left(\frac{c}{x}\right)^m \frac{u_m^*(x)}{u_0^*}\right\} \quad \text{as } y^* \to \infty. \qquad (5.45)$$

Finally the form of the energy balance becomes,

$$\left(\frac{\rho_w k_w}{\rho_s k_s}\right)\frac{1}{P_s}\left(\frac{m+1}{2}\right)\lim_{x\to 0}\left\{x^{-\frac{1}{2}(m+1)}\int_0^x \frac{x^{\frac{1}{2}(m-1)}}{L(x)}\left(\frac{\partial\theta}{\partial y}\right)_{y=0} dx\right\}$$

$$= \int_0^1 \left\{\frac{h_{fg}}{c_{ps}.\Delta T} + \frac{T_s}{\Delta T} - \frac{c_p}{c_{ps}}\cdot\frac{I}{\Delta T}\right\} dy. \qquad (5.46)$$

In equations (6.37) and (6.39) N is given by;

$$N = \lim_{x\to 0}\left\{\frac{2x}{(m+1)}\left(\frac{c}{x}\right)^{2m}\frac{u_m^*(x)}{u_0^*}\frac{d}{dx}\left(\frac{u_m^*(x)}{u_0^*}\right)\right\}. \qquad (5.47)$$

It is not proposed to write out in detail the forms taken by (5.27)-(5.46) for the two problems under discussion. These follow by substituting $m = 1$ with $u_m^*(x) = u_0^* \sin(x/c)$ for the cylinder, and $m = 0$ with $u_m^*(x) = u_0^*\left(1 - \frac{1}{8}\frac{x}{c}\right)$ for the plate.

However with these substitutions we find for the cylinder $N = 1$, for the plate $N = 0$; and the limiting forms of the equations describe condensation in the neighbourhood of a two dimensional stagnation point, and forced flow over a flat plate respectively. The governing equations for these problems have been formulated in Chapter 3. The limiting forms (5.37)-(5.47) are not identical to (3.15)-(3.23) but if one puts

$$F = (m+1)^{1/2} f \quad \text{and} \quad Y = (m+1)^{-1/2} \tilde{Y} ,$$

then (5.37)-(5.47) are transformed into the equations of Chapter 3.

The necessary information to start the integration of the equations formulated in this chapter is therefore available. However to avoid reading very accurate data at X = 0 into the program, subroutines are included which solve the ordinary differential equations using the main matrix inversion procedure.

Method of solution

Solution of the three coupled non-linear partial differential equations is effected by considering the functions $Q = \frac{\partial F}{\partial Y}$, t, θ and $Q^* = \frac{\partial F^*}{\partial Y^*}$. There results a set of parabolic equations, an appropriate method for the solution of which was proposed by Hartree and Womersley [25] and basically involves replacing derivatives in the X-direction by differences and all other quantities by averages. In this manner the solution at the stage $X = X_N + h$ can be found, once that at $X = X_N$ is known, by solving a coupled set of non-linear ordinary differential equations. The previous section has established how the solution is obtained at station X = 0.

Full details of the Hartree-Womersley scheme, quasi-linearisation of the ordinary differential equations and the matrix iteration procedure are given in Appendix C.

Discussion of results

Due to the considerable numerical labour involved solving the partial differential equations, solutions have been computed only with T_W = 0, 70 and 99.99°C for each of the flow configurations. The characteristics of physical interest were introduced in Chapter 3 for the general vapour mainstream velocity $u_m^*(x)$. The particular forms relevant to the plate, $u_m^*(x) = u_o^*(1-\frac{1}{8}\frac{x}{c})$, are obtained on substituting $M(x) = (1-\frac{1}{8}\frac{x}{c})$ and $\alpha = \sqrt{2}$ into the following; those for the case of the cylinder, $u_m^*(x) = u_o^* \sin(x/c)$ follow from putting $M(x) = (\frac{c}{x})\sin(\frac{x}{c})$ and $\alpha = 1$.

$$\frac{\delta(x)}{x}.\ Re_x^{1/2} = \alpha\, t(x)\, M(x)^{\frac{1}{2}} \int_0^1 \frac{\rho_s}{\rho}\, dY,$$

$$\frac{\delta_1}{x}.\ Re_x^{*1/2} = \alpha\, M(x)^{1/2} \lim_{y^*\to\infty} \left\{ y^* + [F^*(x,0) - F^*(x,y^*)]/M(x) \right\},$$

$$\frac{\delta_2}{x}.\ Re_x^{*1/2} = \alpha\, M(x)^{-\frac{1}{2}} \int_0^\infty \frac{\partial F^*}{\partial y^*}\left[1 - \frac{1}{M(x)}\frac{\partial F^*}{\partial y^*}\right] dy^*, \qquad (5.48)$$

$$C_{fw}.\ Re_x^{1/2} = \frac{2}{\alpha}\left(\frac{\rho_w \mu_w}{\rho_s \mu_s}\right) \frac{1}{t(x)^2}\, M(x)^{-3/2} \left[\frac{\partial^2 F}{\partial y^2}\right]_{y=0},$$

$$C_{f_I}.\ Re_x^{1/2} = \frac{2}{\alpha}\, \frac{1}{t(x)^2}\, M(x)^{-3/2} \left[\frac{\partial^2 F}{\partial y^2}\right]_{y=1},$$

$$Nu.\ Re_x^{-\frac{1}{2}} = \frac{1}{\alpha}\, \frac{\rho_w}{\rho_s}\, \frac{1}{t(x)}\, M(x)^{-1/2} \left[\frac{\partial \theta}{\partial y}\right]_{y=0}.$$

Note that the global condensation rate has not been included above. Instead a study will be made of the vapour velocity normal to the interface, which is the local condensation rate. From (6.19) we have;

$$v^*(x,0) = -\left(\frac{2\mu_0^* v_s^* x^{m-1}}{(m+1)c^m}\right)^{\frac{1}{2}} \left\{\frac{(m+1)}{2} F^* + x\frac{\partial F^*}{\partial x}\right\}_{y^*=0},$$

and the dimensionless 'suction' velocity is given by;

$$\frac{v^*(x,0)}{\mu_\infty^*(x)} \cdot Re_x^{*\frac{1}{2}} = -M(x)^{-\frac{1}{2}} \left[\frac{F}{\alpha} + \alpha x \frac{\partial F}{\partial x}\right]_{y^*=0}. \qquad (5.49)$$

Velocity profiles

The velocities in the condensate and vapour phases are given by $u = \mu_0^* \cdot \left(\frac{x}{c}\right) \frac{1}{t(x)} \frac{\partial F}{\partial y}$ and $u^* = \mu_0^* \left(\frac{x}{c}\right) \frac{\partial F^*}{\partial y^*}$ respectively for the cylinder, and by $u = \mu_0^* \frac{1}{t(x)} \frac{\partial F}{\partial y}$ and $u^* = \mu_0^* \frac{\partial F^*}{\partial y^*}$ for the plate. Some of the results for $\frac{\partial F}{\partial y}$ and $\frac{\partial F^*}{\partial y^*}$ at typical cross-sections are given in tables 14-19, where t(X) is also tabulated so that the velocity profiles may be deduced. In addition some profiles are displayed in figures 8, 9 and 10.

In the discussion of the numerical similar solutions T_W was assigned the value $T_W = 99.99^\circ C$ in order to justify the assertion that the vapour flow tended to the Blasius flow as $\Delta T \to 0$. The same value of the wall temperature is used now to establish the fact that the vapour flow tends to the corresponding non-similar single phase flow. The one phase problem over the cylinder has been solved numerically by Terrill [26] and that for the plate by Hartree [27] and later by Leigh [28].

The latter problem was also solved approximately by Howarth [29], whose model is so close to the numerical solutions that it will be used as the yardstick for the vapour boundary layer on the plate.

Comparison between the vapour solution and the corresponding single phase problem is not immediate because of the different choice of variables, but is illustrated by comparing the vapour momentum thickness with the momentum thickness of the corresponding single phase flow. These data are included in tables 22 and 25, which list the physically interesting coefficients as functions of X, when $T_W = 99.99^\circ C$, for the plate and cylinder problems respectively. Table 22 shows that the vapour momentum thickness is marginally less than Howarth's value from X = 0 until beyond three quarters of the way to the separation point X_S. As X_S is approached the thicknesses both increase rapidly. However it is the vapour layer which remains the thinner, and indicates the point of separation in the condensation problem is moved downstream from the single phase location. The same observations can be made from table 23 in relation to the cylinder problem. The magnitude of the shift in X_S is not given since it is very small and to achieve Terrills accuracy a very considerable amount of computing would be necessary.

The fact that condensation delays separation, and the smaller T_W the greater the delay, is more apparent from the tabulated data for the other values of T_W. Figures 11 and 12 show the variation of X_S/C with T_W.

It appears that the delay in separation is more marked in the case of the plate where X_S/C is increased from Howarth's value of 0.96, which is the limiting value as $T_W \longrightarrow 100^\circ C$, to 6.3 when $T_W = 0^\circ C$.

The corresponding values for the cylinder are $x_s/c = 1.823$ radians and $x_s/c = 2.72$ radians. This is due to a fundamental difference between the two vapour mainstreams. The flow over the plate is linearly retarded from the leading edge whereas that over the cylinder is accelerated in the region $0 < x/c < \pi/2$ and is only decelerated for $\pi/2 < x/c < \pi$. If we introduce $\tilde{x}_s/c = x/c - \pi/2$, then the ratio of $\tilde{x}_s/c$ for $T_w = 0^\circ C$ and $T_w = 99.99^\circ C$ becomes 4.5, as against 6.5 for the ratio of x_s/c at the same temperatures for the plate. Even now x_s/c seems more sensitive to T_w, and this is because the pressure gradient varies as $\sin(2x/c)$ round the cylinder and therefore only attains its most restricting value when $x/c = 3\pi/4$.

The fact that the condensate layer acts as a lubricant for the vapour and effectively delays separation is thus quite apparent, however the nature of the flow in the neighbourhood of numerical breakdown and an answer to the question, "In which phase does separation first occur?" are not so obvious. For the single phase linearly retarded flow with the traditional no-slip condition, Goldstein [30] in his classic paper has shown that separation is due to an algebraic singularity in the wall shear $\mu\left(\frac{\partial u}{\partial y}\right)_{y=0}$, of the form;

$$\mu\left(\frac{\partial u}{\partial y}\right)_{y=0} \propto (x - x_s)^{1/2}. \qquad (5.49)$$

Not having similar results available for the behaviour of the wall or interfacial shear stresses in the condensation problems it is not possible to fully appreciate the behaviour of separation. However it is noticed

that the values of the wall and interfacial shear coefficients decrease rapidly as numerical breakdown is approached, so a singularity of the above type is likely to be present.

We will take the criterion for separation to be the vanishing of either the non-dimensional wall shear stress $C_{fw}.Re_x^{1/2}$, or the interfacial shear $C_{f_I}.Re_x^{1/2}$ so that a general conclusion can be attempted.

Tables 20, 21, 22, 23, 24 and 25 show the physical coefficients as functions of x/c and include a comparison of $C_{fw}.Re_x^{1/2}$ and $C_{f_I}.Re_x^{1/2}$ at the typical stages. It is observed that near the leading edge of the plate, or of the forward stagnation point on the cylinder, that $C_{fw}.Re_x^{1/2}$ is never less than $C_{f_I}.Re_x^{1/2}$, the reason for which has been given in Chapter 3, but as numerical breakdown is approached $C_{fw}.Re_x^{1/2}$ becomes the smaller and tends to zero faster. This implies that separation first occurs in the condensate at the body surface.

Figures 8, 9 and 10 confirm the preceding assertion.

All the above remarks have applied to both flow configurations, however there are some differences which are worth noting. In the region $0 < x/c < \pi/2$ for the cylinder it can be seen that the physical properties do not change much, and the switch from $C_{fw}.Re_x^{1/2}$ being the larger shear coefficient to the smaller does not take place until the decelerated zone. In contrast the change over in the plate problems occurs much more steadily.

The same pattern can be seen in the variation of the condensation rate as $^{x}/_{c}$ increases. For the plate $\frac{[v^*]_{y^*=0}}{U^*_{im}(x)} . Re_x^{*\,1/2}$ decreases steadily, whereas it is maintained relatively constant in the accelerated region of the cylinder problem. This observation will account for the reasoning in Chapter 6, that if the vapour phase is considered to be a strong suction boundary layer, then this is a better model for acceleration than for decelerated regions of flow.

Shear Stress

It has been mentioned that values of $C_{fw}.Re_x^{1/2}$ and $C_{f_I}.Re_x^{1/2}$ are included in tables 20-25. In addition figures 13 and 14 display the behaviour of $C_{fw}.Re_x^{1/2}/[C_{fw}.Re_x^{1/2}]_{x=0}$ plotted as functions of $^{x}/_{x_S}$ for the cases T_W = 0,70 and 99.99°C for the plate and cylinder respectively. In each graph it may be noted there is considerable similarity between the curves for each value of T_W. Consequently knowing X_S from either figure 11 or figure 12, and the appropriate value of $[C_{fw}.Re_x^{1/2}]_{x=0}$ from a similarity solution it is possible to deduce the wall shear for any value of T_W in either configuration.

Heat Transfer Rates

The non-dimensional heat transfer rate $Nu.Re_x^{-1/2}$ is tabulated along with $C_{fw}.Re_x^{1/2}$ etc. in tables 20-25. The expected results is that $Nu.Re_x^{-1/2}$ is relatively constant in the accelerated flow region of the cylinder, but in regions of adverse pressure gradient there

is a decrease which becomes increasingly more marked as separation is approached.

Chapter 6

Approximate analytical solution for non-similar condensation problems

Introduction

The previous Chapter has been devoted to the discussion of two examples of this particular type of problem following numerical integration of the governing equations. This was seen to involve considerable labour and consequently approximate methods yielding the flow characteristics are most desirable.

The aim is to extend the thick and thin film approximations, which were developed in Chapter 4, to deal with the general vapour mainstream velocity $u_m^*(x)$. The accuracy of the resulting models will be tested by applying the models to the cases $u_m^*(x) = u_0^* \sin(\frac{x}{c})$ and $u_m^*(x) = u_0^*(1 - \frac{1}{8}\frac{x}{c})$, and comparing the results with the known numerical solutions.

This general two-dimensional flow is described by the set of equations (2.7)-(2.18) and (2.20). Introduce the dimensionless temperature function θ, defined by (2.26), and make the following change of variable;

$$X = x, \quad Y = y/\delta(x), \tag{6.1}$$

where $y = \delta(x)$ is the equation of the vapour-condensate interface. Then the governing equations become:

Condensate phase ($X \geq 0$, $0 \leq Y \leq 1$).

$$u\left(\frac{\partial u}{\partial x} - \frac{1}{\delta} Y \frac{d\delta}{dx} \frac{\partial u}{\partial Y}\right) + \frac{1}{\delta} v \frac{\partial u}{\partial Y} = \frac{\rho_s^*}{\rho} u_m^* \frac{du_m^*}{dx} + \frac{\nu_s}{\delta^2} \frac{\partial}{\partial Y}\left(\frac{\mu}{\mu_s} \frac{\partial u}{\partial Y}\right), \tag{6.2}$$

$$u\left(\frac{\partial\theta}{\partial x} - \frac{1}{\delta} Y \frac{d\delta}{dx}\frac{\partial\theta}{\partial Y}\right) + \frac{1}{\delta} v \frac{\partial\theta}{\partial Y} = \frac{k_s}{\rho_s c_{ps}} \frac{\partial}{\partial Y}\left(\frac{k}{k_s}\frac{\partial\theta}{\partial Y}\right), \tag{6.3}$$

and $$\frac{\partial u}{\partial x} - \frac{1}{\delta} Y \frac{d\delta}{dx}\frac{\partial u}{\partial Y} + \frac{1}{\delta}\frac{\partial v}{\partial Y} = 0. \tag{6.4}$$

Vapour: $(x \geq 0,\ 0 \leq y^* < \infty)$,

$$u^* \frac{\partial u^*}{\partial x} + v^* \frac{\partial u^*}{\partial y^*} = u_m^* \frac{d u_m^*}{dx} + \nu_s^* \frac{\partial^2 u^*}{\partial y^{*2}} \tag{6.5}$$

and $$\frac{\partial u^*}{\partial x} + \frac{\partial v^*}{\partial y^*} = 0. \tag{6.6}$$

Boundary conditions, $(x \geq 0,\ Y = 0)$,

$$u = v = 0, \quad \theta = 0, \tag{6.7}$$

At the interface: $(x \geq 0,\ Y = 1,\ y^* = 0)$, $\theta = 1$, (6.8)

Continuity in mass flow:

$$\rho_s^* v_s^* = -\frac{d}{dx}\left[\delta(x) \int_0^1 \rho u \, dY\right], \tag{6.9}$$

Continuity in tangential velocity:

$$u = u^*, \tag{6.10}$$

Continuity in interfacial stress components:

$$p = p^*, \quad \mu_s \frac{1}{\delta}\frac{\partial u}{\partial Y} = \mu_s^* \frac{\partial u^*}{\partial y^*}, \tag{6.11}$$

Liberation of latent heat at the interface:

$$k_s \cdot \Delta T \cdot \frac{1}{\delta(x)}\left[\frac{\partial\theta}{\partial Y}\right]_{Y=1} = -\rho_s^* v_s^* h_{fg} = \frac{d}{dx}\left[\delta(x) \int_0^1 \rho u h_{fg} \, dY\right]. \tag{6.12}$$

Finally the free stream condition is;

$$u^* \longrightarrow u_m^*(x) \quad , \quad x \gg 0 \quad , \quad y^* \longrightarrow \infty . \tag{6.13}$$

Thin film approximation

This model was introduced in Chapter 4 for the case when $T_w \sim 100^\circ C$ and the condensation rate was slight. It was specified by either of the inequalities $\frac{\Delta T}{T_s} \ll 1$ or $\chi \ll 1$.

A perturbation expansion in terms of $\varepsilon = \chi^{1/3}$ was found to provide the correct limiting form as $\chi \to 0$ for the similar flow over the plate, and there resulted a first order condensate solution which was activated by the shear stress equivalent to the wall shear of the single phase flow satisfying the no-slip condition at $y^* = 0$.

Guided by the analysis of Chapter 4 the vapour velocity is expanded in the form;

$$\underline{q}^* = (u^*, v^*) = \underline{q}_0^* + \varepsilon \underline{q}_1^* + \varepsilon^2 \underline{q}_2^* + \cdots \tag{6.14}$$

and in the condensate the following are taken:

$$u = \varepsilon u_0 + \varepsilon^2 u_1 + \varepsilon^3 u_2 + \cdots \tag{6.15}$$

$$v = \varepsilon^2 v_0 + \varepsilon^3 + v_1 + \varepsilon^4 v_2 + \cdots \tag{6.16}$$

$$\theta = \theta_0 + \varepsilon \theta_1 + \varepsilon^2 \theta_2 + \cdots \tag{6.17}$$

and

$$\delta = \varepsilon \delta_0 + \varepsilon^2 \delta_1 + \varepsilon^3 \delta_2 + \cdots . \tag{6.18}$$

The range of validity of the thin film model will be such that only small temperature changes occur in the condensate, which will therefore be treated as a constant property fluid. On substitution of (6.14)-(6.18) into the simplified forms of (6.2)-(6.13) the zeroth order perturbation functions satisfy the equations:

Condensate: $$\frac{\partial^2 u_0}{\partial y^2} = 0 \quad , \quad \frac{\partial^2 \theta_0}{\partial y^2} = 0 \; ; \tag{6.19}$$

Vapour: $$\frac{\partial u_0^*}{\partial x} + \frac{\partial v_0^*}{\partial y^*} = 0 , \tag{6.20}$$

$$u_0 \frac{\partial u_0^*}{\partial x} + v_0 \frac{\partial u_0^*}{\partial y^*} = u_m^* \frac{d u_m^*}{dx} + \nu_s^* \frac{\partial^2 u_0}{\partial y^{*2}} \; ; \tag{6.21}$$

Boundary conditions: for $X \geq 0$, $Y = 0$:

$$u_0 = v_0 = 0 \quad , \quad \theta_0 = 0 \; ; \tag{6.22}$$

at the interface, $X \geq 0$, $Y = 1$, $y^* = 0$,

$$\theta_0 = 1 , \tag{6.23}$$

$$u_0^* = v_0^* = 0 , \tag{6.24}$$

$$\mu_s \frac{\partial u_0}{\partial y} = \delta_0 \mu_s^* \frac{\partial u_0^*}{\partial y^*} , \tag{6.25}$$

$$\nu_s \frac{\partial \theta_0}{\partial y} = \delta_0 \frac{d}{dx} \left[\delta_0 \int_0^1 u_0 \, dy \right] , \tag{6.26}$$

and as $$y^* \longrightarrow \infty \text{ for } x \geq 0 , \quad u_0^* \longrightarrow u_m^*(x) . \tag{6.27}$$

Firstly note that (6.20), (6.21), (6.24) and (6.27) are simply the equations which govern the single phase flow subject to the no-slip condition at the interface, i.e., to within the current approximations, at the body surface. If the solution to this problem is known then the wall shear is available.

Denoting this by $\tau_w^*(x)$, that is

$$\mu_s^* \frac{\partial u_o^*}{\partial y^*} = \tau_w^*(x), \tag{6.28}$$

the function $\tau_w^*(x)$ can be taken to be a known function wherever it occurs in the solution of the condensate phase.

The zeroth order condensate solution satisfies (6.19), (6.22), (6.23) and (6.25) and hence;

$$\theta_o = Y \quad \text{and} \quad u_o = \frac{\tau_w^*(x)}{\mu_s} \delta_o(x) . Y . \tag{6.29}$$

Now there only remains the energy balance (6.26) to satisfy. Substituting (6.29) in (6.26) we have a differential equation for determining $\delta_o(x)$:

$$\nu_s = \delta_o \frac{d}{dx} \left[\tau_w^*(x) \delta_o(x)^2 / \mu_s \right], \tag{6.30}$$

or

$$\boxed{3 \nu_s \mu_s \tau_w^*(x)^{1/2} = \frac{d}{dx} \left[\tau_w^*(x)^{3/2} \delta_o(x)^3 \right]} \tag{6.31}$$

Since $\tau_w^*(x)$ is known for many two-dimensional flows then $\delta_o(x)$ can be evaluated analytically or by quadratures.

For example if $u_m^*(x) = u_o^*$ then the zeroth order vapour approximation represents the forced single phase flow over a semi-infinite plate, and for this the Blasius solution yields

$$\tau_w^*(x) = A\mu_s^* \left(\frac{u_o^{*3}}{2\nu_s^* x}\right)^{1/2}, \qquad (6.32)$$

where A = 0.4696.

Substitute (6.32) into (6.31), apply the condition that at the leading edge the condensate has zero thickness, then on integrating we have:

$$\delta_o = B^{1/3} x^{1/2}, \quad B = 4\nu_s\mu_s \Big/ \left\{A\mu_s^* \left(\frac{u_o^{*3}}{2\nu_s^* x}\right)^{1/2}\right\}.$$

Hence

$$\frac{\delta(x)}{x} . Re_x^{1/2} = (Bx)^{1/3} x^{-1/2} \left(\frac{u_o . x}{\nu_s}\right)^{1/2} + \ldots,$$

$$= \left(\frac{4\sqrt{2}}{A} . x\lambda\right)^{1/3} + \ldots, \qquad (6.33)$$

which is precisely the zeroth order solution for $\frac{\delta(x)}{x} . Re_x^{1/2}$ derived in Chapter 4.

Consider now the case of flow of saturated vapour past the circular cylinder. The vapour mainstream is

$$u_m^x(x) = u_o^x \sin(x/c),$$

where X is distance measured along the surface from the forward stagnation point and C is the radius of the cylinder.

The single phase flow has been examined by Terrill [26], and $\tau_w^*(x)$ is available in the form

$$\tau_w^*(x) = u_0^* \mu_s^* \left(\frac{u_0^* \rho_s^*}{c \mu_s^2} \right)^{\frac{1}{2}} \tilde{F}(x/c), \qquad (6.34)$$

where the function $\tilde{F}(x/c)$ is given numerically (it is denoted by $\frac{\partial u}{\partial y}$ in the table given on page 93 of Terrill's paper) in the range $0 \leq x/c \leq 1.8206$. At the stagnation point $x/c = 0$, the condensate thickness is finite, and for small X, $\tilde{F} \sim x/c$. Thus on substituting (6.34) into (6.31) we have

$$\delta_0(x) = \left[\frac{3 \nu_s \mu_s}{\mu_s^2 u_0^*} \left(\frac{c \mu_s^*}{u_0^* \rho_s^*} \right)^{1/2} \right]^{\frac{1}{3}} \frac{\left[\int_0^x \tilde{F}(x/c)\, dx \right]^{1/3}}{\tilde{F}^{1/2}(x/c)}. \qquad (6.35)$$

Hence the limiting forms as $x \to 0$ of the characteristics $\frac{\delta(x)}{x} \cdot Re_x^{1/2}$, $C_{fw} \cdot Re_x^{1/2}$ and $Nu \cdot Re_x^{-1/2}$ are:

$$\frac{\delta(x)}{x} \cdot Re_x^{1/2} = \left(\frac{\sin x/c}{x/c} \right)^{1/2} \frac{1}{\tilde{F}(x/c)^{1/2}} \left[\int_0^{x/c} \tilde{F}(x/c)\, d\left(\frac{x}{c}\right) \right]^{\frac{1}{3}} (3\lambda x)^{\frac{1}{3}} + \ldots, \qquad (6.36)$$

$$C_{fw} \cdot Re_x^{1/2} = \frac{2}{\lambda} \frac{\mu_w}{\mu_s} \cdot \frac{\tilde{F}(x/c)}{\sin(x/c)} \left(\frac{x/c}{\sin x/c} \right)^{1/2} + \ldots, \qquad (6.37)$$

$$\text{and } Nu \cdot Re_x^{-\frac{1}{2}} = 1 \Big/ \left(\frac{\delta(x)}{x} Re_x^{1/2} \right). \qquad (6.38)$$

In order to illustrate the validity of the thin-film approximation applied to this non-similar problem the approximate condensate thicknesses are compared with the numerical solutions for $T_W = 99^\circ C$ and $99.99^\circ C$, which was discussed in Chapter 5. To facilitate comparison the dimensionless group $\frac{\delta(x)}{x} \cdot Re_x^{1/2} \chi^{-\frac{1}{3}}$ evaluated from (6.36) is plotted against x/c, along with the numerical solutions, in figure 15. It is sufficient to note that when $T_W = 99.99^\circ C$ the agreement is excellent but there is a noticeable difference (about 5 per cent) when $T_W = 99^\circ C$.

The numerical results have shown that the condensate layer behaves as a lubricant for the vapour and effectively delays separation. Since $P(x/c)$ is only available in the range $0 \leq x/c \leq 1.822$, the thin film model cannot predict the flow characteristics the entire way up to separation. However it is interesting to note that for $T_W = 99.99^\circ C$ the approximate results are accurate right up to x_s/c.

Also the thin film model is unable to give any insight into the nature of separation. An essential feature is the constant condensate shear layer which predicts flow reversal in the liquid and vapour at the same point.

Thick film approximation

In Chapter 4 a thick film approximation was developed for the range of T_W for which the thin film model was invalid. The essential feature of the model was the ability to treat the vapour phase as a strong suction vapour boundary layer. The numerical solutions of the previous chapter suggest the same concepts are likely to be fruitful when applied to

non-similar problems, except perhaps as separation is approached. It has also become apparent that it is a gross simplification to treat the condensate as a constant property fluid when $\Delta T/T_s \sim O(1)$. Accordingly the full form of equations (6.2)-(6.13) are used as a basis for the model. The co-ordinate system is displayed in figure 16.

Denote the unknown vapour velocity normal to the interface, $y^* = 0$, by $w_s^*(x)$ and in view of the preceding remarks suppose it is large. Under such circumstances the vapour boundary layer equations (6.5) and (6.6), for arbitrary distributions of $w_s^*(x)$ and $u_m^*(x)$, can be solved in inverse powers of $w_s^*(x)$ as given by Watson [31].

To utilize Watson's expansion it is only necessary to relax his condition of zero tangential velocity at the surface. From [31] the desired solution is as follows:

$$\psi^* = \int w_s^*(x)\,dx + \frac{\nu_s^* u_m^*}{w_s^*(x)} f^*(x, \zeta^*), \tag{6.39}$$

where $$\zeta^* = \frac{w_s^*(x)}{\nu_s^*} \cdot y^*. \tag{6.40}$$

Hence the velocity components are:

$$u^* = u_m^*(x) \frac{\partial f^*}{\partial \zeta^*}, \tag{6.41}$$

$$v^* = -w_s^*(x) - \frac{\nu_s^*}{w_s^{*2}(x)}\left\{u_m^{*\prime} w_s^* f^* + u_m^* w_s^* \frac{\partial f^*}{\partial x} + u_m^* w_s^{*\prime}\left(\zeta^* \frac{\partial f^*}{\partial \zeta^*} - f^*\right)\right\}, \tag{6.42}$$

where the primes denote differentiation with respect to X.

Substituting (6.41) and (6.42) into (6.5) the vapour momentum equation yields the following equation for determining $f^*(X,\zeta^*)$:

$$\frac{\partial^3 f^*}{\partial \zeta^{*3}} + \frac{\partial^2 f^*}{\partial \zeta^{*2}} + \frac{v_s^*}{w_s^{*3}}\left[u_m^{*\prime}(x)\, w_s^*(x)\left\{1 - \left(\frac{\partial f^*}{\partial \zeta^*}\right)^2 + f^* \frac{\partial^2 f^*}{\partial \zeta^{*2}}\right\}\right.$$

$$\left. + u_m^*(x)\, w_s^*(x)\left\{\frac{\partial f^*}{\partial x}\frac{\partial^2 f^*}{\partial \zeta^{*2}} - \frac{\partial f^*}{\partial \zeta^*}\frac{\partial^2 f^*}{\partial x \partial \zeta^*}\right\} - u_m^*(x)\, w_s^{*\prime}(x)\, f^* \frac{\partial^2 f^*}{\partial \zeta^{*2}}\right] = 0 \qquad (6.43)$$

The chosen condition $v^* = -w_s^*(x)$ at $y^* = 0$, together with (6.13) yield:

$$f^*(x,0) = 0, \qquad (6.44)$$

and

$$\frac{\partial f^*}{\partial \zeta^*} \longrightarrow 1 \quad \text{as} \quad \zeta^* \longrightarrow \infty. \qquad (6.45)$$

Now if $w_s^*(x)$ is large (6.43) is approximately

$$\frac{\partial^3 f^*}{\partial \zeta^{*3}} + \frac{\partial^2 f^*}{\partial \zeta^{*2}} = 0, \qquad (6.46)$$

which subject to (6.44) and (6.45) yields:

$$f^* = \zeta^* + A^*(x)\left(e^{-\zeta^*} - 1\right), \qquad (6.47)$$

where $A^*(x)$ is an arbitrary function of integration. The vapour phase velocity field is now given by the asymptotic formulae:

$$\frac{u}{u_m^*(x)} = \left(1 - A^*(x).e^{-\zeta^*}\right) + O\left(1/w_s^*(x)^3\right), \qquad (6.48)$$

and $$v = -w_s^*(x) - \frac{v_s^*}{w_s^*(x)^2}\Big[u_m^{*\prime}(x)\, w_s^*(x)\{f^* + A^*(x)(e^{-f^*}-1)\}$$

$$+ u_m^*(x) w_s^*(x)\, A^{*\prime}(x)(e^{-f^*}-1)$$

$$- u_m^*(x) w_s^{*\prime}(x)\{A^* f^* e^{-f^*} + A^*(e^{-f^*}-1)\}\Big] + \cdots \quad (6.49)$$

Thus at the interface Y = 1, $f^* = 0$ for $x \geq 0$ and large $w_s^*(x)$,

$$u^*(x,0) = (1 - A^*(x))\, u_m^*(x), \quad (6.50)$$

$$v^*(x,0) = -w_s^*(x), \quad (6.51)$$

and $$\mu_s^* \frac{\partial u^*}{\partial y^*} = \rho_s^* w_s^*(x) A^*(x) u_m^*(x). \quad (6.52)$$

Having solved for the zeroth order vapour solution now we turn to the condensate phase and solve (6.2)-(6.4) subject to (6.7), (6.8), (6.12) and the interfacial conditions (6.9)-(6.11). These together with (6.50)-(6.52) give respectively:

$$\rho_s^* w_s^*(x) = \frac{d}{dx}\left[\delta(x)\int_0^1 \rho u \, dY\right], \quad (6.53)$$

$$u(x,1) = (1 - A^*(x))\, u_m^*(x), \quad (6.54)$$

and $$\mu_s \left(\frac{\partial u}{\partial y}\right)_{Y=1} = \delta(x)\, \rho_s^* w_s^*(x) A^*(x) u_m^*(x). \quad (6.55)$$

When formulating the thick film model for the similar flows, the equations corresponding to this set were solved using the full condensate variable

properties. Then the limiting form of the equations as $\chi \to 0$ was sought and the variable condensate properties approximated to by:

$$\rho = \rho_s, \; c_p = c_{ps}, \; k = k_w + (k_s - k_w)\theta, \; \frac{1}{\mu} = \frac{1}{\mu_w} + \left(\frac{1}{\mu_s} - \frac{1}{\mu_w}\right)\theta. \tag{6.56}$$

The intention now is to omit the full solution of (6.2)-(6.4), (6.7) (6.8), (6.12), (6.53)-(6.55) and to proceed to find the limiting form as $\chi \to 0$ together with the model fluid (6.56).

The necessary expansions are:

$$u = \chi u_m^*(x)\, U(x,Y) + O(\chi^2), \tag{6.57}$$

$$v = \chi u_m^*(x)\, V(x,Y) + O(\chi^2), \tag{6.58}$$

$$w_s^* = \chi W_s^*(x) + O(\chi^2), \tag{6.59}$$

$$\delta = \Delta(x) + O(\chi), \tag{6.60}$$

$$A^* = 1 - \chi B^*(x) + O(\chi^2), \tag{6.61}$$

and

$$\theta = \tilde{H} + O(\chi). \tag{6.62}$$

For all condensates $\frac{\rho_s^*}{\rho_s} \ll 1$ so the vapour induced pressure gradient will be ignored. Substituting (6.57)-(6.62) into the governing equations (6.2)-(6.4), (6.7), (6.8), (6.12), (6.53)-(6.55) the perturbation functions satisfy:

$$\frac{\partial}{\partial Y}\left(\frac{\mu}{\mu_s}\frac{\partial U}{\partial Y}\right) = 0 \quad \text{and} \quad \frac{\partial}{\partial Y}\left(\frac{k}{k_s}\frac{\partial \tilde{H}}{\partial Y}\right) = 0. \tag{6.63}$$

The boundary conditions are:

$$U(x,0) = 0, \; \tilde{H}(x,0) = 0, \; \tilde{H}(x,1) = 1, \tag{6.64}$$

$$\frac{\rho_s}{\rho_s^*}\frac{d}{dx}\left[\Delta(x)\,u_m^*(x)\int_0^1 u\,dy\right] = W_s^*(x), \tag{6.65}$$

$$u(x,1) = B^*(x), \tag{6.66}$$

$$\mu_s\left(\frac{\partial u}{\partial y}\right)_{y=1} = \rho_s^*\,\Delta(x)\,W_s^*(x), \tag{6.67}$$

and $$v_s\left(\frac{\partial \tilde{H}}{\partial y}\right)_{y=0} = \Delta(x)\frac{d}{dx}\left[\Delta(x)u_m^*(x)\int_0^1 u\,dy\right]. \tag{6.68}$$

The equations (6.63) are solved in a similar manner to that introduced for equation (4.55).

Integrating (6.63) we have

$$\frac{k}{k_s}\frac{\partial \tilde{H}}{\partial y} = E(x) \quad \text{and} \quad \frac{\mu}{\mu_s}\frac{\partial u}{\partial y} = D(x), \tag{6.69}$$

where in general E(X) and D(X) are arbitrary functions of X.

The former yields, on using $\tilde{H}(x,0) = 0$:

$$E.Y = \int_0^{\tilde{H}} \frac{k}{k_s}\,d\tilde{H}.$$

Also we have H(X,1) = 1 so that E(X) is determined by

$$E(x) = \int_0^1 \frac{k}{k_s}\,d\tilde{H} = \frac{k_s + k_w}{2k_s}. \tag{6.70}$$

That is E is a constant depending only on the wall and saturation temperatures.

Now (6.65), (6.67) and (6.68) together imply

$$\left(\frac{\partial u}{\partial y}\right)_{y=1} = \left(\frac{\partial \tilde{H}}{\partial y}\right)_{y=1} , \tag{6.71}$$

which together with (6.69) gives:

$$E(x) = D(x) = \frac{k_s + k_w}{2k_s} .$$

From (6.69) $\frac{\partial}{\partial y} = E\frac{k_s}{k}\frac{\partial}{\partial \tilde{H}}$ and hence (6.71) becomes:

$$\frac{\partial u}{\partial \tilde{H}} = \frac{\mu_s k}{k_s \mu} , \tag{6.72}$$

or
$$u = \int_0^{\tilde{H}} \frac{\mu_s k}{k_s \mu}\, d\tilde{H} . \tag{6.73}$$

Thus
$$\int_0^1 u\, dy = \int_0^1 u \cdot \frac{k}{E k_s}\, d\tilde{H}$$

$$= \frac{1}{E}\int_0^1 \left(\frac{k}{k_s}\left[\int_0^{\tilde{H}} \frac{\mu_s k}{\mu k_s}\, d\tilde{H}\right]\right) d\tilde{H} .$$

Therefore
$$\int_0^1 u\, dy = \frac{\varepsilon_p^2}{2E} , \tag{6.74}$$

where
$$\varepsilon_p = \left\{ \frac{8 + 9\frac{k_w}{k_s} + 3\frac{k_w^2}{k_s^2} + \frac{\mu_s}{\mu_w}\left(7 + 21\frac{k_w}{k_s} + 12\frac{k_w^2}{k_s^2}\right)}{60.} \right\}^{\frac{1}{2}} \tag{6.75}$$

On substituting (6.69) and (6.74) into (6.68) then the following differential equation for $\Delta(x)$ is obtained:

$$v_s . E = \Delta(x) \frac{d}{dx}\left(\Delta(x) u_m^*(x) \frac{\varepsilon_p^2}{2E} \right), \tag{6.76}$$

or

$$\boxed{\frac{d}{dx}\left(\Delta^2(x) u_m^{*2}(x) \right) = 4 \frac{E^2}{\varepsilon_p^2} v_s u_m^*(x).} \tag{6.77}$$

The problem of finding the thick film approximation to non-similar flows is now that of solving (6.77), which is a very simple matter once $u_m^*(x)$ is specified.

In the simple case when $u_m^*(x) = u_0^*$, constant then (6.77) gives

$$\Delta(x) = \frac{2E}{\varepsilon_p} \left(\frac{v_s . x}{u_0^*} \right)^{1/2}, \tag{6.78}$$

and hence

$$\frac{\delta(x)}{x} . Re_x^{1/2} = 2E / \varepsilon_p, \tag{6.79}$$

which is the result (4.68) obtained in Chapter 4.

Returning now to the condensation problems onto the flat plate with $u_m^*(x) = u_0^*\left(1 - \frac{1}{8}\frac{x}{c}\right)$ and onto the cylinder where $u_m^*(x) = u_0^* \sin\left(\frac{x}{c}\right)$, then (6.77) is solved to give the following characteristics.

	Plate	Cylinder
$\frac{\delta(x)}{x}.Re_x^{1/2}$	$: \frac{2E}{\varepsilon_p}\left(\frac{1-\frac{1}{16}\frac{x}{c}}{1-\frac{1}{8}\frac{x}{c}}\right)^{1/2}$	$: \sqrt{2}\,\frac{E}{\varepsilon_p}.\left(\frac{\tan x/2c}{x/2c}\right)^{\frac{1}{2}}$
$C_{fw}.Re_x^{1/2}$	$: \chi\varepsilon_p\left(\frac{1-\frac{1}{8}\frac{x}{c}}{1-\frac{1}{16}\frac{x}{c}}\right)^{1/2}$	$:\sqrt{2}\,\chi\varepsilon_p.\left(\frac{x/2c}{\tan x/2c}\right)^{1/2}$ (6.80)
$Nu.Re_x^{-1/2}$	$: \frac{\varepsilon_p}{2}\frac{k_s}{k_w}\left(\frac{1-\frac{1}{8}\frac{x}{c}}{1-\frac{1}{16}\frac{x}{c}}\right)^{1/2}$	$: \frac{\varepsilon_p}{\sqrt{2}}\frac{k_s}{k_w}\left(\frac{x/2c}{\tan x/2c}\right)^{1/2}$

The validity of these formulae can be judged from tables 26, 27, 28 and 29 which compare the approximate dimensionless characteristics with some of the numerical solutions discussed in Chapter 5. Figures 17, 18, 19 and 20 display the comparison graphically.

The accuracy at the leading edge of the plate is of course that obtained using the thick film model in Chapter 4, where it was observed that agreement was excellent for $0 \leq T_W < 60^\circ C$ and within 10 per cent for $T_W = 90^\circ C$. The same is true near the forward stagnation point on the cylinder so it remains to describe the conditions under which the accuracy is maintained as x increases.

When $T_W = 0^\circ C$ the approximations applied to each configuration remain as accurate, except in the vicinity of the point of separation. For the flat plate when $T_W = 70^\circ C$ the model and numerical results diverge from $x = 0$, however for the cylinder, given the same wall temperature, the

agreement at x = 0 is maintained until $\frac{x}{c} = \frac{\pi}{2}$. Only when $\frac{x}{c} > \frac{\pi}{2}$ is the divergence apparent.

The success of the model when $T_w = 70^\circ C$ applied to the cylinder compared with the plate occurs because of the fundamental difference in the flow configurations, which were mentioned in Chapter 5. For the cylinder $0 < \frac{x}{c} < \frac{\pi}{2}$ is a region of favourable pressure gradient, and it is in such a region that the basic assumption, i.e. $w_s^*(x) >> 0$, is most valid. This is evident in figure 21 which displays the variation of $w_s^*(x)$ and also the magnitude of a typical neglected term, $v_s^* w_m^{*\prime}(x) / w_s^*(x)^2$, in (6.43) compared with unity.

A preliminary conclusion is that the model is reliable at the extreme wall temperature $T_w = 0^\circ C$, except near the point of separation, but generally the method is more applicable to accelerated than decelerated flows. It will be shown later that the model is unable to throw any light onto the questions concerning the position and nature of separation.

To further highlight the accuracy of the thick film approximation applied to the accelerated region consider the ratio $\delta(x) / \delta(0)$. From (6.80) we have:

$$\frac{\delta(x)}{\delta(0)} = \sec\,(x/2c), \qquad (6.81)$$

and hence $$\frac{\delta(\pi/2)}{\delta(0)} = \sqrt{2}.$$

Direct numerical integration yields the results $\delta(\frac{\pi}{2}) / \delta(0) = 1.48$ for $T_w = 70^\circ C$, and $\delta(\pi/2) / \delta(0) = 1.418$ for $T_w = 0^\circ C$.

From (6.69) we have $\frac{\mu}{\mu_s}\frac{\partial u}{\partial y} = E$, constant, and consequently

$$\mu_w \left(\frac{\partial u}{\partial y}\right)_{y=0} = \mu_s \left(\frac{\partial u}{\partial y}\right)_{y=\delta(x)} . \tag{6.82}$$

This implies, as the zeroth order solution, a constant condensate shear across any station $^{x}/_{c}$ = const., whereas the numerical solution shows the wall shear to vanish sooner than the interfacial shear.

Moreover (6.80) implies $C_{fw}.Re_x^{1/2}$ only becomes zero at $^{x}/_{c} = 8$ for the plate problem and $^{x}/_{c} = \pi$ for the cylinder, i.e. at the stations where $u_m^*(x)$ disappears. These are compared with the numerical values $^{x_s}/_{c} = 6.3$ for the plate and $^{x_s}/_{c} = 0.84$ for the cylinder.

Thick film method applied to the Falkner-Skan solutions

In Chapter 3 the similar solutions were found for the mainstream vapour velocity

$$u_m^*(x) = u_0^* \left(x/c\right)^m . \tag{6.83}$$

If this form of $u_m^*(x)$ is inserted into (6.77) then

$$\frac{d}{dx}\left[\Delta(x)^2 u_0^2 \left(\frac{x}{c}\right)^{2m}\right] = 4\frac{E^2}{\varepsilon_p^2} v_s u_0 \left(\frac{x}{c}\right)^m . \tag{6.84}$$

Integrating this and using the condition $\Delta(0) = 0$, we have:

$$\Delta(x) = \left(\frac{\nu_s\, x}{(m+1)\,u_0}\right)^{1/2} \frac{2\varepsilon}{\varepsilon_p} \left(\frac{c}{x}\right)^{m/2} . \qquad (6.85)$$

The motivation for Chapter 3 when discussing the numerical solutions of the Falkner-Skan type equations lay in observing the condensate shear in the hope of learning something about the nature of separation. In the thick film model there is a constant condensate shear so we confine ourselves to seeking the point of separation and the accuracy of $C_{fw}.Re_x^{1/2}$ for $m < 0$.

The dimensionless wall shear is defined by

$$C_{fw}.Re_x^{\frac{1}{2}} = \mu_w \left(\frac{\partial u}{\partial y}\right)_{y=0} . Re_x^{1/2} \Big/ \tfrac{1}{2}\rho_s u_m^{*2} . \qquad (6.86)$$

Introducing (6.57) and (6.60) there results:

$$C_{fw}.Re_x^{1/2} = \frac{\mu_w \cdot \frac{1}{\Delta(x)} \cdot x . u_m^*(x) \left[\frac{\partial u}{\partial y}\right]_{y=0}}{\pm \rho_s u_m^{*2}} \cdot \left(\frac{u_m^*(x).x}{\nu_s}\right)^{1/2}$$

$$= (m+1)^{1/2} . x . \varepsilon_p . \qquad (6.87)$$

Thus the thick film model predicts $C_{fw}.Re_x^{1/2} = 0$ when $m = -1$, which is analogous to the values of $x/c = 8$ for the plate with adverse pressure gradient and $x/c = \pi$ for the cylinder.

Figure 5 shows the variation of $C_{fw}.Re_x^{1/2}$ with m. The similarity between the approximate and the full numerical results in the region $0 \geqslant m \geqslant -0.6$ indicates the model is as reliable for $m = -0.6$ as for $m = 0$. Thus agreement is noted over a wider range of m than in the case of condensation in the presence of an adverse pressure gradient. This may be due to the fact that a singularity exists in the model formula (6.87), when $C_{fw}.Re_x^{1/2}$ is considered as a function of m, of the type that Hartree [20] has shown to exist for the single phase flow. Such a singularity is not present in (6.80) whereas the numerical solutions for the cylinder and plate exhibit behaviour similar to that of the single phase flows where a singularity of the type (5.49) is known to be present.

Conclusion for Part I

The main facts that have been established by numerical integration of the full equations are that condensation delays separation and separation first occurs at the body surface and not at the interface.

These results could not be deduced from the approximate methods which predict constant condensate shear layers and vanishing shear when the mainstream velocity is brought to rest. However, the thick and thin models yield sufficiently accurate results, except near separation, so that the enormous effort of computing the full solution is no longer justified.

The real power of these models lies in the simplicity of the formulae they yield. Knowledge of the mainstream velocity is all that is needed to deduce the condensate thickness $\Delta(x)$ from (6.77) in the thick film approximation. For the thin film we must be given the wall shear for the one phase problem in the similar configuration and (6.30) then yields the coefficients.

i	A_i	B_i	C_i	D_i
0	0.98812999	0.99861010	-5.2082931	-6.4709855
1	-0.02176145	0.00338211	-0.83662530	0.09577277
2	-0.01026523	-0.00297578	0.22822022	-0.06905999
3	-0.01337735	0.00457075	-0.07268900	0.02769182
4	-0.00100025	0.08168510	0.03607111	0.20439558
5	0.06409950	-0.02618713	-0.02584258	-0.14554870
6	0.03788946	-0.27551731	-0.04165410	-0.79356270
7	-0.09626597	0.03468912	0.01821563	0.30923446
8	-0.07863884	0.38483344	0.07235524	.1269448
9	0.04632538	-0.01549540	-0.00643871	-0.17973239
10	0.04270481	-0.18014495	-0.03717798	-0.52353273

Table 1

	Units	Water		Steam
		$0^{\circ}C$	$100^{\circ}C$	
Density . ρ	g/c.c.	0.9998	0.578	0.5977×10^{-3}
Specific heat c_p.	cal/g°c	1.0055	1.0078	
Viscosity, μ.	g/sec.cm.	1.782×10^{-2}	2.812×10^{-3}	1.245×10^{-4}
Conductivity, k	cal/sec.cm.°c.	1.316×10^{-3}	1.631×10^{-3}	
Prandtl N_o, P		13.616	1.7370	
Latent heat of condensation, h_{fg}	cal/g.			538.83

Table 2.

x	$\frac{1}{\phi}\frac{\partial f}{\partial y}$	$\left(\frac{\rho\mu}{\rho_s\mu_s}\right)\frac{1}{\phi^2}\frac{\partial^2 f}{\partial y^2}$	G	η^*	$\frac{\partial f^*}{\partial \eta^*}$
0	0	0.0601	0	0	0.0517
0.1	0.00176	0.0601	0.1123	0.05	0.3575
0.2	0.00416	0.0601	0.2198	0.1	0.5897
0.3	0.00725	0.0601	0.3236	0.15	0.7309
0.4	0.01108	0.0601	0.4287	0.2	0.8238
0.5	0.01570	0.0600	0.5241	0.25	0.8849
0.6	0.02114	0.0600	0.6216	0.3	0.9250
0.7	0.02744	0.0599	0.7180	0.35	0.9513
0.8	0.03462	0.0596	0.8132	0.4	0.9684
0.9	0.04272	0.0593	0.9074	0.45	0.9796
1.0	0.05175	0.0588	1	0.5	0.9868
				0.55	0.9915
				0.6	0.9945
				0.65	0.9965
				0.7	0.9978
				0.8	0.9991
				0.9	0.9996
				1.0	0.9999

Table 3 . Veclocity and temperature distributions for forced flow over a flat plate, Tw = 0^{o}C.

x	$\frac{1}{\phi}\frac{\partial f}{\partial y}$	G	η^*	$\frac{\partial f^*}{\partial \eta^*}$
0	0	0	0	0.02701
0.1	0.00225	0.1008	0.1	0.3461
0.2	0.00460	0.2014	0.2	0.5633
0.3	0.00705	0.3020	0.3	0.7106
0.4	0.00959	0.4025	0.4	0.8097
0.5	0.01224	0.5030	0.5	0.8760
0.6	0.01499	0.6032	0.6	0.9199
0.7	0.01784	0.7031	0.7	0.9487
0.8	0.02079	0.8026	0.8	0.9675
0.9	0.02385	0.9014	0.9	0.9796
1.0	0.02701	1	1.0	0.9833
			1.2	0.9953
			1.4	0.9983
			1.6	0.9994
			1.8	0.9999
			2.0	1.0000

Table (4.) velocity and temperature distributions for flow over a flat plate $T_w = 70^{\circ}C$.

x	$\frac{1}{\beta}\frac{\partial f}{\partial y}$	G.	η^*	$\frac{\partial f^*}{\partial \eta^*}$
0	0	0	0	0.01167
0.1	0.00111	0.1004	0.2	0.3071
0.2	0.00223	0.2007	0.4	0.5246
0.3	0.00336	0.3009	0.6	0.6821
0.4	0.00451	0.4010	0.8	0.7935
0.5	0.00567	0.5009	1.0	0.8700
0.6	0.00684	0.6008	1.2	0.9208
0.7	0.00803	0.7005	1.4	0.9534
0.8	0.00923	0.8002	1.6	0.9735
0.9	0.01045	0.9000	1.8	0.9855
1.0	0.01167	1.0000	2.0	0.9923
			2.2	0.9961
			2.4	0.9981
			2.6	0.9991
			2.8	0.9996
			3.0	0.9998

Table (5.) Velocity and temperature distributions for forced flow over the plate $T_w = 90^oC$.

x	$\frac{1}{\phi}\frac{\partial f}{\partial \gamma}$	G.	η^*	$\frac{\partial f^*}{\partial \eta^*}$
0	0	0	0	0.000513
0.1	5.133, -5	0.100	0.2	0.09577
0.2	1.027, -4	0.200	0.4	0.1906
0.3	1.540, -4	0.300	0.6	0.2845
0.4	2.053, -4	0.400	0.8	0.3766
0.5	2.567, -4	0.500	1.0	0.4658
0.6	3.080, -4	0.600	1.2	0.5506
0.7	3.593, -4	0.700	1.4	0.6298
0.8	4.107, -4	0.800	1.6	0.7018
0.9	4.620, -4	0.900	1.8	0.7658
1.0	5.133, -4	1.000	2.0	0.8209
			2.4	0.9039
			2.8	0.9546
			3.2	0.9812
			3.6	0.9932
			4.0	0.9979
			4.4	0.9994
			4.8	0.9999
			5.2	1.0000

Table 6. Velocity and temperature distributions for forced flow over plate. $T_W = 99.99^\circ C$

T_W	$\frac{\delta}{x} Re_x^{1/2}$	$\frac{\delta_1}{x} Re_x^{*1/2}$	$\frac{\delta_2}{x} Re_x^{*1/2}$	$C_{f_W} Re_x^{1/2}$	$C_{f_I} Re_x^{1/2}$	$Nu.Re_x^{-1/2}$	$f^*(o)$.
0.00	3.223	0.159	0.0832	0.0605	0.0588	0.373	8.284
10.00	3.054	0.165	0.0862	0.0579	0.0568	0.381	7.977
20.00	1.896	0.174	0.0907	0.0551	0.0540	0.389	7.570
30.00	2.749	0.187	0.0969	0.0515	0.0505	0.400	7.055
40.00	1.612	0.205	0.1059	0.0471	0.0463	0.413	6.426
50.00	2.484	0.231	0.1187	0.0418	0.0412	0.426	5.680
60.00	2.363	0.271	0.1378	0.0357	0.0353	0.441	4.813
70.00	2.245	0.334	0.1686	0.0288	0.0285	0.459	3.825
80.00	2.120	0.450	0.2214	0.0211	0.0210	0.481	2.717
90.00	1.942	0.699	0.3286	0.0128	0.0127	0.521	1.495
98.00	1.449	1.260	0.5322	0.0058	0.0058	0.689	0.401
99.99	0.290	1.705	0.6602	0.0035	0.0035	3.452	0.010

Table 7. Characteristics for condensation onto a plate with $U_m^*(x) = U_o^*$, constant.

m	0	-0.2	-0.4	-0.6	-0.7	-0.75	-0.763125
Y				$10.\frac{df}{dY}$			
0	0	0	0	0	0	0	0
0.2	0.095	0.105	0.120	0.143	0.157	0.159	0.146
0.4	0.253	0.281	0.321	0.385	0.428	0.437	0.409
0.6	0.482	0.535	0.615	0.741	0.831	0.860	0.820
0.8	0.778	0.877	1.009	1.222	1.379	1.444	1.396
1.0	1.177	1.309	1.506	1.821	2.056	2.167	2.122
t	2.28	2.56	2.97	3.69	4.38	5.05	5.55
η^*				$df^*/d\eta^*$			
0	0.052	0.051	0.051	0.049	0.047	0.043	0.038
0.1	0.589	0.544	0.489	0.409	0.345	0.290	0.249
0.2	0.823	0.781	0.725	0.632	0.549	0.471	0.411
0.3	0.925	0.895	0.853	0.771	0.689	0.605	0.537
0.4	0.968	0.951	0.921	0.858	0.786	0.705	0.636
0.5	0.987	0.977	0.959	0.912	0.853	0.780	0.713
0.6	0.995	0.989	0.978	0.946	0.899	0.836	0.774
0.8	0.999	0.998	0.994	0.980	0.953	0.909	0.861
1.0	1.000	1.000	0.998	0.993	0.978	0.950	0.915
1.2			1.000	0.997	0.990	0.973	0.949
1.4				0.999	0.996	0.986	0.970
1.6				1.000	0.998	0.992	0.982
1.8					0.999	0.996	0.990
2.0					1.000	0.998	0.994
2.2						0.999	0.997
2.4						0.999	0.998
2.6						1.000	0.999
2.8							0.999
3.0							1.000

Table 8: Dimensionless velocities for Falkner Skan mainstream, $u_m^* = 1 \omega^* \left(\frac{x}{c}\right)^m$.

m	$\frac{\delta(x)}{x}.Re_x^{1/2}$	$\frac{\delta_1}{x}.Re_x^{*1/2}$	$\frac{\delta_2}{x}.Re_x^{*1/2}$	$f^{*}(0)$	$C_{f_W}.Re_x^{\frac{1}{2}}$	$C_{f_I}.Re_x^{1/2}$	$Nu.Re_x^{-1/2}$
1	2.27	0.109	0.057	8.32	0.0878	0.0852	0.531
0	3.22	0.159	0.083	8.28	0.0601	0.0588	0.373
-0.1	3.41	0.171	0.087	8.69	0.0566	0.0549	0.353
-0.2	3.62	0.182	0.094	9.21	0.0530	0.0515	0.332
-0.3	3.88	0.197	0.102	9.82	0.0491	0.0477	0.310
-0.4	4.20	0.216	0.112	10.58	0.0448	0.0436	0.286
-0.5	4.62	0.242	0.126	11.53	0.0400	0.0390	0.260
-0.6	5.22	0.282	0.147	12.77	0.0343	0.0337	0.230
-0.7	6.20	0.359	0.187	14.35	0.0265	0.0268	0.194
-0.75	7.14	0.457	0.238	14.94	0.0199	0.0214	0.168
-0.76	7.54	0.510	0.264	14.74	0.0171	0.0194	0.159
-0.7625	7.74	0.540	0.280	14.51	0.0157	0.0185	0.155
-0.763125	7.85	0.556	0.288	14.36	0.0150	0.0180	0.153
-0.763291	7.92	0.569	0.294	14.22	0.0144	0.176	0.152

Table 9

Flow characteristics for Falkner-Skan mainstream.

T_W	EXACT			Approximate formulae (4·28) – (4·30).		
	$\frac{\delta(x)}{x} Re_x^{1/2}$	$C_{fw}.Re_x^{1/2}$	$Nu.Re_x^{-1/2}$	$\frac{\delta(x)}{x}.Re_x^{1/2}$	$C_{fw}.Re_x^{1/2}$	$Nu.Re_x^{-1/2}$
99.99	0.289	0.00354	3.45	0.291	0.00349	3.44
99.9	0.630	0.00375	1.63	0.627	0.00349	1.59
99.5	1.01	0.0043	0.99	1.07	0.00349	0.93
99	1.22	0.0048	0.820	1.35	0.00349	0.740
98	1.45	0.0058	0.689	1.704	0.00349	0.587

Table 10: Comparison of thin film model and numerical solution, $u_m^*(x) = u_0^*$.

	Exact solution			Thick film Solution of (4.48)-(4.51)		
Tw	ϕ	$G'(0)$	$f''(0)$	ϕ	$G'(0)$	$f''(0)$.
0	2.276	1.152	0.0333	2.287	1.152	0.033
20	2.048	1.082	0.0440	2.057	1.082	0.0439
40	1.847	1.041	0.0472	1.858	1.041	0.0470
60	1.671	1.016	0.0414	1.688	1.016	0.0411
80	1.500	1.006	0.0260	1.542	1.006	0.0255
90	1.373	1.004	0.0151	1.476	1.004	0.0140

Table 11 : Comparison of full thick film approximation with numerical similar solutions.

T_w	χ	E	ε_p.
0	0.1077	0.903	0.609
10	0.0969	0.912	0.644
20	0.861	0.939	0.682
30	0.0754	0.952	0.721
40	0.0646	0.964	0.762
50	0.0538	0.974	0.802
60	0.0431	0.982	0.843
70	0.0323	0.989	0.883
80	0.0215	0.993	0.922
90	0.0108	0.998	0.962
98	0.0021	1.000	0.996

Table 12 . Constants E and ε_p of thick film approximation

Tw	Exact results			Thick limit as $\chi \to 0$		
	ϕ	$C_{f_w} Re^{1/2}$	$Nu\, Re^{-1/2}$	ϕ	$C_{f_w} Re^{1/2}$	$Nu\, Re^{-1/2}$
0	2.276	0.0605	0.373	2.099	0.0655	0.377
20	2.048	0.0551	0.389	1.945	0.0588	0.389
40	1.847	0.0471	0.413	1.790	0.0492	0.410
60	1.671	0.0357	0.441	1.648	0.0363	0.437
80	1.500	0.0211	0.481	1.523	0.0199	0.467
90	1.373	0.0128	0.521	1.467	0.0104	0.483

Table 13: Comparison of numerical results with formulae (4.68) of thick film approximation.

	0	1	2	3	4	5	6	6.2
y				10. $\partial F/\partial y$.				
0	0	0	0	0	0	0	0	0
0.2	0.095	0.092	0.088	0.084	0.080	0.074	0.060	0.049
0.4	0.253	0.244	0.235	0.225	0.215	0.203	0.177	0.161
0.6	0.482	0.466	0.449	0.432	0.415	0.396	0.372	0.361
0.8	0.788	0.763	0.737	0.709	0.683	0.657	0.644	0.653
1.0	1.177	1.139	1.100	1.057	1.016	0.972	0.937	0.956
t	2.28	2.53	2.86	3.36	4.05	5.35	8.69	10.37
y^*	$\partial F^*/\partial y^*$							
0	0.052	0.045	0.038	0.031	0.025	0.018	0.011	0.009
0.05	0.375	0.304	0.237	0.172	0.118	0.069	0.026	0.020
0.1	0.589	0.483	0.380	0.279	0.194	0.112	0.041	0.030
0.15	0.730	0.606	0.484	0.360	0.254	0.150	0.056	0.040
0.2	0.823	0.690	0.559	0.422	0.303	0.182	0.069	0.049
0.25	0.885	0.749	0.613	0.470	0.342	0.209	0.082	0.058
0.3	0.925	0.789	0.680	0.506	0.373	0.233	0.094	0.068
0.4	0.968	0.835	0.700	0.554	0.419	0.272	0.117	0.086
0.5	0.987	0.867	0.724	0.582	0.448	0.300	0.137	0.103
0.6	0.995	0.867	0.737	0.560	0.467	0.321	0.155	0.119
0.8	0.999	0.873	0.748	0.612	0.487	0.348	0.186	0.148
1.0	1.000	0.875	0.749	0.617	0.495	0.362	0.209	0.173
1.2			0.750	0.618	0.498	0.369	0.228	0.195
1.4				0.619	0.500	0.374	0.243	0.215
1.6						0.375	0.248	0.221
2.0							0.250	0.225

Table 14. Dimensionless velocity distributions; $u_m^*(x) = u_0^*(1 - \frac{1}{8}\frac{x}{c})$, $T_w = 0°C$.

x/c	0	1.0	2.0	2.5	3.0	3.5	4.0	4.2
Y	$10^2 . \partial F/\partial Y$							
0	0	0	0	0	0	0	0	0
0.2	0.730	0.702	0.666	0.647	0.624	0.592	0.515	0.275
0.4	1.522	0.462	1.396	1.359	1.317	1.265	1.162	0.889
0.6	2.378	2.287	2.190	2.138	2.081	2.019	1.939	1.841
0.8	3.299	3.177	3.048	1.982	1.914	1.850	1.828	3.070
1.0	4.284	4.130	3.969	3.887	3.808	3.741	3.776	4.375
t	1.588	1.796	2.109	2.341	2.674	3.231	4.637	7.09
y^*	$\partial F^*/\partial y^*$							
0.	0.027	0.023	0.018	0.017	0.014	0.012	0.008	0.006
0.1	0.346	0.270	0.197	0.161	0.126	0.090	0.050	0.031
0.2	0.563	0.447	0.333	0.276	0.219	0.159	0.091	0.057
0.3	0.710	0.574	0.437	0.367	0.296	0.220	0.131	0.086
0.4	0.809	0.665	0.517	0.440	0.360	0.273	0.169	0.115
0.5	0.875	0.730	0.577	0.497	0.413	0.320	0.206	0.144
0.6	0.919	0.775	0.623	0.542	0.456	0.360	0.241	0.174
0.8	0.967	0.829	0.683	0.604	0.520	0.425	0.303	0.232
1.0	0.987	0.854	0.715	0.641	0.562	0.472	0.355	0.284
1.2	0.995	0.866	0.733	0.663	0.588	0.504	0.396	0.330
1.4	0.998	0.871	0.742	0.674	0.604	0.526	0.427	0.368
1.6	0.999	0.873	0.746	0.681	0.613	0.540	0.451	0.398
1.8	1.000	0.874	0.748	0.684	0.619	0.549	0.467	0.421
2.0		0.875	0.749	0.685	0.621	0.855	0.479	0.438
2.4			0.750	0.687	0.624	0.560	0.492	0.459
2.8				0.687	0.625	0.562	0.498	0.470
3.2						0.562	0.500	0.473
3.6								0.474
4.0								0.475

Table 15: Dimensionless velocity distributions.

$u_m^*(x) = u_0^* (1 - \frac{1}{8} \frac{x}{c})$; $T_W = 70°C$.

FLAT PLATE $T_w = 99.99^{\circ}C$

x/c	0	0.2	0.4	0.6	0.8	0.9	0.96
Y	$10^4 . \partial F/\partial Y.$						
0	0	0	0	0	0	0	0
0.2	0.210	0.205	0.200	0.193	0.185	0.177	0.160
0.4	0.420	0.411	0.400	0.387	0.372	0.358	0.337
0.6	0.631	0.616	0.600	0.582	0.560	0.545	0.530
0.8	0.841	0.822	0.801	0.778	0.751	0.737	0.741
1.0	1.051	1.028	1.002	0.974	0.943	0.933	0.969
t	0.205	0.220	0.242	0.277	0.353	0.468	0.729
$Y.^*$	$\partial F^*/\partial Y.^*$						
0	0.0005	0.0005	0.0004	0.0004	0.0003	0.0002	0.0001
0.2	0.095	0.082	0.068	0.052	0.033	0.021	0.013
0.4	0.191	0.165	0.138	0.109	0.074	0.051	0.034
0.6	0.285	0.249	0.212	0.171	0.120	0.087	0.063
0.8	0.377	0.334	0.287	0.236	0.173	0.131	0.099
1.0	0.466	0.417	0.364	0.305	0.231	0.181	0.143
1.2	0.551	0.498	0.441	0.375	0.293	0.236	0.193
1.6	0.702	0.647	0.586	0.515	0.424	0.358	0.248
2.0	0.821	0.770	0.712	0.643	0.553	0.486	0.307
2.4	0.904	0.860	0.809	0.749	0.667	0.605	0.554
2.8	0.955	0.917	0.876	0.826	0.758	0.706	0.663
3.2	0.981	0.950	0.915	0.875	0.822	0.782	0.748
3.6	0.993	0.965	0.936	0.903	0.862	0.833	0.808
4.0	0.998	0.972	0.945	0.916	0.884	0.862	0.846
4.4	0.999	0.974	0.948	0.922	0.894	0.877	0.866
4.8	1.000	0.975	0.950	0.924	0.898	0.883	0.875
5.2				0.925	0.899	0.886	0.879
5.6					0.900	0.887	0.881
6.0						0.887	0.881

Table. 16.

$\frac{x}{c}$	0	0.3927	0.7854	1.1781	1.5708	1.9635	2.3562	2.6507	2.719
Y	$10.\ \frac{\partial F}{\partial Y}$								
0	0	0	0	0	0	0	0	0	0
0.2	0.0963	0.0956	0.0937	0.0904	0.0859	0.0800	0.0717	0.0572	0.0431
0.4	0.2549	0.2533	0.2483	0.2400	0.2284	0.2137	0.1944	0.1677	0.1468
0.6	0.4841	0.4819	0.4715	0.4562	0.4351	0.4086	0.3770	0.3478	0.3352
0.8	0.7908	0.7856	0.7715	0.7457	0.7120	0.6703	0.6235	0.5982	0.6103
1.0	1.1827	1.1750	1.1521	1.1150	1.0633	0.9991	0.9238	0.8664	0.8644
t	2.267	2.311	2.455	2.732	3.225	4.146	6.204	11.05	14.40
Y^*	$\frac{\partial F^*}{\partial Y^*}$								
0	0.0522	0.0508	0.0469	0.0408	0.0330	0.0241	0.0149	0.0078	0.0060
0.05	0.3827	0.3677	0.3250	0.2615	0.1872	0.1118	0.0512	0.0169	0.0094
0.1	0.5989	0.5767	0.5133	0.4173	0.3024	0.1851	0.0835	0.0255	0.0129
0.15	0.7400	0.7144	0.6404	0.5270	0.3883	0.2424	0.1149	0.0334	0.0166
0.2	0.8319	0.8048	0.7262	0.6042	0.4523	0.2885	0.1357	0.0411	0.0203
0.3	0.9302	0.9027	0.8226	0.6965	0.5355	0.3548	0.1756	0.0559	0.0278
0.4	0.9713	0.9444	0.8659	0.7418	0.5815	0.3972	0.2060	0.0693	0.0356
0.5	0.9883	0.9620	0.8852	0.7639	0.6067	0.4243	0.2292	0.0817	0.0434
0.6	0.9953	0.9693	0.8937	0.7745	0.6205	0.4415	0.2469	0.0929	0.0511
0.8	0.9993	0.9736	0.8991	0.7821	0.6321	0.4593	0.2704	0.1124	0.0660
1.0	0.9999	0.9743	0.9001	0.7838	0.6354	0.4663	0.2838	0.1281	0.0799
1.2	1.0000	0.9745	0.9003	0.7841	0.6363	0.4690	0.2913	0.1407	0.0924
1.4		0.9745	0.9003	0.7842	0.6366	0.4700	0.2955	0.1504	0.1035
1.6					0.6366	0.4704	0.2977	0.1579	0.1130
2.0						0.4705	0.2996	0.1677	0.1277
2.4							0.3000	0.1729	0.1371
2.8							0.3001	0.1763	0.1451
3.2								0.1777	0.1466
3.6									0.1486
4.0									0.1496
5.0									0.1506

Table 17: Condensation onto cylinder: $T_W = 0^\circ C$.

x/c	0	0.3927	0.7854	1.1781	1.5708	1.9635	2.199	2.327
y	$10^2 \times \partial F/\partial y$							
0	0	0	0	0	0	0	0	0
0.2	0.767	0.761	0.745	0.717	0.677	0.621	0.559	0.284
0.4	1.593	1.581	1.548	1.491	1.411	1.303	1.203	0.891
0.6	2.479	2.462	2.410	2.324	2.204	2.049	1.932	1.806
0.8	3.429	3.405	3.334	3.217	3.057	2.856	2.735	2.945
1	4.444	4.412	4.322	4.172	3.967	3.712	3.584	4.084
t	1.525	1.557	1.663	1.873	2.273	3.173	4.68	9.24
y*	$\partial F^*/\partial y^*$							
0	0.029	0.028	0.026	0.022	0.017	0.012	0.008	0.004
0.1	0.378	0.362	0.317	0.249	0.169	0.088	0.044	0.017
0.2	0.606	0.582	0.514	0.410	0.285	0.153	0.077	0.030
0.3	0.752	0.725	0.646	0.525	0.373	0.208	0.109	0.043
0.4	0.846	0.817	0.735	0.606	0.441	0.255	0.138	0.057
0.5	0.905	0.876	0.793	0.661	0.491	0.294	0.165	0.071
0.6	0.942	0.913	0.831	0.700	0.530	0.326	0.189	0.087
0.8	0.919	0.952	0.873	0.746	0.580	0.376	0.228	0.119
1.0	0.993	0.966	0.889	0.768	0.607	0.410	0.263	0.149
1.2	0.997	0.972	0.896	0.777	0.622	0.432	0.290	0.177
1.4	0.999	0.974	0.899	0.781	0.629	0.447	0.312	0.203
1.6	1.000	0.974_5	0.900	0.783	0.633	0.456	0.328	0.225
1.8				0.784	0.635	0.462	0.340	0.244
2				0.784_2	0.636	0.466	0.348	0.260
2.2					0.636_4	0.468	0.355	0.273
2.4					0.636_6	0.469	0.360	0.283
2.6						0.470	0.362	0.292
2.8						0.470_5	0.364	0.298
3							0.366	0.304
3.4							0.367	0.310
4							0.368	0.313

Table 18: Condensation onto cylinder: $T_W = 70^\circ C$.

x/c	0	0.393	0.785	1.178	1.571	1.728	1.806	1.823
Y	$10^4 \frac{\partial F}{\partial y}$							
0	0	0	0	0	0	0	0	0
0.2	0.291	0.288	0.280	0.268	0.248	0.236	0.221	0.044
0.4	0.581	0.576	0.561	0.535	0.496	0.473	0.451	0.245
0.6	0.870	0.863	0.840	0.801	0.744	0.712	0.689	0.609
0.8	1.159	1.149	1.119	1.067	0.992	0.952	0.936	1.133
1	1.447	1.434	1.396	1.333	1.239	1.193	1.191	1.816
	0.148	0.152	0.166	0.196	0.277	0.389	0.665	1.761
y^*	$\frac{\partial F^*}{\partial y^*}$							
0	9.7×10^{-4}	9.4×10^{-4}	8.4×10^{-4}	6.8×10^{-4}	4.5×10^{-4}	3.1×10^{-4}	1.8×10^{-4}	1.0×10^{-4}
0.2	0.229	0.216	0.180	0.126	0.062	0.032	0.013	0.008
0.4	0.417	0.395	0.333	0.239	0.122	0.067	0.031	0.020
0.6	0.569	0.542	0.462	0.340	0.182	0.105	0.050	0.037
0.8	0.689	0.658	0.569	0.427	0.240	0.146	0.081	0.059
1.0	0.780	0.748	0.654	0.503	0.295	0.187	0.110	0.083
1.2	0.849	0.816	0.773	0.566	0.347	0.229	0.143	0.114
1.6	0.933	0.903	0.840	0.660	0.437	0.309	0.213	0.179
2.0	0.974	0.945	0.875	0.719	0.507	0.381	0.283	0.247
2.4	0.991	0.964	0.890	0.753	0.558	0.441	0.348	0.314
2.8	0.998	0.971	0.897	0.770	0.592	0.487	0.403	0.373
3.2	0.999	0.973	0.899	0.779	0.613	0.520	0.447	0.421
3.6	1.000	0.974	0.900	0.782	0.625	0.542	0.480	0.459
4.0	1.000	0.974	0.900	0.784	0.631	0.555	0.503	0.486
4.4				0.784	0.634	0.563	0.518	0.505
4.8					0.636	0.567	0.527	0.516
5.2						0.570	0.5333	0.523
6.0						0.572	0.537	0.530
7.0							0.538	0.531

Table 19: Condensation onto cylinder: $T_W = 99.99^{\circ}C$.

x/c	$\frac{\delta(x)}{x} \cdot Re_x^{1/2}$	$\frac{\delta_1}{x} \cdot Re_x^{*1/2}$	$\frac{\delta_2}{x} \cdot Re_x^{*1/2}$	$C_{f_w} \cdot Re_x^{1/2}$	$C_{f_I} \cdot Re_x^{1/2}$	$Nu \cdot Re_x^{-1/2}$	$\frac{[v^*]_0}{u_m^*} \cdot Re_x^{*1/2}$
0	3.22	0.159	0.083	0.0606	0.0588	0.372	5.84
0.4	3.27	0.162	0.085	0.0596	0.0579	0.367	5.74
0.8	3.31	0.165	0.086	0.0586	0.0568	0.362	5.64
1.2	3.38	0.168	0.088	0.0575	0.0558	0.356	5.54
1.6	3.43	0.172	0.090	0.0562	0.0546	0.350	5.44
2.0	3.50	0.176	0.092	0.0549	0.0533	0.343	5.33
2.4	3.58	0.181	0.095	0.0534	0.0518	0.336	5.23
2.8	3.67	0.187	0.098	0.0517	0.0502	0.327	5.12
3.2	3.77	0.194	0.101	0.0498	0.0484	0.318	5.00
3.6	3.90	0.203	0.106	0.0478	0.0463	0.308	4.84
4.0	4.05	0.214	0.111	0.0454	0.0439	0.297	4.66
4.4	4.24	0.228	0.118	0.0424	0.0410	0.283	4.46
4.8	4.48	0.246	0.126	0.0389	0.0375	0.267	4.22
5.0	4.64	0.258	0.131	0.0368	0.0354	0.258	4.08
5.2	4.82	0.272	0.137	0.0344	0.0331	0.248	3.94
5.4	5.04	0.289	0.143	0.0317	0.0305	0.237	3.76
5.6	5.30	0.310	0.150	0.0284	0.0274	0.224	3.58
5.8	5.67	0.337	0.157	0.0245	0.0237	0.210	3.36
6.0	6.14	0.372	0.164	0.0196	0.0193	0.191	3.12
6.1	6.49	0.390	0.166	0.0149	0.0178	0.177	2.96
6.2	6.93	0.419	0.168	0.0108	0.0153	0.160	2.78
6.3	7.67	0.440	0.166	0.0047	0.0124	0.137	-

Table 20 : Condensation characteristics, Flat plate

$$u_m^*(x) = u_0^* \left(1 - \frac{1}{8}\frac{x}{c}\right), \quad T_w = 0°C.$$

FLAT PLATE $T_w = 70^{\circ}C$

x/c	$\frac{\delta(x)}{x} Re_x^{1/2}$	$\frac{\delta_1}{x} Re_x^{*1/2}$	$\frac{\delta_2}{x} Re_x^{*1/2}$	$\frac{U_0^*}{U_m^*} Re_x^{*1/2}$	$Cf_w Re_x^{1/2}$	$Cf_I Re_x^{1/2}$	$Nu Re_x^{-1/2}$
0	2.24	0.334	0.169	2.70	0.0288	0.0285	0.459
0.2	2.26	0.339	0.171	2.68	0.0283	0.0281	0.454
0.4	2.28	0.345	0.173	2.65	0.0279	0.0277	0.449
0.6	2.31	0.351	0.175	2.62	0.0274	0.0272	0.444
0.8	2.34	0.356	0.178	2.59	0.0269	0.0268	0.439
1.0	2.37	0.362	0.181	2.55	0.0263	0.0263	0.433
1.2	2.41	0.369	0.184	2.52	0.0257	0.0258	0.427
1.4	2.45	0.377	0.188	1.48	0.0251	0.0252	0.421
1.6	2.49	0.386	0.192	2.44	0.0244	0.0246	0.414
1.8	2.54	0.396	0.197	2.40	0.0236	0.0239	0.406
2.0	2.58	0.407	0.202	2.35	0.0228	0.0232	0.398
2.2	2.64	0.419	0.208	2.30	0.0219	0.0224	0.389
2.4	2.71	0.433	0.214	2.24	0.0210	0.0216	0.380
2.6	2.79	0.450	0.221	2.18	0.0199	0.0206	0.369
2.8	2.88	0.469	0.229	2.11	0.0187	0.0196	0.357
3.0	2.99	0.493	0.239	2.03	0.0173	0.0184	0.344
3.2	3.13	0.521	0.250	1.94	0.0158	0.0171	0.329
3.4	3.31	0.556	0.264	1.84	0.0140	0.0156	0.310
3.6	3.56	0.602	0.280	1.71	0.0120	0.0138	0.288
3.8	3.94	0.664	0.300	1.55	0.0094	0.0116	0.260
3.9	4.23	0.705	0.312	1.45	0.0079	0.0103	0.242
4.0	4.63	0.756	0.325	1.34	0.0062	0.0089	0.219
4.1	5.27	0.839	0.340	1.21	0.0041	0.0072	0.189
4.2	6.64	1.007	0.357	–	0.0007	0.0054	0.127

Table. 21.

$\frac{x}{C}$	$\frac{\delta(x)}{x} \cdot Re_x^{1/2}$	$\frac{\delta_1}{x} \cdot Re_x^{1/2}$	$\frac{\delta_1}{x} \cdot Re_x^{1/2}$ (Howarth)	$\frac{\delta_2}{x} \cdot Re_x^{1/2}$	$Cf_W \cdot Re_x^{1/2}$	$Cf_I \cdot Re_x^{1/2}$	$Nu \cdot Re_x^{-1/2}$
0.0	0.290	1.705	1.72	0.660	0.00354	0.00352	3.452
0.1	0.298	1.751	1.77	0.670	0.00333	0.00334	3.356
0.2	0.308	1.803	1.82	0.681	0.00310	0.00311	3.250
0.3	0.319	1.861	1.88	0.692	0.00286	0.00288	3.131
0.4	0.334	1.927	1.95	0.703	0.00260	0.00262	2.996
0.5	0.352	2.004	2.03	0.716	0.00231	0.00234	2.840
0.6	0.377	2.095	2.12	0.730	0.00200	0.00204	2.654
0.7	0.413	2.206	2.23	0.743	0.00164	0.00169	2.424
0.8	0.473	2.351	2.38	0.758	0.00122	0.00129	2.114
0.9	0.624	2.571	2.62	0.775	0.00067	0.00077	1.604
0.96	0.969	2.908	3.01	0.792	0.00017	0.00028	1.003

Table 22: Characteristics for flat plate with adverse pressure gradient. $T_W = 99.99^{\circ}C$.

x/c	$\frac{\delta(x)}{x} Re_x^{1/2}$	$\frac{\delta_1}{x} . Re_x^{1/2}$	$\frac{\delta_2}{x} . Re_x^{1/2}$	$\frac{[w^*]_{y^*=0}}{w_{\infty}^*} . Re_x^{*\frac{1}{2}}$	$C_{f_w} Re_x^{1/2}$	$C_{f_I} . Re_x^{1/2}$	$Nu . Re_x^{-\frac{1}{2}}$
0	2.27	0.109	0.057	8.32	0.0878	0.0852	0.531
0.1571	2.27	0.110	0.057	8.31	0.0877	0.0877	0.530
0.3142	2.27	0.110	0.057	8.28	0.0874	0.0848	0.529
0.4712	2.29	0.111	0.058	8.24	0.0869	0.0843	0.526
0.6283	2.30	0.112	0.058	8.18	0.0862	0.0835	0.521
0.7854	2.33	0.113	0.059	9.09	0.0852	0.0826	0.516
0.9425	2.36	0.115	0.060	7.99	0.0840	0.0814	0.510
1.100	2.40	0.117	0.061	7.89	0.0824	0.0800	0.501
1.257	2.44	0.119	0.062	7.71	0.0806	0.0782	0.492
1.141	2.50	0.122	0.064	7.53	0.0785	0.0761	0.480
1.571	2.57	0.126	0.066	7.33	0.0759	0.0735	0.467
1.728	2.66	0.132	0.069	7.09	0.0728	0.0706	0.451
1.885	2.77	0.139	0.072	6.84	0.0691	0.0670	0.433
2.042	2.92	0.148	0.076	6.46	0.0646	0.0626	0.411
2.199	3.12	0.160	0.082	6.06	0.0589	0.0571	0.384
2.353	3.40	0.181	0.092	5.69	0.0522	0.0512	0.353
2.513	3.84	0.221	0.117	4.92	0.0419	0.0412	0.310
2.670	4.85	0.331	0.154	4.02	0.0225	0.0231	0.240
2.710	5.40	0.394	0.170	3.72	0.0150	0.0160	0.208
2.719	5.60	0.419	0.174	-	0.0118	0.0130	0.198

Table 23; Cylinder Characteristics $T_W = 0^{\circ}C$.

CYLINDER $T_W = 70^{\circ}C$

x/c	$\frac{\delta(x)}{x} Re_x^{1/2}$	$\frac{\delta_1}{x} Re_x^{1/2}$	$\frac{\delta_2}{x} Re_x^{1/2}$	$Cf_W . Re_x^{1/2}$	$Cf_I . Re_x^{1/2}$	$Nu . Re_x^{-1/2}$	$\frac{V^*(x,0)}{U_\infty^*} Re_x^{1/2}$
0	1.525	0.211	0.106	0.0466	0.0451	0.675	3.98
0.1571	1.526	0.212	0.107	0.0405	0.0450	0.674	3.98
0.3142	1.533	0.213	0.107	0.0463	0.0448	0.672	3.96
0.4712	1.543	0.214	0.108	0.0459	0.0444	0.667	3.93
0.6283	1.558	0.217	0.109	0.0453	0.0439	0.661	3.90
0.7854	1.578	0.220	0.110	0.0445	0.0431	0.652	3.85
0.9425	1.605	0.225	0.113	0.0435	0.0422	0.641	3.78
1.100	1.639	0.231	0.116	0.0422	0.0411	0.628	3.70
1.257	1.682	0.239	0.120	0.0406	0.0397	0.612	3.61
1.414	1.739	0.249	0.125	0.0387	0.0379	0.592	3.49
1.571	1.813	0.263	0.132	0.0363	0.0357	0.567	3.35
1.728	1.917	0.283	0.141	0.0332	0.0330	0.537	3.17
1.885	2.069	0.313	0.154	0.0292	0.0294	0.497	2.93
2.042	2.321	0.360	0.173	0.0236	0.0245	0.443	2.61
2.199	2.875	0.454	0.206	0.0150	0.0171	0.356	2.14
2.278	3.588	0.548	0.230	0.0086	0.0115	0.282	1.82
2.327	5.168	0.662	0.255	0.0012	0.0068	0.170	-

Table .24.

x/c radians.	$\frac{\delta(x)}{x} \cdot Re_x^{1/2}$	$\frac{\delta_1}{x} \cdot Re_x^{1/2}$	$\frac{\delta_2}{x} \cdot Re_x^{1/2}$	$\frac{\delta_1}{x} \cdot Re_x^{1/2}$ (Terrill)	$C_{fw} \cdot Re_x^{1/2}$	$C_{f_I} \cdot Re_x^{1/2}$	$Nu \cdot Re_x^{-1/2}$
0	0.148	0.644	0.291	0.648	0.0132	0.0130	6.734
0.1571	0.149	0.646	0.292	0.650	0.0132	0.0130	6.720
0.3142	0.150	0.652	0.294	0.656	0.0130	0.0128	6.677
0.4712	0.151	0.661	0.298	0.665	0.0128	0.0126	6.604
0.6283	0.154	0.675	0.303	0.680	0.0124	0.0123	6.498
0.7864	0.157	0.695	0.311	0.700	0.0120	0.0118	6.353
0.9425	0.162	0.722	0.320	0.727	0.0113	0.0112	6.164
1.100	0.169	0.759	0.347	0.764	0.0105	0.0104	5.917
1.257	0.179	0.811	0.351	0.816	0.00951	0.00942	5.593
1.414	0.194	0.886	0.374	0.891	0.00817	0.00811	5.153
1.571	0.222	1.005	0.406	1.011	0.00633	0.00633	4.514
1.728	0.295	1.230	0.453	1.25	0.00357	0.00367	3.385
1.806	0.499	1.495	0.485	1.53	0.00124	0.00147	2.003
1.823	1.284	1.627	0.502	-	0.0004	0.0012	0.771

Table 25: Cylinder Characteristics, $T_W = 99.99^{\circ}C$.

x/c	$\frac{\delta(x)}{x} \cdot Re_x^{1/2}$		$C_{fw} \cdot Re_x^{1/2}$		$Nu \cdot Re_x^{-1/2}$	
	Exact	Approx	Exact	Approx	Exact	Approx
0	3.22	2.97	0.0606	0.0655	0.373	0.377
0.8	3.31	3.05	0.0586	0.0638	0.363	0.367
1.6	3.43	3.15	0.0562	0.0618	0.350	0.356
2.4	3.58	3.27	0.0534	0.0595	0.336	0.342
3.2	3.78	3.43	0.0498	0.0567	0.318	0.327
4.0	4.05	3.64	0.0454	0.0535	0.297	0.308
4.8	4.48	3.93	0.0389	0.0495	0.267	0.285
5.6	5.30	4.37	0.0284	0.0445	0.224	0.256
6.0	6.15	4.69	0.0196	0.0414	0.191	0.238

Table 26 : Comparison of thick film formulae (6.80) with full numerical solution, $u_m^*(x) = u_0^*(1-\frac{1}{8}\frac{x}{c})$, $T_w = 0°C$.

x/c	$\frac{\delta(x)}{x} \cdot Re_x^{1/2}$		$Cf_w \cdot Re_x^{1/2}$		$Nu \cdot Re_x^{-1/2}$	
	Exact	Approx	Exact	Approx	Exact	Approx
0	2.24	2.24	0.0288	0.0285	0.459	0.452
0.4.	2.28	2.27	0.0279	0.0282	0.449	0.446
0.8	2.34	2.30	0.0269	0.278	0.439	0.439
1.2	2.41	2.34	0.0257	0.0273	0.427	0.433
1.6	2.49	2.38	0.0244	0.0269	0.414	0.426
2.0	2.58	2.42	0.0228	0.0264	0.398	0.418
2.4	2.71	2.47	0.0210	0.0259	0.380	0.410
2.8	2.88	2.52	0.0187	0.0253	0.357	0.400
3.2	3.13	2.59	0.0158	0.0247	0.329	0.391
3.6	3.56	2.66	0.0120	0.6240	0.288	0.380
4.0	4.63	2.74	0.0062	0.0233	0.219	0.369
4.2	6.64	2.79	0.0007	0.0229	0.127	0.362

Table 27 : Comparison of full numerical results and thick film formulae (6.80) applied the flat plate, $U_m^*(x) = U_0^* \left(1 - \frac{1}{8}\frac{x}{c}\right)$ and Tw = 70°C.

	$\frac{\delta(x)}{x} \cdot Re_x^{1/2}$		$C_{fw} \cdot Re_x^{1/2}$		$Nu \cdot Re_x^{-1/2} \cdot$	
$\frac{x}{c} \cdot \pi$	Exact	Approx	Exact	Approx	Exact	Approx
0	2.27	2.10	0.0878	0.0927	0.531	0.533
0.125	2.29	2.11	0.0870	0.0921	0.527	0.530
0.25	2.33	2.16	0.0852	0.0902	0.516	0.519
0.375	2.42	2.24	0.0814	0.0870	0.496	0.501
0.5	2.57	2.37	0.0759	0.0821	0.467	0.473
0.625	2.84	2.59	0.0671	0.0750	0.423	0.432
0.75	3.40	3.00	0.0522	0.0647	0.353	0.373
0.8	3.84	3.29	0.0419	0.0592	0.310	0.341
0.84	4.66	3.64	0.0166	0.0533	0.198	0.307

Table 28. Thick film formulae (680) compared with full numerical solutions for cylinder, $T_w = 0^\circ c$.

$\frac{x}{c}.\pi$	$\frac{\delta(x)}{x}.Re_x^{1/2}$		$C_{fw}.Re_x^{1/2}$		$Nu.Re_x^{-1/2}$	
	Exact	Approx	Exact	Approx	Exact	Approx
0	1.53	1.58	0.0466	0.0403	0.675	0.639
0.125	1.54	1.59	0.0461	0.0401	0.670	0.634
0.25	1.58	1.63	0.0445	0.0393	0.652	0.622
0.375	1.66	1.69	0.0415	0.0379	0.620	0.600
0.5	1.81	1.79	0.0363	0.0358	0.567	0.566
0.625	2.17	1.96	0.0267	0.0327	0.474	0.517
0.76	3.49	2.19	0.0093	0.0292	0.291	0.463

Table 29 : Thick film formulae (6.80) compared with full numerical solution for cylinder Tw = 70°c.

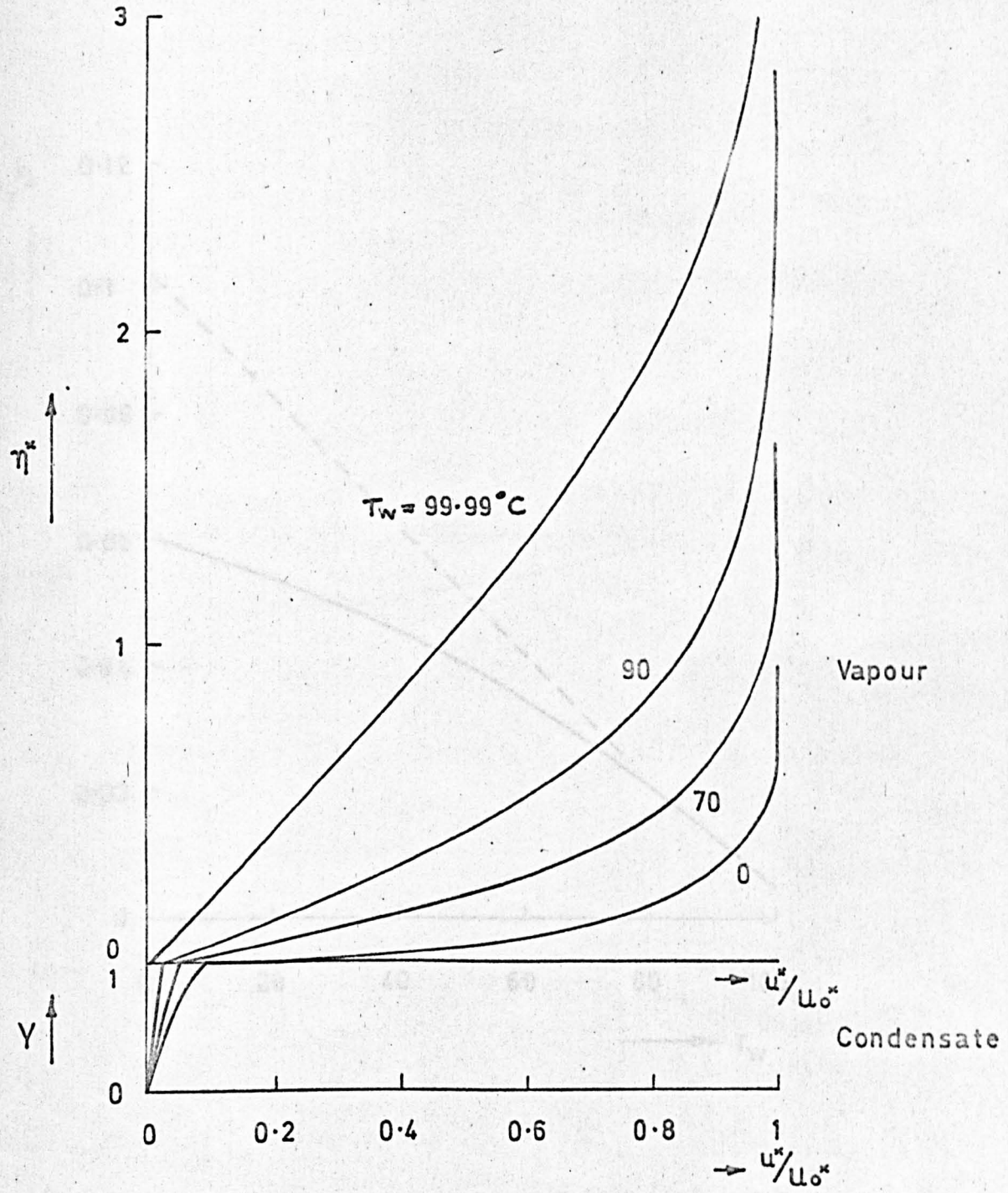

Figure.1. Velocity profiles for flow over flat plate, $u_m^*(x) = u_o^*$.

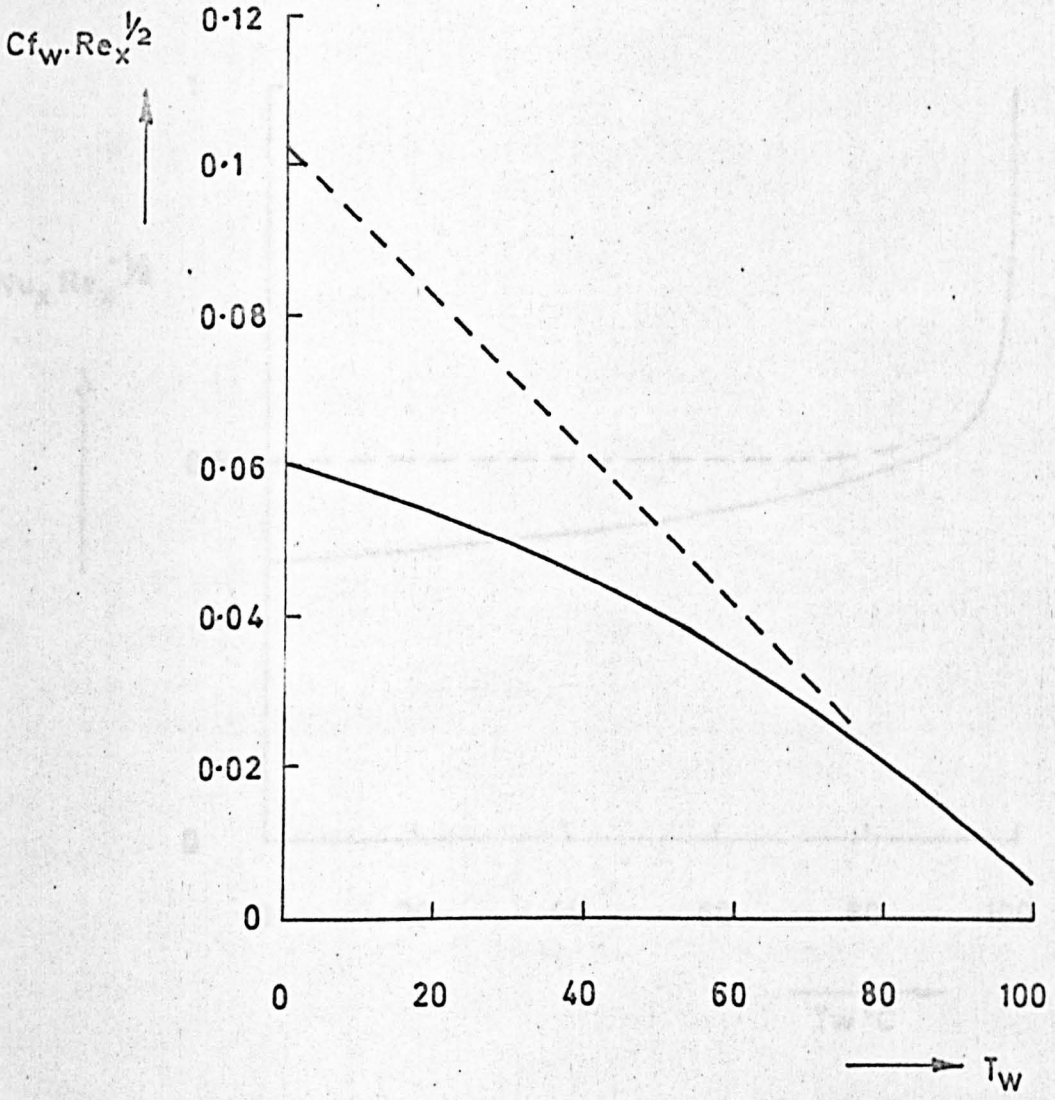

Figure 2. Non-dimensional wall shear; condensation onto plate; $u_m^*(x) = u_0^*$. —— current results, ---- Cess' results.

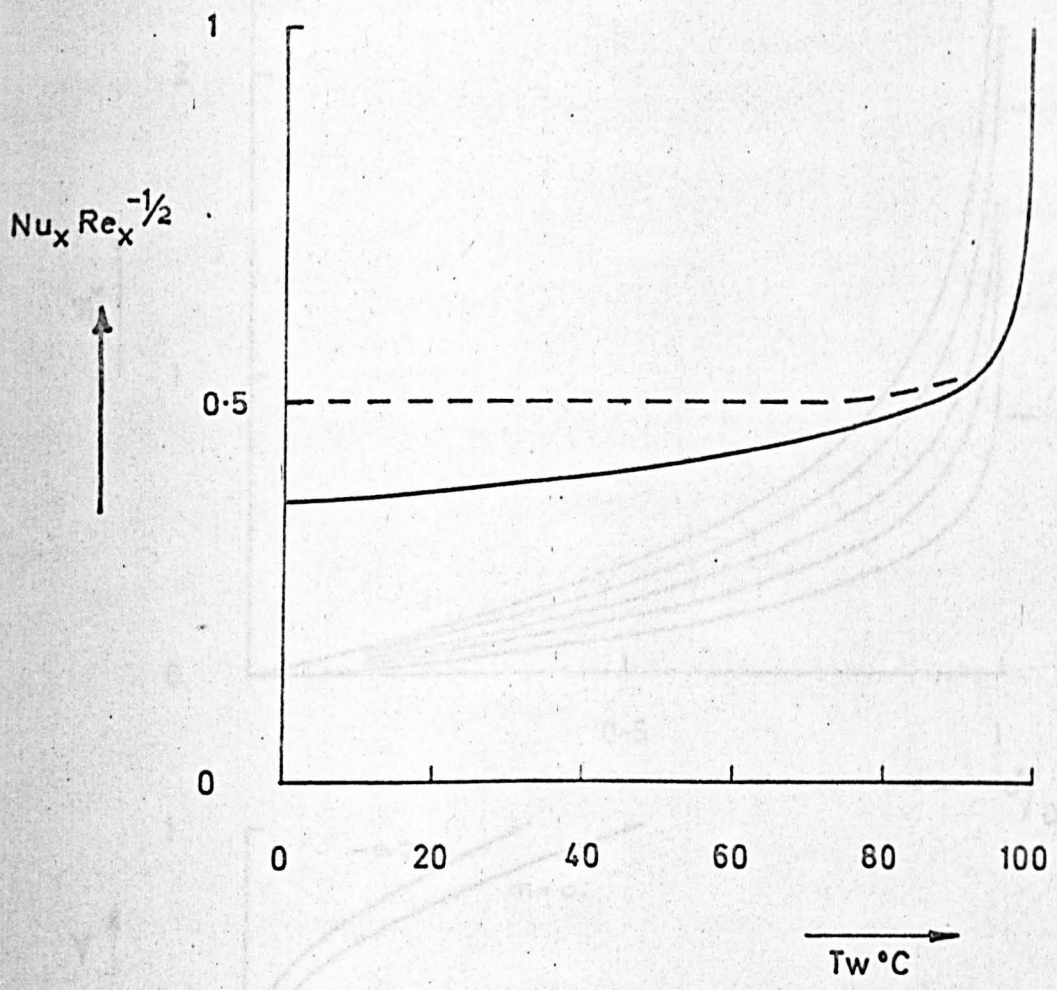

Figure 3. Nusselt number, condensation onto flat plate $\overline{Nu}^*(x) = Nu^*$.

——— current results, - - - - Cess.

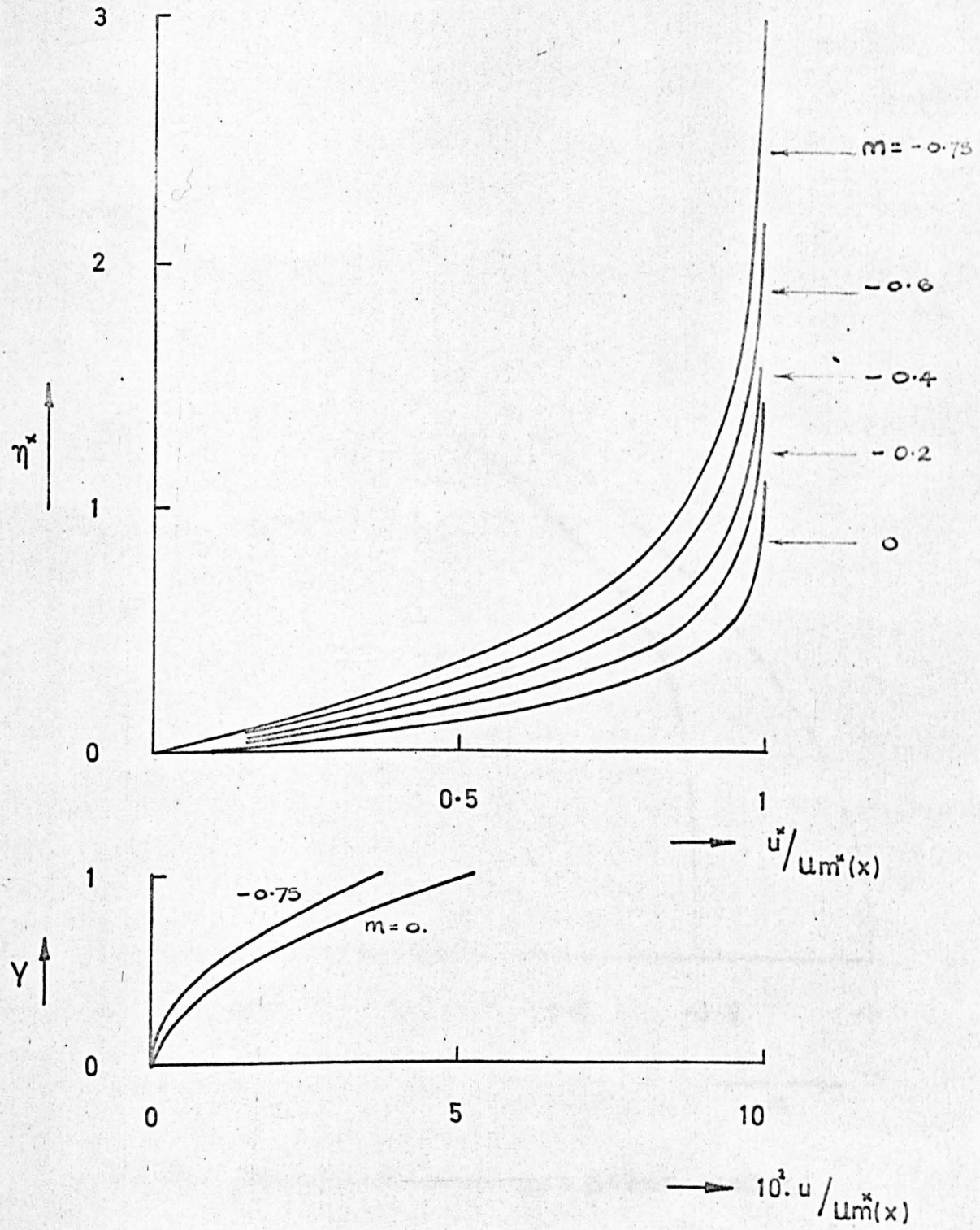

Figure 4. Velocity profiles with $U_m^*(x) = U_o^* (x/c)^m$, $T_w = 0^\circ C$, $m = 0, -0.2, -0.4, -0.6, -0.75$.

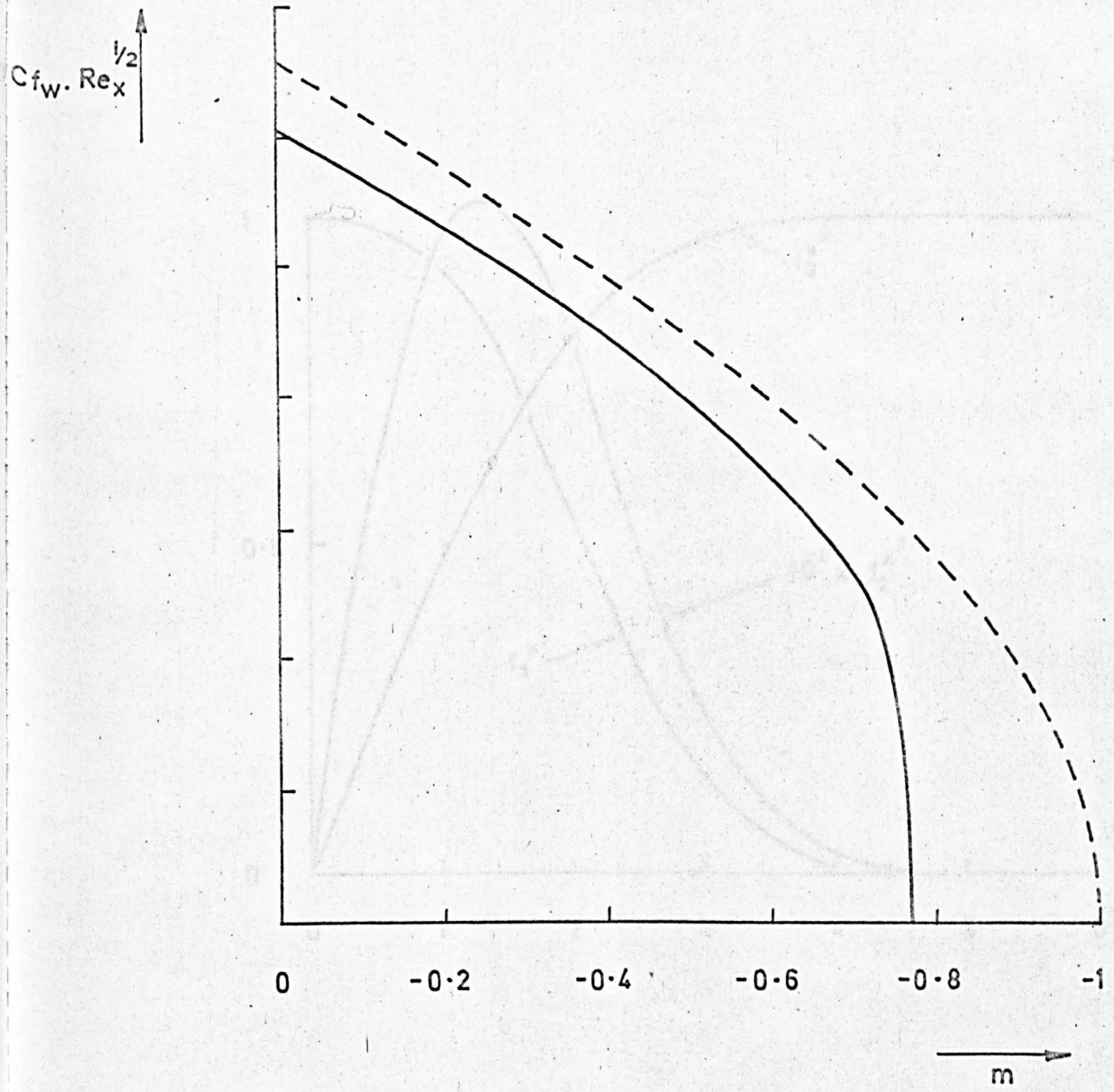

Figure 5. Non-dimensional wall shear plotted against m, Falkner-Skan mainstream. ——— numerical solution, - - - Thick film approx. (6.87).

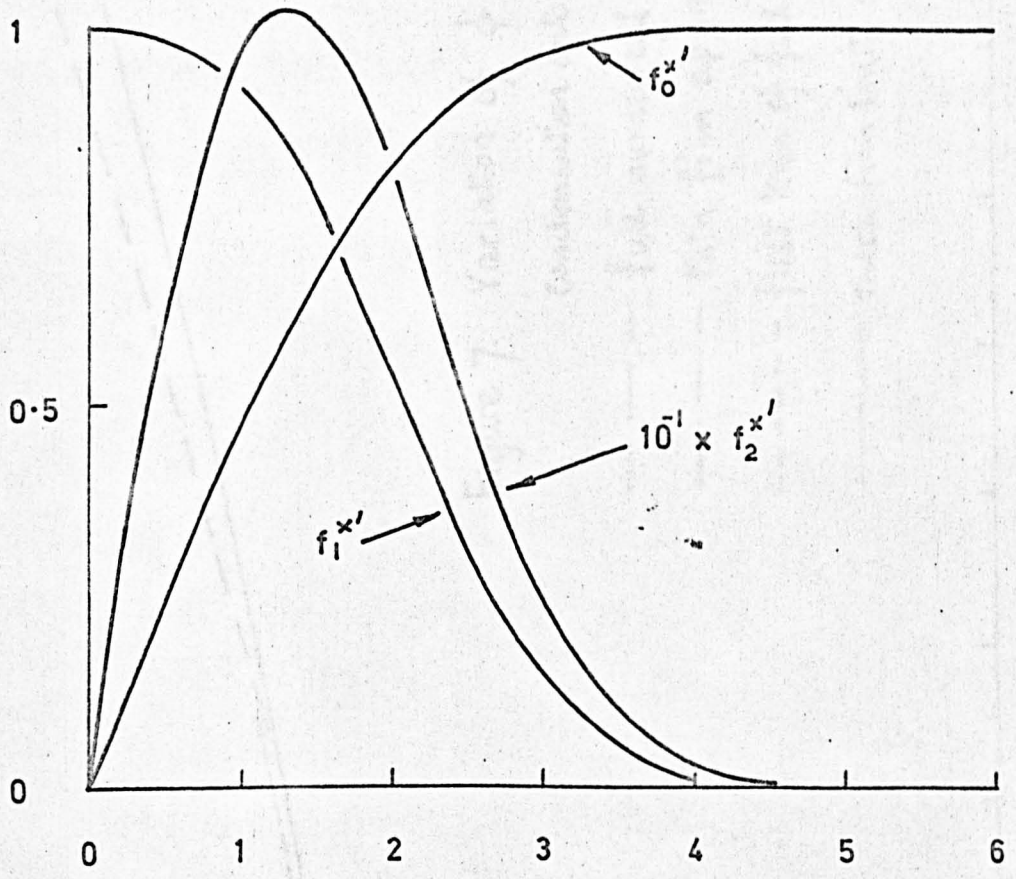

Figure 6. Thin film perturbation functions (4.14) for vapour.

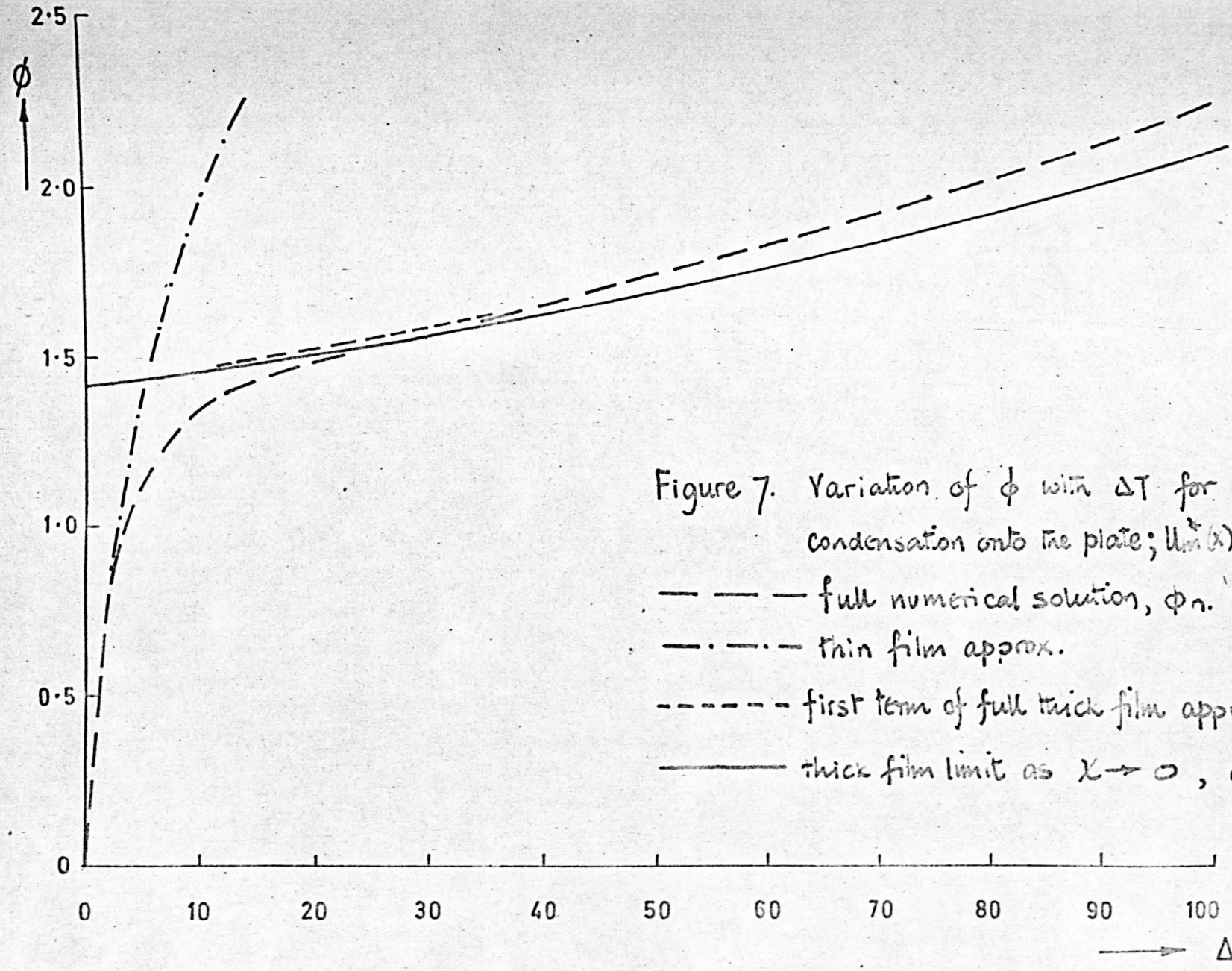

Figure 7. Variation of ϕ with ΔT for condensation onto the plate; $U_{in}^*(x) = U_0^*$.

— — — full numerical solution, ϕ_n.

—·—·— thin film approx.

- - - - - - first term of full thick film approx. ϕ_T.

——— thick film limit as $x \to 0$, $\phi_{T,x}$.

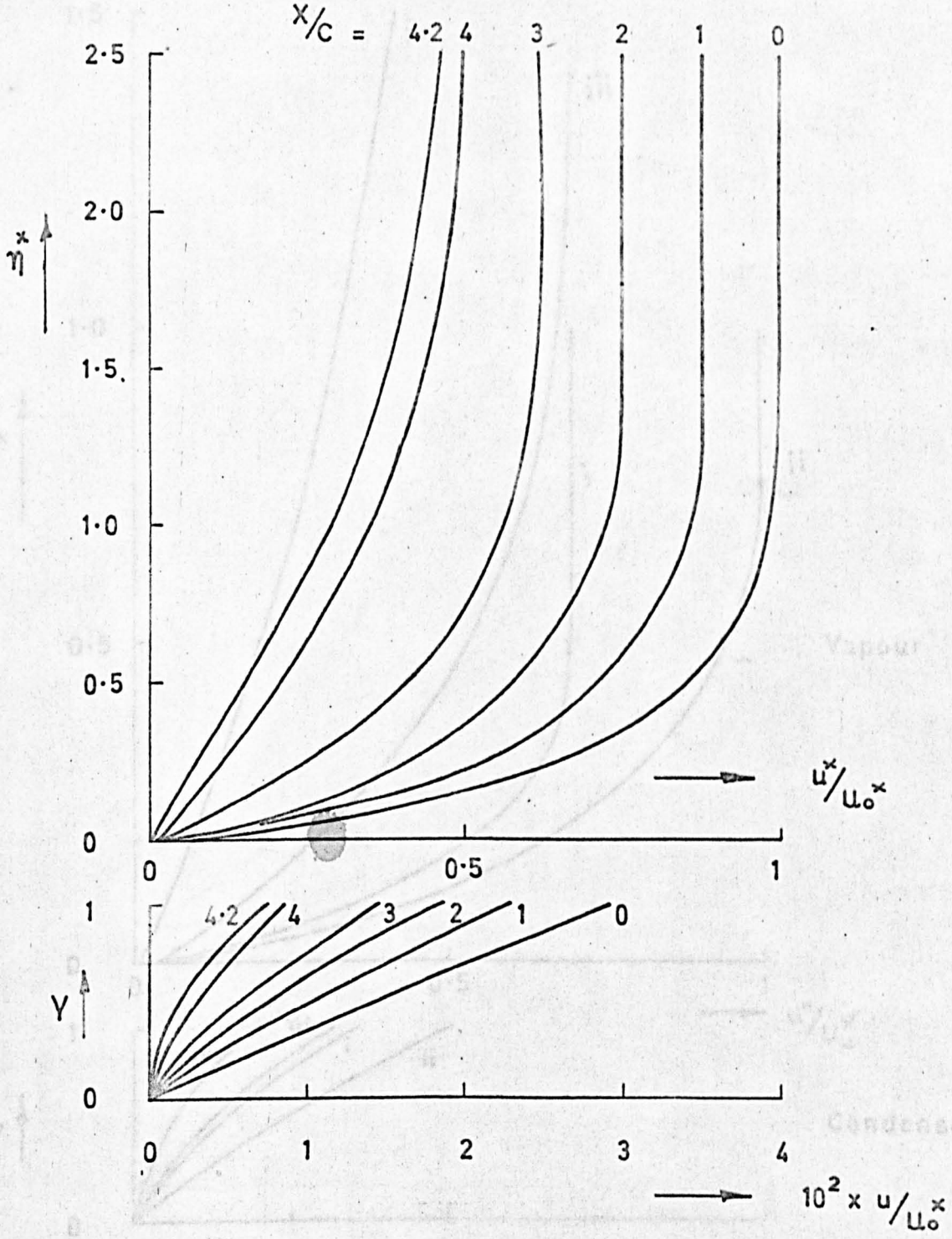

Figure 8. Flat plate, $u_{m}^{*}(x) = u_{0}^{*}(1 - \frac{1}{8}\frac{x}{c})$, $T_W = 70°C$.
Velocity profiles at $\frac{x}{c} = 0, 1, 2, 3, 4$ and 4·2.

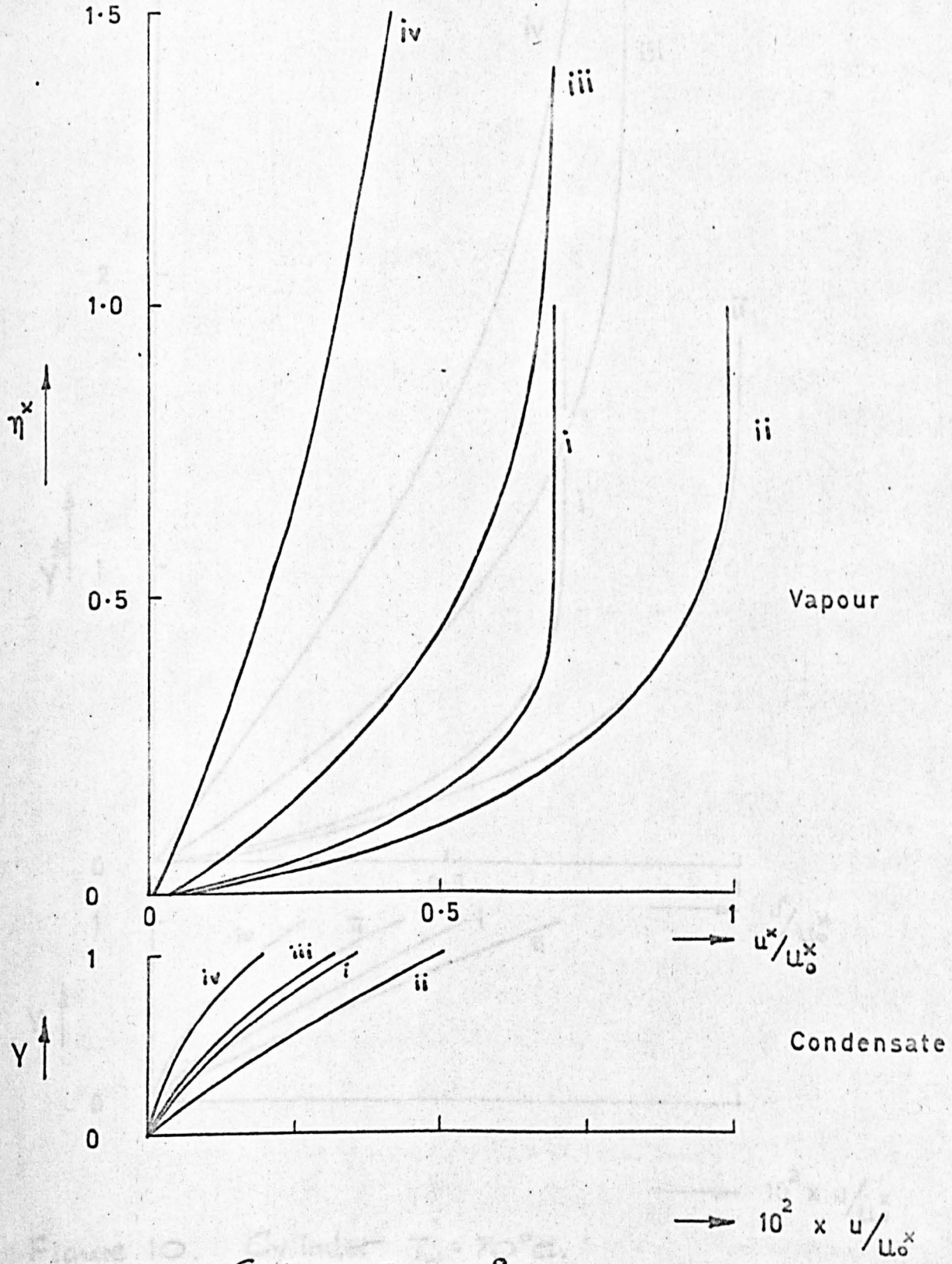

Figure 9. Cylinder $T_w = 0°C$

Velocity profiles : (i) $\frac{x}{L} = \frac{\pi}{4}$, (ii) $\frac{x}{L} = \frac{\pi}{2}$, (iii) $\frac{x}{L} = \frac{3\pi}{4}$, (iv) $\frac{x}{L} = 2.719$ rads

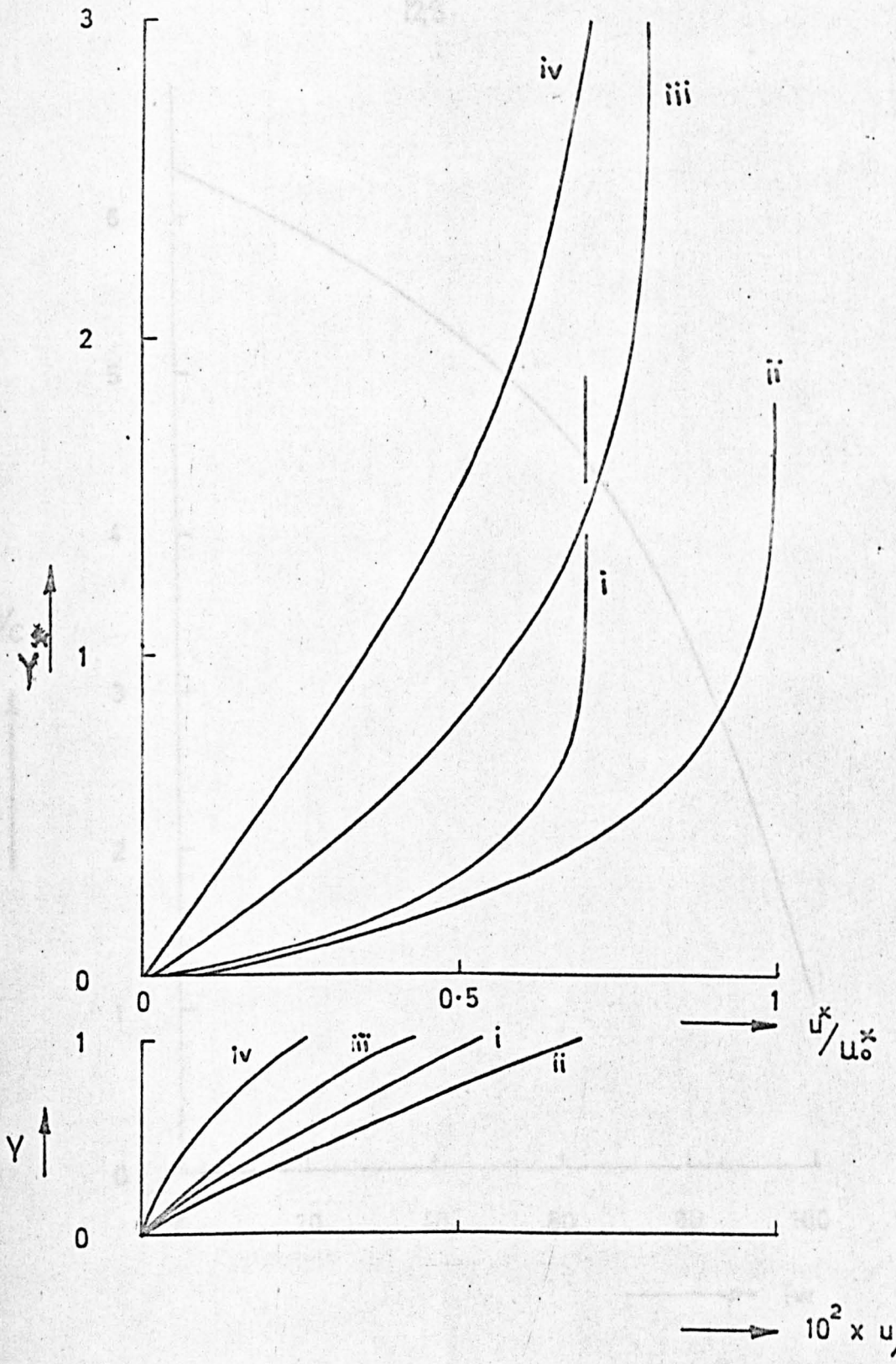

Figure 10. Cylinder $T_W = 70°C$.

Velocity profiles: (i) $x/c = \frac{\pi}{4}$, (ii) $\frac{x}{c} = \frac{\pi}{2}$, (iii) $\frac{x}{c} = \frac{3\pi}{4}$, (iv) $\frac{x}{c} = 2.327$ rads.

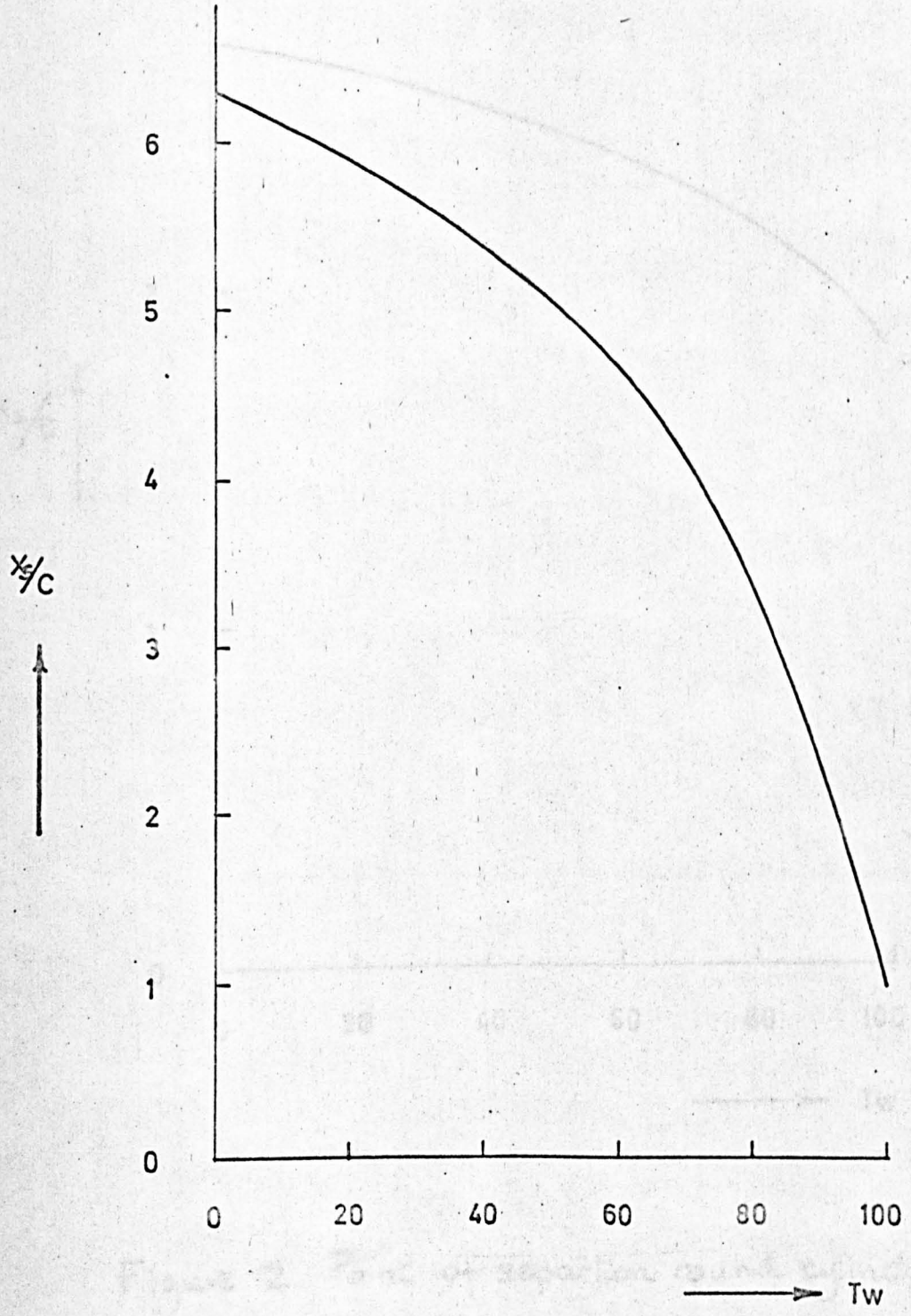

Figure 11. Point of separation along flat plate.
$M_m^*(x) = M_0^*(1 - \frac{1}{8}\frac{x}{c})$.

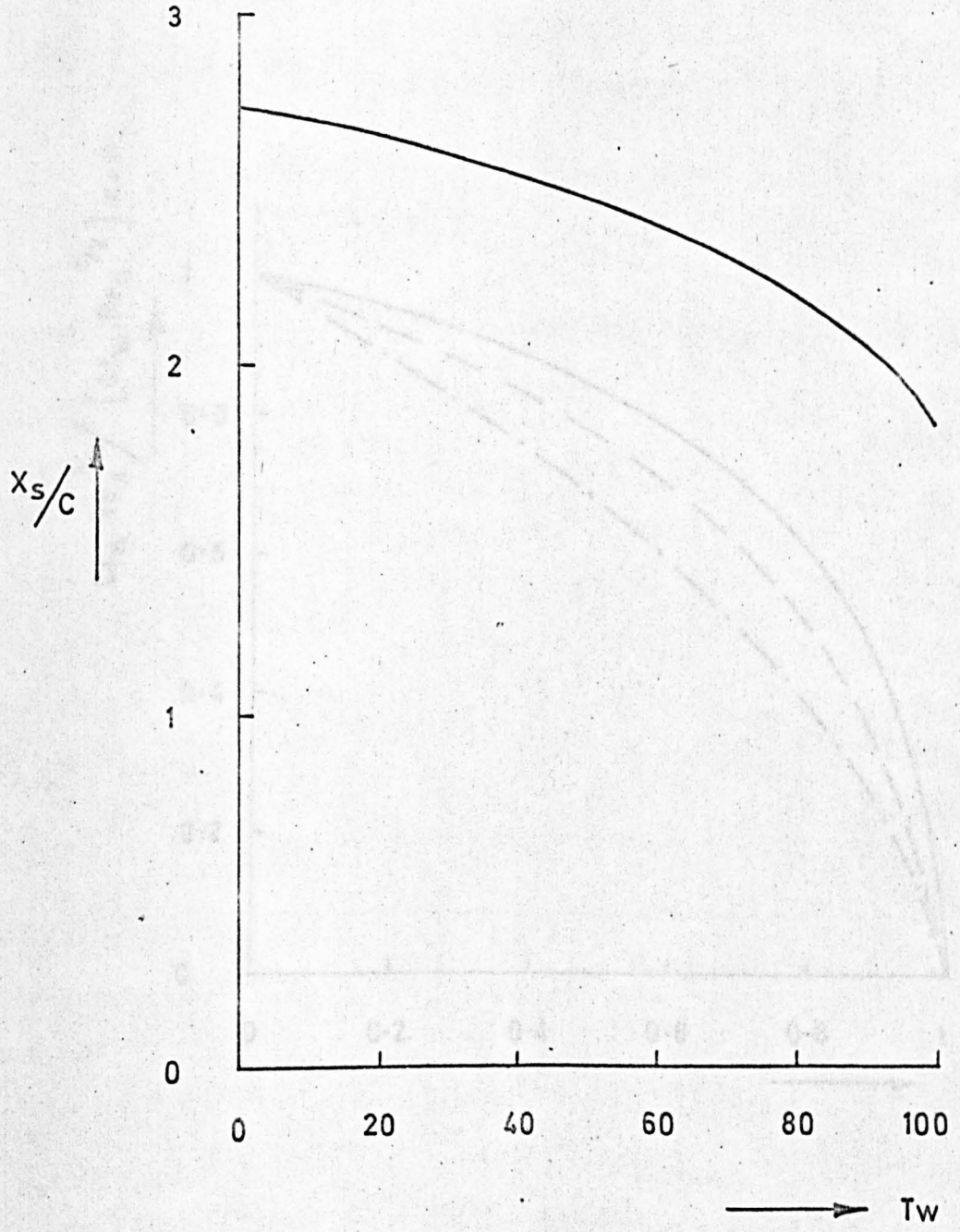

Figure 12. Point of separtion round cylinder,

$M_{n}^{*}(x) = M_{0}^{*} \sin(x/c)$.

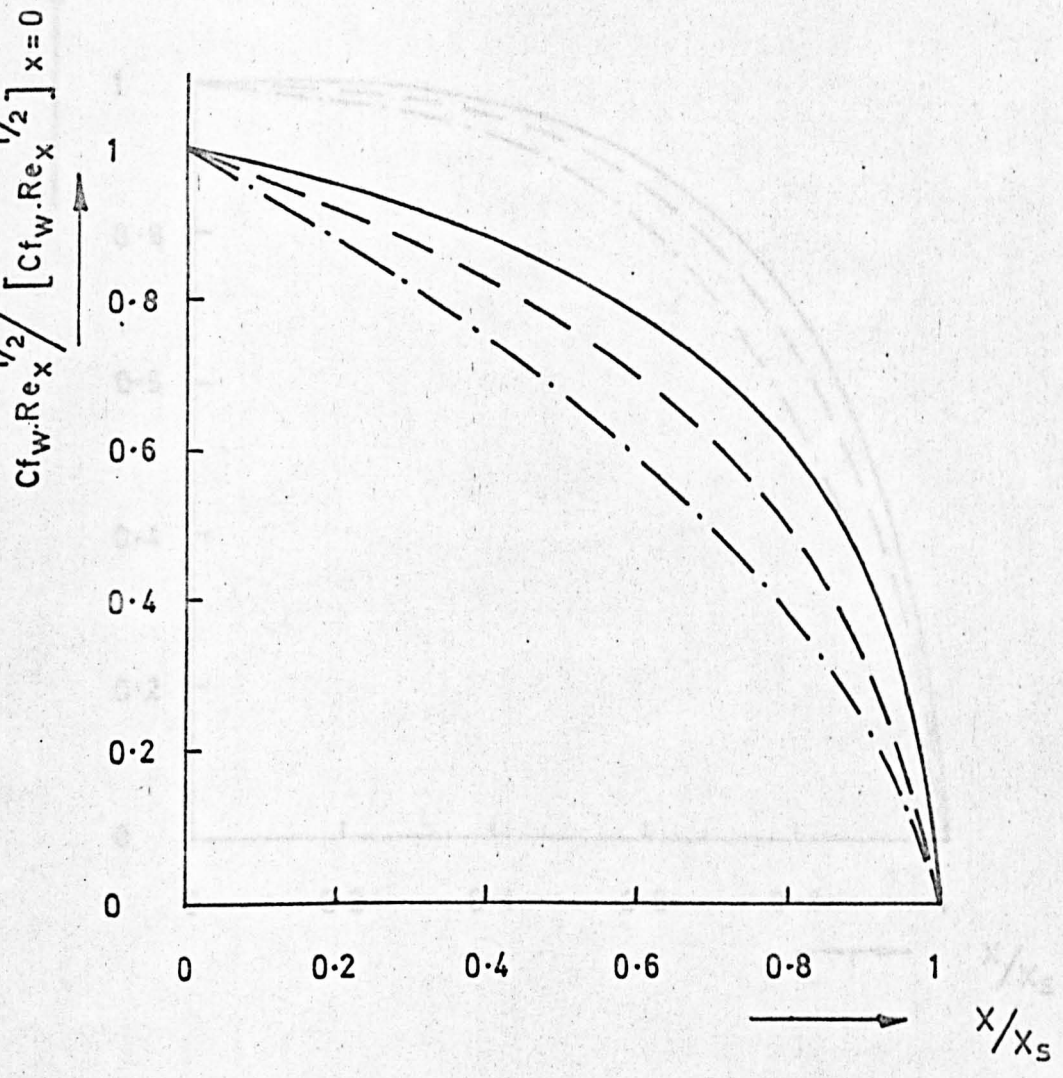

Figure 13: Wall shear coefficients for flat plate.

——— $T_w = 0°C$, – – – $T_w = 70°C$, —·— 99·99%.

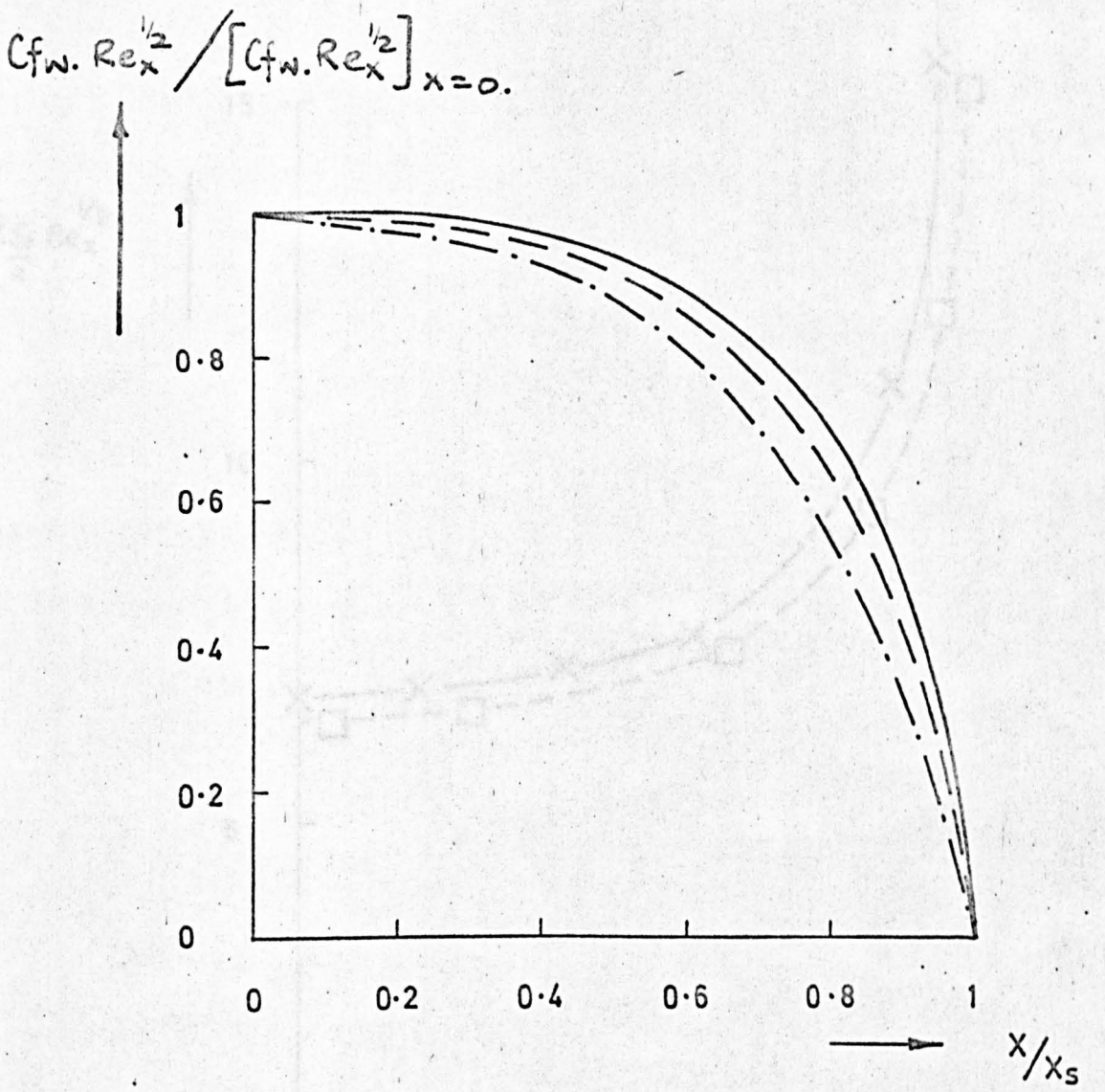

Figure 14. Wall shear coefficients for the cylinder.

—— T_w=0°C, — — — T_w=70°C, —·—·— T_w=99.99°C.

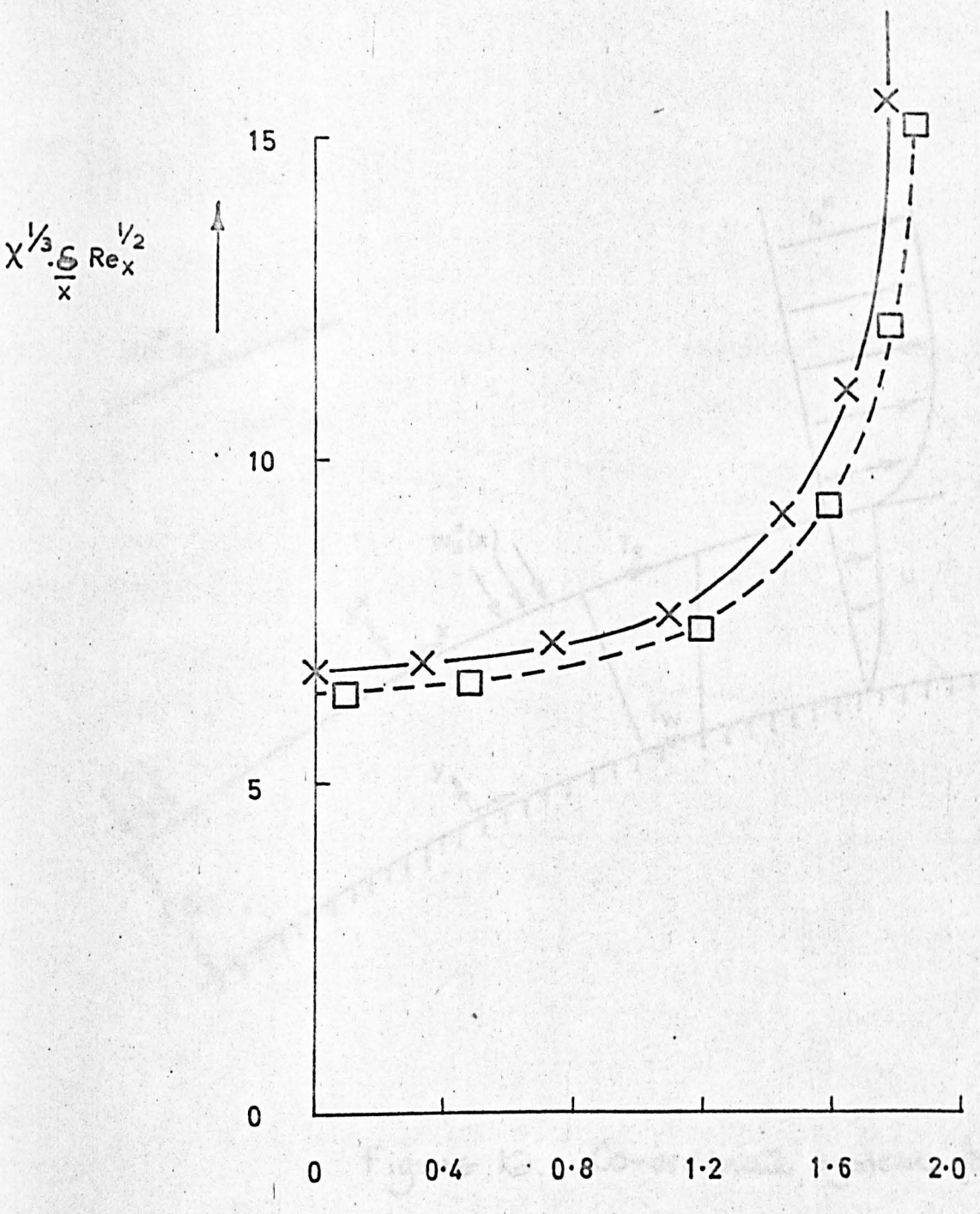

Figure 15. Comparison of thin film approximation applied to the cylinder and numerical solutions. ——(6.36), × numerical values for $T_w = 99.99°C$, □ for $T_w = 99°C$.

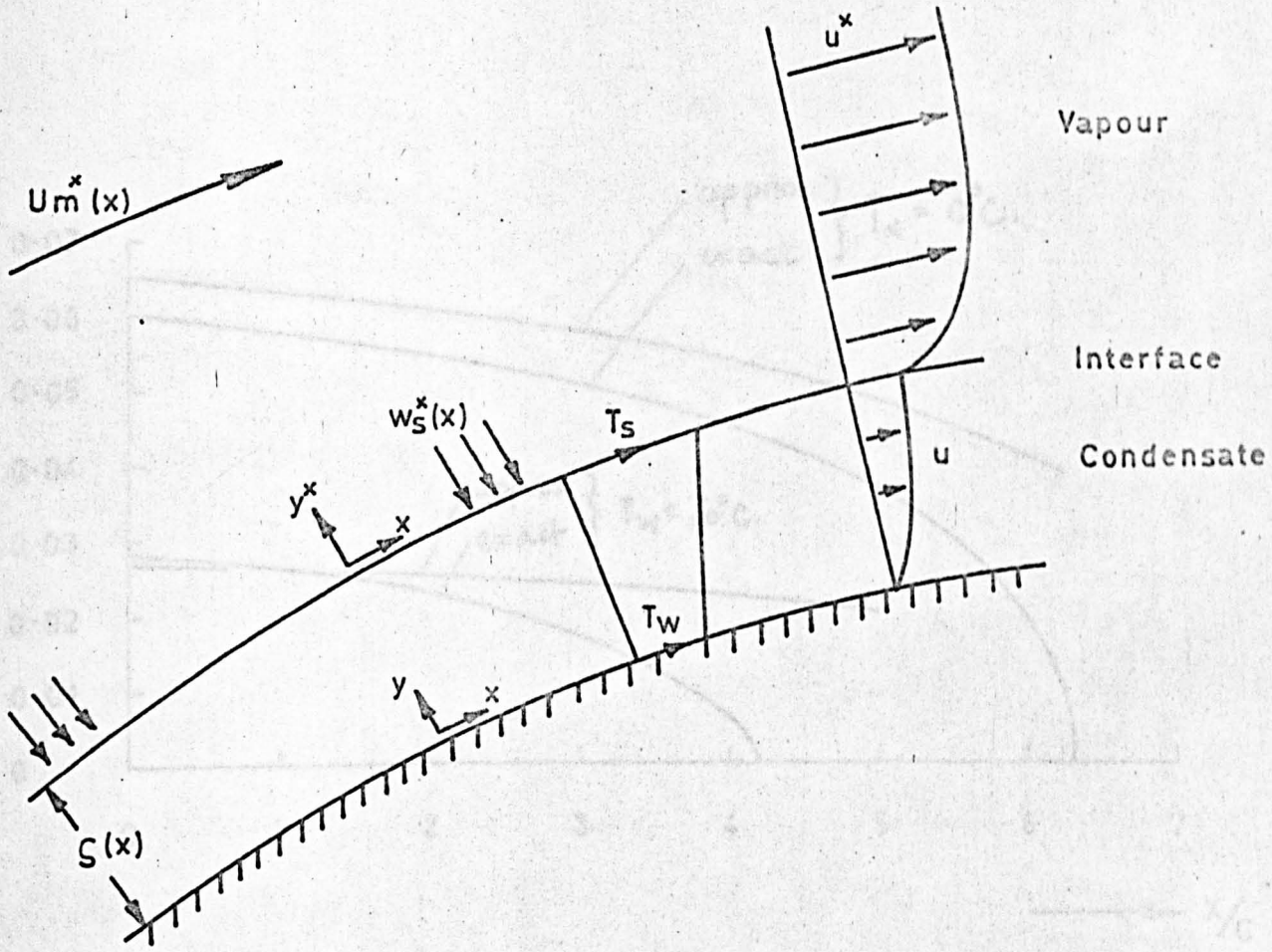

Figure 16. Co-ordinate system for thick film approximation applied to non-similar flows.

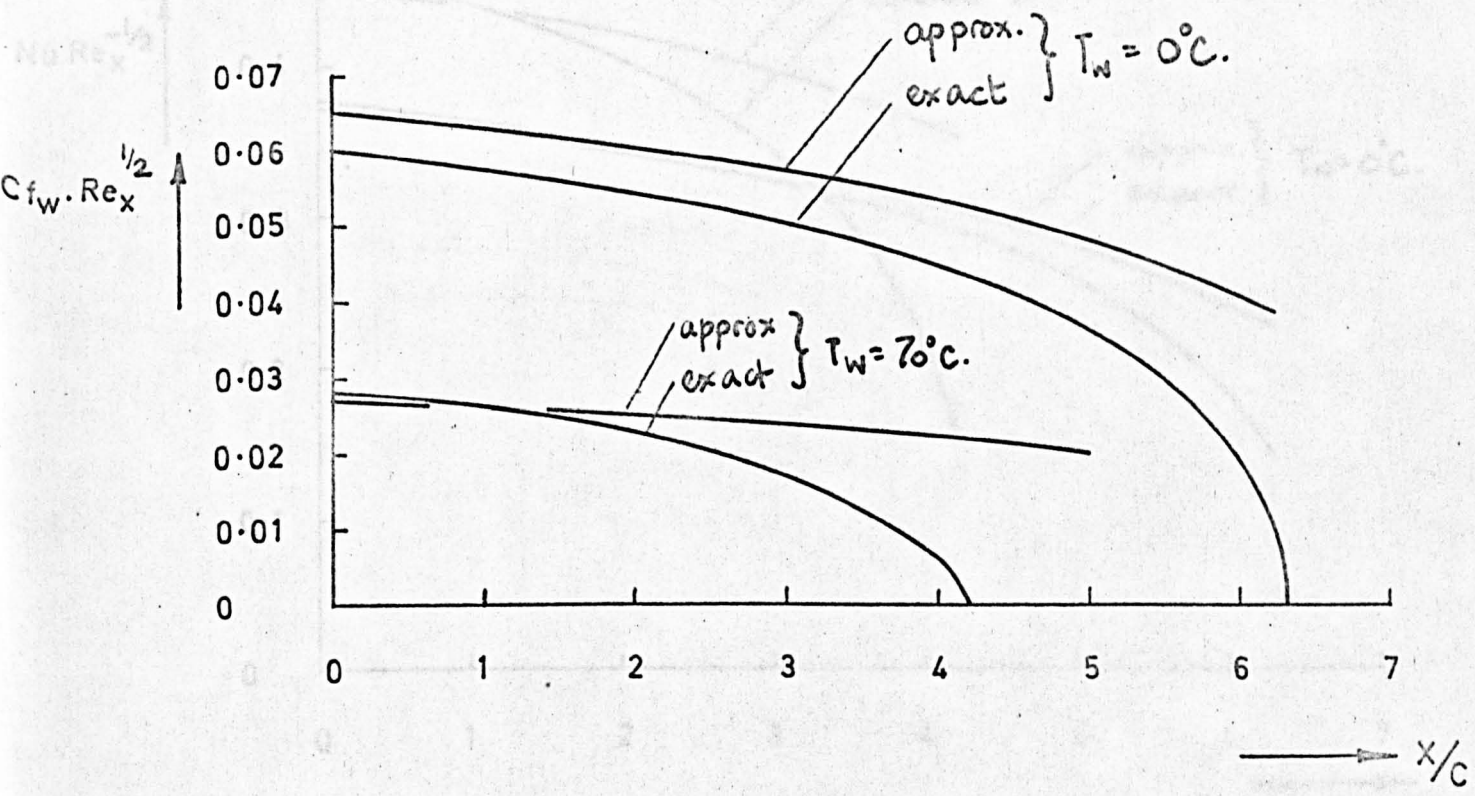

Figure 17. Comparison of wall shear from thick-film approximation (6.80) with numerical solutions for flat plate, $u_m^*(x) = u_0^*(1 - \frac{1}{8}\frac{x}{c})$.

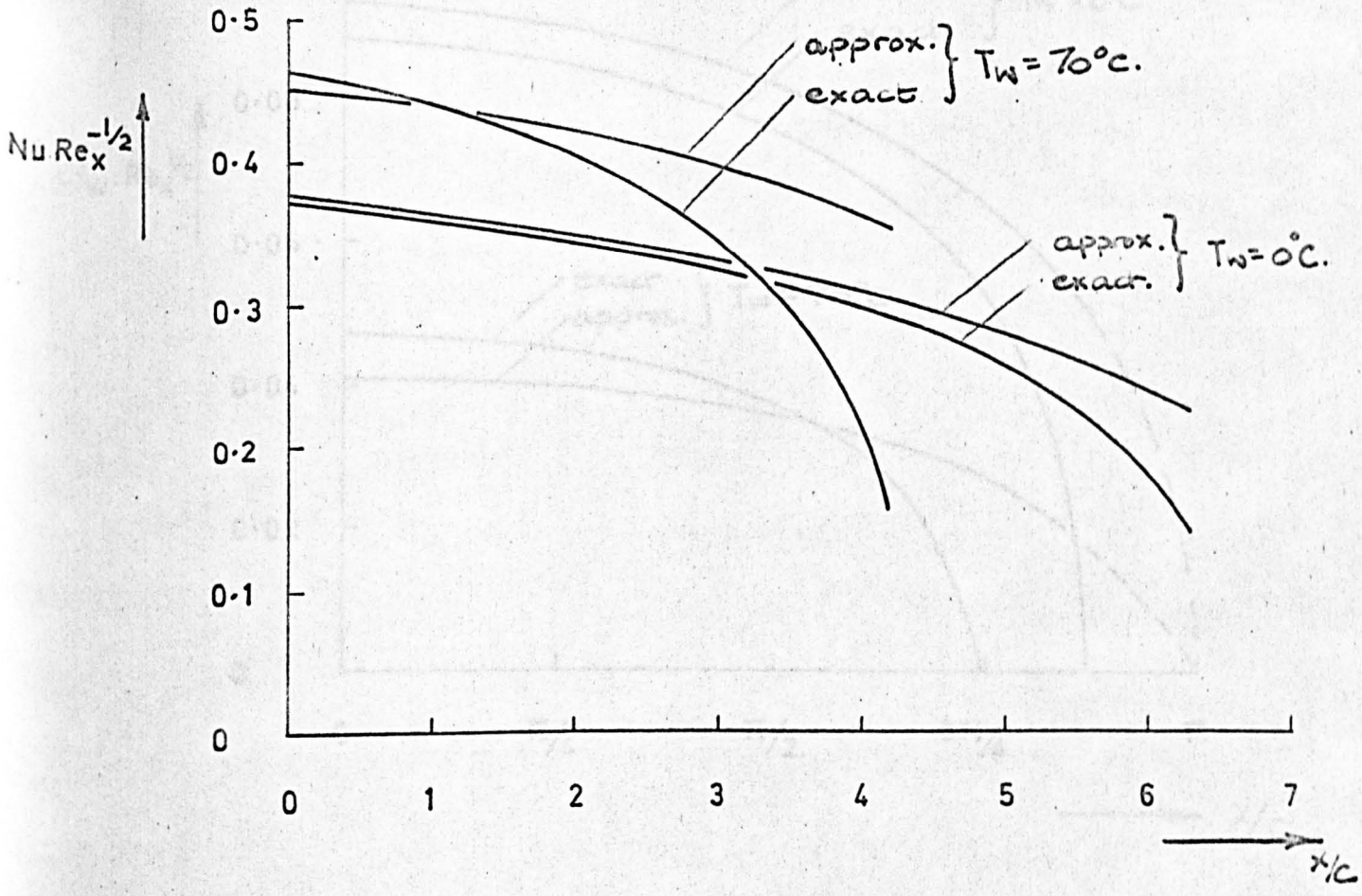

Figure 18. Comparison of heat transfer over plate given by thick film approximation (6.80) and numerical solution.

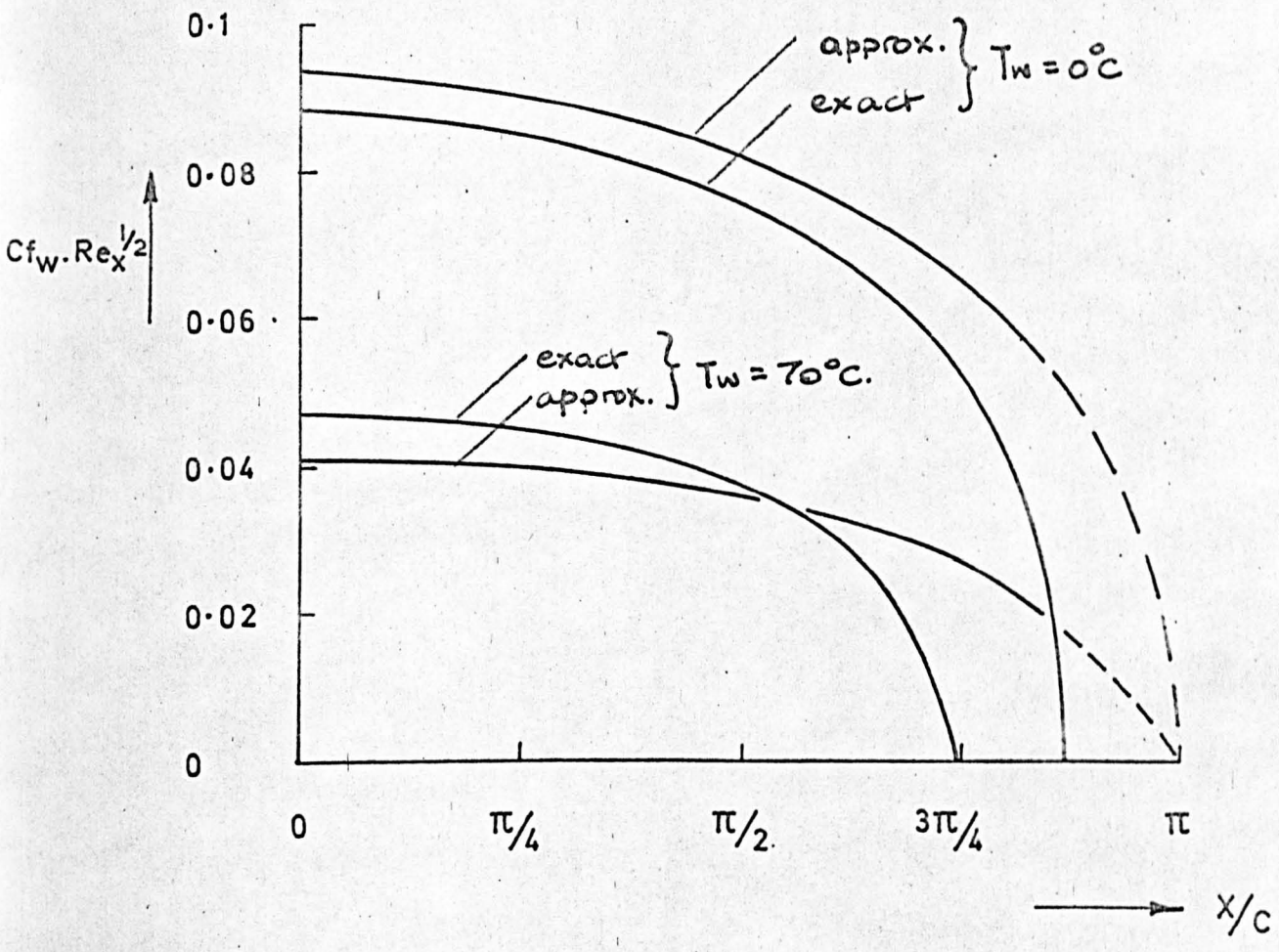

Figure 9. Comparison of cylinder wall shear from (6·80) compared with numerical solution.

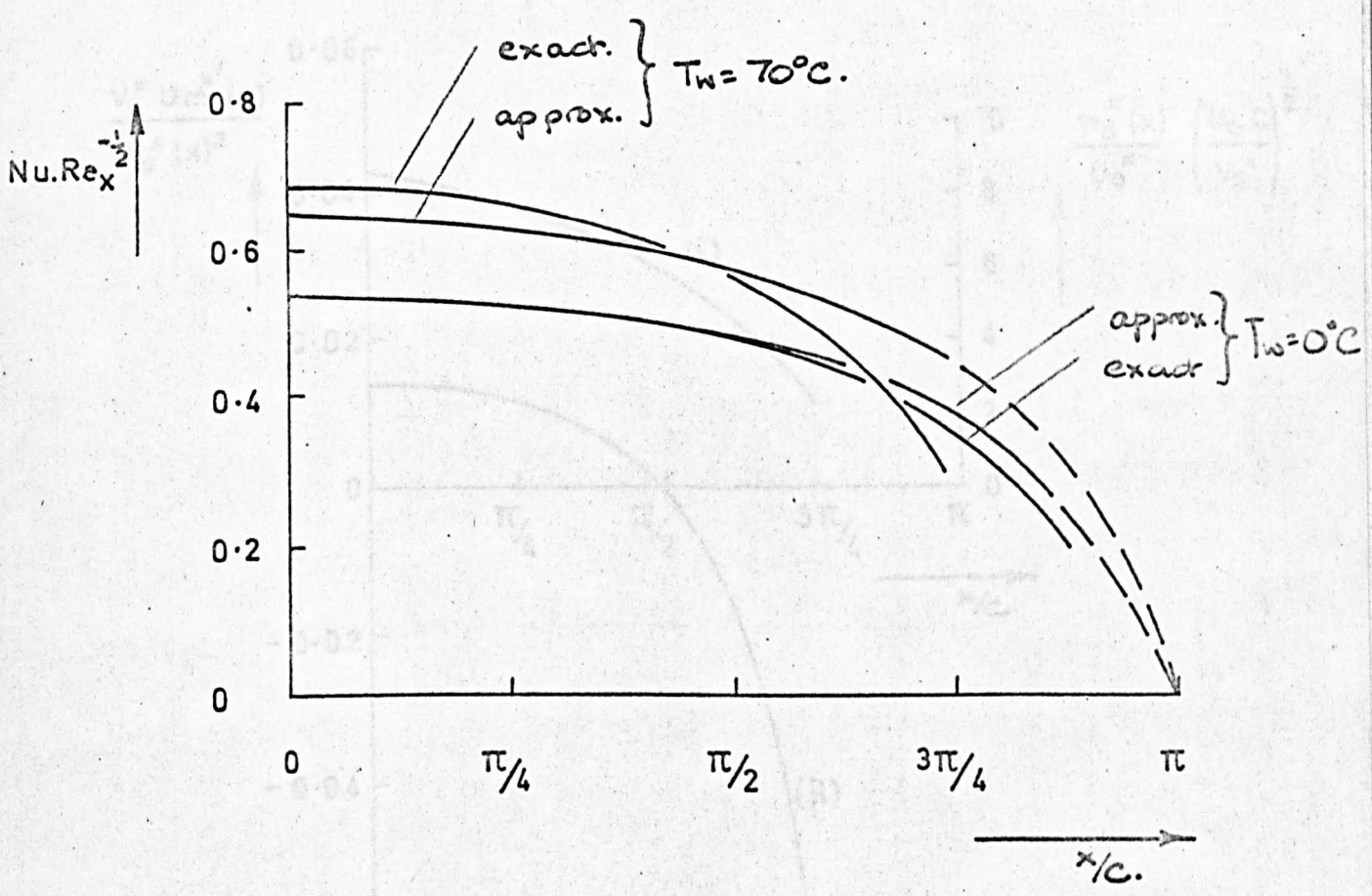

Figure 20. Comparison of heat transfer rate over cylinder given by (6.80) and numerical solution.

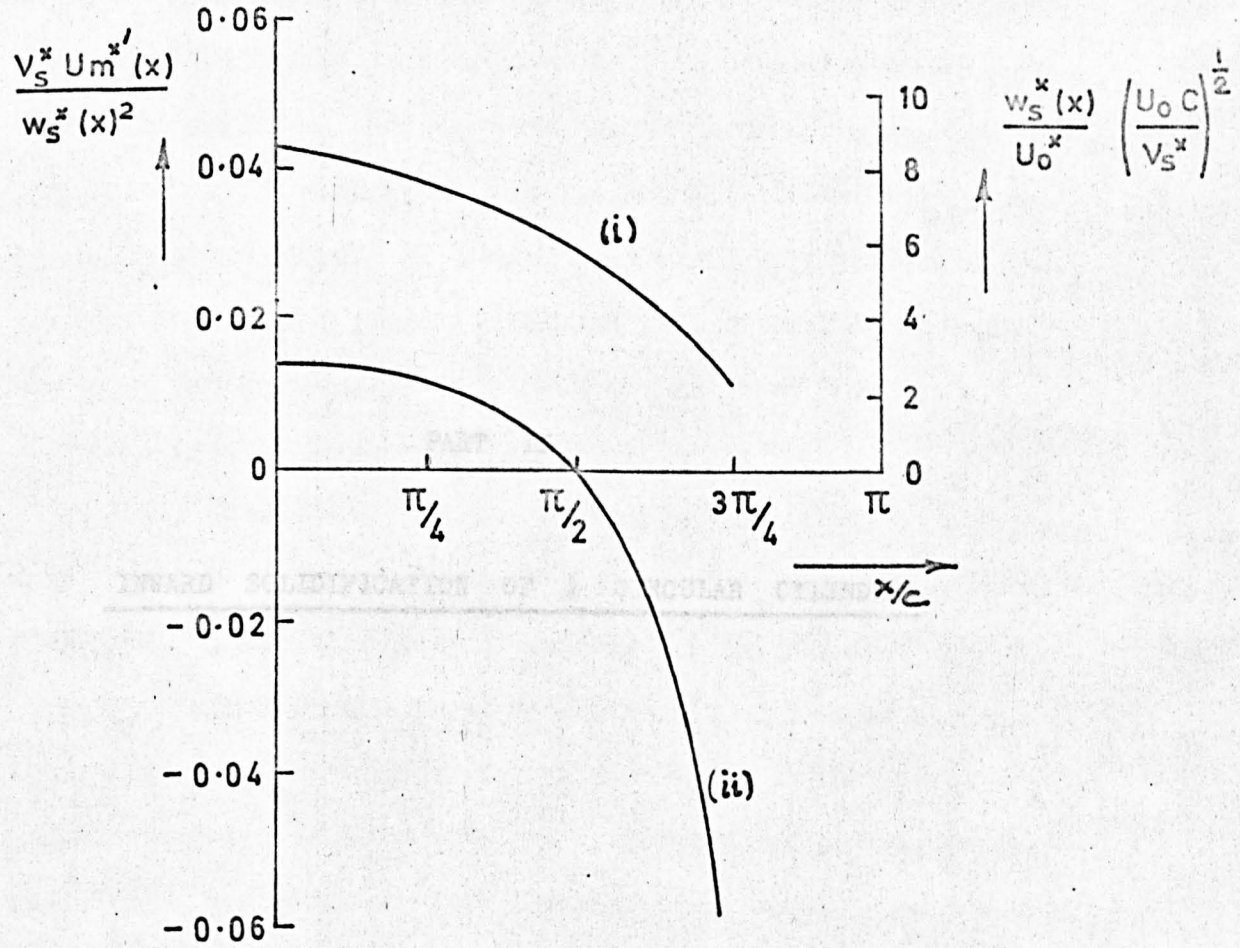

Figure 21. (i) Vapour velocity normal to interface,

(ii) Neglected Term in (6.43),

Condensation onto cylinder $T_w = 70°C$.

PART II

INWARD SOLIDIFICATION OF A CIRCULAR CYLINDER.

Introduction

When liquid initially at the fusion temperature is suddenly exposed to an environment whose temperature is below fusion, then a process of solidification begins at the boundary through which the heat is being drawn, and the solid-liquid interface moves into the liquid from this boundary as time progresses. In the work presented in this section it will be assumed that during the process of solidification the liquid remains at fusion temperature, the properties of the solid are independent of temperature and that there is a sharply defined fusion temperature.

These assumptions immediately deny us the possibility of predicting many important results of solidification. For example when metal solidifies in ingots, or more complicated castings, it is contraction in the solidified phase which causes unsoundness in many cases and which necessitates the employment of such devices as exothermic sleeves to ensure a supply of molten metal to the centres of the more massive sections of the casting. This phenomenon is common to most solidifying liquids but there is an important exception in the case of water because as ice forms its density being less than water would cause compression in the liquid phase.

In order to justify pursuing solutions of solidification problems under these simplifying assumptions, it is only necessary to state that there is a general lack of accurate numerical results on such problems. Most of the earlier work was completed on desk machines with crude finite difference approximations.

In addition to this shortage of results there are several aspects of solidification problems which have not been satisfactorily discussed and which add greater stimulation to looking once again at this class of problem. Of particular interest is the behaviour as the time of complete solidication is approached and, for example, an answer to the question: "At what rate does the solid-liquid interface approach the centre of the cylinder?"

The main difficulty in obtaining analytical solutions of solidification problems stems from the fact that as the liquid undergoes a change of phase from liquid to solid, thermal energy in the form of latent heat of fusion is liberated at the moving interface and this leads to a non-linear boundary condition at the unknown interface. One of the few exact analytical solutions (see Carslaw and Jaeger [32]) is that found by Neumann and Stefan relating to the solidification of the semi-infinite region when the surface wall temperature is suddenly decreased below fusion. The inherent non-linearity can be removed by adjusting the wall temperature so that a constant solidification rate results, and it is this technique which is used by Stefan (see Ingersoll et. al. [33]) for the semi-infinite region and by Kreith and Rommie [34] for the inward solidification of the cylinder and sphere.

Several authors have offered numerical methods applied to problems which retain the non-linearity, in particular Allen and Severn [35] and [36] have been very ingenious in applying relaxation methods to treat the unidimensional problems of the semi-infinite region and the cylinder. Though the method applied to the former is quite accurate the conclusion

of the present work is that the same method when applied to the cylinder yields inaccurate results. This is apparent on comparison with the work of Poots [37] who has found a series solution, which is exact for small values of the time. This series solution is developed in a similar manner to that described by Goldstein and Rosenhead [38] in the discussion of boundary layer growth when a cylinder is impulsively started from rest.

There is now considerable incentive for reconsidering this class of problem and in particular to the problem of inward solidification of the cylinder. The exact solution is computed using the Hartree-Womersley technique applied to parabolic partial differential equations and in addition more terms of the series solution are sought in view of the possible insight they may give into the convergence of Goldstein and Rosenhead type series. Two additional terms to those given by Poots will be found, but the analytical solution will be left at that point and further terms found using an algorithm.

Governing equations and boundary conditions

Under the assumptions made earlier the temperature distribution in the solidified phase is given by the thermal diffusion equation

$$k \nabla^2 T = \rho C \frac{\partial T}{\partial t}, \qquad (7.1)$$

where k is the thermal conductivity, ρ is the density of the solid (and will also be the density of the liquid), C is the specific heat, ∇^2 is the form of the Laplacian in cylindrical polar coordinates, and

the temperature will be assumed a function of r only.

The location of the solid-liquid interface is defined by

$$r = a - E, \tag{7.2}$$

where a is the radius of the cylinder and E(t) denotes the depth of penetration of the front.

Initially the entire cylindrical region is occupied by liquid at the fusion temperature T_F and then at time $t = 0$ the outer surface is switched to $T_o < T_F$.

Thus when t = 0

$$E = 0; \quad T = T_F, r < a; \quad T = T_o, r = a; \tag{7.3}$$

and at subsequent times we have:

$$\begin{aligned} T &= T_F, \quad 0 \le r \le a - E(t), \\ T &= T_o, \quad r = a. \end{aligned} \tag{7.4}$$

In addition there is the boundary condition associated with the liberation of latent heat, L, at the interface:

$$K \frac{\partial T}{\partial r} = -\rho L \frac{dE}{dt}. \tag{7.5}$$

Common to the numerical and series solutions are the following transformations.

Introduce dimensionless moduli and new variables :

$$\varepsilon = \frac{E}{a}, \qquad \theta(\eta,\tau) = \frac{T - T_0}{T_F - T_0},$$

$$\eta = \frac{a-r}{a\varepsilon}, \qquad \tau = \frac{tk}{a^2}, \tag{7.6}$$

$$\beta = \frac{L}{c(T_F - T_0)}.$$

Then the governing equation and boundary conditions become:

$$\frac{\partial^2\theta}{\partial\eta^2} + \eta\varepsilon\frac{d\varepsilon}{d\tau}\frac{\partial\theta}{\partial\eta} - \varepsilon^2\frac{\partial\theta}{\partial\tau} = \frac{\varepsilon}{1-\varepsilon\eta}\frac{\partial\theta}{\partial\eta}, \tag{7.7}$$

subject to

$$\theta = 0 \text{ at } \eta = 0,$$

$$\theta = 1 \text{ and } \frac{\partial\theta}{\partial\eta} = \beta\varepsilon\frac{d\varepsilon}{d\tau} \text{ at } \eta = 1. \tag{7.8}$$

It is to (7.7) and (7.8) that the two distinct methods mentioned previously are now applied.

Method 1: Series expansions for θ and ε in powers of τ.

Following Poots the unknown functions ε and θ are expanded as follows.

$$\varepsilon = \sum_{r=0}^{\infty} e_r \tau^{\frac{1}{2}(1+r)}, \tag{7.9}$$

$$\text{and } \theta = \sum_{r=0}^{\infty} f_r(\eta)\tau^{r/2}.$$

By doing this it will transpire that the complication of the non-linearity is removed, and on comparing the coefficients of like powers

of τ in the equation, having substituted (7.8) and (7.9), then ordinary linear differential equations for $f_r(\eta)$ have to be solved. The first three terms in each series are available in the work of Poots and it is the intention in this section to find the next two terms analytically and also to describe a procedure for computing any number of terms.

1(a) Analytic solution of $f_r(\eta)$.

Substitution of (7.9) into (7.6) and (7.7) and the subsequent comparison of the coefficients of powers of τ yields the following sets of equations and boundary conditions.

First order solution.

$$f_0'' + 2\xi f_0' = 0,$$
$$f_0(0) = 0, f_0\left(\tfrac{e_0}{2}\right) = 1, \quad f_0'\left(\tfrac{e_0}{2}\right) = e_0\beta. \tag{7.10}$$

where ξ is a new independent variable defined by $\xi = \frac{1}{2}e_0\eta$ and the dashes denote now differentiation w.r.t. ξ ;

Second order solution:

$$f_1'' + 2\xi f_1' - 2f_1 = \left(\frac{2}{e_0}\right)(e_0 - 3e_1\xi)f_0', \tag{7.11}$$
$$f_1(0) = f_1\left(\tfrac{e_0}{2}\right) = 0, \quad f_1'\left(\tfrac{e_0}{2}\right) = 3e_1\beta;$$

Third order solution:

$$f_2'' + 2\xi f_2' - 4f_2 = \left(\frac{2}{e_0}\right)(e_0 - 3e_1\xi)f_1' + 4\frac{e_1}{e_0}f_1 + \left(\frac{2}{e_0^2}\right)(e_1e_0 + \xi(2e_0^2 - 2e_1^2 - 4e_0e_2))f_0'. \tag{7.12}$$
$$f_2(0) = f_2\left(\tfrac{e_0}{2}\right) = 0, \quad f_2'\left(\tfrac{e_0}{2}\right) = \frac{\beta}{e_0}(4e_0e_2 + 2e_1^2).$$

Fourth order solution:

$$f_3'' + 2\zeta f_3' - 6f_3 = \left(\frac{2}{e_0}\right)(e_0 - 3e_1\zeta) f_2'$$
$$+ \left(\frac{2}{e_0^2}\right)\left[e_0e_1 + 2\zeta(e_0^2 - e_1^2 - 2e_0e_2)\right] f_1'$$
$$+ \left(\frac{2}{e_0^2}\right)\left[e_0e_2 + \zeta(4e_0e_1 - 5e_0e_3 - 5e_1e_2) + 4e_0^2\zeta^2\right] f_0' \qquad (7.13)$$
$$+ \left(\frac{2}{e_0^2}\right)\left[(e_1^2 + 2e_0e_2) f_1 + 4e_0e_1 f_2\right],$$

$$f_3(0) = f_3\left(\frac{e_0}{2}\right) = 0, \quad f_3'\left(\frac{e_0}{2}\right) = \frac{5\beta}{e_0}(e_0e_3 + e_1e_2).$$

Fifth order solution:

$$f_4'' + 2\zeta f_4' - 8f_4 = \frac{2}{e_0}(e_0 - 3\zeta e_1) f_3'$$
$$+ \frac{2}{e_0^2}(e_0e_1 + 2\zeta[e_0^2 - e_1^2 - 2e_0e_2]) f_2'$$
$$+ \frac{2}{e_0^2}(e_0e_2 + \zeta[4e_0e_1 - 5e_0e_3 - 5e_1e_2] + 4e_0^2\zeta^2) f_1'$$
$$+ \frac{2}{e_0^2}\Big(e_0e_3 + \zeta\left[2e_1^2 + 4e_0e_2 - 6e_0e_4 - 6e_1e_3 - 3e_2^2\right] \qquad (7.14)$$
$$+ 12e_0e_1\zeta^2 + 8e_0^2\zeta^3\Big) f_0'$$
$$+ \frac{4}{e_0^2}\left([e_0e_3 + e_1e_2] f_1 + [e_1^2 + 2e_0e_2] f_2 + 3e_0e_1 f_3\right),$$

$$f_4(0) = f_4\left(\frac{e_0}{2}\right) = 0, \quad f_4'\left(\frac{e_0}{2}\right) = \frac{3\beta}{e_0}\left(2e_0e_4 + 2e_1e_3 + e_2^2\right).$$

Poots has solved (7.10)-(7.12) and gives e_0, e_1 and e_2 in his paper. For the sake of completeness these are included below together with the corresponding function $f_i(\eta)$, i = 0,1, and 2.

The system (7.10) is solved to give

$$f_0(\eta) = A_1^0 \operatorname{erf} \eta \quad , \quad A_1^0 = \frac{\sqrt{\pi}}{2} \beta e_0 e^{(\frac{1}{2}e_0)^2} , \tag{7.15}$$

and e_0 is found to satisfy the transcendental equation

$$\frac{\sqrt{\pi}}{2} \beta e_0 e^{(\frac{1}{2}e_0)^2} \operatorname{erf}\left(\frac{e_0}{2}\right) = 1. \tag{7.16}$$

With (7.15) substituted in (7.11) the solution for the second terms in each series is

$$f_1(\eta) = A_1' \eta + A_2' \operatorname{erf} \eta + A_3' \eta e^{-\eta^2},$$

$$e_1 = \frac{e_0^2}{6 + e_0^2},$$

where $A_1' = -(1 + \beta e_1)$,

$$A_2' = A_1^0 ,$$

$$A_3' = 2 A_1^0 e_1 / e_0 \sqrt{\pi} . \tag{7.17}$$

Proceeding to solve (7.12) then we have

$$f_2(\xi) = A_1^2 \xi + A_2^2 \xi^2 + \operatorname{erf} \xi \,.\, [A_3^2 + A_4^2 \xi + A_5^2 \xi^2] + e^{-\xi^2} [A_6^2 \xi + A_7^2 \xi^2 + A_8^2 \xi^3],$$

and $$e_2 = \frac{e_0}{\beta} \left\{ 1 + \beta \left[3\frac{e_1^2}{e_0} - \frac{e_1}{2} + \frac{5}{4} - \frac{3}{8} e_0^2 + \frac{e_0^2 e_1}{4} - \frac{e_1^2 e_0^2}{8} + \frac{3}{4} e_1^2 \right] - \frac{(1+\beta)}{2 + e_0^2(1+\beta)} \left[2 + e_0^2 + \frac{\beta}{2} \left(3e_0^2 + e_1^2 e_0^2 + 4e_1^2 \right) \right] \right\} \Bigg/ \left\{ 3 + \frac{e_0^2}{2} + \frac{2e_0^2(1+\beta)}{2 + e_0^2(1+\beta)} \right\},$$

where $A_1^2 = A_1^1 \, e_1/e_0,$

$A_2^2 = A_1^1,$ (7.18)

$$A_5^2 = \frac{\beta\sqrt{\pi}\, e_0 e^{(\frac{1}{2}e_0)^2}}{(2 + e_0^2(1+\beta))} \left[\frac{1}{2}(2 + e_0^2) + \frac{\beta}{4}\left(3e_0^2 - 4e_0 e_2 + e_0^2 e_1^2 + 4e_1^2 \right) \right],$$

$$A_3^2 = \tfrac{1}{2} A_5^2 - \frac{1}{2 \operatorname{erf}(\frac{1}{2}e_0)},$$

$$A_4^2 = e_1 / e_0 \operatorname{erf}(\tfrac{1}{2}e_0),$$

$$A_6^2 = -\tfrac{1}{4}\beta e^{(\frac{1}{2}e_0)^2} (3e_0 - 4e_2) + A_5^2 / \sqrt{\pi},$$

$$A_7^2 = e_1 \beta e^{(\frac{1}{2}e_0)^2}, \quad A_8^2 = -\frac{e_1}{e_0} A_7^2 \,.$$

The method used to solve (7.10)-(7.12) is exactly that which will be described in the following analysis when the next two sets of equations (7.13) and (7.14) are solved.

To obtain the fourth term in each series then the functions $f_0(\eta)$, $f_1(\eta)$ and $f_2(\eta)$, as stated above, are substituted in (7.13) and there results the following equation for $f_3(\eta)$:

$$f_3''' + 2\eta f_3'' - 6f_3 = \alpha_1 + \alpha_2\eta + \alpha_3\eta^2 + \alpha_4\eta\left(\alpha_4 + \alpha_5\eta + \alpha_6\eta^2\right) \quad (7.19)$$
$$+ e^{-\eta^2}\left(\alpha_7 + \eta\alpha_8 + \eta^2\alpha_9 + \eta^3\alpha_{10} + \eta^4\alpha_{11} + \eta^5\alpha_{12}\right),$$

where

$$\alpha_1 = 4A_1^2, \qquad \alpha_2 = 4A_1'(2 - e_2/e_0),$$

$$\alpha_3 = -\alpha_1, \qquad \alpha_4 = 4A_5^2\, e_1/e_0,$$

$$\alpha_5 = 4A_5^2 + 2A_4^2\, e_1/e_0 + 2A_1^0(2 - 2e_2/e_0 - e_1^2/e_0^2),$$

$$\alpha_6 = -\alpha_4,$$

$$\alpha_7 = \frac{4}{\sqrt{\pi}} A_3^2 + 2A_6^2 + \frac{4}{\sqrt{\pi}} A_1^0\left(2e_1^2/e_0^2 + e_2/e_0\right), \quad (7.20)$$

$$\alpha_8 = \frac{4}{\sqrt{\pi}} A_4^2 + 4A_7^2 - 6\frac{e_1}{e_0}\left(\frac{2}{\sqrt{\pi}}A_3^2 + A_6^2\right) + 2A_3'\left(2 - \frac{e_1^2}{e_0} - 2\frac{e_2}{e_0}\right)$$

$$+ \frac{5}{\sqrt{\pi}} A_1^0 \frac{e_1}{e_0}\left(1 - \frac{e_2}{e_0}\right) - \left[\frac{20\,A_1^0}{\sqrt{\pi}.\,e_0}\right]e_3 + 8\frac{e_1}{e_0}A_6^2,$$

$$\alpha_9 = \frac{4}{\sqrt{\pi}} A_5^2 - 4A_6^2 + 18 A_8^2 - \frac{12}{\sqrt{\pi}} \frac{e_1}{e_0} A_4^2 - 4 \frac{e_1}{e_0} A_3^1 + 8 \frac{e_1}{e_0} A_7^2$$

$$+ \frac{8}{\sqrt{\pi}} A_1^0 \left(3 - e_1^2/e_0^2 - 2 e_2/e_0\right), \qquad (7.20)$$

$$\alpha_{10} = -4A_7^2 - \frac{12}{\sqrt{\pi}} A_5^2 . e_1/e_0 + 12 A_6^2 e_1/e_0$$

$$- 10 A_8^2 e_1/e_0 - 8 A_3^1 (1 - e_1^2/e_0^2 - 2e_2/e_0),$$

$$\alpha_{11} = -16 A_8^2,$$

$$\alpha_{12} = 12 A_8^2 . e_1/e_0.$$

The problem is now to solve equation (7.19) subject to

$$f_3(0) = f_3\left(\frac{e_0}{2}\right) = 0 \quad , \quad f_3'\left(\frac{e_0}{2}\right) = \frac{5\beta}{e_0} (e_0 e_3 + e_1 e_2) ; \qquad (7.21)$$

the three conditions being required since e_3, which appears in the R.H.S. of (7.19), is unknown.

Define the operator $\mathcal{L}_n(D)$ by

$$\mathcal{L}_n(D) f = (D^2 - 2\xi D - 2n) f , \quad D = \frac{d}{d\xi} . \qquad (7.22)$$

Consequently the differential equations which need to be solved for each $f_i(\xi)$ are of the form

$$\mathcal{L}_n(D) f_n = \Lambda_n(\xi), \qquad (7.23)$$

which is linear in $f_n(\xi)$ and so the general solution may be obtained by adding particular integrals to the complementary function.

In order to proceed we note :

$$\mathcal{L}_n(D)\left[\xi^m e^{-\xi^2}\right] = e^{-\xi^2}\left\{m(m-1)\xi^{m-2} - 2(m+n+1)\xi^m\right\}, \tag{7.24}$$

$$\mathcal{L}_n(D)\left[\xi^m \operatorname{erf}\xi\right] = m(m-1)\xi^{m-2} + \frac{4}{\sqrt{\pi}} m\xi^{m-1}e^{-\xi^2} + 2(m-n)\xi^m \operatorname{erf}\xi, \tag{7.25}$$

and $$\mathcal{L}_n(D)\xi^m = m(m-1)\xi^{m-2} + 2(m-n)\xi^m. \tag{7.26}$$

Firstly (7.25) indicates that to obtain the terms involving the error function on the right hand side of (7.19) then the particular integral must be of the same form. Assuming such a form, utilising (7.25) and comparing coefficients then we find:

$$\mathcal{L}_3(D)\left[\operatorname{erf}\xi\left(-\tfrac{1}{6}[\alpha_4+\alpha_6] - \tfrac{1}{4}\alpha_5\xi - \tfrac{1}{2}\alpha_6\xi^2\right)\right] \tag{7.27}$$

$$= (\alpha_4 + \alpha_5\xi + \alpha_6\xi^2)\operatorname{erf}\xi - \left(\frac{\alpha_5}{\sqrt{\pi}} + \frac{4}{\sqrt{\pi}}\alpha_6\right)e^{-\xi^2}.$$

Thus it is now necessary to find a solution of

$$\mathcal{L}_3(D) f_3 = e^{-\zeta^2}\{\alpha_7^* + \alpha_8^* \zeta + \alpha_9 \zeta^2 + \alpha_{10}\zeta^3 + \alpha_{11}\zeta^4 + \alpha_{12}\zeta^5\} + \{\alpha_1 + \alpha_2\zeta + \alpha_3\zeta^2\}, \tag{7.28}$$

where $\alpha_7^* = \alpha_7 + \frac{\alpha_5}{\sqrt{\pi}}$ and $\alpha_8^* = \alpha_8 + \frac{4}{\sqrt{\pi}}\alpha_6$.

The formulae (7.24) and (7.26) enable the correct form of a particular integral of (7.28) to be assumed. On application of (7.24) and (7.26) there results a solution to which is added the operand on the left hand of (7.27) to give as a particular solution of (7.19):

$$\begin{aligned} f_{3p} = {} & (B_1^3 + B_2^3\zeta + B_3^3\zeta^2) \\ & + (B_4^3 + B_5^3\zeta + B_6^3\zeta^2)\operatorname{erf}\zeta \\ & + (B_7^3 + B_8^3\zeta + B_9^3\zeta^2 + B_{10}^3\zeta^3 + B_{11}^3\zeta^4 + B_{12}^3\zeta^5)e^{-\zeta^2}; \end{aligned} \tag{7.29}$$

where

$$\begin{aligned} & B_1^3 = -\tfrac{1}{6}(\alpha_1+\alpha_3),\ B_2^3 = -\tfrac{1}{4}\alpha_2,\ B_3^3 = -\tfrac{1}{2}\alpha_3, \\ & B_4^3 = -\tfrac{1}{6}(\alpha_4+\alpha_6),\ B_5^3 = -\tfrac{1}{4}\alpha_5,\ B_6^3 = -\tfrac{1}{2}\alpha_6, \\ & B_7^3 = -\tfrac{1}{8}(\alpha_7^* + \tfrac{1}{9}\alpha_9 + \tfrac{1}{8}\alpha_{11}),\ B_8^3 = -\tfrac{1}{10}(\alpha_8^* + \tfrac{3}{7}\alpha_{10} + \tfrac{10}{21}\alpha_{12}), \\ & B_9^3 = -\tfrac{1}{12}(\alpha_9 + \tfrac{3}{4}\alpha_{11}),\ B_{10}^3 = -\tfrac{1}{14}(\alpha_{10} + \tfrac{10}{9}\alpha_{12}), \\ & B_{11}^3 = -\tfrac{1}{16}\alpha_{11},\ B_{12}^3 = -\tfrac{1}{18}\alpha_{12}. \end{aligned} \tag{7.30}$$

To (7.29) we must now add the complementary function of (7.19), i.e. f_{3c}.

This will be found by considering the repeated integrals of the error function. These have been studied and tabulated by Hartree [39]; the relevant relations are to be found in Carslaw and Jaeger [32], Appendix II. Write

$$i^n \operatorname{erfc} \eta = \int_\eta^\infty i^{n-1} \operatorname{erfc} \xi \, d\xi \tag{7.31}$$

with

$$i^0 \operatorname{erfc} \eta = \operatorname{erfc} \eta. \tag{7.32}$$

On integrating by parts we have

$$i^1 \operatorname{erfc} \eta = \frac{1}{\sqrt{\pi}} e^{-\eta^2} - \eta \operatorname{erfc} \eta, \tag{7.33}$$

and

$$i^2 \operatorname{erfc} \eta = \tfrac{1}{4}[\operatorname{erfc} \eta - 2\eta \, i^1 \operatorname{erfc} \eta] \tag{7.34}$$

$$= \tfrac{1}{4}\left[(1+2\eta^2)\operatorname{erfc} \eta - \frac{2}{\sqrt{\pi}} \eta e^{-\eta^2}\right]. \tag{7.35}$$

The general recurrence relation is

$$2n \, i^n \operatorname{erfc} \eta = i^{n-2} \operatorname{erfc} \eta - 2\eta \, i^{n-1} \operatorname{erfc} \eta \tag{7.36}$$

which shows that $f(\eta) = i^n \operatorname{erfc} \eta$ satisfies the differential equation

$$\frac{d^2f}{d\zeta^2} + 2\zeta \frac{df}{d\zeta} - 2nf = 0 , \qquad (7.37)$$

and this is the homogeneous part of (7.23).

Consequently a complementary solution of equation (7.19) is

$$f_3(\zeta) = i^3 \operatorname{erfc} \zeta , \qquad (7.38)$$

$$= \left[\left(\tfrac{1}{4}\zeta + \tfrac{1}{6}\zeta^3\right)\operatorname{erf}\zeta + \frac{(1+\zeta^2)}{6\sqrt{\pi}} e^{-\zeta^2}\right] + \left[\tfrac{1}{4}\zeta + \tfrac{1}{6}\zeta^3\right]. \qquad (7.39)$$

Each of the terms in square brackets of (7.39) is a solution of (7.37) and so the complete complementary function is:

$$f_{3c}(\zeta) = \lambda^*\left[3\zeta + 2\zeta^3\right] + \tilde{\lambda}\left[\frac{2}{\sqrt{\pi}}(1+\zeta^2)e^{-\zeta^2} + (3\zeta + 2\zeta^3)\operatorname{erf}\zeta\right]. \qquad (7.40)$$

where $\tilde{\lambda}$ and λ^* are constants. The general solution of (7.19) is:

$$f_3(\zeta) = \lambda^*\left[3\zeta + 2\zeta^3\right] + \tilde{\lambda}\left[\frac{2}{\sqrt{\pi}} e^{-\zeta^2}(1+\zeta^2) + (3\zeta + 2\zeta^3)\operatorname{erf}\zeta\right]$$

$$+ \left[B_1^3 + B_2^3\zeta + B_3^3\zeta^2\right] + \left[B_4^3 + B_5^3\zeta + B_6^3\zeta^2\right]\operatorname{erf}\zeta$$

$$+ \left[B_7^3 + B_8^3\zeta + B_9^3\zeta^2 + B_{10}^3\zeta^3 + B_{11}^3\zeta^4 + B_{12}^3\zeta^5\right] e^{-\zeta^2}. \qquad (7.41)$$

Since $f_3(0)=0$ then it follows that

$$\tilde{\lambda} = -\tfrac{1}{2}\sqrt{\pi}\,[B_1^3 + B_7^3]. \tag{7.42}$$

Also we have $f_3(\tfrac{1}{2}e_0)=0$, and hence

$$\lambda^* \gamma_0 + \gamma_1 + e_3 \gamma_2 = 0\,; \tag{7.43}$$

where $\gamma_0 = \left(\frac{3e_0}{2} + \frac{e_0^3}{4}\right)$,

$$\gamma_1 = -\tfrac{1}{2}\sqrt{\pi}\left(B_1^3 + B_7^3\right)\left(\frac{2}{\sqrt{\pi}} e^{-(\frac{1}{2}e_0)^2}\left[1+\tfrac{1}{4}e_0^2\right] + \left[\tfrac{3}{2}e_0 + \tfrac{1}{4}e_0^2\right]\operatorname{erf}(\tfrac{1}{2}e_0)\right)$$

$$+\left(B_1^3 + B_2^3\frac{e_0}{2} + \tfrac{1}{4}B_3^3 e_0^2\right) + \left(B_4^3 + \tfrac{1}{2}B_5^3 e_0 + \tfrac{1}{4}B_6^3 e_0^2\right)\operatorname{erf}(\tfrac{1}{2}e_0)$$

$$+\left(B_7^3 + \bar{B}_8^3\frac{e_0}{2} + B_9^3\frac{e_0^2}{4} + B_{10}^3\frac{e_0^3}{8} + B_{11}^3\frac{e_0^4}{16} + B_{12}^3\frac{e_0^5}{32}\right)e^{-(\frac{1}{2}e_0)^2}, \tag{7.44}$$

$$\gamma_2 = \frac{1}{\sqrt{\pi}}\, A_1^0\, e^{-(\frac{1}{2}e_0)^2},$$

and $$\bar{B}_8^3 = B_8^3 - 2A_1^0 e_3 / \sqrt{\pi}.e_0 .$$

The boundary condition has been put in the form (7.43) since e_3 is still unknown. It is on solving this equation simultaneously with that resulting from the last condition in (7.21) that both λ^* and e_3 are now found.

On differentiating (7.34) there results:

$$f_3'(\tfrac{1}{2}e_0) = \gamma_3 + \gamma_4 e_3 + \gamma_5 \lambda^*, \tag{7.45}$$

where $\gamma_3 = -\frac{1}{2}\sqrt{\pi}\left(B_1^3 + B_7^3\right)\left(\frac{3e_0}{\sqrt{\pi}} e^{-(\frac{1}{2}e_0)^2} + \left(3 + \frac{3}{2}e_0^2\right)\operatorname{erf}\frac{1}{2}e_0\right)$

$$+ \left(B_2^3 + e_0 B_3^3\right) + \left(B_5^3 + e_0 B_6^3\right)\operatorname{erf}\left(\tfrac{1}{2}e_0\right)$$

$$+ \left\{\frac{2}{\sqrt{\pi}} B_4^3 + \bar{B}_8^3 + \left(\frac{2}{\sqrt{\pi}} B_5^3 + 2B_9^3 - 2B_7^3\right)\frac{e_0}{2}\right.$$

$$+ \left(\frac{2}{\sqrt{\pi}} B_6^3 + 3B_{10}^3 - 2\bar{B}_8^3\right)\frac{e_0^2}{4} + \left(4B_{11}^3 - 2B_9^3\right)\frac{e_0^3}{8}$$

$$\left. + \left(5B_{12}^3 - 2B_{10}^3\right)\frac{e_0^4}{16} - \frac{1}{16}B_{11}^3 e_0^5 - \frac{1}{32}B_{12}^3 e_0^6\right\} e^{-(\frac{1}{2}e_0)^2}, \qquad (7.46)$$

$$\gamma_4 = \frac{2}{\sqrt{\pi}}\frac{A_1^0}{e_0} e^{-(\frac{1}{2}e_0)^2}\left(1 - \tfrac{1}{2}e_0^2\right),$$

$$\gamma_5 = 3 + \frac{3}{2}e_0^2.$$

Then (7.21) yields

$$\gamma_3 + \gamma_4 e_3 + \gamma_5 \lambda^* = 5\beta e_3 + 5\beta e_1 e_2 / e_0.$$

$$\text{or} \quad e_3(\gamma_4 - 5\beta) + \gamma_5 \lambda^* = 5\beta \frac{e_1 e_2}{e_0} - \gamma_3. \qquad (7.47)$$

Equations (7.43) and (7.47) can now be solved to give:

$$e_3 = \frac{\gamma_0\gamma_3 - \gamma_1\gamma_5 - 5\beta e_1 e_2/e_0}{\gamma_2\gamma_5 + 5\beta\gamma_0 - \gamma_0\gamma_4}, \qquad (7.48)$$

$$\text{and} \quad \lambda^* = -\frac{1}{\gamma_0}\left(\gamma_1 + e_3\gamma_2\right).$$

Hence the form of $f_3(\xi)$ becomes:

$$f_3(\xi) = A_0^3 + A_1^3\xi + A_2^3\xi^2 + A_3^3\xi^3 + (A_4^3 + A_5^3\xi + A_6^3\xi^2 + A_7^3\xi^3)\operatorname{erf}\xi + (A_8^3 + A_9^3\xi + A_{10}^3\xi^2 + A_{11}^3\xi^3 + A_{12}^3\xi^4 + A_{13}^3\xi^5)e^{-\xi^2}, \tag{7.49}$$

where

$$A_0^3 = B_1^3,\ A_1^3 = B_2^3 + 3\lambda^*,\ A_2^3 = B_3^3,\ A_3^3 = 2\lambda^*,$$
$$A_4^3 = B_4^3,\ A_5^3 = B_5^3 + 3\tilde{\lambda},\ A_6^3 = B_6^3,\ A_7^3 = 2\tilde{\lambda},$$
$$A_8^3 = B_7^3 + 2\tilde{\lambda}/\sqrt{\pi},\ A_9^3 = B_8^3,\ A_{10}^3 = B_9^3 + 2\tilde{\lambda}/\sqrt{\pi}, \tag{7.50}$$
$$A_{11}^3 = B_{10}^3,\ A_{12}^3 = B_{11}^3,\ A_{13}^3 = B_{12}^3.$$

Thus we have completed the solution for e_3 and $f_3(\xi)$ and are now in a position to seek the next terms in the expansions. Substituting the known solutions e_i and $f_i(\xi)$, for $i \leq 3$, into the right hand side of the differential equations (7.14) we obtain:

$$f_4'' + 2\xi f_4' - 8f_4 = \bar{\alpha}_0 + \bar{\alpha}_1\xi + \bar{\alpha}_2\xi^2 + \bar{\alpha}_3\xi^3 + (\bar{\alpha}_4 + \bar{\alpha}_5\xi + \bar{\alpha}_6\xi^2 + \bar{\alpha}_7\xi^3)\operatorname{erf}\xi + (\bar{\alpha}_8 + \bar{\alpha}_9\xi + \bar{\alpha}_{10}\xi^2 + \bar{\alpha}_{11}\xi^3 + \bar{\alpha}_{12}\xi^4 + \bar{\alpha}_{13}\xi^5 + \bar{\alpha}_{14}\xi^6 + \bar{\alpha}_{15}\xi^7)e^{-\xi^2}, \tag{7.51}$$

where $\bar{\alpha}_0 = \sigma_2 A_1^2 + \sigma_4 A_1^1 + \sigma_{12} A_0^3 + 2A_1^3$,

$\bar{\alpha}_1 = 4A_2^3 + (\sigma_1 + \sigma_{12}) A_1^3 + 2\sigma_2 A_2^2$,

$+ (\sigma_5 + \sigma_{10}) A_1^1 + (\sigma_3 + \sigma_{11}) A_1^2 + \alpha_{12} A_1^3$,

$\bar{\alpha}_2 = 6A_3^3 + (2\sigma_3 + \sigma_{11}) A_2^2 + 8A_1^1 + (\sigma_{12} + 2\sigma_1) A_2^3$,

$\bar{\alpha}_3 = (3\sigma_1 + \sigma_{12}) A_3^3$,

$\bar{\alpha}_4 = 2A_5^3 + \sigma_2 A_4^2 + \sigma_4 A_3^1 + \sigma_{11} A_3^2 + \sigma_{12} A_4^3$,

$\bar{\alpha}_5 = 4A_6^3 + (\sigma_1 + \sigma_{12}) A_5^3 + 2\sigma_2 A_5^2 + (\sigma_5 + \sigma_{10}) A_1^0$

$+ (\sigma_{11} + \sigma_3) A_4^2$, (7.52)

$\bar{\alpha}_6 = 6A_7^3 + (2\sigma_1 + \sigma_{12}) A_6^3 + (2\sigma_3 + \sigma_{11}) A_5^2 + 8A_1^0$,

$\bar{\alpha}_7 = (3\sigma_1 + \sigma_{12}) A_7^3$,

$\bar{\alpha}_8 = 2A_9^3 + \frac{4}{\sqrt{\pi}} A_4^3 + \sigma_2 (A_6^2 + \frac{2}{\sqrt{\pi}} A_3^2) + \sigma_4 A_3^1$

$+ \sigma_6 \cdot \frac{2}{\sqrt{\pi}} A_1^0 + \sigma_{12} A_8^3$,

$\bar{\alpha}_9 = 4A_{10}^3 + \frac{4}{\sqrt{\pi}} A_5^3 - 4A_8^3 + \sigma_1 (A_9^3 + \frac{2}{\sqrt{\pi}} A_4^3) + \sigma_2 (2A_7^2 + \frac{2}{\sqrt{\pi}} A_4^2)$

$+ \sigma_3 (A_6^2 + \frac{2}{\sqrt{\pi}} A_3^2) + (\sigma_{10} + \sigma_5) A_3^1 + \frac{2}{\sqrt{\pi}} (\sigma_4 + \sigma_7) A_1^0$

$+ \frac{2}{\sqrt{\pi}} e_4 \sigma_8 A_1^0 + \sigma_{11} A_6^2 + \sigma_{12} A_9^3$,

$\bar{\alpha}_{10} = 6A_{11}^3 + \frac{4}{\sqrt{\pi}} A_6^3 - 4A_9^3 + \sigma_1 (2A_{10}^3 + \frac{2}{\sqrt{\pi}} A_5^3 - 2A_8^3)$

$+ \sigma_2 (3A_8^2 + \frac{2}{\sqrt{\pi}} A_5^2 - 2A_6^2) + \sigma_3 (2A_7^2 + \frac{2}{\sqrt{\pi}} A_4^2) + \sigma_{11} A_7^2$

$+ \frac{2}{\sqrt{\pi}} (\sigma_5 + \sigma_9) A_1^0 + (8 - 2\sigma_4) A_3^1 + \sigma_{12} A_{10}^3$,

$$\bar{\alpha}_{11} = 8A_{12}^3 + 4A_7^3 - 4A_{10}^3 + \sigma_1\left(3A_{11}^3 + \frac{2}{\sqrt{\pi}}A_6^3 - 2A_9^3\right)$$
$$- 2\sigma_2 A_7^2 + \sigma_3\left(3A_8^2 + \frac{2}{\sqrt{\pi}}A_5^2 - 2A_6^2\right) + \frac{48}{\sqrt{\pi}}A_1^0$$
$$- 2\sigma_5 A_3^1 + \sigma_{11} A_8^2 + \sigma_{12} A_{11}^3, \qquad (7.52)\ \text{cont.}$$

$$\bar{\alpha}_{12} = 10A_{13}^3 - 4A_{11}^3 + \sigma_1\left(4A_{12}^3 + 2A_7^3 - 2A_{10}^3\right)$$
$$- 2\sigma_2 A_8^2 - 2\sigma_3 A_7^2 - 16A_3^1 + \sigma_{12} A_{12}^3,$$

$$\bar{\alpha}_{13} = -4A_{12}^3 + \sigma_1(5A_{13}^3 - 2A_{11}^3) - 2\sigma_3 A_8^2 + \sigma_{12} A_{13}^3,$$

$$\bar{\alpha}_{14} = -4A_{13}^3 - 2\sigma_1 A_{12}^3, \qquad \bar{\alpha}_{15} = -2\sigma_1 A_{13}^3.$$

Moreover in the above :

$$\sigma_1 = -6e_1/e_0, \quad \sigma_2 = 2e_1/e_0, \quad \sigma_3 = \frac{4}{e_0^2}(e_0^2 - e_1^2 - 2e_0e_2),$$
$$\sigma_4 = 2e_2/e_0, \quad \sigma_5 = \frac{2}{e_0^2}[4e_0e_1 - 5e_0e_3 - 5e_1e_2], \quad \sigma_6 = 2e_3/e_0,$$
$$\sigma_7 = \frac{2}{e_0^2}(2e_1^2 + 4e_0e_2 - 6e_1e_3 - 3e_2^2), \quad \sigma_8 = -12/e_0,$$
$$\sigma_9 = 24e_1/e_0, \quad \sigma_{10} = \frac{4}{e_0^2}(e_0e_3 + e_1e_2),$$
$$\sigma_{11} = \frac{4}{e_0^2}(e_1^2 + 2e_0e_2), \quad \sigma_{12} = 12e_1/e_0.$$

The general solution of (7.52) is found in the identical manner to that described for the solution of (7.19) and is :

$$f_4 = \mu^*(3+12\xi^2+4\xi^4) + \tilde{\mu}\left[(3+12\xi^2+4\xi^4)\operatorname{erf}\xi + \frac{1}{\sqrt{\pi}}(10\xi+4\xi^3)e^{-\xi^2}\right]$$
$$+ (B_0^4 + B_1^4\xi + B_2^4\xi^2 + B_3^4\xi^3) + (B_4^4 + B_5^4\xi + B_6^4\xi^2 + B_7^4\xi^3)\operatorname{erf}\xi$$
$$+ (B_8^4 + B_9^4\xi + B_{10}^4\xi^2 + B_{11}^4\xi^3 + B_{12}^4\xi^4 + B_{13}^4\xi^5 + B_{14}^4\xi^6 + B_{15}^4\xi^7)e^{-\xi^2}, \quad (7.53)$$

where $B_0^4 = -\frac{1}{16}[\bar{\alpha}_2 + 2\bar{\alpha}_0]$, $B_1^4 = -\frac{1}{6}(\bar{\alpha}_1 + 3\bar{\alpha}_3)$,

$B_2^4 = -\frac{1}{4}\bar{\alpha}_2$, $B_3^4 = -\frac{1}{2}\bar{\alpha}_3$, $B_4^4 = -\frac{1}{16}(\bar{\alpha}_6 + 2\bar{\alpha}_4)$,

$B_5^4 = -\frac{1}{6}(\bar{\alpha}_5 + 3\bar{\alpha}_7)$, $B_6^4 = -\frac{1}{4}\bar{\alpha}_6$, $B_7^4 = -\frac{1}{2}\bar{\alpha}_7$,

$B_8^4 = -\frac{1}{10}\left(\bar{\alpha}_8 + \frac{32}{21\sqrt{\pi}}\bar{\alpha}_7 + \frac{2}{3\sqrt{\pi}}\bar{\alpha}_5 + \frac{1}{7}\bar{\alpha}_{10} + \frac{2}{21}\bar{\alpha}_{12} + \frac{10}{77}\bar{\alpha}_{14}\right)$,

$B_9^4 = -\frac{1}{12}\left(\bar{\alpha}_9 + \frac{2}{\sqrt{\pi}}\bar{\alpha}_6 + \frac{3}{8}\bar{\alpha}_{11} + \frac{3}{8}\bar{\alpha}_{13} + \frac{21}{32}\bar{\alpha}_{15}\right)$, (7.54)

$B_{10}^4 = -\frac{1}{14}\left(\bar{\alpha}_{10} + \frac{6}{\sqrt{\pi}}\bar{\alpha}_7 + \frac{2}{3}\bar{\alpha}_{12} + \frac{10}{11}\bar{\alpha}_{14}\right)$,

$B_{11}^4 = -\frac{1}{16}\left(\bar{\alpha}_{11} + \bar{\alpha}_{13} + \frac{7}{4}\bar{\alpha}_{15}\right)$, $B_{12}^4 = -\frac{1}{18}\left(\bar{\alpha}_{12} + \frac{15}{11}\bar{\alpha}_{14}\right)$,

$B_{13}^4 = -\frac{1}{20}\left(\bar{\alpha}_{13} + \frac{7}{4}\bar{\alpha}_{15}\right)$, $B_{14}^4 = -\frac{1}{22}\bar{\alpha}_{14}$, $B_{15}^4 = -\frac{1}{24}\bar{\alpha}_{15}$.

In the general solution (7.53) there are three unknowns, μ^*, $\tilde{\mu}$ and e_4, which will be specified on applying the conditions given in (7.14); namely

$$f_4(0) = f_4\left(\frac{e_0}{2}\right) = 0, \quad f_4'\left(\frac{e_0}{2}\right) = \frac{3}{e_0}\left(2e_0e_4 + 2e_1e_3 + e_2^2\right)\beta. \quad (7.55)$$

The first condition yields,

$$\mu^* = -\tfrac{1}{3}(B_0^4 + B_8^4), \tag{7.56}$$

and the second can be written as

$$\bar{\gamma}_0 \tilde{\mu} + \bar{\gamma}_1 + \bar{\gamma}_2 e_4 = 0. \tag{7.57}$$

Here
$$\bar{\gamma}_0 = (3 + 3e_0^2 + \tfrac{1}{4}e_0^4)\,\mathrm{erf}(\tfrac{1}{2}e_0) + \frac{1}{\sqrt{\pi}}(5e_0 + \tfrac{1}{2}e_1^2),$$

$$\begin{aligned}\bar{\gamma}_1 = {} & -\tfrac{1}{3}(B_0^4 + B_8^4)(3 + 3e_0^2 + \tfrac{1}{4}e_0^4) + (B_0^4 + \tfrac{1}{2}B_1^4 e_0 + \tfrac{1}{4}B_2^4 e_0^2 + \tfrac{1}{8}B_3^4 e_0^3) \\ & + (B_4^4 + \tfrac{1}{2}B_5^4 e_0 + \tfrac{1}{4}B_6^4 e_0^2 + \tfrac{1}{8}B_7^4 e_0^3)\,\mathrm{erf}(\tfrac{1}{2}e_0) \\ & + \Big\{B_8^4 + \bar{B}_9^4 \frac{e_0}{2} + \tfrac{1}{4}B_{10}^4 e_0^2 + \tfrac{1}{8}B_{11}^4 e_0^3 + \tfrac{1}{16}B_{12}^4 e_0^4 \\ & + B_{13}^4\left(\frac{e_0}{2}\right)^5 + B_{14}^4\left(\frac{e_0}{2}\right)^6 + B_{15}^4\left(\frac{e_0}{2}\right)^7\Big\} e^{-(\frac{1}{2}e_0)^2},\end{aligned} \tag{7.58}$$

$$\bar{\gamma}_2 = -\frac{\sigma_8}{12\sqrt{\pi}} A_1^0 e^{-(\frac{1}{2}e_0)^2},$$

and
$$\bar{B}_9^4 = B_9^4 + \frac{1}{6\sqrt{\pi}} e_4 \sigma_8 A_1^0.$$

In order to utilise the boundary condition associated with the liberation of latent heat in (7.55) we must write down the differentiated

form of $f_4(\zeta)$ evaluated at $\zeta = \frac{1}{2}e_0$. This can be taken as

$$f_4'(\tfrac{e_0}{2}) = \bar{\gamma}_3 + \bar{\gamma}_4 e_4 + \bar{\gamma}_5 \tilde{\mu}, \tag{7.59}$$

where
$$\begin{aligned}\bar{\gamma}_3 = {} & \mu^*(12e_0 + 2e_0^3) + (B_1^4 + B_2^4 e_0 + 3B_3^4(\tfrac{e_0}{2})^2) \\ & + (B_5^4 + B_6^4 e_0 + \tfrac{3}{4}B_7^4 e_0^2)\,\mathrm{erf}(\tfrac{1}{2}e_0) \\ & + \Big\{(\bar{B}_9^4 + \tfrac{2}{\sqrt{\pi}}B_4^4) + (B_{10}^4 + \tfrac{1}{\sqrt{\pi}}B_5^4 - B_8^4)e_0 \\ & + (3B_{11}^4 + \tfrac{2}{\sqrt{\pi}}B_6^4 - 2\bar{B}_9^4)(\tfrac{e_0}{2})^2 \\ & + (4B_{12}^4 + \tfrac{2}{\sqrt{\pi}}B_7^4 - 2B_{10}^4)(\tfrac{e_0}{2})^3 + (5B_{13}^4 - 2B_{11}^4)(\tfrac{e_0}{2})^4 \\ & + (6B_{14}^4 - 2B_{12}^4)(\tfrac{e_0}{2})^5 + (7B_{15}^4 - 2B_{13}^4)(\tfrac{e_0}{2})^6 \\ & - 2B_{14}^4(\tfrac{e_0}{2})^7 - 2B_{15}^4(\tfrac{e_0}{2})^8\Big\} e^{-(\frac{1}{2}e_0)^2},\end{aligned} \tag{7.60}$$

$$\bar{\gamma}_4 = \frac{1}{6\sqrt{\pi}}(\tfrac{1}{2}e_0^2 - 1)e^{-(\frac{1}{2}e_0)^2}\cdot\sigma_8 A_1^0,$$

$$\bar{\gamma}_5 = (12e_0 + 2e_0^3)\,\mathrm{erf}(\tfrac{1}{2}e_0) + \frac{4}{\sqrt{\pi}}(4 + e_0^2)e^{-(\frac{1}{2}e_0)^2}.$$

Thus substituting (7.59) in (7.55),

$$(\bar{\gamma}_4 - 6e_0\beta)e_4 + \bar{\gamma}_5\tilde{\mu} = \frac{3\beta}{e_0}(2e_1e_3 + e_2^2) - \bar{\gamma}_3, \tag{7.61}$$

we have a second equation linking the remaining unknowns $\tilde{\mu}$ and e_4. Solving simultaneously (7.57) and (7.61):

{

$$e_4 = \frac{(\bar{\gamma}_1 \bar{\gamma}_5 + \frac{3\beta}{\epsilon_0}(2e_1 e_3 + e_2^2) - \bar{\gamma}_3 \bar{\gamma}_6)}{(\bar{\gamma}_4 \bar{\gamma}_0 - 6e_0 \beta \bar{\gamma}_0 - \bar{\gamma}_2 \bar{\gamma}_5)}, \qquad (7.62)$$

and $$\tilde{\mu} = -\frac{1}{\bar{\gamma}_0}(\bar{\gamma}_1 + \bar{\gamma}_2 e_4). \qquad (7.63)$$

The final step to complete the determination of fifth terms in the series is to write down $f_4(\xi)$.

$$f_4(\xi) = (A_0^4 + A_1^4 \xi + A_2^4 \xi^2 + A_3^4 \xi^3 + A_4^4 \xi^4)$$
$$+ (A_5^4 + A_6^4 \xi + A_7^4 \xi^2 + A_8^4 \xi^3 + A_9^4 \xi^4) \operatorname{erf} \xi$$
$$+ e^{-\xi^2}(A_{10}^4 + A_{11}^4 \xi + A_{12}^4 \xi^2 + A_{13}^4 \xi^3 + A_{14}^4 \xi^4 + A_{15}^5 \xi^5 + A_{16}^4 \xi^6 + A_{17}^4 \xi^7) \qquad (7.64)$$

where $A_0^4 = B_0^4 + 3\mu^*$, $A_1^4 = B_1^4$, $A_2^4 = B_2^4 + 12\mu^*$,

$A_3^4 = B_3^4$, $A_4^4 = 4\mu^*$, $A_5^4 = B_4^4 + 3\tilde{\mu}$, $A_6^4 = B_5^4$,

$A_7^4 = B_6^4 + 12\tilde{\mu}$, $A_8^4 = B_7^4$, $A_9^4 = 4\tilde{\mu}$, $A_{10}^4 = B_8^4$,

$A_{11}^4 = B_9^4 + \frac{10}{\sqrt{\pi}}\tilde{\mu}$, $A_{12}^4 = B_{10}^4$, $A_{13}^4 = B_{11}^4 + 4\tilde{\mu}$, (7.65)

$A_{14}^4 = B_{12}^4$, $A_{15}^4 = B_{13}^4$, $A_{16}^4 = B_{14}^4$, $A_{17}^4 = B_{15}^4$.

{NB the numbering of pages 164 & 165.

$$\frac{2\varepsilon}{e_0\left(1-\frac{2\varepsilon\beta}{e_0}\right)}\frac{\partial\theta}{\partial\beta}=\left(\frac{2}{e_0}\right)\sum_{r=1}^{\infty}\left\{\sum_{p=0}^{r-1}V_p\,f'_{r-p-1}(\beta)\right\}\tau^{r/2}, \tag{7.70}$$

where in this last expansion V_r is defined by

$$\varepsilon\left(1+2\frac{\beta\varepsilon}{e_0}+\left(2\frac{\beta\varepsilon}{e_0}\right)^2+\cdots\right)=\sum_{r=0}^{\infty}V_r\,\tau^{\frac{1}{2}(r+1)}. \tag{7.71}$$

In order to determine the form of V_r let

$$\varepsilon^s=\sum_{i=0}^{\infty}W_{s,i}\,\tau^{\frac{1}{2}(i+1)}, \tag{7.72}$$

so that

$$\varepsilon^1=\sum_{i=0}^{\infty}W_{1,i}\,\tau^{\frac{1}{2}(i+1)},\quad W_{1,i}=e_i, \tag{7.73}$$

$$\left.\begin{aligned}W_{s,i}&=\sum_{u=0}^{i-1}e_{i-u-1}\,W_{s-1,u}\quad\text{for } i\geq 1\\ W_{s,0}&=0,\end{aligned}\right\}\ \text{for } s>1, \tag{7.74}$$

and then

$$V_r=\sum_{j=1}^{r+1}W_{j,r}\left(\frac{2\beta}{e_0}\right)^{j-1}. \tag{7.75}$$

1(b): Numerical solution of $f_r(\zeta)$.

The preceding analysis can be readily extended to obtain further terms in the expansions but the work involved becomes increasingly more laborious. The present aim is to derive the functions $f_r(\zeta)$ and the constants e_r numerically.

As before introduce $\zeta = \frac{1}{2}e_0\eta$ so that (7.6) becomes

$$\frac{\partial^2\theta}{\partial\zeta^2}\left(\frac{4}{e_0^2}\right)\varepsilon\zeta\frac{d\varepsilon}{d\tau}\frac{\partial\theta}{\partial\zeta} - \left(\frac{4}{e_0^2}\right)\varepsilon^2\frac{\partial\theta}{\partial\tau} = \left(\frac{2}{e_0}\right)\left(\frac{\varepsilon}{1-\frac{2\varepsilon}{e_0}\zeta}\right)\frac{\partial\theta}{\partial\zeta}. \quad (7.66)$$

On substituting (7.8) and (7.9) into each term of this equation the series expressions for each component of (7.66) become:

$$\frac{\partial^2\theta}{\partial\zeta^2} = \sum_{r=0}^{\infty} f_r''(\zeta)\,\tau^{r/2}, \quad (7.67)$$

$$\left(\frac{4}{e_0^2}\right)\varepsilon\zeta\frac{d\varepsilon}{d\tau}\frac{\partial\theta}{\partial\zeta} = \left(\frac{4\zeta}{e_0^2}\right)\sum_{r=0}^{\infty}\left\{\sum_{q=0}^{r}\left(f_q'(\zeta)\left[\sum_{p=0}^{r-q}(r-q-p+1)e_p e_{r-p-q}\right]\right)\right\}\tau^{r/2}, \quad (7.68)$$

$$-\left(\frac{4}{e_0^2}\right)\varepsilon^2\frac{\partial\theta}{\partial\tau} = -\left(\frac{4}{e_0^2}\right)\sum_{r=1}^{\infty}\left\{\sum_{q=1}^{r}\frac{1}{2}q\,f_q(\zeta)\left[\sum_{p=0}^{r-q}e_p e_{r-q-p}\right]\right\}\tau^{r/2}, \quad (7.69)$$

We now equate the coefficients of $\tau^{r/2}$, for r ≥ 0 and obtain differential equations governing $f_r(\xi)$. The boundary conditions to impose on these are realised by substituting (7.8) and (7.9) into

$$\theta = 0 \quad \text{at} \quad \xi = 0,$$
$$\theta = 1 \quad \text{and} \quad \frac{\partial\theta}{\partial\xi} = \left(\frac{2}{e_0}\right)\beta\varepsilon\frac{d\varepsilon}{d\tau} \quad \text{at} \quad \xi = \tfrac{1}{2}e_0. \tag{7.76}$$

which result when $\xi = \frac{1}{2}e_0\eta$ is introduced into (7.7). Thus we have

$$f_0(0) = 0, \quad f_0\left(\frac{e_0}{2}\right) = 1, \tag{7.77}$$

$$f_n(0) = f_n\left(\frac{e_0}{2}\right) = 0 \quad \text{for } n \geq 1, \tag{7.78}$$

and

$$\sum_{r=0}^{\infty} f_r'\left(\frac{e_0}{2}\right)\tau^{r/2} = \left(\frac{\beta}{e_0}\right)\sum_{r=0}^{\infty}\left\{\sum_{j=0}^{r}(r-j+1)e_j e_{r-j}\right\}\tau^{r/2}. \tag{7.99}$$

Equating the zeroeth order terms in (7.76) and (7.79) we obtain (7.10) as the equations governing $f_0(\xi)$ and e_0 and thus we have, as before,

$$f_0(\zeta) = \frac{\sqrt{\pi}}{2}\,\beta\, e_0\, e^{(\frac{1}{2}e_0)^2}\, \mathrm{erf}\,\zeta$$

where e_0 is the root of (7.80)

$$\frac{\sqrt{\pi}}{2}\,\beta\, e_0\, e^{(\frac{1}{2}e_0)^2}\, \mathrm{erf}\,(\tfrac{1}{2}e_0) = 1.$$

The root is unique since $\psi(e_0) = \frac{\sqrt{\pi}}{2}\beta e_0 e^{(\frac{1}{2}e_0)^2}\mathrm{erf}(\frac{1}{2}e_0) - 1$ is a monotonic increasing function.

As in the analytic solution it is necessary to know $f_i(\zeta)$ and e_i for $0 \le i \le r-1$ when calculating $f_r(\zeta)$ and e_r. The method for finding the r^{th} terms will thus be described assuming the preceding terms are known.

Comparing coefficients of $\tau^{r/2}$ in (7.66) and using (7.67)-(7.75) the equation to be solved for $f_r(\zeta)$ is:

$$f_r''(\zeta) + \left(\frac{2\zeta}{e_0^2}\right)\sum_{q=0}^{r}\left\{f_q'(\zeta)\left[\sum_{p=0}^{r-q}(r-q-p+1)\,e_p\,e_{r-p-q}\right]\right\}$$

$$-\left(\frac{2}{e_0}\right)\sum_{q=1}^{r}\left\{q\,f_q(\zeta)\left[\sum_{p=0}^{r-q} e_p\,e_{r-q-p}\right]\right\} = \left(\frac{2}{e_0}\right)\sum_{p=0}^{r-1} V_p\, f'_{r-p-1}(\zeta), \qquad (7.81)$$

This leads to the differential recurrence relation:

$$f_r''(\rho) + 2\rho f_r'(\rho) - 2r f_r(\rho)$$

$$= \left(\frac{2}{\epsilon_0}\right)\sum_{p=0}^{r-1} V_p f'_{r-p-1}(\rho) + \left(\frac{2}{\epsilon_0^2}\right)\sum_{q=1}^{r-1} q f_q(\rho)\left[\sum_{p=0}^{r-q} e_p e_{r-q-p}\right]$$

$$-\left(\frac{2\rho}{\epsilon_0^2}\right)\sum_{q=0}^{r-1}\left(f_q'(\rho)\left[\sum_{p=0}^{r-q}(r-q-p+1)\, e_p e_{r-p-q}\right]\right). \qquad (7.82)$$

In addition to $f_r(\rho)$ being unknown in this equation e_r is as yet unspecified. Fortunately e_r only occurs once on the right hand side, in the last term, so is easily isolated and (7.82) is regrouped as follows:

$$f_r''(\rho) + 2\rho f_r'(\rho) - 2r f_r(\rho) = \phi_r(\rho) + e_r \psi_r(\rho), \qquad (7.83)$$

where $$\phi_r(\rho) = \left(\frac{2}{\epsilon_0}\right)\sum_{p=0}^{r-1} V_p f'_{r-p-1}(\rho) + \left(\frac{2}{\epsilon_0^2}\right)\sum_{q=1}^{r-1} q f_q(\rho)\left[\sum_{p=0}^{r-q} e_p e_{r-p-q}\right]$$

$$-\left(\frac{2\rho}{\epsilon_0^2}\right)\sum_{q=1}^{r-1} f_q'(\rho)\left[\sum_{p=0}^{r-q}(r-q-p+1)\, e_p e_{r-p-q}\right]$$

$$-\left(\frac{2\rho}{\epsilon_0^2}\right) f_0'(\rho)\sum_{p=1}^{r-1}(r-p+1)\, e_p e_{r-p}, \qquad (7.84)$$

and $$\psi_r = -\left(\frac{2\rho}{\epsilon_0}\right)(r+2) f_0'(\rho).$$

The boundary conditions for (7.83) come from (7.78) and (7.79). These are

$$f_r(0) = f_r\left(\frac{e_0}{2}\right) = 0, \tag{7.85}$$

and

$$f_r'\left(\frac{e_0}{2}\right) = H_r + e_r K_r, \tag{7.86}$$

where

$$H_r = \left(\frac{\beta}{e_0}\right) \sum_{j=1}^{r-1} (r-j+1)\, e_j\, e_{r-j} \tag{7.87}$$

and

$$K_r = (r+2)\beta.$$

Introduce again the operator $\mathcal{L}_r(D)$ defined by (7.22), then we wish now to solve

$$\mathcal{L}_r(D) f_r(\xi) = \phi_r(\xi) + e_r \psi_r(\xi) \tag{7.88}$$

subject to (7.85) and (7.86).

Firstly seek solutions $f_r^*(\xi)$ and $f_r^{**}(\xi)$ of the equations

$$\mathcal{L}_r f_r^*(\xi) = \phi_r(\xi) \tag{7.89}$$

subject to

$$f_r^*(0) = f_r^*\left(\frac{e_0}{2}\right) = 0 \tag{7.90}$$

and also $$\mathcal{L}_r f_r^{**}(\eta) = \psi_r(\eta)$$

subject to $$f_r^{**}(0) = f_r^{**}\left(\frac{e_0}{2}\right) = 0. \qquad (7.91)$$

The method of integration employed to solve these equations is Gill's modification of the Runge-Kutta scheme, and solutions are constructed as follows.

Solve

$$\mathcal{L}_r F_r^*(\eta) = 0, \; F_r^*(0) = 0, \; F_r^{*\prime}(0) = 1, \qquad (7.92)$$

and

$$\mathcal{L}_r \bar{F}_r^*(\eta) = \phi_r(\eta), \; \bar{F}_r^*(0) = 0, \; \bar{F}_r^{*\prime}(0) = 0, \qquad (7.93)$$

so that if

$$f_r^*(\eta) = A_r F_r^*(\eta) + \bar{F}_r^*(\eta), \; A_r \text{ constant} \qquad (7.94)$$

then (7.89) is satisfied, $f_r^*(0) = 0$ and $f_r^*\left(\frac{e_0}{2}\right) = 0$ provided

$$A_r = -\bar{F}_r^*\left(\frac{e_0}{2}\right) \Big/ F_r^*\left(\frac{e_0}{2}\right).$$

A similar pair of functions to $F_r^*(\eta)$ and $\bar{F}_r^*(\eta)$ is introduced to solve (7.91).

Now let $$f_r(\eta) = f_r^*(\eta) + e_r f_r^{**}(\eta) \qquad (7.95)$$

so this function $f_r(\zeta)$ satisfies (7.88) and (7.85). To determine e_r evaluate the differentiated form of (7.95) at $\zeta = \frac{1}{2}e_0$, i.e.

$$f_r'\left(\frac{e_0}{2}\right) = f_r^{*\prime}\left(\frac{e_0}{2}\right) + e_r f_r^{**\prime}\left(\frac{e_0}{2}\right) \qquad (7.96)$$

and solve this simultaneously with (7.86).

The function $f_r(\zeta)$ is then obtained by substituting the value of e_r into (7.95), thus completing the cycle which determines the r^{th} terms from the previous terms.

2. Direct numerical solution of the governing equations

The previous series expansion for ε shows for small τ that $\varepsilon \sim \tau^{\frac{1}{2}}$ and consequently $\frac{d\varepsilon}{d\tau}$ is singular at $\tau = 0$. For this reason any attempt to start the numerical solution at $\tau = 0$ will lead to errors, and in order to avoid this problem the previously obtained series solution will be used to start the integration procedure at some finite small time. Consequently we take the governing equations in the form (7.66), i.e.

$$\frac{\partial^2\theta}{\partial\zeta^2} + \left(\frac{4}{e_0^2}\right)\varepsilon\zeta\frac{d\varepsilon}{d\tau}\frac{\partial\theta}{\partial\zeta} - \left(\frac{4}{e_0^2}\right)\varepsilon^2\frac{\partial\theta}{\partial\tau} = \left(\frac{2}{e_0}\right)\left(\frac{\varepsilon}{1-2\varepsilon\frac{\zeta}{e_0}}\right)\frac{\partial\theta}{\partial\zeta} \qquad (7.100)$$

and the boundary conditions (7.76), i.e.:

$$\theta = 0 \text{ at } \zeta = 0 \; ; \; \theta = 1 \text{ at } \zeta = \tfrac{1}{2}e_0 \qquad (7.101)$$

and $$\frac{\partial\theta}{\partial\zeta} = \left(\frac{2}{e_0}\right)\beta\varepsilon\frac{d\varepsilon}{d\tau} \text{ at } \zeta = \tfrac{1}{2}e_0. \qquad (7.102)$$

Equation (7.100) will be solved in a similar manner to the partial differential equations which arose in the study of non-similar condensation flows in Part I of this thesis. In this case the solution is available for small time, say at $\tau = \tau_0$, from the series solution, and knowing this, the solution at time $\tau = \tau_1$ is deduced by approximating to the equation at the time $\tau = \frac{1}{2}(\tau_0 + \tau_1)$ using the Hartree-Womersley technique. Knowing the solution at a general time, $\tau = \tau_N$, that at the time $\tau = \tau_{N+1}$ is similarly found solving (7.100) at $\tau = \frac{1}{2}(\tau_N + \tau_{N+1})$.

Applying the Hartree-Womersley scheme at a general time location we have:

$$\left[\frac{\partial^2\theta_N}{\partial\xi^2} + \frac{\partial^2\theta_{N+1}}{\partial\xi^2}\right] + \left(\frac{2}{\varepsilon_0^2}\right)\xi\,(\varepsilon_N + \varepsilon_{N+1})\left(\frac{\varepsilon_{N+1} - \varepsilon_N}{\tau_{N+1} - \tau_N}\right)\left[\frac{\partial\theta_{N+1}}{\partial\xi} + \frac{\partial\theta_N}{\partial\xi}\right]$$

$$-\left(\frac{4}{\varepsilon_0^2}\right)(\varepsilon_{N+1}^2 + \varepsilon_N^2)\left[\frac{\theta_{N+1} - \theta_N}{\tau_{N+1} - \tau_N}\right] = \frac{1}{\varepsilon_0}\left(\frac{\varepsilon_{N+1}}{1 - 2\xi\frac{\varepsilon_{N+1}}{\varepsilon_0}} + \frac{\varepsilon_N}{1 - 2\xi\frac{\varepsilon_N}{\varepsilon_0}}\right)\left[\frac{\partial\theta_{N+1}}{\partial\xi} + \frac{\partial\theta_N}{\partial\xi}\right], \quad (7.103)$$

which can be written as

$$\frac{\partial^2\theta_{N+1}}{\partial\xi^2} + \xi_1\frac{\partial\theta_{N+1}}{\partial\xi} + \xi_2\theta_{N+1} + \xi_3 = 0 \quad (7.104)$$

where

$$\xi_1 = \left(\frac{2\xi}{\varepsilon_0^2}\right)\left[\frac{\varepsilon_{N+1}^2 - \varepsilon_N^2}{\tau_{N+1} - \tau_N}\right] - \frac{1}{\varepsilon_0}\left(\left[\frac{\varepsilon_{N+1}}{1 - 2\xi\frac{\varepsilon_{N+1}}{\varepsilon_0}}\right] + \left[\frac{\varepsilon_N}{1 - 2\xi\frac{\varepsilon_N}{\varepsilon_0}}\right]\right),$$

$$\xi_2 = -\left(\frac{4}{\varepsilon_0^2}\right)\left(\frac{\varepsilon_{N+1}^2 + \varepsilon_N^2}{\tau_{N+1} - \tau_N}\right), \quad (7.105)$$

$$\xi_3 = \frac{\partial^2\theta_N}{\partial\xi^2} + \left\{\frac{2\xi}{\varepsilon_0^2}\left[\frac{\varepsilon_{N+1}^2 - \varepsilon_N^2}{\tau_{N+1} - \tau_N}\right] - \frac{1}{\varepsilon_0}\left[\frac{\varepsilon_{N+1}}{1 - 2\varepsilon_{N+1}\xi} + \frac{\varepsilon_N}{1 - 2\xi\frac{\varepsilon_N}{\varepsilon_0}}\right]\right\}\frac{\partial\theta_N}{\partial\xi}$$

$$+\left(\frac{4}{\varepsilon_0^2}\right)\left(\frac{\varepsilon_{N+1}^2 + \varepsilon_N^2}{\tau_{N+1} - \tau_N}\right)\theta_N.$$

The condition (7.102) must also be approximated to at and yields

$$e_0 \left(\frac{\partial \theta_{N+1}}{\partial \zeta} + \frac{\partial \theta_N}{\partial \zeta} \right)_{\zeta = \frac{1}{2} e_0} = \beta \left(\frac{\varepsilon_{N+1}^2 - \varepsilon_N^2}{\tau_{N+1} - \tau_N} \right), \qquad (7.106)$$

whilst (7.101) holds at $\tau = \tau_{N+1}$ so that

$$\theta_{N+1} = 0 \; ; \; \zeta = 0 \; ; \quad \theta_{N+1} = 1, \; \zeta = \tfrac{1}{2} e_0. \qquad (7.107)$$

Appendix C states that quasi-linearisation of the equation and boundary conditions leads to the most rapidly convergent process for dealing with the equations arising in condensation problems. The same will be true here but the linearisation of (7.103) to include a term $\zeta_4 \varepsilon_{N+1}$ is by no means a simple matter and so the following procedure has been developed.

At the time $\tau = \tau_{N+1}$ a value of ε_{N+1} is assumed and (7.104) solved, in a similar manner to (C·47) [see Appendix C], subject to (7.107). The error in the boundary condition is noted and then ε_{N+1} is perturbed by a small amount and a second solution obtained. Assuming that the error in (7.106) can be expanded as a Taylor series in ε_{N+1} then a new estimate of ε_{N+1} is calculated as in the Newton-Raphson method. The entire process is repeated until ε_{N+1} has converged to sufficient accuracy at $\tau = \tau_{N+1}$.

In order to maintain accuracy as τ varies the method applied in Appendix C to the condensation problems is now applied. That is the converged accurate solution at time $\tau = \tau_N$ is used to find that at $\tau = \tau_N + \Delta\tau$. This is now used to compute the solution at $\tau = \tau_N + 2\Delta\tau$ which is then compared with the solution at this time obtained by taking twice the time step length from $\tau = \tau_N$. If the discrepancy is less than an allowed tolerance ($0.00001 \times \varepsilon_N$) then the solution at $\tau = \tau_N + 2.\Delta\tau$ obtained by taking the two steps is accepted and the procedure continued with the same time step length. Otherwise the time step length is halved and the process re-started at $\tau = \tau_N$.

Discussion of results

Considering the non-dimensional form of the governing equation and boundary conditions (7.6)-(7.8), then it is apparent that the time history of the solidification of a cylindrical bar of any material for any temperature difference ΔT can be deduced if solutions are known throughout the range of $\beta = \frac{L}{c_p \Delta T}$, $0 < \beta < \infty$.

In order to see which part of this range is likely to be important physically, table (30) has been included giving details of material properties. For freezing water $L/Cp = 160$ and since the temperature difference is likely to be only a few degrees, a large value of β is expected. The tabulated data for the metals cannot be accurate since they depend on the exact specifications, but they do give an idea of the magnitude of the various properties and it can be seen for the metals

listed that $^{L}/Cp \sim 400$. Since the cooling of a metal bar is controlled by radiation from the surface during the solidification process, it is not realistic to stipulate a fixed low wall temperature which would yield $\beta < 1$, and again we have $\beta > 1$.

Consequently the solutions are sought for $\beta = 10$ and $\beta = 20$ in the zone of expected physical interest, and for $\beta = 0.1$ at the low end. To illustrate the nature for $\beta \sim 1$ the specific value of $\beta = 1.5613$ has been chosen. This value can be traced back to Jones [40] and all subsequent authors on the problem have used this case for comparison purposes. Consider firstly then the case $\beta = 1.5613$ and examine the accuracy of previous solutions.

The full numerical solution, if started at $\tau = 0.025$ from the series solution involving five terms, yields results which are given in table 31 . The time history of the interface is also displayed graphically in figure 22 , where comparison is made with the numerical solution obtained by Allen and Severn [36] and also with an approximate method formulated by Poots [37], based on a modification of the Karman-Pohlhausen technique due to Tani [41]. The times of complete solidification by these authors are $\tau_f = 0.47$ and $\tau_f = 0.52$ respectively while the full numerical solution predicts $\tau_f = 0.548$.

The series solutions with respectively five and twenty-three terms yield results which are to be found in tables 31 and 33 . The shorter series agrees with the full numerical solution to within 5 per cent for 90 per cent of the total solidification time, while the longer agrees to

within 0.2 per cent throughout the solidification period and predicts $\tau_f = 0.55$.

All these models, with the exception of the series involving only five terms, predict that the interfacial velocity decreases from its infinite value at $\tau = 0$ but accelerates as the time of complete solidification is approached. The singularity at $\tau = 0$ has been avoided in the numerical scheme by starting at a finite value of τ but there is also an apparent singularity in (7.100) at $\xi = 1$ and $\beta = \frac{1}{2}e_0$ which must lead to errors in any of the methods. Allen and Severn neglect both singularities, and though no doubt one cause for their loss in accuracy is the size of the mesh length used in the relaxation method, it is doubtful whether the scheme as presented could produce the correct solutions even if the mesh was refined.

The solutions for $\beta = 10$ and $\beta = 20$, which are given in tables 34 and 35 and displayed graphically in figures 23 and 24, exhibit similar forms to those for $\beta = 1.5613$. The temperature profiles across the solidified annulus are initially almost linear but as time progresses they become increasingly more concave so that $\frac{\partial\theta}{\partial\eta}$ at $\eta = 1$ is increasing. As before the interface accelerates towards the axis as $\tau \to \tau_f$. The solution for $\beta = 0.1$ only behaves in part like those for $\beta > 1$, in that the velocity decreases from its infinite value at $\tau = 0$ and then increases. In contrast though as time progresses the concavity is in the opposite direction and $\frac{\partial\theta}{\partial\eta}$ at $\eta = 1$ now decreases, which is apparent from table 36 and figure 25.

The times of complete solidification are given in table 37 for β = 0.1, 0.2, 1.5613, 4.10 and 20.

The two-fold incentive for this problem has been stated and having produced and discussed the numerical solutions we are now in a better position to study the convergence of the series solution.

The radius of convergence, τ_R , of the series

$$\varepsilon = \sum_{r=0}^{\infty} e_r \tau^{\frac{1}{2}(r+1)} \qquad (7.108)$$

is given by

$$\tau_R = \lim_{r\to\infty} \left(e_r / e_{r+1} \right)^2. \qquad (7.109)$$

The first twenty-three terms of (7.108) have been computed for the case β = 1.5613, the coefficients e_r being listed in tahle 38 , but from this it is not possible to conclude that there is a specific radius of convergence since the ratio e_r/e_{r+1} is decreasing almost linearly as r increases. However it is possible to deduce from the following that the radius of convergence cannot be greater than τ_f .

To establish this consider the equation (7.7) and specifically its form as the time of complete solidification is approached. In this region $\varepsilon \to 1$ and the solidified phase is given by $0 \leq \eta \leq 1$. Thus it is apparent that the series cannot converge for $\tau = \tau_f$ because the expansion of $(1-\varepsilon\eta)^{-1}$ only converges for $\varepsilon\eta < 1$.

It has already been acknowledged that this singularity causes the full numerical scheme to predict erroneous behaviour very close to $\tau = \tau_f$,

but if $\tau_f = 0.548$ is accepted when $\beta = 1.5613$ then $\tau_R < 0.548$. The fact that longer series agrees so well with the 'exact' solution must indicate there is a non-zero radius of convergence, and it seems plausible to suggest that the series will converge for $\tau < \tau_f$ but not for $\tau = \tau_f$.

The corresponding data to that given for $\beta = 1.5613$ is given for the case $\beta = 20$ in tables 32, 35 and 39. Comparing these one is able to reach the same conclusion as from the data for $\beta = 1.5613$.

Material	State	Thermal conductivity cal/sec.cm.°C	Specific heat.cp cal/g/°C	denisty g/Cm^3	Latent Heat cal/g	L/cp °C.
Water	-	0.000144	1.0	1.0	80	160
Ice	-	0.0053	0.502	0.92		
Steel	molten	0.038	0.2	7.2	70	424
	solid	0.076	0.165	7.5		
Aluminium	molten	0.411	0.251	2.377	90	450
	solid	0.411	0.206	2.70		
Brass	molten	-	-	-	36	400
	solid	0.25	0.09	8.5		

Table. 30.

τ	0.1		0.2		0.3		0.4		0.5		0.548	
η	N	S	N	S	N	S	N	S	N	S	N	S
0	0	0	0	0	0	0	0	0	0	0	0	0
0.2	0.190	0.190	0.176	0.177	0.163	0.165	0.151	0.155	0.137	0.145	0.132	0.147
0.4	0.389	0.390	0.366	0.368	0.344	0.349	0.321	0.322	0.295	0.315	0.283	0.322
0.6	0.593	0.594	0.568	0.572	0.542	0.522	0.512	0.534	0.473	0.516	0.540	0.524
0.8	0.789	0.779	0.799	0.785	0.758	0.773	0.729	0.763	0.682	0.754	0.639	0.751
1	1.000	1.000	1.000	1.000	1.000	1.000	1.000	1.000	1.000	1.000	1.000	1.000
ε	0.346	0.346	0.506	0.505	0.642	0.637	0.772	0.757	0.912	0.871	1.000	0.887
$\frac{d\varepsilon}{d\tau}$	1.855	1.854	1.435	1.417	1.303	1.247	1.315	1.164	1.580	0.121	2.395	0.954

Table 31 . Temperature distributions and interfacial positions for the case $\beta = 1.5613$.

N- Numerical solution; S- Series solution involving 5 terms.

τ	0	1	2	3	4	5	5.3	5.45
ε	0	0.334	0.492	0.627	0.761	0.914	0.969	1.000
$\frac{d\varepsilon}{d\tau}$	∞	0.181	0.142	0.132	0.139	0.174	0.195	0.208

Table 32. . . Interface position and velocity β = 20.

Series solution using 20 terms.

τ	0	0.1	0.2	0.3	0.4	0.5	0.548	0.55
ε	0	0.346	0.506	0.642	0.772	0.915	0.997	1.001
$\frac{d\varepsilon}{d\tau}$	∞	1.855	1.435	1.308	1.329	1.575	1.834	1.872

Table 33 . Interface position and velocity, β = 1.5613

Series solution involving 23 terms.

τ	0.4875		0.9875		1.4875		1.9875		2.4875		2.693	
η	N	S	N	S	N	S	N	S	N	S	N	S
0	0	0	0	0	0	0	0	0	0	0	0	0
0.2	0.175	0.176	0.159	0.162	0.143	0.151	0.126	0.141	0.102	0.132	0.087	0.128
0.4	0.361	0.363	0.334	0.341	0.307	0.324	0.274	0.307	0.226	0.292	0.192	0.286
0.6	0.560	0.563	0.529	0.540	0.496	0.520	0.453	0.503	0.382	0.487	0.319	0.480
0.8	0.772	0.775	0.749	0.759	0.721	0.746	0.680	0.733	0.598	0.721	0.485	0.716
1	1.000	1.000	1.000	1.000	1.000	1.000	1.000	1.000	1.000	1.000	1.000	1.000
ε	0.327	0.326	0.483	0.477	0.616	0.600	0.745	0.708	0.896	0.807	1.000	0.846
$\frac{d\varepsilon}{d\tau}$	0.361	0.356	0.280	0.266	0.257	0.228	0.268	0.206	0.369	0.192	0.908	0.187

Table 34. Temperature distributions and interfacial positions for the case $\beta = 10$

N-Numerical solution; S- Series solution involving 3 terms.

τ	1		2		3		4		5		5.3	
η	N	S	N	S	N	S	N	S	N	S	N	S
0	0	0	0	0	0	0	0	0	0	0	0	0
0.2	0.172	0.173	0.155	0.159	0.139	0.148	0.120	0.138	0.090	0.128	0.074	0.126
0.4	0.356	0.359	0.328	0.337	0.299	0.318	0.262	0.302	0.202	0.286	0.165	0.281
0.6	0.555	0.558	0.522	0.534	0.486	0.514	0.437	0.496	0.346	0.479	0.281	0.474
0.8	0.768	0.771	0.743	0.755	0.712	0.740	0.665	0.727	0.556	0.715	0.454	0.711
1	1.000	1.000	1.000	1.000	1.000	1.000	1.000	1.000	1.000	1.000	1.000	1.000
ε	0.334	0.333	0.492	0.485	0.627	0.609	0.761	0.718	0.923	0.819	0.998	0.848
$\frac{d\varepsilon}{d\tau}$	0.181	0.178	0.142	0.134	0.132	0.115	0.140	0.104	0.206	0.097	0.322	0.048

Table 35 . Temperature distributions and interfacial positions for the case $\beta = 20$.

N- Numerical solution; S- Series solution involving 3 terms.

τ	0.02		0.04		0.06		0.08		0.1		0.114	
η	N	S	N	S	N	S	N	S	N	S	N	S
0	0	0	0	0	0	0	0	0	0	0	0	0
0.2	0.281	0.281	0.272	0.272	0.265	0.265	0.260	0.260	0.257	0.253	0.258	0.249
0.4	0.542	0.542	0.531	0.532	0.522	0.523	0.515	0.515	0.511	0.508	0.513	0.503
0.6	0.755	0.755	0.745	0.747	0.737	0.740	0.730	0.733	0.725	0.727	0.725	0.724
0.8	0.906	0.906	0.900	0.902	0.895	0.898	0.890	0.895	0.883	0.892	0.877	0.890
1	1.000	1.000	1.000	1.000	1.000	1.000	1.000	1.000	1.000	1.000	1.000	1.000
ε	0.367	0.368	0.530	0.529	0.663	0.656	0.784	0.767	0.904	0.867	1.000	0.932
$\frac{d\varepsilon}{d\tau}$	9.58	9.54	7.16	6.99	6.24	5.89	5.92	5.23	6.22	4.80	7.55	0.457

Table 36 . Temperature distributions and interfacial positions for the case $\beta = 0.1$

N- Numerical solution; S- series solution involving 3 terms.

β	τ_f
0.1	0.114
0.2	0.153
1.5613	0.548
4	1.19
10	2.69
20	5.30

Table 37.

r	e_r	e_r/e_{r+1}.	$(e_r/e_{r+1})^2$
0	1.0337	6.838	46.76
1	0.15118	1.603	2.569
2	0.09432	1.235	1.525
3	0.07640	1.086	1.179
4	0.070369	1.005	1.010
5	0.07005	0.953	0.908
6	0.07348	0.918	0.843
7	0.08004	0.892	0.769
8	0.08971	0.873	0.762
9	0.10281	0.847	0.734
10	0.11997	0.844	0.712
11	0.14208	0.834	0.696
12	0.17034	0.825	0.681
13	0.20637	0.813	0.669
14	0.25227	0.812	0.659
15	0.31086	0.806	0.650
16	0.38554	0.801	0.642
17	0.48114	0.797	0.635
18	0.60366	0.793	0.629
19	0.76105	0.790	0.627
20	0.96360	0.787	0.619
21	1.22486	0.784	0.615
22	1.56250	-	-

Table 38. Coefficients e_r in series expansion for ε, (7.19). $\beta = 1.5613$

r	e_r	e_r/e_{r+1}	$(e_r/e_{r+1})^2$
0	3.136×10^{-1}	19.44	378
1	1.613×10^{-2}	4.837	23.4
2	3.333×10^{-3}	3.755	14.10
3	8.881×10^{-4}	3.320	11.02
4	2.675×10^{-4}	3.083	9.506
5	8.676×10^{-5}	2.934	8.609
6	2.957×10^{-5}	2.832	8.022
7	1.044×10^{-5}	2.757	7.599
8	3.787×10^{-6}	2.701	7.296
9	1.402×10^{-6}	2.655	7.048
10	5.281×10^{-7}	2.620	6.862
11	2.016×10^{-7}	2.589	6.702
12	7.787×10^{-8}	2.564	6.574
13	3.037×10^{-8}	2.544	6.470
14	1.194×10^{-8}	2.524	6.370
15	4.731×10^{-9}	2.508	6.292
16	1.886×10^{-9}	2.494	6.219
17	7.563×10^{-10}	2.482	6.161
18	3.047×10^{-10}	2.471	6.107
19	1.233×10^{-10}	2.461	6.057
20	0.501×10^{-11}	-	-

Table 39 . Coefficients e_r in series expansion for ε (7.19), $\beta = 20$

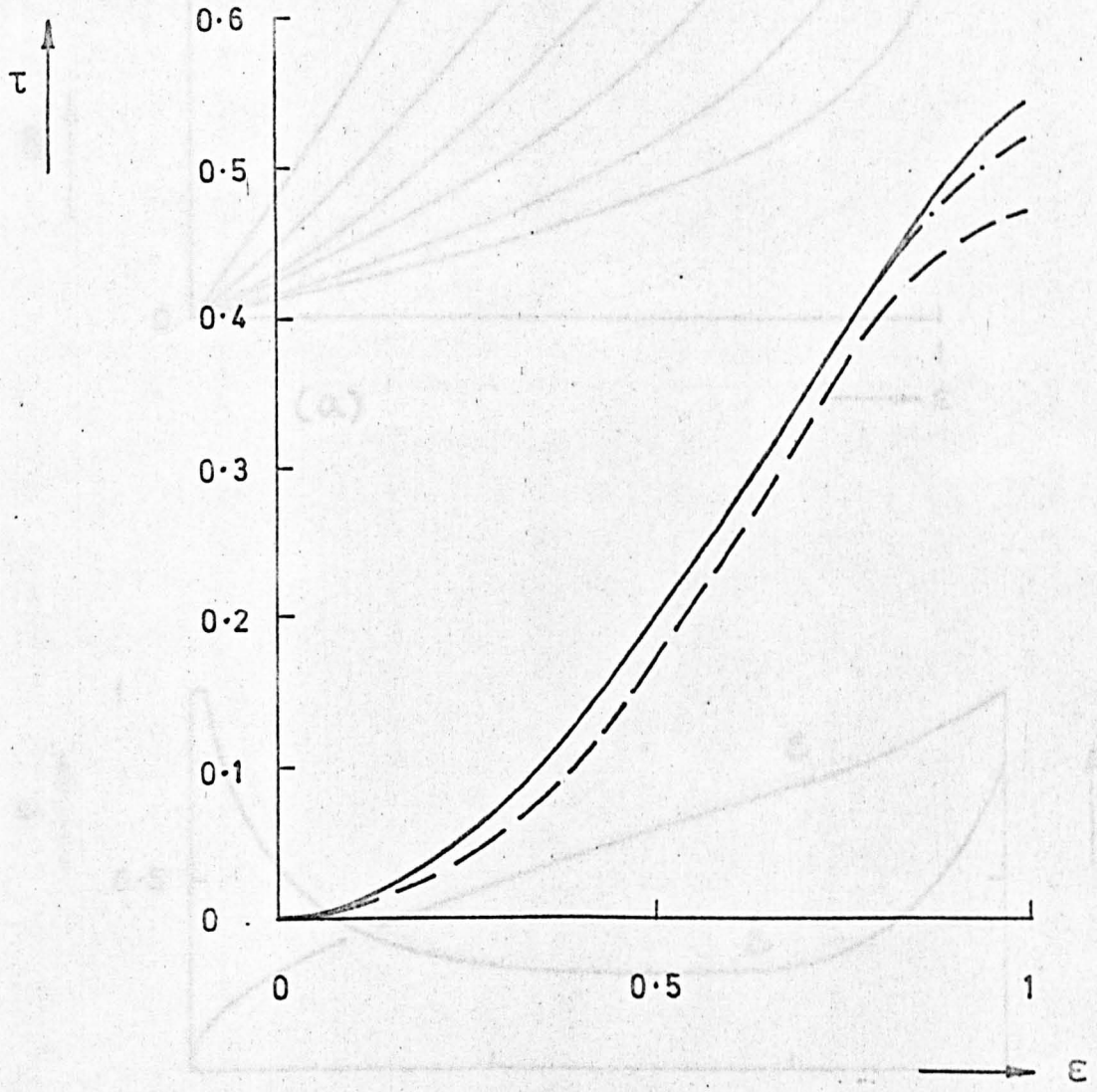

Figure 22. Time history of solidification front, $\beta = 1.5613$.

——— full numerical solution,

— — — Allen and Severn,

—·—·— Tani method applied by Poots.

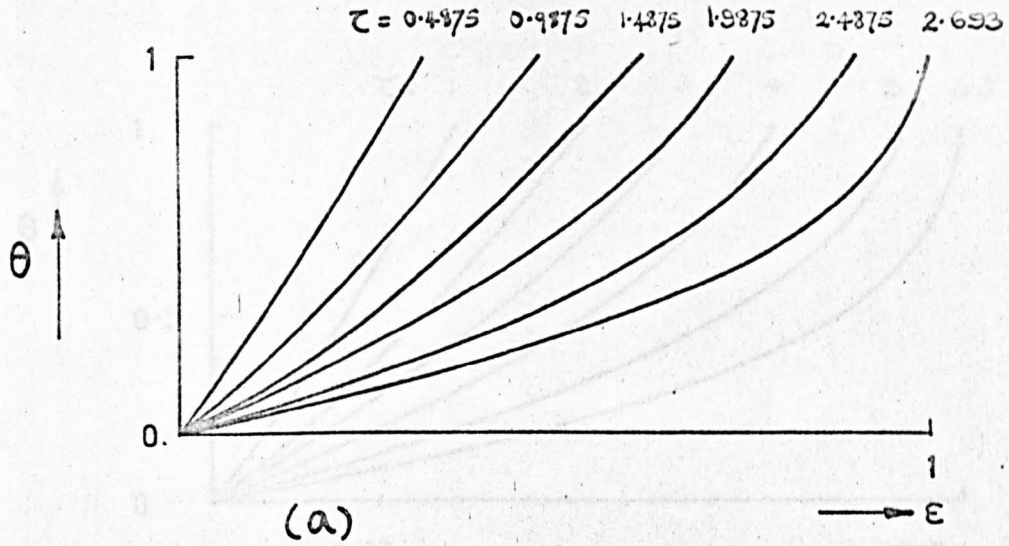

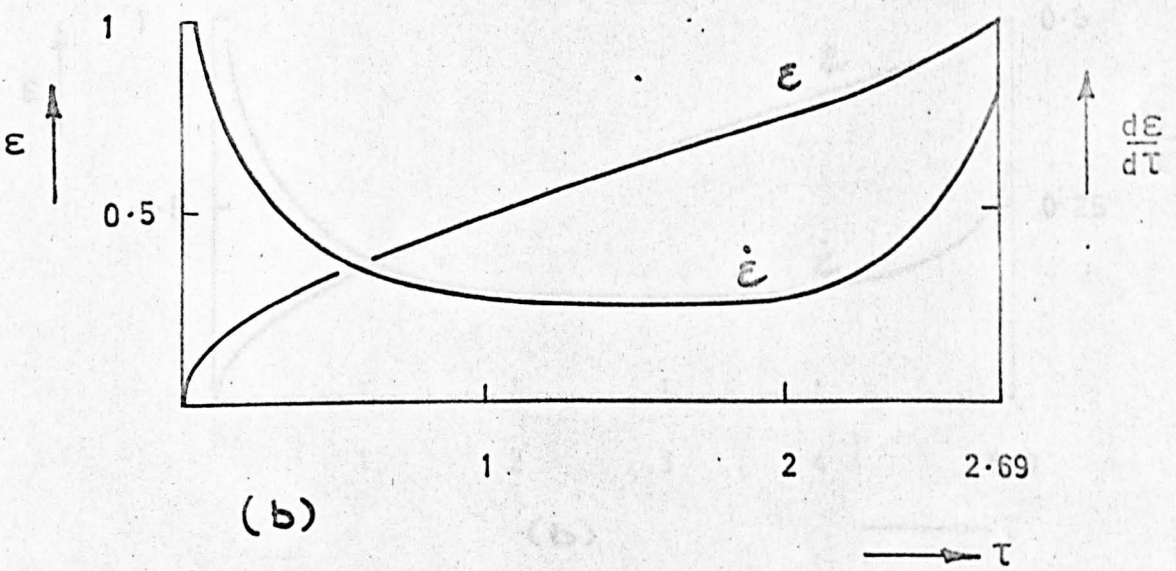

Figure 23. $\beta = 10$. (a) Thermal profiles.
(b) History of solidification front.

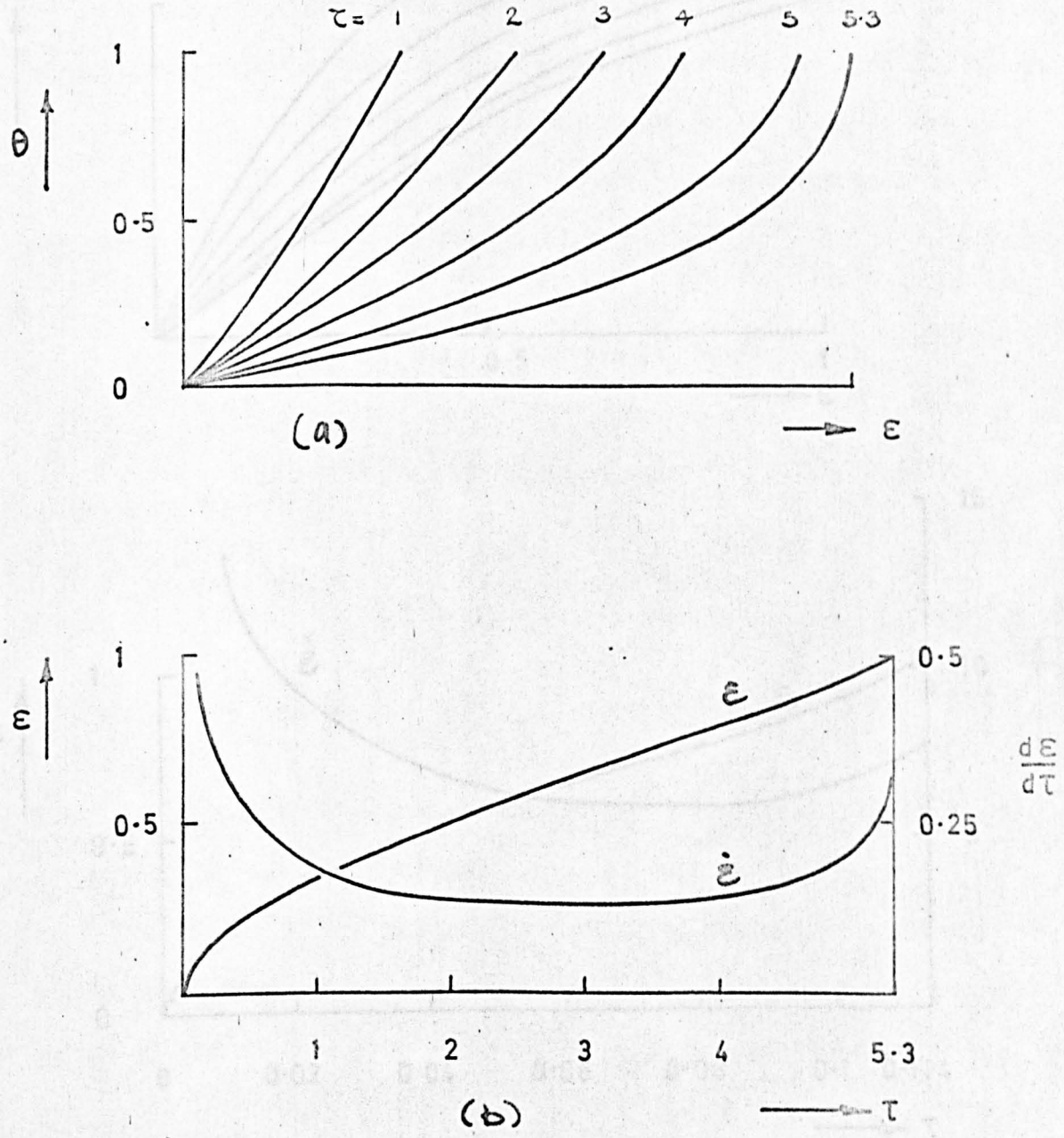

Figure 24. $\beta = 20$. (a) Thermal profiles
(b) History of solidification front.

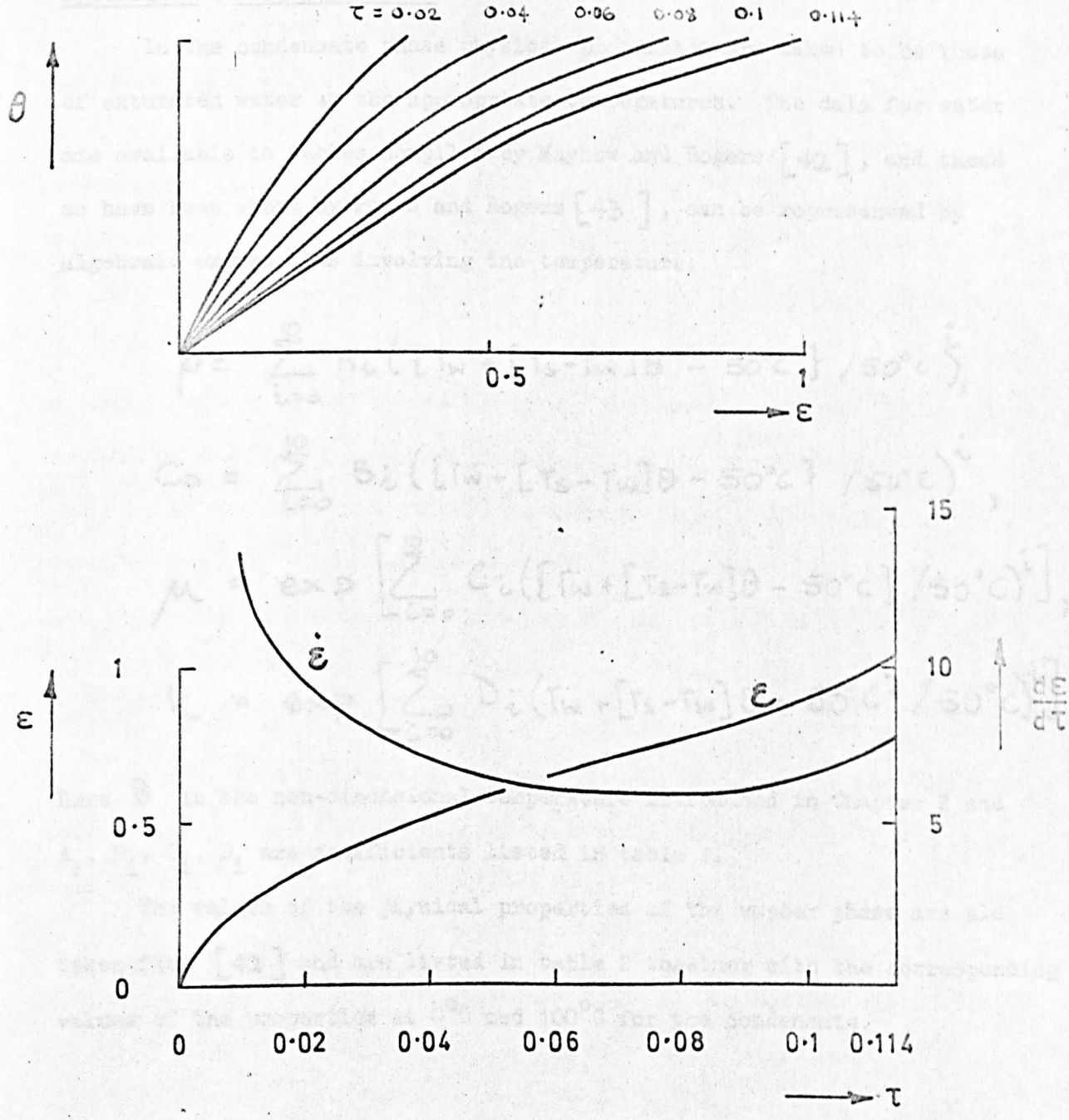

Figure 25. $\beta = 0{\cdot}1$ (a) Temperature profiles.
(b) History of solidification front.

Appendix A: Property values

In the condensate phase physical properties are taken to be those of saturated water at the appropriate temperatures. The data for water are available in tables compiled by Mayhew and Rogers [42], and these as have been shown by Poots and Rogers [43], can be represented by algebraic expressions involving the temperature.

$$\rho = \sum_{i=0}^{10} A_i \left(\{ T_w + [T_s - T_w]\theta - 50^\circ C \} / 50^\circ C \right)^i,$$

$$C_p = \sum_{i=0}^{10} B_i \left(\{ T_w + [T_s - T_w]\theta - 50^\circ C \} / 50^\circ C \right)^i,$$

$$\mu = \exp \left[\sum_{i=0}^{10} C_i \left(\{ T_w + [T_s - T_w]\theta - 50^\circ C \} / 50^\circ C \right)^i \right],$$

$$k = \exp \left[\sum_{i=0}^{10} D_i \left(T_w + [T_s - T_w]\theta - 50^\circ C \} / 50^\circ C \right)^i \right].$$

Here θ is the non-dimensional temperature introduced in Chapter 2 and A_i, B_i, C_i, D_i are coefficients listed in table 1.

The values of the physical properties of the vapour phase are also taken from [42] and are listed in table 2 together with the corresponding values of the properties at 0°C and 100°C for the condensate.

Appendix B: Integration of ordinary differential equations (Runge-Kutta)

Here the numerical method for solving the ordinary differential equations (3.15)-(3.23) is discussed.

The equations governing the transport of momentum and energy in the condensate phase yield a third order equation for f and a second order equation for G, both of which contain the unknown constant ϕ. At Y = 0 we have G(0) = 0 and f(0) = f'(0) = 0; which is insufficient information to start step by step integration from that point. However if values for f''(0), G'(0) and ϕ are assumed then the procedure can begin. Using Gill's modification of the Runge-Kutta technique the two equations are solved for $0 \leq Y \leq 1$ and the value of G(1) is stored. Using the interfacial conditions (3.20)-(3.22) values of f*(0), f*'(0) and f*''(0) are calculated and the vapour equation (3.17) integrated from $\eta^* = 0$ to $\eta^* = \tilde{\eta}^*$ (at which point f*'' is zero to within any desired accuracy). The value of $f^{*\prime}(\eta^*)$ is then stored. At this stage no reference has been made to the energy balance (3.23), and the object is now to discover the values of f''(0), G'(0) and ϕ which then yeild the functions f, G and f* such that G(1) = 1, $f^{*\prime}(\tilde{\eta}^*) = 1$ and, moreover, satisfy the energy balance.

It has been found that the following scheme is not convergent for arbitrary values of f''(0), G'(0) and ϕ, and indeed quite accurate data must be provided. This is readily available from the formulae given in Chapter 5. Denoting the values of G'(0), f''(0) and ϕ respectively by α, β and $\bar{\phi}$ the procedure is as follows.

With $\bar{\phi}$ fixed, solutions of the equations are found taking

(i) $G'(0) = \alpha$, $f''(0) = \beta$

(ii) $G(0) = \alpha + \delta\alpha$, $f''(0) = \beta$

(iii) $G(0) = \alpha$, $f(0) = \beta + \delta\beta$

where $\delta\alpha$ and $\delta\beta$ are small compared with α and β. Then since $G(1)$ and $f^{*\prime}(\infty)$ are functions in α and β which can be expanded in Taylor series, new estimates of $f''(0)$ and $G'(0)$ can be found such that $G(1)$ and $f^{*\prime}(\infty)$ are nearer to unity. With $\bar{\phi}$ still fixed this routine is repeated until $G(1)-1$ and $f^{*\prime}(\infty)-1$ are both as small as may be required. A measure of the error in the energy balance is stored.

With ϕ perturbed to $\bar{\phi} + \delta\phi$, where $\delta\phi$ is small compared with $\bar{\phi}$, the procedure is repeated, and assuming the error in the energy balance to be a function of ϕ, and expandable in a Taylor series, a new estimate of ϕ is obtained. It is also possible to regard α and β as functions of ϕ, so that knowing the values of α and β when $\phi = \bar{\phi}$ and $\phi = \bar{\phi} + \delta\phi$ then the values of α and β corresponding to the new ϕ can be approximated.

The entire process is then repeated until the conditions on $G(1)$, $f^{*\prime}(\infty)$ and the energy balance are satisfied.

Appendix C: Integration procedure for partial differential equations

In this appendix details are given of the numerical scheme applied to solve the equations arising in the problems of condensation onto the plate with a retarded vapour flow, and onto the cylinder.

These are parabolic non-linear partial differential equations. The solutions are obtained using an iterative scheme stepping along the body surface. Denoting the distance along the surface of the n^{th} stage by X_N the problem is that of finding the solution at X_{N+1} once that at X_N is known. To this end the equations are considered at $X_{N+\frac{1}{2}}$, and at this station derivatives in the X direction are replaced by central differences, and all other quantities by averages. This yields ordinary differential equations for the functions at X_{N+1}, and because the solution at X_N appears in the coefficients, the solution is found using matrix iterative techniques.

This is the method proposed by Hartree and Womersley [25], which has been found to provide a stable convergent process.

To start the step by step procedure the solution is demanded at $X = 0$, and, as was noted in Chapter 4, although this knowledge is available from Runge-Kutta techniques, this solution will be obtained using the matrix inversion routine.

The methods for the cylinder and the plate differ only because of the variation of m and $U_m^*(x)$ in the two problems, and it will suffice to give details for the case of the cylinder since all the terms in the differential equations are retained.

Consider firstly the momentum equation for the condensate phase.

$$\frac{\partial}{\partial y}\left(\frac{\rho\mu}{\rho_s\mu_s}\frac{\partial^2 F}{\partial y^2}\right) + t(x)F\frac{\partial^2 F}{\partial y^2} - t(x)\left(\frac{\partial F}{\partial y}\right)^2 + x t(x)\left\{\frac{\partial F}{\partial x}\frac{\partial^2 F}{\partial y^2} - \frac{\partial F}{\partial y}\frac{\partial^2 F}{\partial x \partial y}\right\}$$

$$+ x\frac{dt}{dx}\left(\frac{\partial F}{\partial y}\right)^2 + t(x)^3\frac{\rho_s^*}{\rho}\left(\frac{c}{x}\right)\sin\left(\frac{x}{c}\right)\cos\left(\frac{x}{c}\right) = 0. \qquad (C.1)$$

Taking each term individually they are replaced using the Hartree - Womersley technique as follows:

$$\frac{\partial}{\partial y}\left(\frac{\rho\mu}{\rho_s\mu_s}\frac{\partial^2 F}{\partial y^2}\right) = \frac{1}{2}\left\{\left[\frac{\rho_{N+1}\mu_{N+1}}{\rho_s\mu_s}F_{N+1}''\right]' + \left[\frac{\rho_N\mu_N}{\rho_s\mu_s}F_N''\right]'\right\}, \qquad \text{I}$$

$$t(x)F\frac{\partial^2 F}{\partial y^2} = \frac{1}{8}(t_N + t_{N+1})(F_N + F_{N+1})(F_{N+1}'' + F_N''), \qquad \text{II}$$

$$-t(x)\left(\frac{\partial F}{\partial y}\right)^2 = -\frac{1}{8}(t_N + t_{N+1})(F_N' + F_{N+1}')^2, \qquad \text{III}$$

$$x\,t(x)\left\{\frac{\partial F}{\partial x}\frac{\partial^2 F}{\partial y^2} - \frac{\partial F}{\partial y}\frac{\partial^2 F}{\partial x\partial y}\right\} = \left(\frac{x_N + x_{N+1}}{2}\right)\left(\frac{t_N + t_{N+1}}{2}\right)\left\{\frac{F_{N+1} - F_N}{x_{N+1} - x_N}\frac{F_{N+1}'' + F_N''}{2} - \frac{F_{N+1}' - F_N'}{x_{N+1} - x_N}\frac{F_{N+1}' + F_N'}{2}\right\}, \qquad \text{IV}$$

$$x\frac{dt}{dx}\left(\frac{\partial F}{\partial y}\right)^2 = \frac{1}{8}(x_{N+1} + x_N)(F_{N+1}' + F_N')^2\left[\frac{t_{N+1} - t_N}{x_{N+1} - x_N}\right], \qquad \text{V}$$

$$t(x)^3\frac{\rho_s^*}{\rho}\left(\frac{c}{x}\right)\sin\left(\frac{x}{c}\right)\cos\left(\frac{x}{c}\right) = \left(\frac{t_{N+1} + t_N}{8}\right)^3\frac{\rho_s^*}{2}\left[\frac{1}{\rho_N} + \frac{1}{\rho_{N+1}}\right]\left\{\frac{\sin\frac{x_{N+1}}{c}\cos\frac{x_{N+1}}{c}}{x_{N+1}/c} + \frac{\sin\frac{x_N}{c}\cos\frac{x_N}{c}}{x_N/c}\right\}$$

VI

In these expressions the subscripts N and N+1 denote that the functions are evaluated across the N^{th} or $(N+1)^{th}$ stations, and dashes now denote differentiation w.r.t. Y. In addition let

$$\gamma = \frac{x_{N+1}+x_N}{x_{N+1}-x_N} \quad \text{and} \quad \Lambda(x_{N+1}) = \left\{ \frac{\sin\frac{x_{N+1}}{c}\cos\frac{x_{N+1}}{c}}{x_{N+1}/c} + \frac{\sin\frac{x_N}{c}\cos\frac{x_N}{c}}{x_N/c} \right\}.$$

Then recombining the above terms there results an ordinary differentiation equation for F_{N+1}:

$$\left[\frac{\rho_{N+1}\mu_{N+1}}{\rho_s\mu_s} F_{N+1}''\right]' + \xi_1 F_{N+1}'' + \xi_2 F_{N+1} + \xi_3 t_{N+1} + \xi_4 F_{N+1}'$$
$$+ \xi_5 F_{N+1} F_{N+1}'' + \xi_6 t_{N+1} F_{N+1}'' + \xi_7 F_{N+1}'^2 + \xi_8 t_{N+1} F_{N+1} \qquad (C.2)$$
$$+ \xi_9 t_{N+1} F_{N+1} F_{N+1}'' + \xi_{10} t_{N+1} F_{N+1}' + \xi_{14} t_{N+1} (F_{N+1}')^2$$
$$+ \xi_{13} + \xi_{11} (t_N + t_{N+1})^3 \cdot \frac{1}{\rho_{N+1}} + \xi_{12} (t_N + t_{N+1})^3 = 0,$$

where
$$4\xi_1 = (1-\gamma) t_N F_N, \qquad 4\xi_8 = (1+\gamma) F_N'',$$
$$4\xi_2 = (1+\gamma) t_N F_N'', \qquad 4\xi_9 = (1+\gamma),$$
$$4\xi_3 = (1-\gamma) F_N F_N'' - (1-2\gamma) F_N'^2, \qquad 4\xi_{10} = -2(1-\gamma) F_N',$$
$$4\xi_4 = -2(1+\gamma) t_N F_N', \qquad 16\xi_{11} = \rho_s^* \Lambda(x_{N+1}), \qquad (C.3)$$
$$4\xi_5 = (1+\gamma) t_N, \qquad \xi_{12} = \xi_{11}/\rho_N,$$
$$4\xi_6 = (1-\gamma) F_N, \qquad 4\xi_{14} = -1,$$
$$4\xi_7 = -(1+2\gamma) t_N,$$
$$4\xi_{13} = 4\left[\frac{\rho_N\mu_N}{\rho_s\mu_s} F_N''\right]' + (1-\gamma) t_N F_N F_N'' - t_N (F_N')^2.$$

Equation (C.2) is a non-linear ordinary differential equation for F_{N+1}, and in order to solve this using a matrix inversion procedure it must be linearized in some way. Several possibilities are open to us, and though many are simpler and easier to program we shall linearize everything utilising the quasilinearization technique described by Bellman and Kalaba [44]. This is essentially an extension of the Newton-Raphson development of a sequence of approximation to a root of the scalar equation $f(X) = 0$.

Consider a general function of m variables

$$F(x_1, x_2, \cdots, x_m). \tag{C.5}$$

In an iterative method to solve equations involving $F(x_1, \ldots, x_m)$, let the p^{th} iterate be the set $\{x_{1p}, \ldots, x_{mp}\}$, and suppose that this is not far removed from the true solution $\{x_1, \ldots, x_m\}$. Then expanding in a Taylor series about $\{x_{1p}, \cdots, x_{mp}\}$ we have

$$F(x_1, \ldots, x_m) = F(x_{1p}, \ldots x_{mp}) + \sum_{s=1}^{m} \left\{ \left(\frac{\partial F}{\partial x_s} \right)_{(x_{1p}, \ldots x_{m,p})} (x_s - x_{sp}) \right\} + \cdots \tag{C.6}$$

Neglecting the terms of $O(x_s - x_{sp})^2$ then the right hand side is linear in X_i and replaces $F(x_1, \ldots, x_m)$ in the equations.

As an example choose $F(x_1, x_2, x_3) = x_1 \cdot x_2 \cdot x_3$, then replacing $\{x_{1p}, \ldots, x_{mp}\}$ by $\{\bar{x}_1, \ldots \bar{x}_m\}$ the above yields as a linearization of $x_1 \cdot x_2 \cdot x_3$:

$$\begin{aligned} x_1 x_2 x_3 &= \bar{x}_1 \bar{x}_2 \bar{x}_3 + \bar{x}_2 \bar{x}_3 (x_1 - \bar{x}_1) + \bar{x}_1 \bar{x}_3 (x_2 - \bar{x}_2) + \bar{x}_1 \bar{x}_2 (x_3 - \bar{x}_3) \qquad (C.7) \\ &= x_1 (\bar{x}_2 \bar{x}_3) + x_2 (\bar{x}_1 \bar{x}_3) + x_3 (\bar{x}_1 \bar{x}_2) - 2 \bar{x}_1 \bar{x}_2 \bar{x}_3. \end{aligned}$$

An analogous way of reaching this linearization is to assume the latest iterate $\{\bar{x}_1, \bar{x}_2, \bar{x}_3\}$ is not far removed from the true solution $\{x_1, x_2, x_3\}$, so that if

$$x_1 = \bar{x}_1 + x_1' \,, \quad x_2 = \bar{x}_2 + x_2' \,, \quad x_3 = \bar{x}_3 + x_3' \qquad (C.8)$$

the primed quantities are small.

Consequently by taking

$$x_1 x_2 x_3 = (\bar{x}_1 + x_1')(\bar{x}_2 + x_2')(\bar{x}_3 + x_3'),$$

expanding the right hand side and neglecting second order terms in the primed quantities we have:

$$x_1 x_2 x_3 = \bar{x}_1 \bar{x}_2 \bar{x}_3 + x_1' \bar{x}_2 \bar{x}_3 + x_2' \bar{x}_1 \bar{x}_3 + x_3' \bar{x}_2 \bar{x}_1 .$$

Substituting for X_i' from (C.8) then (C.7) results.

This method of linearizing has been used in 1957 by Poots [45], indeed many problems in stability analysis introduce disturbances through equations similar to (C.8), after which products of the disturbances are presumed neglegible. The rather heuristic approach of others was put on a proper formal basis by Bellman [44].

As one illustration of the power of this scheme consider the following differential equation. This was used by Davies and James [46] to illustrate the way in which the convergence of the basic Cauchy iteration could be improved.

$$\frac{dy}{dx} = y^2 + 1 \; ; \quad y = 0 \,, \; x = 0 \,. \qquad (C.9)$$

The exact solution is $y = \tan x$ so $y = 1$ when $x = \frac{\pi}{4}$. Using the Cauchy iteration the equation is replaced by :

$$\frac{dy_p}{dx} = y_{p-1}^2 + 1 \; ; \quad y_p = 0 \,, \; x = 0 \,,$$

and the following early terms in the sequence $\{y_p\}$ result:

$$y_0 = 0, \quad y_1 = x, \quad y_2 = x + \tfrac{1}{3}x^3. \tag{C.10}$$

Alternatively Davies and James suggest replacing (C.9) by

$$\frac{dy_p}{dx} = y_p y_{p-1} + 1 \; ; \quad y_p = 0 \; , \; x = 0 \; ,$$

which yields:

$$y_0 = 0 \; , \; y_1 = x \; , \; y_2 = \exp(\tfrac{1}{2}x^2) \int_0^x \exp(-\tfrac{1}{2}u^2)\, du. \tag{C.11}$$

If we now apply the Bellman linearization to (C.9) then we have

$$\frac{dy_p}{dx} = 2y_p y_{p-1} - y_{p-1}^2 + 1 \; ; \quad y_p = 0 \; , x = 0.$$

For this set of equati ns we obtain as leading terms of the sequence $\{y_p\}$:

$$y_0 = 0, \quad y_1 = x, \quad y_2 = \tfrac{1}{2}x + \tfrac{1}{2}\exp(x^2) \int_0^x \exp(-u^2)\, du. \tag{C.12}$$

For $x = \frac{\pi}{4}$ we know the exact solution is $y = 1$, so the accuracy of the third function, y_3, in each sequence will be compared by putting $x = \pi/4$.

From (C.10) : Basic Cauchy : $y_3(\pi/4) = 0.947$

(C.11) : Modified Cauchy iteration : $y_3(\pi/4) = 0.968$

(C.12) : Bellman method : $y_3(\pi/4) = 0.995$

As further and more relevant illustration of the power of the method, the solution to the Blasius problem will be found iteratively using the modified Cauchy method and the Bellman scheme. The equation to be solved for $f(\eta)$ is

$$f'''(\eta) + f(\eta) f''(\eta) = 0 \; ,$$

subject to

$$f(0) = f'(0) = 0 \; , \quad f'(\infty) = 1 \; ,$$

where dashes denote differentiation w.r.t. η.

The iterative processes following the modified Cauchy and Bellman linearizations are respectively,

(A) $f_n''' + f_{n-1} f_n'' = 0$; $f_n(0) = f_n'(0) = 0$, $f_n'(\infty) = 1$,

(B) $f_n''' + f_n f_{n-1}'' + f_{n-1} f_n'' - f_{n-1} f_{n-1}'' = 0$; $f_n(0) = f_n'(0) = 0$, $f_n'(\infty) = 1$.

Solutions are effected by introducing $Q_n = f_n'$ and $Q_{n-1} = f_{n-1}'$, replacing the derivatives by finite differences and the integrals using the Trapezoidal rule. As a measure of the accuracy, the characteristic $f''(0)$ is given in table (40) at each iteration.

n	A	B
0	0.133333	0.133333
1	0.339236	0.863298
2	0.424364	0.582174
3	0.455999	0.485417
4	0.465567	0.470036
5	0.468425	0.46961523
6	0.469267	0.46961620
7	0.469514	0.46961619

Table 40.

This solution was found using steps of 0.1, taking 6 units in the η direction and with $f_0(\eta) = \eta^2/2$. Such a step length with the particular simple finite difference representation has not yielded $f''(0)$ to more than four decimal places, but the solution does show the excellent convergence of the Bellman iteration. Initially the poor initial estimate for f is modified better in (A), but once the solutions get close to the

converged solution the Bellman scheme is far more rapidly convergent. The disadvantage of (B) lies in the necessity to have the lower half of the matrix complete, making the inversion time of course slower.

Further evidence of the usefulness of quasi-linearization is given by Ames [47], who states that the full benefit is only accrued if the boundary conditions also are linearized in the same way.

Have digressed enough we now readdress ourselves to the problem of fitting (C.2) into a matrix scheme, and linearize according to the Bellman method.

Dropping the sufficies (N+1) from the terms in (C.2) and linearizing, the the approximating form is:

$$\left(\frac{\rho\mu}{\rho_s\mu_s}F''\right)' + \xi_1 F'' + \xi_2 F + \xi_3 t + \xi_4 F' + \xi_5\left(F\bar{F}'' + \bar{F}F'' - \bar{F}\bar{F}''\right)$$
$$+ \xi_6\left(t\bar{F}'' + \bar{t}F'' - \bar{t}\bar{F}''\right) + \xi_7\left(2\bar{F}'F' - (\bar{F}')^2\right)$$
$$+ \xi_8\left(t\bar{F} + \bar{t}F - \bar{t}\bar{F}\right) + \xi_9\left(t\bar{F}\bar{F}'' + \bar{t}\bar{F}''F + \bar{t}\bar{F}\bar{F}'' - 2\bar{t}\bar{F}\bar{F}''\right)$$
$$+ \xi_{10}\left(t\bar{F}' + \bar{t}F' - \bar{t}\bar{F}'\right) + \left(\xi_{12} + \tfrac{1}{\rho}\xi_{11}\right)\left\{3(t+t_N)(\bar{t}+t_N)^2 - 2(\bar{t}+t_N)^3\right\}$$
$$+ \xi_{13} + \xi_{14}\left(t(\bar{F}')^2 + 2\bar{t}\bar{F}'F' - 2\bar{t}[\bar{F}']^2\right) = 0, \qquad \text{(C.14)}$$

where $\bar{t}$ and $\bar{F}$ denote the most recent estimates of t and F in the iterative process.

Introducing the new dependent variable Q defined by

$$Q = \frac{\partial F}{\partial y}\left(= F'\right), \qquad \text{(C.15)}$$

and taking $\bar{Q} = \bar{F}$, then equation (C.13) becomes:

$$\left(\frac{\rho\mu}{\rho_s\mu_s}\,Q'\right)' + \chi_1 Q' + \chi_2 Q + \chi_3 \int_0^Y Q\,dY + \chi_4 t + \chi_5 = 0, \quad \text{(C.15)}$$

where $\chi_1 = \xi_1 + \xi_5 \int_0^Y \bar{Q}\,dY + \xi_6 \bar{t} + \xi_9 \bar{t} \int_0^Y \bar{Q}\,dY$,

$$\chi_2 = \xi_4 + 2\xi_7 \bar{Q} + \xi_{10} \bar{t} + 2\xi_{14} \bar{t}\,\bar{Q}, \quad \text{(C.16)}$$

$$\chi_3 = \xi_2 + \xi_5 \bar{Q}' + \xi_8 \bar{t} + \xi_9 \bar{t}\,\bar{Q}',$$

$$\chi_4 = \xi_3 + \xi_6 \bar{Q}' + \xi_8 \int_0^Y \bar{Q}\,dY + \xi_9 \bar{Q} \int_0^Y \bar{Q}\,dY + \xi_{10} \bar{Q} + \xi_{14} \bar{Q}^2 + 3(\bar{t} + t_N)^2 \left(\xi_{12} + \tfrac{1}{\rho}\xi_{11}\right),$$

and $\chi_5 = \xi_{13} - \xi_5 \bar{Q}' \int_0^Y \bar{Q}\,dY - \xi_6 \bar{t}\,\bar{Q}' - \xi_7 \bar{Q}^2 - \xi_8 \bar{t} \int_0^Y \bar{Q}\,dY - 2\xi_9 \bar{t}\,\bar{Q} \int_0^Y \bar{Q}\,dY - \xi_{10} \bar{t}\,\bar{Q} - 2\xi_{14} \bar{t}\,\bar{Q}^2 + \left\{(t_N + \bar{t})^2 (t_N - 2\bar{t}) \left(\xi_{12} + \tfrac{1}{\rho}\xi_{11}\right)\right\}.$

By making the transformation (C.5) it has been possible to reduce the third order equation in F to a second order equation in Q. Of the original boundary conditions we have now used $F(x,0) = 0$ in deriving the substitued form $F = \int_0^Y Q\,dY$ from (C.15).

In order to solve equation (C.15) the range of Y is divided into m equal intervals of length h, so that $h = 1/m$, and the differential equation approximated to at the m-1 interior points using finite differences. Denote the j^{th} point across the $(N+1)$ station by (X_{N+1}, Y_j), and the values of Q, ρ, μ evaluated at this point by Q_j, ρ_j and μ_j. Then the derivatives are replaced according to :

$$Q_j' = \frac{1}{2h}(Q_{j+1} - Q_{j-1}) - \frac{h^2}{6} Q^{(3)},$$

$$\left(\frac{\rho_j \mu_j}{\rho_s \mu_s} Q_j'\right)' = \frac{1}{h^2}\left\{\frac{(\rho\mu)_{j+\frac{1}{2}}}{\rho_s \mu_s} Q_{j+1} - \left[\frac{(\rho\mu)_{j+\frac{1}{2}} + (\rho\mu)_{j-\frac{1}{2}}}{\rho_s \mu_s}\right] Q_j + \frac{(\rho\mu)_{j-\frac{1}{2}}}{\rho_s \mu_s} Q_{j-1}\right\}, \quad (C.17)$$

and $\int_0^Y Q\, dy$ is replaced using the traperzoidal rule, i.e.

$$\int_0^Y Q\, dy = h\left(Q_1 + Q_2 + \cdots + Q_{j-1} + \tfrac{1}{2} Q_j\right).$$

The derivatives and integrals of Q_N and $\bar{Q}$ are replaced using the same formulae.

As a result of these substitutions the approximate form of (C.6) at (X_{N+1}, Y_j) is:

$$\left[\frac{(\rho\mu)_{j+\frac{1}{2}}}{\rho_s \mu_s} \cdot \frac{1}{h^2} + \frac{1}{2h} \chi_1\right] Q_{j+1} + \left[\chi_2 - \frac{1}{h^2}\left\{\frac{(\rho\mu)_{j+\frac{1}{2}}}{\rho_s \mu_s} + \frac{(\rho\mu)_{j-\frac{1}{2}}}{\rho_s \mu_s}\right\} + \frac{h}{2}\chi_3\right] Q_j$$

$$+ \left[\frac{(\rho\mu)_{j-\frac{1}{2}}}{\rho_s \mu_s} \cdot \frac{1}{h^2} - \frac{\chi_1}{2h} + \frac{h}{2}\chi_3\right] Q_{j-1}$$

$$+ h\chi_3 [Q_{j-2} + Q_{j-3} + \cdots + Q_1] + \chi_4 t = -\chi_5. \quad (C.18)$$

Now return to the vapour momentum equation:

$$\frac{\partial^3 F^*}{\partial y^{*3}} + F^* \frac{\partial^2 F^*}{\partial y^{*2}} - \frac{\partial F^{*2}}{\partial y^*} + \chi\left\{\frac{\partial F^*}{\partial x}\frac{\partial^2 F^*}{\partial y^{*2}} - \frac{\partial F^*}{\partial y^*}\frac{\partial^2 F^*}{\partial x\, \partial y^*}\right\} \quad (C.19)$$

$$+ \left(\frac{c}{x}\right) \sin\left(\frac{x}{c}\right) \cos\left(\frac{x}{c}\right) = 0.$$

The Hartree-Womersley scheme is applied to this in exactly the way as to the condensate equation (C.1), and corresponding to (C.2) we have

$$F_{N+1}^{*'''} + \xi_1^* F_{N+1}^{*''} + \xi_2 F_{N+1}^{*} + \xi_5^* F_{N+1}^{*} F_{N+1}^{*''}$$
$$+ \xi_7^* (F_{N+1}^{*'})^2 + \xi_3^* F_{N+1}^{*'} + \xi_{13}^* = 0, \qquad (C.20)$$

where dashes now denote differentiation with respect to Y*, and

$$2\xi_1^* = (1-\gamma) F_N^*, \quad 2\xi_2^* = (1+\gamma) F_N^{*''},$$
$$2\xi_3 = -2F_N^{*'}, \quad 2\xi_5^* = (1+\gamma), \quad 2\xi_7^* = -(1+\gamma),$$
$$2\xi_{13}^* = (1-\gamma) F_N^* F_N^{*''} - (1-\gamma)(F_N^{*'})^2 + 2F_N^{*''} + 2\Lambda(x_{N+1}). \qquad (C.21)$$

Dropping the suffixes (N+1) from (C.21) and linearizing then:

$$F^{*'''} + x_1^* F^{*''} + x_2^* F^{*'} + x_3^* F + x_4^* = 0, \qquad (C.22)$$

where
$$x_1^* = \xi_1^* + \xi_5^* \bar{F}^*,$$
$$x_2^* = \xi_3^* + 2\xi_7^* \bar{F}^{*'},$$
$$x_3^* = \xi_2^* + \xi_5^* \bar{F}^{*''}, \qquad (C.23)$$

and
$$x_4^* = \xi_{13}^* - \xi_5^* \bar{F}^* \bar{F}^{*''} - \xi_7^* (\bar{F}^{*'})^2.$$

Still following the method employed on the condensate momentum equation, a new dependent variable is introduced by

$$Q^* = \frac{\partial F^*}{\partial Y^*}. \qquad (C.24)$$

Integrating this we have

$$F^*(x_{N+1}, Y^*) = \int_0^{Y^*} Q^* dY^* + F^*(x_{N+1}, 0), \qquad (C.25)$$

where here $F^*(x_{N+1}, 0) \neq 0$, and so remains in the differential equations as an unknown quantity.

With (C.24) and (C.25) substituted into (C.22) we have

$$Q^{*\prime\prime} + \chi_1^* Q^{*\prime} + \chi_2^* Q^* + \chi_3^* \int_0^{Y^*} Q^* \, dY + \chi_3^* F^*(x_{N+1}, 0) + \chi_4^* = 0. \quad [C.26]$$

This is equivalent to (C.15) for the condensate phase and is also to be represented by finite differences. Unlike the condensate phase there is no definite range across the vapour boundary layer and there arises the problem of deciding how far to extend to solution in the Y* direction. Fortunately the similarity solutions can indicate this range at the leading edge of the plate, or the stagnation point of the cylinder, and there is some indication of the rate at which the vapour momentum thickness might grow from the work of Leigh and Terrill. If the same finite difference formulae are used for Q* as for Q, then the vapour step length would have to be as small as h (or smaller since a typical error term $h^2 Q^{(3)}$ would be larger for the vapour phase) and a considerable number of steps taken across the vapour layer. Instead more accurate finite differences are introduced into the vapour phase thus cutting down the number of points, making the matrix smaller and increasing the speed of inversion. If n steps each of length h_s are taken in the Y* direction, the j^{th} point across the $(N+1)^{st}$ station denoted by (X_{N+1}, Y^*_j), and the value of Q* at this point by Q^*_j, then the derivatives are replaced using for first order derivatives:

$$Q_1^{*\prime} = \frac{1}{12h_s}(-3Q_0^* - 10Q_1^* + 18Q_2^* - 6Q_3^* + Q_4^*) - \frac{h_s^4}{20}Q^{*(5)},$$

$$Q_{n-1}^{*\prime} = \frac{1}{12h_s}(-Q_{n-4}^* + 6Q_{n-3}^* - 18Q_{n-2}^* + 10Q_{n-1}^* + 3Q_n^*), \qquad (C.27)$$

and for $2 \le j \le n-2$,

$$Q_j^{*\prime} = \frac{1}{12h_s}(Q_{j-2}^* - 8Q_{j-1}^* + 8Q_{j+1}^* - Q_{j+2}^*) + \frac{h_s^4}{30}Q^{*(5)},$$

and for the second order derivatives:

$$Q_1^{*\prime\prime} = \frac{1}{12h_s^2}(10Q_0^* - 15Q_1^* - 4Q_2^* + 14Q_3^* - 6Q_4^* + Q_5^*),$$

$$Q_{n-1}^{*\prime\prime} = \frac{1}{12h_s^2}(10Q_n^* - 15Q_{n-1}^* - 4Q_{n-2}^* + 14Q_{n-3}^* - 6Q_{n-4}^* + Q_{n-5}^*),$$

and for $2 \le j \le n-2$, (C.28)

$$Q_j^{*\prime\prime} = \frac{1}{12h_s^2}(-Q_{j-2}^* + 16Q_{j-1}^* - 30Q_j^* + 16Q_{j+1}^* - Q_{j+2}^*).$$

The integral $\int_0^{Y_j} Q^* \, dY^*$ is evaluated using the formulae:

$$\int_0^{Y_1^*} Q^* \, dY^* = \frac{1}{2}h_s(Q_0^* + Q_1^*),$$

$$\int_0^{Y_3^*} Q^* \, dY^* = \frac{3}{8}h_s(Q_0^* + 3Q_1^* + 3Q_2^* + Q_3^*), \qquad (C.29)$$

$$\int_0^{Y_j^*} Q^* \, dY^* = \frac{1}{3}h_s(Q_0^* + 4Q_1^* + 2Q_2^* + \cdots + 4Q_{j-1}^* + Q_j^*), \text{ if } j \text{ even}$$

and $\int_0^{Y_j^*} Q^* \, dY^* = \int_0^{Y_3^*} Q^* \, dY + \frac{h_s}{3}(Q_3^* + 4Q_4^* + \cdots + Q_j^*)$ if $j \ge 3$ and odd.

Note that the use of such accurate difference formulae can be dangerous if too much detail concerning the vapour layer is used. However accurate soluitions are available at X = 0 from the Runge-Kutta integration procedure, and these were used to choose the finite differential representation and step length h_s.

When solving the condensate momentum equation the latest estimate of the temperature is used in the evaluation of μ, ρ, C_p and k, so consequently for the purposes of solving (C.1) and (C.19) the temperature is a constant. The momentum equations are coupled through the boundary conditions and will be solved simultaneously. Having taken m intervals across the condensate layer there are m pivotal values of Q to find, i.e. Q_j for j = 1(1)m, and n values of Q^* to be determined, i.e. Q^*_j for j = 0(1)n-1. In addition t and $F^*(X_{N+1}, 0)$ are also unknown making a total of (m + n + 2) unknowns at the $(N + 1)^{st}$ station. The representations of the momentum equations at interior points of the intervals $[0,1]$ and $[0, n^*h_s]$ give a total of (m + n - 2) simultaneous equations in Q and Q^*. To these are added linearized versions of (5.32), (5.33), (5.34) and (5.36).

Take firstly, (5.32):

$$\left(\frac{\rho_s \mu_s}{\rho_s^* \mu_s^*}\right)^{1/2} \frac{1}{t^2}\left[\frac{\partial^2 F}{\partial y^2}\right]_{y=1} = \left[\frac{\partial^2 F^*}{\partial y^{*2}}\right]_{y^*=0},$$

which on the introduction of Q and Q^* becomes:

$$\lambda \left[Q'\right]_{y=1} = t^2 \left[Q^{*\prime}\right]_{y^*=0}. \qquad (C.30)$$

This equation holds at $X = X_{N+1}$ and is linearized using the Bellman method:

$$\lambda \left[Q'\right]_{y=1} = 2t\bar{t}\left[\bar{Q}^{*\prime}\right]_{y^*=0} + \bar{t}^2\left[Q^{*\prime}\right]_{y^*=0} - \bar{t}^2\left[\bar{Q}^{*\prime}\right]_{y^*=0},$$

$$\text{or} \quad -\lambda\left[Q'\right]_{y=1} + \bar{t}^2\left[Q^{*\prime}\right]_{y^*=0} + \left(2\bar{t}\left[\bar{Q}^{*\prime}\right]_{y^*=0}\right)t = \bar{t}^2\left[\bar{Q}^{*\prime}\right]_{y^*=0}. \qquad (C.31)$$

Replacing $[Q']_{y=1}$ and $[Q^{*\prime}]_{y^*=0}$, using

$$Q_{m'} = \frac{1}{6h}\left(-2Q_{m-3} + 9Q_{m-2} - 18Q_{m-1} + 11Q_m\right) \quad (C.32)$$

and $$Q_0^{*\prime} = \frac{1}{60n_S}\left(-137Q_0^* + 300Q_1^* - 300Q_2^* + 200Q_3^* - 75Q_4^* + 12Q_5^*\right),$$

then we have another linear relationship between the Q_i and Q_i^*.

Continuity of velocity tangential to the interface yields (5.33)

or

$$Q_m = t\,Q_0^*,$$

which is now linearized to give

$$Q_m = \bar{t}\,Q_0^* + t\,\bar{Q}_0^* - \bar{t}\,\bar{Q}_0^*. \quad (C.33)$$

The continuity of mass flow across the interface yields the equation

$$\lambda F(x_{N+1}, 1) = F^*(x_{N+1}, 0),$$

which is already linear, and on the introduction of Q becomes:

$$\lambda \int_0^1 Q\,dY = F^*(x_{N+1}, 0). \quad (C.34)$$

All that has been written so far concerning the numerical procedure applies to both the plate and the cylinder problems, but in the energy balance, which provides the last necessary equation linking Q and t, there are differences arising when m = 0 or 1 which effect the method of introduction into the matrix scheme.

We have the global energy balance:

$$\left(\frac{\rho_w k_w}{\rho_s k_s}\right)\frac{1}{P_s}\frac{(m+1)}{2x^{\frac{1}{2}(m+1)}}\int_0^x \frac{x^{\frac{1}{2}(m-1)}}{t(x)}\left(\frac{\partial\theta}{\partial y}\right)_{y=0} dx$$

$$= \int_0^1 \left\{\frac{h_{fg}}{c_{ps}\cdot\Delta T} + \frac{T_s}{\Delta T} - \frac{c_p}{c_{ps}}\cdot\frac{T}{\Delta T}\right\}\frac{\partial F}{\partial y}\, dy. \qquad (C.35)$$

Common to both problems, the integral on the left hand side is written as follows :

$$\int_0^{x_{N+1}} \frac{x^{\frac{1}{2}(m-1)}}{t(x)}\left(\frac{\partial\theta}{\partial y}\right)_{y=0} dx = \int_0^{x_N} \frac{x^{\frac{1}{2}(m-1)}}{t(x)}\left[\frac{\partial\theta}{\partial y}\right]_{y=0} dx + \int_{x_N}^{x_{N+1}} \frac{x^{\frac{1}{2}(m-1)}}{t(x)}\left(\frac{\partial\theta}{\partial y}\right)_{y=0} dx$$

$$= \text{INTEG} + \int_{x_N}^{x_{N+1}} \frac{x^{\frac{1}{2}(m-1)}}{t(x)}\left(\frac{\partial\theta}{\partial y}\right)_{y=0} dx,$$

where INTEG is the value of the integral up to the point X_N and will be known during the evaluation of Q_{N+1} etc.

Now for the case of the cylinder m = 1, therefore (C.35) becomes:

$$\frac{m+1}{2x^{\frac{1}{2}(m+1)}}\int_0^{x_{N+1}} \frac{x^{\frac{1}{2}(m-1)}}{t(x)}\left(\frac{\partial\theta}{\partial y}\right)_{y=0} dx = \frac{1}{x_{N+1}}\left[\text{INTEG} + \int_0^{x_{N+1}} \frac{1}{t(x)}\left(\frac{\partial\theta}{\partial y}\right)_{y=0} dx\right].$$

Putting $\int_{x_N}^{x_{N+1}} \frac{1}{t(x)}\left(\frac{\partial\theta}{\partial y}\right)_{y=0} dx = \frac{(x_{N+1}-x_N)}{2}\left[\frac{1}{t_N}\left[\frac{\partial\theta_N}{\partial y}\right]_{y=0} + \frac{1}{t_{N+1}}\left(\frac{\partial\theta_{N+1}}{\partial y}\right)_{y=0}\right],$ (C.36)

then the energy balance becomes:

$$\int_0^1 \left\{h_{fg}/c_{ps}.\Delta T + \frac{T_s}{\Delta T} - \frac{c_p}{c_{ps}}\frac{T}{\Delta T}\right\} t_{N+1}\, Q_{N+1}\, dy \qquad (C.37)$$

$$= \left(\frac{\rho_w k_w}{\rho_s k_s}\right)\frac{1}{P_s}\left\{\frac{\text{INTEG}.\, t_{N+1}}{x_{N+1}} + \frac{(x_{N+1}-x_N)}{2t_N x_{N+1}}\left(\frac{\partial\theta_N}{\partial y}\right)t_{N+1} + \frac{(x_{N+1}-x_N)}{2x_{N+1}}\left(\frac{\partial\theta_{N+1}}{\partial y}\right)_{y=0}\right\}.$$

The integral on the left is non-linear in the quantities unknown at the (N+1) station. Hence it is quasilinearized to give, dropping the suffix (N+1),

$$\int_0^1 \left\{ \frac{h_{fg}}{c_{ps}\Delta T} + \frac{T_s}{\Delta T} - \frac{c_p}{c_{ps}} \frac{T}{\Delta T} \right\} (t\bar{Q} + \bar{t}Q - \bar{t}\bar{Q}) \, dY .$$

The linearized form of the energy balance is now:

$$\bar{t} \int_0^1 \alpha(Y) Q \, dY + t \left[\int_0^1 \alpha(Y) \bar{Q} \, dY - \left(\frac{\rho_w k_w}{\rho_s k_s} \right) \frac{1}{P_s} \left\{ \frac{\text{INTEG}}{x_{N+1}} + \frac{x_{N+1} - x_N}{2 t_N x_{N+1}} \left(\frac{\partial \theta_N}{\partial Y} \right)_{Y=0} \right\} \right] \tag{C.38}$$

$$= \bar{t} \int_0^1 \alpha(Y) \bar{Q} \, dY + \left(\frac{\rho_w k_w}{\rho_s k_s} \right) \frac{1}{P_s} \frac{x_{N+1} - x_N}{2 x_{N+1}} \left(\frac{\partial \theta_{N+1}}{\partial Y} \right)_{Y=0} ,$$

where $$\alpha(Y) = \left(\frac{h_{fg}}{c_{ps} \Delta T} + \frac{T_s}{\Delta T} - \frac{c_p}{c_{ps}} \cdot \frac{T}{\Delta T} \right).$$

When X = 0 then INTEG = 0, and this the value when N = 1. Thereafter INTEG is updated at each station by taking the converged solution at X_{N+1} and adding

$$\text{INTEG} + \int_{x_N}^{x_{N+1}} \frac{1}{t(x)} \left(\frac{\partial \theta}{\partial Y} \right)_{Y=0} dx = \text{INTEG} + \frac{(x_{N+1} - x_N)}{2} \left[\frac{1}{t_N} \left(\frac{\partial \theta_N}{\partial Y} \right)_{Y=0} + \frac{1}{t_{N+1}} \left(\frac{\partial \theta_{N+1}}{\partial Y} \right)_{Y=0} \right] \tag{C.39}$$

before proceeding to the stage N+2.

For the case of the plate m = 0, then (C.35) becomes:

$$\frac{(m+1)}{2 x_{N+1}^{\frac{1}{2}(m+1)}} \int_0^{x_{N+1}} \frac{x^{\frac{1}{2}(m-1)}}{t(x)} \left(\frac{\partial \theta}{\partial Y} \right)_{Y=0} dx = \frac{1}{2 x_{N+1}^{1/2}} \int_0^{x_{N+1}} \frac{1}{x^{\frac{1}{2}} t(x)} \left(\frac{\partial \theta}{\partial Y} \right)_{Y=0} dx$$

$$= \frac{1}{2 x_{N+1}^{1/2}} \left[\text{INTEG} + \int_{x_N}^{x_{N+1}} \frac{1}{x^{1/2}} \frac{1}{t(x)} \left(\frac{\partial \theta}{\partial Y} \right)_{Y=0} dx \right].$$

when N > 1 then the procedure is similar to that outlined for the cylinder case with $\int_{x_n}^{x_{n+1}} f(x)\,dx = \frac{1}{2}(x_{n+1}-x_n)(f_n + f_{n+1})$. , but if N = 1 then we must deal separately with

$$\int_0^{x_1} \frac{1}{t(x).x^{1/2}} \left(\frac{\partial\theta}{\partial y}\right)_{y=0} dx. \qquad (C.40)$$

Near the leading edge t and $\left(\frac{\partial\theta}{\partial y}\right)_{y=0}$ are only weakly dependent upon X, therefore let

$$\frac{1}{t(x)}\left(\frac{\partial\theta}{\partial y}\right)_{y=0} = A + Bx,$$

where A and B are found in terms of t_N, t_{N+1}, $\left(\frac{\partial\theta_0}{\partial y}\right)_{y=0}$ and $\left(\frac{\partial\theta_1}{\partial y}\right)_{y=0}$.

Hence we find

$$\int_0^{x_1} \frac{1}{t(x).x^{1/2}} \left(\frac{\partial\theta}{\partial y}\right)_{y=0} dx = \frac{2}{3}t_1\left(\frac{\partial\theta_1}{\partial y}\right)_{y=0} + \frac{4}{3}t_0\left(\frac{\partial\theta_0}{\partial y}\right)_{y=0}. \qquad (C.41)$$

This is also used in calculating the value of INTEG which is carried into the procedure for finding the solution at the second stage. Apart from this, the method of multuplying across by t_{N+1} and linearizing is the same used when m = 1 for all N.

We now have (m + n + 2) equations for the (m + n + 2) unknowns, i.e. Q_i (i = 1(1)m), Q_i (i = 0(1)n-1), t and $F^*(0)$.

The equations are written in matrix form as

$$\underline{A}\ \underline{B} = \underline{R}, \qquad (C.42)$$

where $\underline{B}^T = (Q_1, \ldots, Q_m, Q_0^*, \ldots Q_{n-1}^*, t, F_0^*)$, (C.43)

$\underline{B}^T$ the transpose of $\underline{B}$, $\underline{R}$ is a column vector the elements of which are the right hand sides of the linearized equations [C.16] etc. , and the element s of $\underline{A}$ are:

$\underline{A} =$

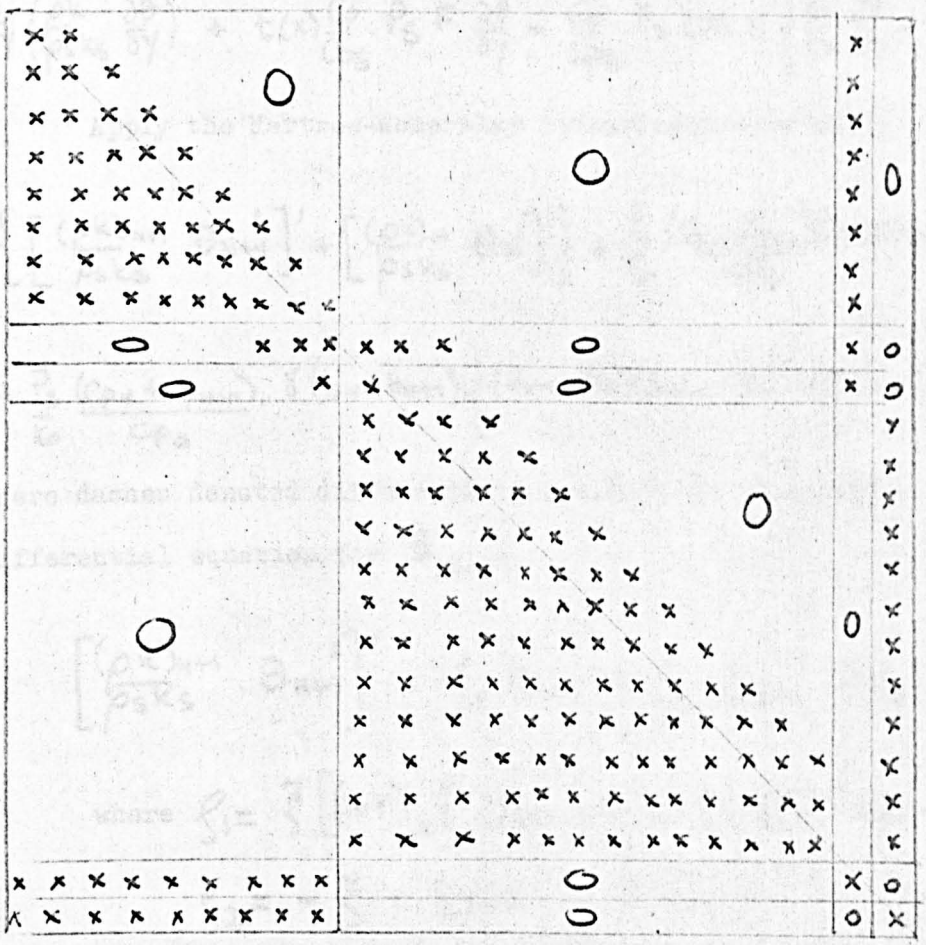

[C·44]

Solving (C.42) thus yeilds a better aprroximation for Q, Q^*, t and $F^*(X_{N+1}, 0)$ at the $(N+1)^{st}$ station, and to complete the iterative cycle the new values of t and Q are used in the solution of the energy equation (5.28).

We have for the case of the cylinder:

$$\frac{\partial}{\partial y}\left(\frac{\rho k}{\rho_s k_s}\frac{\partial \theta}{\partial y}\right) + t(x)\frac{c_p}{c_{ps}}.\rho_s F\frac{\partial \theta}{\partial y} + \frac{c_p}{c_{ps}}.\rho_s t(x).\times\left\{\frac{\partial F}{\partial x}\frac{\partial \theta}{\partial y} - \frac{\partial F}{\partial y}\frac{\partial \theta}{\partial x}\right\} = 0. \quad (C.45)$$

Apply the Hartree-Womersley linearization to this:

$$\frac{1}{2}\left\{\left[\left(\frac{\rho k}{\rho_s k_s}\right)_{N+1}\theta'_{N+1}\right]' + \left[\left(\frac{\rho k}{\rho_s k_s}\right)_N \theta'_N\right]'\right\} + \frac{P_s}{16}\left(\frac{c_{pN}+c_{pN+1}}{c_{ps}}\right)(t_N+t_{N+1})(F_{N+1}+F_N)(\theta_N+\theta_{N+1})$$

$$+ \frac{P_s}{16}\left(\frac{c_{pN}+c_{pN+1}}{c_{ps}}\right).\gamma(t_N+t_{N+1})\left\{(F_{N+1}-F_N)(\theta'_{N+1}+\theta'_N) - (F'_{N+1}+F'_N)(\theta_{N+1}-\theta_N)\right\} = 0, \quad [C.46]$$

where dashes denoted differentiation w.r.t. Y. This is an ordinary differential equation for θ_{N+1};

$$\left[\left(\frac{\rho k}{\rho_s k_s}\right)_{N+1}\theta'_{N+1}\right]' + f_1\theta'_{N+1} + f_2\theta_{N+1} + f_3 = 0, \quad (C.47)$$

where
$$f_1 = \tilde{\zeta}\left[(1+\gamma)\int_0^Y Q_{N+1}\,dY + (1-\gamma)\int_0^Y Q_N\,dY\right],$$
$$f_2 = -\tilde{\zeta}.\gamma\left[Q_{N+1}+Q_N\right],$$
$$f_3 = \tilde{\zeta}\left\{(1+\gamma)\theta'_N\int_0^Y Q_{N+1}\,dY + (1-\gamma)\theta'_N\int_0^Y Q_N\,dY + \gamma\theta_N\left[Q_N+Q_{N+1}\right]\right\} + \left[\frac{\rho_N k_N}{\rho_s k_s}\theta'_N\right]', \quad (C.48)$$

and
$$\tilde{\zeta} = \frac{1}{8}\frac{P_s}{c_{ps}}(c_{pN}+c_{pN+1})(t_N+t_{N+1}).$$

The ordinary differential equation (C.47) for θ_{N+1} is already

linear and can be introduced into a matrix scheme as it stands. We have $\vartheta_{N+1} = 0$ when Y = 0, and $\vartheta_{N+1} = 1$ when Y = 1 so there are only the (m-1) interior points unknown. Solving (C.47) at these (m-1) points ϑ_{N+1} can be determined. The finite differences used for Q in the condensate momentum equation are those used for ϑ in the above.

The iteration procedure at the $(N+1)^{st}$ station, given the solution at the N^{th} station, is to repeatedly solve (C.42) and (C.47) until successive approximations differ by less than a prescribed set of tolerances. This is a rapidly convergent process needing only two or three iterations near X = 0, but becomes markedly worse as separation is approached. In order to ascertain that this convergenced solution at X_{N+1} is close enough to the true solution we proceed as follows. Firstly two steps each of length $\frac{1}{2}(X_{N+1} - X_N)$ are taken from X_N to X_{N+1}, and then this solution at X_{N+1} is compared with the solution obtained by taking just one step from X_N to X_{N+1}. If the difference between t_{N+1} obtained by the two methods is greater than an allowable limit then the step lengths in the x-direction are halved and the procedure repeated, otherwise the solution obtained by taking two steps is accepted at X_{N+1}.

It remains to describe the manner in which the solution is started from X = 0.

The limiting forms of (C.1) and (C.19) as $X \to 0$ yield differential equations in which there is no differentiation with respect to X so they are already in forms analogous to (C.2) and (C.20). These are linearized using the Bellman technique, and there result differential equations the coefficients of which are functions of the previous iterate.

The boundary conditions (5.31)-(5.33) remain unaltered as $X \to 0$ so are introduced into the matrix in the same way as before, and it remains to consider the limiting form of the energy balance as $X \to 0$.

In the neighbourhood of $X = 0$ then $t(x)$ and $\left(\frac{\partial\theta}{\partial y}\right)_{y=0}$ will be taken to be constant, and for small X the left hand side of (C.35) becomes

$$\left(\frac{\rho_w k_w}{\rho_s k_s}\right)\frac{1}{P_s}\frac{(m+1)}{2x^{\frac{1}{2}(m+1)}}\frac{1}{t(0)}\left(\frac{\partial\theta_0}{\partial y}\right)_{y=0}\int_0^X x^{\frac{1}{2}(m-1)}\,dx$$

$$= \left(\frac{\rho_w k_w}{\rho_s k_s}\right)\frac{1}{P_s}\frac{1}{t(0)}\left(\frac{\partial\theta}{\partial y}\right)_{y=0}.$$

Thus the limiting form of (C.35) is:

$$\left(\frac{\rho_w k_w}{\rho_s k_s}\right)\frac{1}{P_s}\left(\frac{\partial\theta_0}{\partial y}\right)_{y=0} = \int_0^1 \left\{\frac{h_{fg}}{c_{ps}\Delta T} + \frac{T_s}{\Delta T} - \frac{c_p}{c_{ps}}\frac{T}{\Delta T}\right\} Q.t.\,dy,$$

which is treated in the same way as (C.37).

In this way a matrix equation analogous to (C.44) results and enables more accurate solutions Q, Q^*, t, and $F^*(0,0)$ at $X = 0$ to be found. The iterative cycle is completed by solving the energy equation (C 45), the limiting form as $X \to 0$ of which is a linear (in θ) ordinary differential equation and is solved by the method outlined for (C.47).

References

1. H. W. Emmons, Trans. Inst. Chem. Engrs. 35, 109 (1939).
2. A. Umur and P. Griffith, Mechanism of dropwise condensation, J. Heat Transfer, 87, 275, (1965)
3. L. Trefethen, Drop Condensation and Possible Importance of circulation within drops caused by Surface Tension Effects, GEL Report No. 58GL47, General Electric Co., Schenectady. N.Y. Feb. 3, 1958.
4. B. B. Mikic, On mechanism of dropwise condensation, Int. J. Heat Transfer, 12, 1311, (1969).
5. W. H. McAdams, Heat Transmission, 3rd Ed., p.334, McGraw-Hill, New York. (1954).
6. H. Schlichting, Grenzchicht-Theorie, Karlsruhe. (1951).
7. P. L. Kapitsa, Zh. Ekper., Teoret. Fiz, 18, 1, (1948).
8. W. J. Minkowycz and E. M. Sparrow, The effect of superheating on condensation heat transfer in a forced convection boundary layer flow, Int. J. Heat Mass Transfer, 12, 147, (1969).
9. E. M. Sparrow, W. J. Minkowycz and M. Saddy, Forced convection condensation in the presence of non-condensables and interfacial resistance, Int. J. Heat Mass Transfer, 10, 1829, (1967).
10. W. Nusselt, Die Oberflachenkondensation des Wasserdampfes, Z. Ver. Dt. Ing., 60, 541, (1916).

11. R. G. Miles and G. Poots, Effects of variable physical properties on laminar film condensation of saturated steam on a vertical flat plate, Int. J. Heat Mass Transfer, 10, 1677, (1967).

12. R. D. Cess, Laminar film condensation on a flat plate in the absence of a body force, Z. Angew. Math. Phys., 11, 426, (1960).

13. J. C. Y. Koh, Film condensation in a forced-convection boundary layer, Int. J. Heat Mass Transfer, 5, 941, (1962).

14. I. G. Shekriladze and V. I. Gomelauri, Theoretical study of laminar film condensation of flowing vapour, Int. J. Heat Mass Transfer 9, 581, (1966).

15. L. Prandtl, Mechanics of viscous liquids. In Aerodynamics by V. Durend, Vol.3, Oborongiz, Moscow (1939).

16. E. M. Sparrow and J. L. Gregg, J. Heat Transfer, 81, 113 (1959)

17. P. C. Hudson, Ph.D. Thesis, Applied Mathematics Department, University of Hull. (1970).

18. R. G. Miles, Ph.D. Thesis, Applied Mathematics Department, University of Hull. (1968).

19. W. M. Falkner and S. W. Skan, Solution of the boundary layer equations, Phil. Mag (7), 12, 865, (1913).

20. D. R. Hartree, On an equation occurring in Falkner and Skan's approximate treatment of the equations of the boundary layer, Proc. Camb. Phil. Soc., 33, 223, (1937).

21. K. Stewartson, Further solutions of the Falkner-Skan equation, Proc. Cam. Phil. Soc., 50, 454, (1954).

22. H. W. Emmons and D. C. Leigh, Tabulation of the Blasius function with suction and blowing, Fluid Motion Sub-Committee, Aero. Res. Coun., Rep. No. FM1915 (1953).

23. K. D. Voskresenskiy, Calculation of Heat Transfer in Film Condensation allowing for the temperature dependence of the physical properties of the condesnate, U.S.S.R. Acad. Sci. O.T.K. (1948).

24. D. A. Labuntsov. Effect of temperature dependence of the physical parameters of the condensate on heat transfer in film condensation of steam. Teploenergetika, 4(2), 49,(1957).

25. D.R. Hartree and J. R. Womersley. A method for the numerical or mechanical solution of certain types of partial differential equations. Proc. Roy. Soc. A, 161, 353,(1937).

26. R. M. Terrill, Laminar boundary layer near separation with and without suction, Phil. Trans. A. 253, 55 (1960).

27. D.R. Hartree, A solution of the laminar boundary layer equation for retarded flow, Rep. Memor. Aero. Res. Coun. No. 2426 (1939, issued 1949).

28. D. C. F. Leigh, The laminar boundary layer equation: a method of solution by means of an automatic computer, Proc. Cam. Phil. Soc., 51, 320, (1955).

29. L. Howarth. On the Solution of the laminar boundary equations, Proc. Roy. Soc. A, 164, 547 (1938).

30. S. Goldstein, On laminar boundary layer flow near a position of separation, Quart, J. Mech., 1, 43 (1948).

31. E. J. Watson, The asymptotic theory of boundary layer flow with suction, Rep. Memor, aero. Res. Coun., London. No. 2619, 252, (1947).

32. H. S. Carslaw and J. C. Jaeger, Conduction of Heat in Solids, Second Edition, Oxford (1959).

33. L. R. Ingersol, O. J. Zoebel and A. C. Ingersoll, Heat Conduction with Engineering and Geological Applications, McGraw-Hill, New York (1948).

34. F. Kreith and F. E. Rommie, Proc. Phys. Soc., B 68, 277, (1955).

35. D. N. de G. Allen and R. T. Severn, The application of relaxation methods to the solution of non-elliptic partial differential equations, II the solidification of liquids. Quart J. Mech. and App. Math., IV pt. 4, 447, (1952).

36. D. N. de G. Allen and R. T. Severn, The application of relaxation method to the solution of non-elliptic partial differential equations, III Heat Conduction, with a change of state, in two space dimensions. Quart. J. Mech. and Appl. Math., XV pt.1, 53, (1962).

37. G. Poots, On the application of integral methods to the solution of problems involing the solidification of liquids initially at fusion temperature, Int. J. Heat Mass Transfer, 5, 525, (1962).

38. S.Goldstein and L. Rosenhead, Boundary Layer Growth, Proc. Cam. Phil. Soc., 32, 392, (1936).

39. D. R. Hartree, Mem. Manc. Lit. Phil. Soc., 80, 85, (1935).

40. H. Jones, Unpublished Ministry of Supply report.

41. I. Tani, J. Aero. Sci. 21, 487 (1954).

42. Y. R. Mayhew and G. F. C. Rogers, Thermodynamics and transport properties of fluids (MKS Units), Blackwell, Oxford (1964).

43. G. Poots and M. H. Rogers, Laminar flow between parallel flat plates, of water with variable fluid properties, Int. J. Heat Mass Transfer, 8, 1515, (1965).

44. R. Bellman and R. Kalaba, Some numerical experiments using Newton's method for non-linear parabolic and elliptic boundary value problems, Rand. Corp. (Santa Monica, Calif.), Rep. No. P-2200, (1961).

45. G. Poots, A solution of the compressible laminar boundary layer equations with heat transfer and adverse pressure gradient, Quart. J. Mech. and Appl. Math., XIII (1), 57, (1960).

46. T. V. Davies and E. M. James, Non-linear Differential Equations, Addison-Wesley, (1966).

47. W. F. Ames, Non-linear Partial Differential Equations in Engineering, Academic Press, New York (1965).